Regulation of Integrin-Mediated Linkages
during Cell Migration

by

Sean P. Palecek

B.ChE. Chemical Engineering
University of Delaware, 1993

M.S. Chemical Engineering
University of Illinois at Urbana-Champaign, 1995

Submitted to the Department of Chemical Engineering
in Partial Fulfillment of the Requirements for the Degree of

Doctor of Philosophy in Chemical Engineering

at the

Massachusetts Institute of Technology

September, 1998

© 1998 Massachusetts Institute of Technology.
All rights reserved.

Signature of Author: ....
Department of Chemical Engineering
July 27, 1998

Certified by: ....
Douglas A. Lauffenburger
Professor of Chemical Engineering
Director of the Center for Biomedical Engineering
Thesis Supervisor

Accepted by: ....
Robert E. Cohen
St. Laurent Professor of Chemical Engineering
Chairman, Committee for Graduate Students
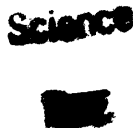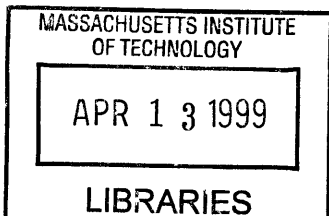
Regulation of Integrin-Mediated Linkages
during Cell Migration

by

Sean P. Palecek

Submitted to the Department of Chemical Engineering on July 27, 1998
in Partial Fulfillment of the Requirements for the Degree of
Doctor of Philosophy in Chemical Engineering

ABSTRACT

The objective of this study was to determine how integrin adhesion interact with both cytoskeletal elements and ligands to determine cell migration speed. An understanding of these parameters will aid in developing methods to control cell migration to treat diseases such as cancer, to aid wound healing, or to design tissue engineering matrices.

A Chinese hamster ovary (CHO) cell system was constructed to allow us to vary integrin-ligand binding by altering extracellular matrix (ECM) concentration, integrin expression level, and integrin-ligand binding. As these parameters change, cell migration speed remains a constant, biphasic function of cell-substratum adhesiveness. We can regulate cell speed by varying the number and nature of cell-substratum bonds. The mechanism of cell-substratum detachment is also different as cell adhesiveness varies. At low adhesiveness integrin-ECM bonds preferentially dissociate while at high adhesiveness integrin-cytoskeletal linkages fracture and rear retraction occurs by extraction of ligand-bound integrin from the cell membrane. At high adhesiveness cell-substratum detachment is the rate-limiting step in cell migration speed while at low adhesiveness other factors, such as the formation of new adhesions, are likely to limit cell speed. We identified calpain, a calcium-dependent protease, as a regulator of rear retraction and cell speed at high adhesiveness. Calpain inhibition strengthens integrin-cytoskeletal linkages and greatly reduces integrin-extraction during rear retraction. These experiments demonstrate that we can change cell speed by altering how integrins interact with both the ECM and cytoskeleton.

A mathematical model of rear retraction during cell migration was developed to help explain how integrin-ECM and integrin-cytoskeleton binding can regulate retraction rate and mechanism. The model predicts two different detachment phenotypes. Rear retraction can occur by either rapid release of integrin-ECM bonds or by slower cleavage of integrin-cytoskeletal linkages followed by extraction of integrin from the cell membrane. Rapid detachment rate is regulated by integrin-ligand affinity and concentrations while slow detachment is regulated by integrin-cytoskeleton binding and calpain activity. The transition from slow to rapid detachment can be induced by reducing integrin-ligand affinity, increasing integrin:ligand concentration ratio, or increasing intracellularly generated force. This model can explain why highly motile cells do not release integrin during rear retraction but slower cells tend to detach by integrin extraction.

Thesis Supervisor: Douglas A. Lauffenburger
Title: Professor of Chemical Engineering and Director of the Center for Biomedical Engineering

Acknowledgments

Table of Contents

5

List of Figures

7

List of Tables

Chapter 1: Introduction and Background

1.1 Cell Migration in Health and Medicine

The processes of cell adhesion and cell migration are essential for normal embryonic development and the maintenance of health throughout life; but may also contribute to pathologic conditions which threaten health. Survival of many cell types requires adhesion to extracellular matrix (ECM) proteins (Meredith and Schwartz, 1997) and the loss of anchorage dependent growth is characteristic of tumorigenicity (Schwartz, 1997). Adhesion-dependent growth can depend on both biochemical and mechanical events (Shyy and Chien, 1997). Cell motility is first apparent during early embryonic development in morphogenic processes where different cells both aggregate and segregate to form diverse tissues and organs. These morphogenic migrations are intricate, highly specific, and reproducible. In the adult, cellular migrations are required for the development of an immune response whereby immune cells migrate out of the vasculature and into areas of inflammation. While this process is required for normal immune function, it may also contribute to the pathogenesis of inflammatory disorders such as arthritis or asthma. Cell adhesion and migration are also crucial for wound healing (Racine-Samson et al., 1997; Gailit and Clark, 1994). Fibroblasts migrate into the wound, attach to the matrix, and contract to close the wound. Cell migrations also contribute to diseases such as cancer, in which migration of cells from the primary tumor mass to distant sites is the hallmark of the conversion of a benign to a malignant tumor (Keely et al., 1998; Giancotti and Mainiero, 1994; Van Roy and Mareel, 1992). Thus, a molecular understanding of migration is central to our understanding of basic organismal biology. It is also critical to developing therapeutic strategies against several important pathologic conditions including vascular disease, cancer, and chronic and acute inflammation. Finally, it promises to aid efforts to accelerate wound repair and the production and utilization of replacement tissues (Cima and Langer, 1993).

The complex process of cell migration can be usefully analyzed as comprised of several distinct, dynamic events: these include membrane protrusion and extension, formation of stable but dynamic contacts between the cell and its substratum, translocation of cell cortex, and release of cell-substratum adhesions at the rear of the cell. This parsing of migration into distinct events underscores the spatially distributed nature of the component processes, which therefore require coordination -- temporal as well as spatial -- to accomplish locomotion. Understanding the mechanisms of cell migration, along with their regulation and coordination, is especially challenging because of this central role for physical integration. Different proportions of integration likely give rise to qualitatively different movement appearances among particular cell types or under various environmental conditions. For instance, effective coordination of

12

lamellipod protrusion, cytoskeletal contraction, and cell-substratum de-adhesion may result in highly efficient "gliding" motion, as seen in keratocytes and neutrophils on substrata of relatively low adhesion. More distinct extension and retraction processes yield locomotion by relatively discrete "steps", as observed in fibroblasts and endothelial cells; at the same time, keratocyte and neutrophil movement behavior on highly adhesive substrata can become more saltatory and resemblent of fibroblasts. In a comparable vein, the process rate-limiting for movement may differ among cell types or across a span of conditions. For example, under some circumstances the rate of cell locomotion can be governed by events at the cell front (Wessels et al., 1994). However, cell speed is generally not limited by the rate of lamellipod protrusion (Abercrombie et al., 1970; Felder and Elson, 1990; Condeelis, 1993); sometimes lamellipodia are not able to form stable attachments to the substratum (Bard and Hay, 1975), and often cell/substratum adhesions at the cell rear are determinative, particularly on highly adhesive substrata. It is conceivable, therefore, that the fundamental molecular mechanisms underlying the processes comprising migration are similar among different cell types despite apparent phenomenological variation.

1.2 Formation of Adhesions at the Cell Front

To initiate migration, cells must extend membrane protrusions and form new attachments to the substratum at their front. Nascent attachments may subsequently become highly organized structures which are connected to the actin cytoskeleton. Protrusions at the leading edge include broad, flat, veil-like protrusions called lamellipodia and needle-like projections called filopodia. These protrusions are primarily driven by polymerizing actin (Stossel, 1993; Mitchison and Cramer, 1996). These adhesive sites generate forward-based traction necessary for migration. Recent studies have contributed fresh insights into the basic mechanisms of adhesion formation.

Cell adhesion to ECM, an important component of migration, is mediated by a number of transmembrane glycoprotein adhesion receptors, including members of the integrin family (for reviews see Buck and Horwitz, 1987; Ruoslahti and Pierschbacher, 1987; Hynes, 1992; Sonnenberg, 1993). Integrins are heterodimeric proteins composed of an α and a β subunit whose extracellular domains form a binding site for one or more ECM proteins with specificity (Hogg et al., 1994; Smith and Cheresh, 1988). Integrins also bind to cytoskeletal proteins, such as talin or α-actinin, via a short cytoplasmic domain sequence on the β subunit to transmit the force of cytoskeletal tension to the substratum (Horwitz et al., 1986; Burridge et al., 1988; Otey et al., 1990). In nonmotile fibroblasts, integrins and associated cytoskeletal components associate into highly organized focal adhesions, shown in Figure 1.1, which mediate a close attachment between the cell and its substratum (Hynes, 1987; Buck and Horwitz, 1987). Attachments between

integrins and the cytoskeleton are less well organized in migrating fibroblasts, but integrins interact with the substratum and cytoskeleton through similar linkages (Regen and Horwitz, 1992).

Formation of integrin-containing adhesive complexes during cell migration has been examined using low-light level video microscopy and immunofluorescence (Regen and Horwitz, 1992) and laser optical trapping and nanometer level motion analysis (Schmidt et al., 1993). In migrating cells, nascent adhesions containing aggregated integrins, vinculin, FAK, and various phosphoproteins, form preferentially along the periphery of lamellipodia and the tips of filipodia (Nobes and Hall, 1995). Integrin-ligand binding appears to be a crucial step in regulating adhesion structure association with the cytoskeleton (Felsenfeld et al., 1996). On the ventral (lower) surface, these aggregates tend to remain-fixed to the substratum, increasing in size and organization as the cell moves over them until they reach the rear (Regen and Horwitz, 1992). Thus the motile process actively removes integrins from the leading edge and concentrates them at the rear. This raises an important question. How are integrins replenished to the cell front so new adhesions can form? One potential mechanism is provided by polarized vesicle trafficking in which receptors on the cell surface, especially those at the rear, are endocytosed and delivered toward the cell front where they can supply integrins for nascent adhesions (Lawson and Maxfield, 1995; Bretscher, 1996; Bretscher, 1989). This appears to be an important mechanism for neutrophils; but its relative contribution in other cell types is less clear. Another mechanism, which may complement the endocytic mechanism just discussed, involves molecular motors carrying integrins to the cell front, thus having a similar replenishing effect. Experimental evidence supporting this notion has been obtained for integrins through tracking studies in which colloidal gold particles attached to small $\beta 1$ integrin aggregates on the dorsal (upper) surface at the cell front were found to translocate to the leading edge (Schmidt et al., 1993).

In addition to preferential integrin localization to the cell front, mechanisms also exist to deliver actin, and perhaps other adhesion-related molecules, to the leading edge. The mRNA for β-actin localizes to the lamellipodia of motile cells (Bassell and Singer, 1997). Furthermore, inhibiting β-actin mRNA localization or its translation into protein, reduces motility in fibroblasts (Kislauskis et al., 1997). In summary, it is now clear that various mechanisms ensure that the cell front is supplied with the building blocks for nascent adhesions and actin protrusion. Precise determination of the mechanisms involved and the importance of these delivery modes among different cell types, as well as discovery of new mechanisms will give more insights into how the molecular constituents concentrate at the leading edge.

The mechanisms which govern adhesion formation and actin organization at the leading edge are not yet fully understood. Recent progress has elucidated some of the signaling molecules and mechanisms which regulate adhesion and cytoskeletal organization during migration. These include tyrosine phosphorylation, rho family proteins, and growth factor signaling pathways.

Tyrosine phosphorylation has a prominent role in adhesion formation and migration (however it is also implicated in adhesive release as discussed below). Inhibition of tyrosine phosphorylation of cytoskeletal proteins abrogates formation of adhesions, cell spreading and decreases motility (Gilmore and Romer, 1996; Romer et al., 1994; Burridge et al., 1992). Though the phosphoproteins responsible for initiating and assembling adhesions have not been clearly defined, the focal adhesion kinase (FAK) has received much attention in this context. FAK associates with the cytoplasmic domains of integrins, is present in nascent adhesions and has a well defined role in cell migration (Schlaepfer and Hunter, 1998; Schaller and Parsons, 1994). FAK-deficient mice are embryonic lethals that exhibit general mesodermal defects at the eighth day into development (Ilic et al., 1995). Fibroblast-like cells cultured from FAK-deficient mice have a more rounded morphology, an increased number of focal adhesions and dramatically reduced motility compared to analogous cells derived from wild-type mice. Further evidence supporting a role for this kinase in regulating migration is provided by CHO cells that overexpress FAK. These cells show an enhanced motility on fibronectin, although the mechanism contributing to this phenotype has not been elucidated (Cary et al., 1996).

Another group of molecules that appear to be key regulators of adhesion formation during migration are those belonging to the rho family, and in particular, rac. The rho family of small GTPases direct adhesive complex formation and also serve as actin architects, sculpting actin networks and linking them to these adhesive complexes. The most intensely studied members of this family include cdc42, rac, and rho. G-protein linked and growth factor receptors activate the rho family proteins (Machesky and Hall, 1996). Like ras, these proteins act as molecular switches controlling downstream signaling cascades: they are inactive when bound to GDP and are active when bound to GTP, which seems to occur concurrently with membrane localization. Three groups of regulatory molecules control the activity of these proteins: guanine nucleotide exchange factors (GEFs), which catalyze exchange of GDP for GTP; GTPase activating proteins (GAPs), which catalyze the hydrolysis of GTP to GDP; and GDP dissociation inhibitors (GDIs), which stabilize the inactive state.

Microinjection studies demonstrate that cdc42 induces filopod formation, rac orchestrates lamella extension and membrane ruffling, while rho coordinates stress fiber and focal adhesion assembly (Ridley and Hall, 1992; Kozma et al., 1995; Nobes and Hall, 1995). Cdc42 and rac also induce formation of adhesion complexes which have the same components as rho-induced focal adhesions (clustered integrin, talin, vinculin, phosphorylated FAK and paxillin) but are smaller in size (Nobes and Hall, 1995). Rac appears to stimulate lamella extension through phosphorylation of p130CAS which allows CAS to couple to Crk (Klemke et al., 1998). The rho family proteins are linked in a hierarchical cascade: cdc42 activates rac which activates rho, a

temporal order consistent with the chronology of actin polymerization for membrane protrusion followed by attachment.

Motile cells have membrane ruffles and lamellipodia at the leading edge, and diminished stress fibers relative to non-motile cells. Rac, which stimulates formation of membrane ruffles and lamellipodia, appears to have a paramount role in migration. For example, the expression of rac or Tiam1, a rac GEF, confers an invasive phenotype to T-lymphoma cells (Michiels et al., 1995). Furthermore, active rac is essential for NGF- and PMA-induced motility of PC12 cells (Altun-Gultekin and Wagner, 1996). Rho, on the other hand, stimulates formation of strong adhesions and stress fibers through generating contractility (Chrzanowska-Wodnicka and Burridge, 1996), and its role in migration is less well defined. Some evidence exists that downregulation of rho is necessary for migration to occur. Microinjection of activated rho inhibits scatter factor / hepatocyte growth factor-induced migration of MDCK cells, while inhibition of rho does not affect motility (Ridley et al., 1995). Alternatively, rho-stimulated contractility may be important in release of adhesions at the cell rear during migration (see below). The role of cdc42 in migration has not been examined, though this molecule is likely to be important as it directs filopodial formation. The relationship between these short-term ruffling events and longer-term sustained locomotion, however, is not clear at present. A plausible hypothesis may be that these short-term events are involved in initial reorganization of cytoskeleton from that of sessile cells to that required for effective force transmission in locomoting cells (Craig and Johnson, 1996). Alternatively, the rho family-mediated events could remain important for continuing rounds of lamellipod/filopod extension during sustained migration. This issue merits further investigation.

Recently, a great deal of progress has been made towards elucidating the downstream effectors of the rho proteins (Tapon and Hall, 1997). This has given insights into how these proteins form adhesions and stimulate actin polymerization. The rho pathway appears to link the growth factor response to cytoskeletal organization and adhesion formation (Santos et al., 1997). One of the most intensely studied downstream effectors of rac and rho is phosphatidylinositol 5-kinase (PI 5-kinase), which elevates phosphatidyinositol 4,5-bisphospate (PIP$_2$) levels (Chong et al., 1994; Tolias et al., 1995; Hartwig et al., 1995). This is interesting because PIP$_2$ has many activities that may contribute to adhesion formation and cytoskeletal architecture. In particular, PIP$_2$ unmasks cryptic actin and talin binding sites on vinculin which is necessary for adhesion complex assembly (Gilmore and Burridge, 1996). It also modulates actin polymerization through interactions with numerous actin-binding proteins including gelsolin, capZ, α-actinin and profilin (Stossel, 1993). PIP$_2$ also apparently has a role in activating ERM (ezrin-radixin-moesin) proteins, which act as cross-linkers between plasma membranes and the actin cytoskeleton (Hirao et al., 1996; Niggli et al., 1995). Highlighting the cumulative effect of these activities,

microinjection of PIP$_2$ antibodies inhibits stress fiber and focal adhesion assembly (Gilmore and Burridge, 1996).

Another important downstream effector of rac and cdc42 is phosphatidylinositol 3-kinase (PI 3-kinase), whose activity is regulated by rho (Zhang et al., 1993; Zheng et al., 1994, Kumagai et al., 1993). This is interesting because PI 3-kinase is implicated in growth factor-mediated motogenic signaling pathways (see below). How PI 3-kinase influences motility is not understood but it is known to regulate integrin receptor avidity (Kovacsovics et al., 1995). Furthermore, PI 3-kinase catalyzes the synthesis of D3-phosphorylated inositides which activate various protein kinase C (PKC) family isoforms (Nakanishi et al., 1993; Toker et al., 1994). Activation of PKC has been shown to stimulate focal adhesion formation (Woods and Couchman, 1992) and enhance cell migration (Harrington et al., 1997).

Finally, growth factor receptors and certain downstream effectors have been implicated as regulators of adhesion in motile cells. Studies of chemotaxis towards growth factors have given insights into motogenic signaling pathways. Many growth factor receptors are tyrosine kinases whose activities are stimulated upon ligand binding, resulting in receptor autophosphorylation. Upon phosphorylation, several molecules associate with the growth factor receptors via SH2 domains, including PI 3-kinase, phospholipase C-γ (PLC-γ), rho GTPase activating protein (rhoGAP), and the GRB2-SOS complex. The motogenic and mitogenic pathways stimulated by growth factors are distinct; PI 3-kinase and PLC-γ are implicated in generating motogenic signals. The ability of platelet-derived growth factor (PDGF) to stimulate chemotaxis correlates positively In another study, both PI 3-kinase and PLC-γ were found to be essential in the motile response mediated by PDGF receptor, while rasGAP had an antagonistic effect (Kundra et al., 1994). PLC-γ is also important in epidermal growth factor (EGF) receptor-initiated motility (Chen et al., 1994). Various inhibitors of PLC-γ abrogate the ability of EGF receptor to signal motogenically (Chen et al., 1994).

The manner in which PI 3-kinase and PLC-γ stimulate locomotion is unknown. Both these molecules can alter actin organization. PI 3-kinase is discussed above as being a downstream effector of rho proteins. In addition, this lipid kinase has been found to mediate PDGF-induced activation of rac (Hawkins et al., 1995). The EGF receptor stimulates motility at least partially through PLC-γ-mediated gelsolin release (Chen et al., 1996). PLC-γ hydrolyzes PIP$_2$ releasing membrane bound gelsolin, which can function as an actin-severing protein, freeing actin monomers for polymerization. Consistent with this activity, membrane extension rates in fibroblasts are increased via a PLC-γ pathway upon stimulation by EGF, proportional to but not entirely commensurate with enhanced migration speed (Ware et al., in press).

Much progress has been made towards discerning the mechanisms that orchestrate adhesion formation during migration; in particular the role of rho family proteins and interactions

among focal adhesion components. Despite this however, much remains unknown concerning the upstream regulators and targets of the rho family regulatory proteins.

1.3 Release of Adhesions at the Cell Rear

While there has been much progress in recent years toward understanding adhesive events at the front of motile cells, less is known about events at the cell rear. Although the rate of rear release determines the migration rate under many conditions (Chen, 1981), the mechanisms regulating this process are poorly understood. Understanding the dynamics of cell-substratum adhesions at the rear of a migrating cell may help contribute insight into release mechanisms. In fact, many focal adhesions in migrating cells disassemble at the leading edge so understanding the processes which govern disassembly of adhesions may also give insight into cell protrusion (Burridge et al., 1997). Breakage of cell-substratum attachments needed to allow locomotion can, in principle, occur by either intracellular or extracellular fracture of the cytoskeletal-integrin-ECM linkage. Previous studies suggest that under some conditions extraction of membrane components occurs at the rear of migrating cells both in vitro and in vivo (Chen, 1981; Hay, 1985; Niggemann et al., 1997). Using anti-integrin antibodies conjugated with fluorescent derivatives, the fates of integrin receptors at the cell rear have been characterized in fibroblasts. Studies using migrating fibroblasts demonstrate that a substantial fraction of integrin receptors can be released from the cell surface and remain on the substratum after detachment (Regen and Horwitz, 1992; Palecek, et al. 1996). A smaller fraction of the integrin receptor remains on the cell surface after fibroblasts detach from the substratum. Integrin remaining on the cell surface may subsequently be taken up into endocytic vesicles which accumulate near the nucleus in fibroblasts. Alternatively, integrin may also remain on the cell surface as an aggregate which can move along the cell edge and reattach to the surface, or it may disperse along the cell surface. The different mechanisms of adhesion disruption and the ensuing reuse of integrins are shown in Figure 1.2.

The factors contributing to adhesive release at the cell rear are likely to involve a combination of contractile forces and biochemical regulatory mechanisms. There is increasing evidence supporting a role for contraction in the breakdown of adhesions at the rear of the cell. Several lines of evidence support a role for myosin II-based contraction (Jay et al., 1995). Amoebae deficient in myosin II have decreased migration rates which are exaggerated on more adhesive substrata (Wessels et al., 1988, Jay et al., 1995). Myosin II also localizes to the rear of migrating fibroblasts (Conrad et al., 1993), suggesting a functional role in that area. Furthermore, injection of antibodies to myosin light chain kinase inhibits macrophage migration (Wilson et al., 1991). Using a permeabilized system to study mechanisms of adhesive release, additional evidence supports a role for contraction in cell detachment. Addition of exogenous ATP to the

permeabilized cells promotes contraction and a breakdown of focal adhesions (Crowley and Horwitz, 1995). The importance of contraction and actin-myosin interactions is also demonstrated by the inhibition of focal adhesion breakdown by peptides that inhibit actin-myosin interactions. Externally-induced signaling pathways could elicit appropriate contractile activity for purposes of regulating detachment. For instance, MAP kinase activity stimulated by EGF has been found to cause disassembly of focal adhesions in fibroblasts with corresponding decrease in adhesion strength (Xie et al., 1997). The potential importance of contractility in migration is further suggested by a recent study which showed that MAP kinase enhances migration through activating myosin light chain (MLC) kinase activity, thus increasing MLC phosphorylation (Klemke et al., 1997). A particular locus for effects of MLC kinase activity has not been identified; it could operate over the entire cell for cytoskeletal reorganization, or possibly primarily at the cell rear to facilitate detachment.

Upon application of force, cell-substratum linkages can be broken at two different loci: the integrin-ligand bond or the integrin-cytoskeletal bond. In general, the comparative probabilities of breakage at two alternative loci are inversely proportional to the square root of the comparative bond affinities (Saterbak and Lauffenburger, 1996). In migrating fibroblasts, the majority of integrin remains on the substratum suggesting preferential severing of the integrin-cytoskeletal bond at the rear of migrating fibroblasts. Direct evidence for this is demonstrated by studies showing that the integrin-cytoskeletal linkage is weaker at the rear of migrating fibroblasts (Schmidt et al., 1993). Optical trapping studies using integrin antibodies show that there is a large differential in cytoskeletal linkage between the cell front and rear, with at least a four fold lower probability of an integrin linking with the cytoskeleton at the cell rear.

As discussed below, the application of force to cell-substratum attachments can either strengthen or weaken the cytoskeletal linkages. Thus, if linkages at the cell rear need to be preferentially broken while those at the front need to be preferentially strengthened, some biochemical mechanism must exist to provide a differential effect. Regulation of cell detachment likely involves signal transduction pathways, although the roles of these pathways are not yet clearly defined. The small GTP-binding protein rho is among signal transduction pathways that are implicated in rear release. Inhibitors of rho induce cell rounding and detachment (Miura et al., 1993, Paterson et al., 1990). Tyrosine phosphorylations also appear to play a role in cell detachment. Infection of cells with transforming viruses such as Rous sarcoma virus promote a rounded morphology and less organized adhesive structures as a result of increased pp60src tyrosine kinase expression (Burridge et al., 1988). Further evidence for a role for tyrosine phosphorylation is supported by studies using a permeabilized system which implicate tyrosine phosphorylation in the breakdown of focal adhesions. Although the evidence suggests that tyrosine phosphorylation is involved in adhesive release, the pathway involved is unknown.

Gradients of calcium, with higher concentrations seen at the cell rear, have been demonstrated in migrating eosinophils and are implicated in release of adhesions (Brundage et al., 1991). Buffering calcium inhibits migration of neutrophils on both fibronectin and vitronectin by inhibiting the release of adhesions at the rear (Maxfield, 1993). One target for calcium appears to be the calcium/calmodulin-dependent phosphatase calcineurin. Addition of a peptide inhibitor of calcineurin inhibits neutrophil detachment on vitronectin, suggesting that calcineurin is a calcium-dependent release mechanism specifically for the $\alpha v \beta 3$ interaction with vitronectin (Hendey et al., 1992). The calcium-dependent protease calpain may also play an important role in the release of integrin-mediated adhesions. Calpain localizes to focal adhesions, cleaves many focal adhesion proteins including FAK, talin and the integrin cytoplasmic domain (Beckerle et al., 1987; Du et al., 1996; Cooray et al., 1996), and therefore is a likely candidate to play a role in severing the integrin-cytoskeletal linkage during migration.

In addition to mechanisms altering integrin-cytoskeletal linkages during rear retraction, alteration in the strength of integrin-ligand interactions may also play a regulatory role during rear release. It is possible, for example, that integrins at the cell front have a high affinity while those at the rear have a lower affinity, producing an adhesive asymmetry within the cell. The weaker adhesions at the rear would favor release while the stronger adhesions at the front would support adhesion. To date there is no direct evidence supporting a role for this kind of gradient in integrin affinity. However, the affinity of integrin receptors does contribute to migration. In immune cell migration, for example, transient activation is required for the transmigration of immune cells. The cells neither adhere nor migrate with their $\beta 2$ receptors in their low affinity state (Springer, 1995). However locking $\beta 1$, $\beta 2$, or $\beta 3$ integrin receptors in a high affinity state inhibits cell migration in several cell types (Kuijpers et al., 1993, Huttenlocher et al., 1996). The high integrin affinity inhibits migration by inhibiting release at the cell rear, as revealed by video imaging. Lowering the substrate ECM concentration can compensate for increased integrin affinity to result in efficient migration (Huttenlocher et al., 1996). This is in accord with the notion that migration is inhibited because of a reduction in the rate of rear release with high affinity integrin.

1.4 Forces as Mechanical and Molecular Integrators during Migration

While the formation and release of adhesions are essential during migration, the function of adhesions, once formed, is to transmit intracellularly generated forces to its environment. Adhesions serve primarily to provide the traction necessary for force transmission and cortical movement. Cellular forces also serve mechanistic roles in the release and formation of adhesions mentioned previously. At least two types of forces, protrusive and contractile, are required for cell locomotion. Protrusive forces are required to extend lamellipodia or filopodia. These forces must

overcome the drag of the membrane and the deformation of the surrounding environment. Actin polymerization is the most likely origin of protrusive forces (Mitchison and Cramer, 1996). Actin-binding and crosslinking proteins have been implicated in regulating actin polymerization and membrane protrusion. Contractile forces are required to move the cell body forward and to detach cell-substratum adhesions at the rear. Contractile forces presumably depend on muscle-like actin-myosin interactions and on myosin motors.

At least two mechanisms have been suggested for generating the contractile forces which move the cell body forward (see Figure 1.3). Actin filament contraction in which filaments of opposite polarity slide past each other, as in muscle sarcomeres, could generate tension aiding cortical translocation or rear retraction. Alternately, myosin motors could function to move one population of actin filaments forward over a track of stationary actin filaments on the ventral surface of migrating cells. A recent study of actin filament polarity in migrating cells supports both of these models (Cramer et al., 1997). A small population of actin filaments are organized in bundles which alternate in polarity. This is consistent with their role as mediators of contractile events. Another, larger population of actin filament bundles is organized in ventrally located bundles in which the polarity gradually changes along the length of the bundle. This arrangement is expected for filaments involved in track migration. Recently, observations on migrating cells demonstrate that one fraction of actin filaments in the cell body remains fixed with respect to the substratum and another moves forward at the rate of cell body translocation (Cramer et al., 1997) This suggests that track-like movement generates cortical translation. Earlier observations point to contractile events during release at the cell rear, which is consistent with the actin filament arrangement predominantly found there (Conrad et al., 1993). An analysis of the organization of the actin-myosin II system in fish epidermal keratocytes is inconsistent with both sarcomeric contraction and transport along arrays of actin (Svitkina et al., 1997). Actin filaments and myosin II clusters form in the lamellipodia. As the cells migrate forward, these structures remain fixed with respect to the substratum. In the cell body, actin and myosin filaments align and form contractile elements, aligned parallel to the leading edge, which may drive forward movement of the cell body. Similar organization of actin and myosin has been reported in fibroblasts (Verkhovsky et al., 1995; Verkhovsky et al., 1997).

Contractile forces are transmitted from the actin cytoskeleton to the extracellular environment through adhesive complexes. The transmission of these contractile forces to the environment leads to the exertion of a traction force on the surface. Likewise, the surface exerts an equal but opposite force on the cell. The magnitude of the traction force is obviously related to the magnitude of the tension generated by forces discussed above; but it is also influenced by properties of the cytoskeleton-adhesion receptor-ECM linkage. The notion of a "molecular clutch" has been used to explain how contractile forces can be used to propel a cell through its environment

21

(Choquet et al., 1997; Heidemann and Buxbaum, 1998). In this model the actin network treadmills across the cell by polymerizing at the cell front and depolymerizing at the cell rear. Adhesions can engage the actin network, allowing the cell to treadmill forward. Adhesions can also disengage and the cell then treadmills in place.

Contractile forces can also play a key role in allowing cell body translocation and cell-substratum detachment (Lauffenburger and Horwitz, 1996). Measuring local contractile forces is technically challenging, but these forces have been measured on deformable silicone rubber substrata for migrating fibroblasts (Harris et al., 1980) and keratocytes (Lee et al., 1994), and by a micropatterned force-transducing surface for fibroblasts (Galbraith and Sheetz, 1997). Faster moving cells which glide over a substrate, such as keratocytes, tend to be less adherent and exert lower traction forces on the substrate than slower cells, like fibroblasts. Traction forces range from about 2×10^{-8} N for keratocytes to about 2×10^{-7} N for fibroblasts, with neutrophils intermediate (Oliver et al., 1995). Migrating keratocytes do not exert detectable traction forces at the front of the cell where actin polymerization is thought to provide protrusive forces. Keratocytes exert inward-directed traction forces at the cell periphery near the cell rear. Fibroblasts also do not exert traction forces at the front of the cell. Behind the leading edge, however, fibroblasts exert large, inward directed forces, throughout the entire cell, that are oriented perpendicular to the peripheral contour of the cell. The differences in magnitude of these traction forces reflect the differences in cell-substratum adhesiveness among the cell types. The force required to overcome viscous drag on a migrating cell is about 3×10^{-13} N (Lee et al., 1994), much lower than the contractile force exerted by any cell type. The large contractile forces are instead required to facilitate detachment of cell-substratum adhesions. As mentioned above, the linkage can be disrupted either between the ECM ligand and adhesion receptor or between intracellular cytoskeletal bonds. As the force on a bond increases, the probability of bond dissociation increases (Alon et al., 1995). The differences in the direction of exerted traction forces in fibroblasts and keratocytes possibly reflects the differences in coordination between extension and retraction in keratocytes and fibroblasts. Keratocytes must be very coordinated and move very quickly while fibroblasts do not need to move as quickly but must be able to generate larger forces for processes such as wound retraction.

Contractile forces serve not only to disrupt cell-substratum linkages during migration; but they also function to strengthen their interactions with cytoskeletal elements. Application of mechanical stress through integrins increases cytoskeletal stiffness proportionally with the applied stress (Wang et al., 1993). The stiffening requires an intact cellular architecture of actin filaments, microtubules, and intermediate filaments, suggesting that structural rearrangement of the cytoskeleton contributes to the mechanically induced stiffening (Wang and Ingber, 1994). Using a laser optical trap to exert forces on fibronectin-coated beads on a cell surface, Choquet et al. (1997)

also demonstrated that reinforcement of integrin-cytoskeletal linkages is proportional to the applied force. The linkage strengthening requires occupancy of the ligand-binding site and is inhibited by a phosphatase inhibitor. This phenomenon may be involved in cell guidance since linkages on rigid substrates will be stronger than linkages on compliant substrates, steering cells toward rigidity (Choquet et al., 1997). Mechanical forces applied to integrins can also induce biochemical signals. Stressing the $\alpha2$ or $\beta1$ subunit induces tyrosine phosphorylation of MAP kinases in an osteosarcoma cell line (Schmidt et al., 1998). Contractility can affect matrix proteins as well as integrins. For example, mechanically stretching fibronectin can expose cryptic sites which induce fibronectin matrix assembly (Zhong et al., 1998).

Cell migration requires that the intracellularly generated forces be transmitted to the substratum in a spatially asymmetric manner (Lauffenburger and Horwitz, 1996; Sheetz, 1994). This front vs. rear asymmetry in contractility or cell-substratum adhesiveness can be satisfied in a number of ways. The spatial distribution of adhesion receptors may lead to higher adhesiveness or reduced transmission of contractile forces at the cell front than at the cell rear. The triangular shape of many cells, with more contact area at the cell front than rear, may produce such a polarity. Asymmetries in adhesion receptor-ECM ligand affinity could also result in an adhesive gradient in the cell. As discussed above, locking integrins in a high-affinity state inhibits eosinophil migration (Kuijpers et al., 1993); this could be due to a superoptimal overall adhesiveness or loss of front-versus-rear gradient in adhesiveness. Also, locking $\beta2$ integrin in a high-affinity conformation for ICAM prevents lymphocyte locomotion (Dustin et al., 1997). Adhesion receptor-cytoskeleton linkage avidity appears to exhibit a spatial asymmetry in the cell; integrin linkages to the cytoskeleton in migrating NIH 3T3 fibroblasts are more prevalent in the cell front than at the cell rear (Schmidt et al., 1993). Spatial concentrations of signaling molecules may also contribute to the asymmetry. For example, intracellular Ca^{+2} or phophoinositide levels may regulate contractile forces or the strength of adhesive linkages. In migrating leukocytes, calcium concentration, and myosin-II based contractility, increases from the front to rear of the cell (Hahn et al., 1992). Also, intracellular calcium transients are required for detachment of the cell rear during neutrophil migration (Maxfield, 1993). Kinases and/or phosphatases may regulate the activity or affinity of adhesion complex components.

Contractility and adhesiveness must cooperate during the rear retraction phase of migration so that the front of the cell remains anchored while the rear detaches from the substratum. According to a theoretical model for migration (DiMilla et al., 1991) the magnitude of the front vs. rear asymmetry governs the ranges of contractile forces and cell-substratum adhesiveness promoting locomotion. Cells with a large asymmetry are predicted to exhibit migration over a wide range of adhesiveness while cells with a low asymmetry are predicted to migrate only over a narrow range of adhesiveness. Therefore, adhesive and contractile asymmetries are candidates for

explaining why some cell types (e.g. neutrophils) are able to migrate through many different environments while others (e.g. fibroblasts) only migrate under more specific conditions.

1.5 Regulation of Migration by Cell-Substratum Adhesiveness

As discussed above, the major function of cell substrate adhesion is to generate the traction required for translocation of the cell cortex; consequently, the adhesive strength between a cell and its substratum affects migration speed (see Figure 1.4). At low adhesiveness sufficient traction cannot be generated with the substrate to efficiently move the cell while at high adhesiveness the cell cannot generate enough contractile force to fracture attachments at the rear. At intermediate adhesiveness the cell can both efficiently form new attachments at the front and release attachments at the rear. A quantitative model of cell migration confirms this simple analysis and suggests principles governing the dependence of cell migration speed on integrin-ECM ligand binding and cell mechanical properties (DiMilla et al., 1991). In this model, maximum migration speed occurs at an intermediate ratio of cell-substratum adhesiveness to intracellular contractile force. Considerable experimental evidence in many different cell systems supports the prediction that cell-substratum adhesiveness regulates cell migration speed, which is maximal at intermediate adhesiveness. Cell-substratum adhesiveness can be altered in many ways, including changes in ECM protein composition or concentration, integrin expression levels or spatial distribution, integrin-ligand affinity, cytoskeletal protein expression, or integrin-cytoskeletal affinity.

Human smooth muscle cells and murine myoblasts migrate maximally at intermediate concentrations of fibronectin and collagen, and laminin respectively (DiMilla et al., 1993; Goodman et al., 1989). Tenascin enhances glioma cell migration on fibronectin substrates presumably by modulating cell-substratum adhesiveness (Deryugina and Bourdon, 1996) through interactions with the cell-surface receptor annexin II (Chung et al., 1996). Furthermore, addition of fibronectin to collagen type I gels inhibits migration of polymorphonuclear leukocytes through the gels due to increased cell adhesion (Kuntz and Saltzman, 1997).

Changes in adhesion receptor expression can also have varied effects on cell migration. Cell speed is maximal on collagen at intermediate levels of $\alpha2$ integrin subunit expression (Keely et al, 1995) and on fibronectin at intermediate levels of $\alpha5\beta1$ expression (Giancotti and Ruoslahti, 1990; Bauer et al., 1992). Expression of $\alpha2\beta1$ can either increase or decrease tumor cell motility, both in vitro and in vivo, by altering cell-substratum adhesiveness (Ho et al., 1997). Neurons can actually modulate expression of $\alpha6\beta1$ integrin based on laminin concentration (Condic and Letourneau, 1997). At low laminin levels, $\alpha6\beta1$ integrin expression and cell adhesiveness increases. allowing the neurite to continue growing. This integrin regulation may allow the growth

24

Goodman et al., 1989). Tenascin enhances glioma cell migration on fibronectin substrates presumably by modulating cell-substratum adhesiveness (Deryugina and Bourdon, 1996) through interactions with the cell-surface receptor annexin II (Chung et al., 1996). Furthermore, addition of fibronectin to collagen type I gels inhibits migration of polymorphonuclear leukocytes through the gels due to increased cell adhesion (Kuntz and Saltzman, 1997).

Changes in adhesion receptor expression can also have varied effects on cell migration. Cell speed is maximal on collagen at intermediate levels of $\alpha 2$ integrin subunit expression (Keely et al, 1995) and on fibronectin at intermediate levels of $\alpha 5 \beta 1$ expression (Giancotti and Ruoslahti, 1990; Bauer et al., 1992). Expression of $\alpha 2 \beta 1$ can either increase or decrease tumor cell motility, both in vitro and in vivo, by altering cell-substratum adhesiveness (Ho et al., 1997). Neurons can actually modulate expression of $\alpha 6 \beta 1$ integrin based on laminin concentration (Condic and Letourneau, 1997). At low laminin levels, $\alpha 6 \beta 1$ integrin expression and cell adhesiveness increases, allowing the neurite to continue growing. This integrin regulation may allow the growth cone to respond to its environment and maintain a constant rate of motility over a variety of laminin concentrations.

Other receptors may interact with integrins to regulate integrin function and also promote adhesion and migration. For example, the urokinase-type plasminogen activator receptor (uPAR) interacts with $\alpha v \beta 3$ integrin in human embryonic kidney 293 cells to enhance adhesion and migration on vitronectin (Chapman, 1997; Wei et al., 1996). Likewise, plasminogen activator inhibitors can promote cell motility by blocking cell adhesion (Waltz et al., 1997). uPAR association with $\alpha x \beta 2$ oscillates with time and this signal may coordinate proteolysis, cell adhesion, and cell migration (Kindzelskii et al., 1997).

Changes in cytoskeletal protein expression also lead to changes in cell adhesion and migration. A decrease in vinculin or α-actinin expression in 3T3 cells increases motility (Fernandez et al., 1993; Gluck and Ben-Ze'ev, 1994) while a decrease in vinculin expression in PC12 cells diminishes neurite outgrowth by decreasing lamellipod stability (Varnum-Finney and Reichardt, 1994).

Integrin-ECM ligand affinity also regulates cell adhesion and migration. Integrins may be activated into a high affinity state by cytoplasmic domain alterations in either the α or β chains which presumably disrupt specific interactions between the α and β subunits (Hughes et al., 1996). Integrins may also be activated by specific antibodies which alter integrin conformation (Frelinger et al., 1991). CHO cells transfected with $\alpha IIb \beta 3$ integrin migrate maximally on intermediate concentrations of fibrinogen, with the concentration promoting maximum migration decreasing as $\alpha IIb \beta 3$/fibrinogen affinity increases (Huttenlocher et al., 1996). Neural crest cells are able to form focal adhesions and migrate on antibodies to the $\beta 1$ integrin subunit (Duband et al., 1991). The antibody concentration required for optimal cell migration cells is lower for cells

25

on high-avidity polyclonal antibodies than for cells on lower avidity monoclonal antibodies. CC chemokines can affect monocyte cell speed on fibronectin by transiently regulating $\alpha4\beta1$ and $\alpha5\beta1$ integrin avidity, and thus altering cell adhesiveness (Weber et al., 1996).

Altered integrin-cytoskeleton interactions can result in altered cell-substratum adhesion and motility. CHO cells transfected with different $\alpha4$ cytoplasmic domain chimeras demonstrate a maximum in migration speed at an intermediate adhesiveness (Kassner et al., 1995). The A and B variants of $\alpha6\beta1$ integrin stimulate adhesion and maximum migration speed at different laminin concentrations (Shaw and Mercurio, 1994). Expression of the $\beta1B$ isoform reduces cell motility through cell adhesiveness with respect to $\beta1A$ since $\beta1B$ does not localize to focal adhesion sites (Balzac et al., 1994). $\beta1$-$\beta5$ integrin chimeras demonstrate that preventing integrin localization to focal adhesions can enhance cell speed under certain conditions (Pasqualini and Hemler, 1994). Truncation of the $\beta3$ cytoplasmic domain alters integrin-cytoskeletal interactions and inhibits focal adhesion formation (Huttenlocher et al., 1996). CHO cells transfected with this variant show maximum motility at higher fibrinogen concentrations than wild-type cells. Maximum migration speed does not change in a random migration assay but haptotaxis is inhibited in the truncation mutant. These results suggest that haptotaxis may be regulated differently than random motility.

Transmembrane or secreted matrix metalloproteinases (MMPs) are also involved in regulation of cell migration. For example, integrin signaling induces expression of collagenases in fibroblasts, keratinocytes, and melanoma cells (Werb et al., 1989; Larjava et al., 1993; Seftor et al., 1993). Expression of Kuzbanian, metalloproteinase/disintegrin of the ADAM family, is required for axonal extension in Drosophila (Fambrough et al., 1996). Matrix metalloproteinase MMP-2 can directly bind $\alpha v\beta3$ integrin in angiogenic blood vessels and melanoma cells in vivo (Brooks et al., 1996; Deryugina et al., 1997). Clustering CD3 and $\alpha L\beta2$, $\alpha4\beta1$, or $\alpha5\beta1$ integrin in T lymphocytes leads to induction of uPAR transcription and translation (Bianchi et al., 1996). These proteinases can regulate cell locomotion by a number of different mechanisms. At the cell leading edge they can degrade the matrix, reducing the force required to extend membrane protrusions through the surrounding environment. At the cell rear the matrix-degradation activity of MMPs may disrupt cell/substratum bonds, thereby decreasing cell/substratum adhesiveness. Intracellular proteases such as calpain can affect adhesion by modifying integrin-cytoskeleton linkages. Calpain can stimulate initial lymphocyte adhesion strengthening by increasing $\alpha L\beta2$ integrin mobility (Stewart et al., 1998) but may decrease adhesion at later stages by cleaving integrin-cytoskeleton linkages (Huttenlocher et al., 1997). Intracellular calcium buffering inhibits rear retraction in neutrophils migrating through three-dimensional amnion matrices (Mandeville and Maxfield, 1997), possibly by inhibiting calpain activity. Calpain may also allow cell spreading by promoting cytoskeletal remodeling at the front of the cell (Potter et al., 1998). Understanding how these very complicated proteinases help govern migration will require devotion of quantitative and

model has not been rigorously tested by varying several cell-substratum binding parameters and measuring the corresponding effects on cell speed and adhesiveness. We have developed a Chinese Hamster Ovary (CHO) cell system which we use to vary integrin expression, extracellular matrix ligand concentration, and integrin-ligand affinity. Quantitative measurements of cell speed are related to quantitative measurements of cell-substratum adhesiveness as these three cell-substratum binding parameters change. Thus, we determined cell-substratum binding regulates migration speed through cell adhesiveness.

Next, we sought to determine some of the molecular mechanisms which may be responsible for regulating cell speed through adhesiveness. Due to a lack of understanding of the factors which regulate cell-substratum detachment, we investigated how varying cell-substratum binding parameters affects cytoskeleton-integrin-ECM linkage fracture. Previous experiments have demonstrated that in certain circumstances the integrin-cytoskeleton bond can rupture while in other circumstances the integrin-ECM bond dissociates. We measured the amount of integrin which rips from the rear of migrating CHO cells as we vary integrin expression, ECM concentration, and integrin-ECM affinity. From these experiments we can determine which bond in the linkage is a more appropriate target for regulation of cell speed at different experimental conditions.

Regulation of the integrin-cytoskeletal bond is likely to occur by biochemical as well as biophysical means. To explore one possible biochemical mechanism of regulation of this linkage we examined the role of calpain in allowing cell-substratum detachment. Measurements of cell detachment rate and integrin-cytoskeleton bond dissociation probability suggest that calpain activity can allow rear retraction by weakening integrin-cytoskeleton linkages.

We constructed a mathematical model of cell-substratum detachment at the rear of a migrating cell. This model predicts retraction rate and the amount of integrin which the cell releases as a function of kinetic binding parameters and force transmission within the cytoskeleton-integrin-ECM linkages. 2 distinct phenotypes of rear release occur in the model. In one, release is rapid and limited by the rate of integrin-ligand dissociation and in the other release is slow and rate-limited by cleavage of cytoskeleton-integrin bonds. We predict that detachment phenotype can be determined by the fraction of integrin which is extracted from the cell membrane during rear retraction.

1.7 Implications of Thesis Work

The experimental and theoretical work outlined in this thesis has expanded our knowledge on the fundamental processes which comprise cell motility. Specifically, we now have a better scientific understanding of how adhesion receptor interactions with both the ECM and the cytoskeleton can impact migration speed. We have also illustrated the conditions where each of

these interactions is important. For example, at high adhesiveness release of adhesions at the cell rear limits cell speed but at low adhesiveness other factors are rate-limiting. Therefore, targeting rear release is an effective method for altering cell speed only at high adhesiveness. We have also characterized both extracellular and intracellular biophysical and biochemical process which affect migration. Increasing integrin-receptor binding can have very different effects than strengthening integrin-cytoskeleton interactions.

This increased understanding of the role of cell-substratum linkages in cell migration also has implications on technological applications. In some applications control of extracellular parameters is advantageous while in other applications affecting intracellular molecular interactions may be a better option. For example, in tissue engineering design we can choose or modify biomaterials while the cell type we require may be more rigid. In pharmaceutical design, however, modifying intracellular interactions in the cytoskeleton or in signal transduction pathways may be more specific than targeting the extracellular environment. This work, along with other studies, has established some of the design parameters for biomaterials We know that changing the ligand type or density on a material will alter cell speed in a manner related to cell substratum adhesiveness. By identifying and characterizing targets for pharmacological intervention, this work also has aided pharmaceutical design to either enhance or inhibit cell migration. We can inhibit migration of adherent cells by inhibiting calpain activity in the cells, or by other methods which strengthen integrin-cytoskeleton linkages. The integrin-ECM bond can also be an important intervention target and will yield different results than varying integrin-cytoskeleton binding.

1.8   References

Abercrombie, M., Heaysman, J. E. M., and Pegrun, S. M. (1970). The locomotion of fibroblasts in culture. I. Movements of the leading edge. *Exp. Cell Res.* **59**, 393-398.

Alon, R., Hammer, D. A., and Springer, T. A. (1995). Lifetime of the P-selectin-carbohydrate bond and its response to tensile force in hydrodynamic flow. *Nature.* **374**, 539-542.

Altun-Gultekin, Z. F., and Wagner, J. A. (1996). Src, ras, and rac mediate the migratory response elicited by NGF and PMA in PC12 cells. *J. Neurosci. Res.* **44**, 308-327.

Balzac, F., Retta, S. F., Albini, A., Melchiorri, A., Koteliansky, V. E., Geuna, M., Silengo, L., and Tarone, G. (1994). Expression of β1B integrin isoform in CHO cells results in a dominant negative effect on cell adhesion and motility. *J. Cell Biol.* **127**, 557-565,

Bard, J. B. L., and Hay, E. D. (1975). The behavior of fibroblasts from the developing avian cornea. *J. Cell Biol.* **67**, 400-418.

Bassell, G., and Singer, R. H. (1997). mRNA and cytoskeletal filaments. *Curr. Opin. Cell Biol.* **9**, 109-115.

Bauer, J. S., Schreiner, C., Giancotti, F. G., Ruoslahti, E., and Juliano, R. L. (1992). Motility of fibronectin receptor-deficient cells on fibronectin and vitronectin: collaborative interactions among integrins. *J. Cell Biol.* **116**, 477-487.

Beckerle, M. C., Burridge, K., DeMartino, G. N., and Croall, D. E. (1987). Colocalization of calcium-dependent protease II and one of its substrates at sites of cell adhesion. *Cell.* **51**, 569-577.

Bianchi, E., Ferrero, E., Fazioli, F., Mangili, F., Wang, J., Bender, J. R., Blasi, F., and Pardi, R. (1996). Integrin-dependent induction of functional urokinase receptors in primary T lymphocytes. *J. Clin. Invest.* **98**, 1133-1141.

Bretscher, M. S. (1996). Getting membrane flow and the cytoskeleton to cooperate in moving cells. *Cell.* **87**, 601-606.

Bretscher, M. S. (1989). Endocytosis and recycling of the fibronectin receptor in CHO cells. *EMBO J.* **8**, 1341-1348.

Brooks, P. C., Stromblad, S., Sanders, L. C., von Schalscha, T. L., Aimes, R. T., Stetler-Stevenson, W. G., Quigley, J. P., and Cheresh, D. A. (1996). Localization of matrix metalloproteinase MMP-2 to the surface of invasive cells by interaction with integrin $\alpha v \beta 3$. *Cell.* **85**, 683-693.

Brundage, R. A., Fogarty, K. E., Tuft, R. A., and Fay, F. S. (1991). Calcium gradients underlying polarization and chemotaxis of eosinophils. *Science.* **254**, 703-706.

Buck, C. A., and Horwitz, A. F. (1987). Integrin, a transmembrane glycoprotein complex mediating cell-substratum adhesion. *J. Cell Sci. Suppl.* **8**, 231-250.

Burridge, K., Fath, K., Kelly, T., Nuckolls, G., and Turner, C. (1988). Focal adhesions: transmembrane junctions between the extracellular matrix and the cytoskeleton. *Annu. Rev. Cell Biol.* **4**, 487-525.

Burridge, K., Turner, C. E., and Romer, L. H. (1992). Tyrosine phosphorylation of paxillin and pp125FAK accompanies cell adhesion to extracellular matrix: a role in cytoskeletal assembly. *J. Cell Biol.* **119**, 893-903.

Burridge, K., Chrzanowska-Wodnicka, M., and Cuiling, Z. (1997). Focal adhesion assembly. *Trends Cell Biol.* **7**, 342-347.

Cary, L. A., Chang, J. F., and Guan, J. L. (1996). Stimulation of cell migration by overexpression of focal adhesion kinase and its association with Src and Fyn. *J. Cell Sci.* **109**, 1787-1794.

Chapman, H. A. (1997). Plasminogen activators, integrins, and the coordinated regulation of cell adhesion and migration. *Curr. Opin. Cell Biol.* **9**, 714-724.

Chen, P., Xie, H., Sekar, M. C., Gupta, K., and Wells, A. (1994). Epidermal growth factor receptor-mediated cell motility: phospholipase C activity is required, but mitogen-activated protein kinase activity is not sufficient for induced cell movement. *J. Cell Biol.* **127**, 847-857.

Chen, P., Murphy-Ullrich, J. E., and Wells, A. (1996). A role for gelsolin in actuating epidermal growth factor receptor-mediated cell motility. *J. Cell Biol.* **134**, 689-698.

Chen, W. -T. (1981). Mechanism of retraction of the trailing edge during fibroblast movement. *J. Cell Biol.* **90**, 187-200.

Chong, L. D., Traynor-Kaplan, A., Bokoch, G. M., and Schwartz, M. A. (1994). The small GTP-binding protein rho regulates a phosphatidylinositol 4-phosphate 5-kinase in mammalian cells. *Cell.* **79**, 507-513.

Choquet, D., Felsenfeld, D. P., and Sheetz, M. P. (1997). Extracellular matrix rigidity causes strengthening of integrin-cytoskeleton linkages. *Cell.* **88**, 39-41.

Chrzanowska-Wodnicka, M., and Burridge, K. (1996). Rho-stimulated contractility drives the formation of stress fibers and focal adhesions. *J. Cell Biol.* **133**, 1403-1415.

Chung, C. Y., Murphy-Ullrich, J. E., and Erickson, H. P. (1996). Mitogenesis, cell migration, and loss of focal adhesions induced by tenascin-C interacting with its cell surface receptor, annexin II. *Mol. Biol. Cell.* **7**, 883-892.

Cima, L. G. and Langer, R. (1993). Engineering human tissue. *Chem. Eng. Progr.* June, 46-54.

Condeelis, J. (1993). Life at the leading edge. *Annu. Rev. Cell Biol.* **9**, 411-444.

Condic, M. L., and Letourneau, P. C. (1997). Ligand-induced changes in integrin expression regulate neuronal adhesion and neural outgrowth. *Nature.*, 852-856.

Conrad, P. A., Giuliano, K. A., Fisher, G., Collins, K., Matsudaira, P. T., and Taylor, D. L. (1993). Relative distribution of actin, myosin I, and myosin II during the wound healing response of fibroblasts. *J. Cell Biol.* **120**, 1381-1391.

Cooray, P., Yuan, Y., Schoenwaelder, S. M., Mitchell, C. A., Salem, H. H., and Jackson, S. P. (1996). Focal adhesion kinase (pp125Fak) cleavage and regulation by calpain. *Biochem. J.* **318**, 41-47.

Craig, S. W. and Johnson, R. P. (1996). Assembly of focal adhesions: progress, paradigms, and portents. *Curr. Opin. Cell Biol.* **8**, 74-85.

Cramer, L. P., Siebert, M., and Mitchison, T. J. (1997). Identification of novel graded polarity actin filament bundles in locomoting heart fibroblasts: implications for the generation of motile force. *J. Cell Biol.* **136**, 1287-1305.

Crowley, E., and Horwitz, A. F. (1995). Tyrosine phosphorylation and cytoskeletal tension regulate the release of fibroblast adhesions. *J. Cell Biol.* **131**, 525-537.

Deryugina, E. I., and Bourdon, M. A. (1996). Tenascin mediates human glioma cell migration and modulates cell migration on fibronectin. *J. Cell Sci.* **109**, 643-652.

Deryugina, E. I., Bourdon, M. A., Luo, G. X., Reisfeld, R. A., and Strongin, A. (1997). Matrix metalloproteinase-2 activation modulates glioma cell migration. *J. Cell Sci.* **110**, 2473-2482.

DiMilla, P. A., Barbee, K., and Lauffenburger, D. A. (1991). Mathematical model for the effects of adhesion and mechanics on cell migration speed. *Biophys. J.* **60**, 15-37.

DiMilla, P. A., Stone, J. A., Quinn, J. A., Albeda, S. M., and Lauffenburger, D. A. (1993). Maximal migration of human smooth muscle cells on fibronectin and type IV collagen occurs at an intermediate attachment strength. *J. Cell Biol.* **122**, 729-737.

Du, X., Saido, T. C., Tsubuki, S., Indig, F. E., Williams, M. J., and Ginsberg, M. H. (1996). Calpain cleavage of the cytoplasmic domain of the integrin β3 subunit. *J. Biol. Chem.* **270**, 26146-26151.

Duband, J. L., Dufour, S., Yamada, S. S., Yamada, K. M., and Thiery, J. P. (1991). Neural crest cell locomotion induced by antibodies to β1 integrins. A tool for studying the roles of substratum molecular avidity and density in migration. *J. Cell Sci.* **98**, 517-532.

Dustin, M. L., Bromley, S. K., Kan, Z., Peterson, D. A., and Unanue, E. R. (1997). Antigen receptor engagement delivers a stop signal to migrating T lymphocytes. *Proc. Natl. Acad. Sci. USA.* **94**, 3909-3913.

Fambrough, D., Pan, D., Rubin, G. M., and Goodman, C. S. (1996). The cell surface metalloprotease/disintegrin Kuzbanian is required for axonal extension in Drosophila. *Proc. Natl. Acad. Sci. USA.* **93**, 13233-13238.

Felder, S., and Elson, E. L. (1990). Mechanics of fibroblast locomotion: quantitative analysis of forces and motions at the leading lamellas of fibroblasts. *J. Cell Biol.* **111**, 2527-2536.

Felsenfeld, D. P., Choquet, D., and Sheetz, M. P. (1996). Ligand binding regulates the directed movement of β1 integrins on fibroblasts. *Nature.* **383**, 438-440.

Fernandez, J. L. R., Geiger, B., Salomon, D., and Ben-Ze'ev, A. (1993). Suppression of vinculin expression by antisense transfection confers changes in cell morphology, motility, and anchorage-dependent growth of 3T3 cells. *J. Cell. Biol.* **122**, 1285-1294.

Frelinger, A. L., Du, X., Plow, E. F., and Ginsberg, M. H. (1991). Monoclonal antibodies to ligand-occupied conformer of integrin αIIbβ3 (glycoprotein IIb-IIa) alter receptor affinity, specificity and function. *J. Biol. Chem.* **266**, 17106-17111.

Gailit, J., and Clark, R. A. F. (1994). Wound repair in the context of extracellular matrix. *Curr Opin. Cell Biol.* **6**, 717-725.

Galbraith, C. G., and Sheetz, M. P. (1997). A micromachined device provides a new bend on fibroblast traction forces. *Proc. Natl. Acad. Sci, USA.* **94**, 9114-9118.

Giancotti, F. G., and Ruoslahti, E. (1990). Elevated levels of the α5β1 fibronectin receptor suppress the transformed phenotype of Chinese hamster ovary cells. *Cell.* **60**, 849-859.

Giancotti, F. G., and Mainiero, F. (1994). Integrin-mediated adhesion and signaling in tumorigenesis. *Biochim. Biophys.* **1198**, 47-64.

Gilmore, A. P., and Burridge, K. (1996). Regulation of vinculin binding to talin and actin by phosphatidyl-inositol-4-5-bisphosphate. *Nature.* **381**, 531-535.

Gilmore, A. P. and Romer, L. H. (1996). Inhibition of focal adhesion kinase (FAK) signaling in focal adhesions decreases cell motility and proliferation. *Mol. Biol. Cell.* **7**, 1209-1224.

Gluck, U., and Ben-Ze'ev, A. (1994). Modulation of α-actinin levels affects cell motility and confers tumorigenicity on 3T3 cells. *J. Cell Sci.* **107**, 1773-1782.

Goodman, S. L., Risse, G., and von der Mark, K. (1989). The E8 subfragment of laminin promotes locomotion of myoblasts over extracellular matrix. *J. Cell Biol.* **109**, 799-809.

Hahn, K., DeBiasio, R., and Taylor, D. L. (1992). Patterns of elevated free calcium and calcineurin activation in living cells. *Nature.* **359**, 736-738.

Harrington, E. O., Loffler, J., Nelson, P. R., Kent, K. C., Simons, M., and Ware, J. A. (1997). Enhancement of migration by protein kinase Cα and inhibition of proliferation and cell cycle progression by protein kinase Cδ in capillary endothelial cells. *J. Biol. Chem.* **272**, 7390-7397.

Harris, A. K., Wild, P., and Stopak, D. (1980). Silicone rubber substrata: a new wrinkle in the study of cell locomotion. *Science.* **208**, 177-179.

Hartwig, J. H., Bokoch, G. M., Carpenter, C. L., Janmey, P. A., Taylor, L. A., Toker, A., and Stossel, T. P. (1995). Thrombin receptor ligation and activated rac uncap actin filament barbed ends through phosphoinositide synthesis in permeabilized human platelets. *Cell.* **82**, 643-653.

Hawkins, P. T., Equinoa, A., Qui, R.-G., Stokoe, D., Cooke, F. T., Walters, R., Wennstrom, S., Claesson-Welsh, L., Evans, T., Symons, M., and Stephens, L. (1995). PDGF stimulates and increase in GTP-rac via activation of phosphoinositide 3-kinase. *Curr. Biol.* **5**, 393-403.

Hay, E. D. (1985). Interaction of migrating embryonic cells with extracellular matrix. *Exp. Biol. Med.* **10**, 174-193.

Heidemann, S. R., and Buxbaum, R. E. (1998). Cell crawling: first the motor, now the transmission. *J. Cell Biol.* **141**, 1-4

Hendey, B., Klee, C. B., and Maxfield, F. R. (1992). Inhibition of neutrophil chemotaxis on vitronectin by inhibitors of calcineurin. *Science.* **258**, 296-299.

Hirao, M., Sato, N., Kondo, T., Yonemura, S., Monden, M., Sasaki, T., Takai, Y., Tsukita, Sh., and Tsukita, Sa. (1996). Regulation mechanism of ERM protein/plasma membrane association: possible involvement of phosphatidylinositol turnover and rho-dependent signaling pathway. *J. Cell Biol.* **135**, 37-52.

Ho, W., Heinemann, C., Hangan, D., Uniyal, S., Morris, V. L., and Chan, B. M. C. (1997). Modulation of in vivo migratory function of α2β1 integrin in mouse liver. *Mol. Biol. Cell.* **8**, 1863-1875.

Hogg, N., R. C. Landis, P. A. Bates, P. Stanley, and Randi, A. M. (1994). The sticking point: how integrins bind to their ligands. *Trends Cell Biol.* **4**, 379-382.

Horwitz, A., K. Duggan, C. Buck, M. C. Beckerle, and Burridge, K. (1986). Interaction of plasma membrane fibronectin receptor with talin. A transmembrane linkage. *Nature.* **320**, 531-532.

Hughes, P. E., Diaz-Gonzalez, F., Leong, L., Wu, C., McDonald, J. A., Shattil, S., and Ginsberg, M. H. (1996). Breaking the integrin hinge: a defined structural constraint regulates integrin signaling. *J. Biol. Chem.* **271**, 6571-6574.

Huttenlocher, A, Ginsberg, M. H., and Horwitz, A. F. (1996). Modulation of cell migration by integrin-mediated cytoskeletal linkages and ligand-binding affinity. *J. Cell Biol.* **134**, 1551-1562.

Huttenlocher, A., Palecek, S. P., Lu, Q., Zhang, W., Mellgren, R. L., Lauffenburger, D. A., Ginsberg, M. H., and Horwitz, A. F. (1997). Regulation of cell migration by the calcium-dependent protease calpain. *J. Biol. Chem.* **272**, 32719-32722.

Hynes, R. O. (1992). Integrins: versatility, modulation, and signaling in cell adhesion. *Cell.* **69**, 11-25.

Hynes, R. O. (1987). Integrins: a family of cell surface receptors. *Cell.* **48**, 549-554.

Ilic, D., Furuta, Y., Kanazawa, S., Takeda, N., Sobue, K., Nakatsuji, N., Nomura, S., Fujimoto, J., Okada, M., Yamamoto, T., and Aizawa, S. (1995). Reduced cell motility and enhanced focal adhesion contact formation in cells from FAK-deficient mice. *Nature.* **377**, 539-544.

Jay, P. Y., Pham, P. A., Wong, S. A., and Elson, E. L. (1995). A mechanical function of myosin II in cell motility. *J. Cell Sci.* **108**, 387-393.

Kassner, P. D., Alon, R., Springer, T. A., and Hemler, M. E. (1995). Specialized functional properties of the integrin α_4 cytoplasmic domain. *Mol. Biol. Cell.* **6**, 661-674.

Keely, P. J., Fong, A. M., Zutter, M. M., and Santoro, S. A. (1995). Alteration of collagen-dependent adhesion, motility, and morphogenesis by the expression of antisense $\alpha2$ integrin mRNA in mammary cells. *J. Cell Sci.* **108**, 595-607.

Keely, P., Parise, L., and Juliano, R. (1998). Integrins and GTPases in tumor cell growth, motility, and invasion. *Trends Cell Biol.* **8**, 101-106.

Kindzelskii, A. L., Eszes, M. M., Todd, R. F., and Petty, H. R. (1997). Proximity oscillations of complement type 4 ($\alpha x \beta 2$) and urokinase receptors on migrating neutrophils. *Biophys. J.* **73**, 1777-1784.

Kislauskis, E. H., Zhu, X-C., and Singer, R. H. (1997). β-actin messenger RNA localization and protein synthesis augment cell motility. *J. Cell Biol.* **136**, 1263-1270.

Klemke, R. L., Cai, S., Giannini, A. L., Gallagher, P. J., de Lanerolle, P., and Cheresh, D. A. (1997). Regulation of cell motility by mitogen-activated protein kinase. *J. Cell Biol.* **137**, 481-492.

Klemke, R. L., Leng, J., Molander, R., Brooks, P. C., Vuori, K., and Cheresh, D. A. (1998). CAS/Crk coupling serves as a "molecular switch" for induction of cell migration. *J. Cell Biol.* **140**, 961-972.

Kovacsovics, T. J., Bachelot, C., Toker, A., Viahos, C. J., Duckworth, B., Cantley, L. C., and Hartwig, J. H. (1995). Phosphoinositide 3-kinase inhibition spares actin assembly in activating platelets but reverses platelet aggregation. *J. Biol. Chem.* **270**, 11358-11366.

Kozma, R., Ahmed, S., Best, A., and Lim, L. (1995). The ras-related protein cdc42Hs and bradykinin promote formation of peripheral actin microspikes and filopodia in Swiss 3T3 fibroblasts. *Mol. Cell. Biol.* **15**, 1942-1952.

Kuijpers, T. W., Mul, E. P. J., Blom, M., Kovach, N. L., Gaeta, F. C. A., Tollefson, V., Elices, M. J., and Harlan, J. M. (1993). Freezing adhesion molecules in a state of high-avidity binding blocks eosinophil migration. *J. Exp. Med.* **178**, 279-284.

Kumagai, N., Morii, N., Fujisawa, K., Nemoto, Y., and Narumiya, S. (1993). ADP-ribosylation of rho p21 inhibits lysophosphatidic acid-induced protein tyrosine phosphorylation and phosphatidylinositol 3-kinase activation in cultured Swiss 3T3 cells. *J. Biol. Chem.* **268**, 24535-24538.

Kundra, V., Escodedo, J. A., Kaziauskas, A., Kim, H. K., Rhee, S. G., Williams, L. T., and Zetter, B. R. (1994). Regulation of chemotaxis by the platelet-derived growth factor receptor-β. *Nature.* **367**, 474-476.

Kuntz, R. M., and Saltzman, W. M. (1997). Neutrophil motility in extracellular matrix gels: mesh size and adhesion affect speed of migration. *Biophys. J.* **72**, 1472-1480.

Larjava, H., Lyons, J. G., Salo, T., Makela, M., Koivisto, L., Birkedal-Hansen, H., Akiyama, S. K., Yamada, K. M., and Heino, J. (1993). Anti-integrin antibodies induce type IV collagenase expression in keratinocytes. *J. Cell. Physiol.* **157**, 190-200.

Lauffenburger, D. A. and Horwitz, A. F. (1996). Cell migration: a physically integrated molecular process. *Cell.* **84**, 359-369.

Lawson, M. A., and Maxfield, F. R. (1995). Ca^{2+}-and calcineurin-dependent recycling of an integrin to the front of migrating neutrophils. *Nature.* **377**, 75-79.

Lee, J., Leonard, M., Oliver, T., Ishihara, A., and Jacobson, K. (1994). Traction forces generated by locomoting keratocytes. *J. Cell Biol.* **127**, 1957-1964.

Machesky, L. M., and Hall, A. (1996). Rho: a connection between membrane signalling and the cytoskeleton. *Trends Cell Biol.* **6**, 304-310.

Mandeville, J. T. and Maxfield, F. R. (1997) Effects of buffering intracellular free calcium on neutrophil migration through three-dimensional matrices. *J. Cell. Physiol.* **171**, 168-178.

Maxfield, F. R. (1993). Regulation of leukocyte locomotion by Ca^{2+}. *Trends Cell Biol.* **3**, 386-391.

Meredith, J. E. and Schwartz, M. A. (1997). Integrins, adhesion, and apoptosis. *Trends Cell Biol.* **7**, 146-150.

Michiels, F., Habets, G. G. M., Stam, J. C., van der Kammer, R. A., and Collard, J. G. (1995). A role for rac in tiam1-induced membrane ruffling and invasion. *Nature.* **375**, 338-340.

Mitchison, T. J., and Cramer, L. P. (1996). Actin-based cell motility and cell locomotion. *Cell.* **84**, 371-379.

Miura, Y., Kikuchi, A., Musha, T., Kuroda, S., Yaku, H., Sasaki, T., and Takai, Y. (1993). Regulation of morphology by rho p21 and its inhibitory GDP/GTP exchange protein (rho GDI) in Swiss 3T3 cells. *J. Biol. Chem.* **268**, 510-515.

Nakanishi, H., Brewer, K. A., and Exton, J. H. (1993). Activation of the ζ isozyme of protein kinase C by phosphatidylinositol 3,4,5-triphosphate. *J. Biol. Chem.* **268**, 13-16.

Niggimann, B., Maaser, K., Lu, H., Kroczek, R., Zanker, K. S., and Friedl, P. (1997). Locomotory phenotypes of human tumor cell lines and T lymphocytes in a three-dimensional collagen lattice. *Cancer Lett.* **118**, 173-180.

Niggli, V., Andreoli, C., Roy, C., and Mangeat, P. (1995). Identification of a phoshatidylinositol-4,5-bisphosphate-binding domain in the N-terminal region of ezrin. *FEBS Lett.* **376**, 172-176.

Nobes, C. D., and Hall, A. (1995). Rho, rac, and cdc42 GTPases regulate the assembly of multimolecular focal complexes associated with actin stress fibers, lamellipodia, and filopodia. *Cell.* **81**, 53-62.

Oliver, T., Dembo, M., and Jacobson, K. (1995). Traction forces in locomoting cells. *Cell Motility Cyto.* **31**, 225-240.

Otey, C., Pavalko, F., and Burridge, K. (1990). An interaction between α-actinin and the β1-integrin subunit in vitro. *J. Cell. Biol.* **111**, 721-729.

Palecek, S. P., Schmidt, C. E., Lauffenburger, D. A., and Horwitz, A. F. (1996). Integrin dynamics on the tail region of migrating fibroblasts. *J. Cell Sci.* **109**, 941-952.

Pasqualini, R. and Hemler, M. E. (1994). Contrasting roles for integrin β1 and β5 cytoplasmic domains in subcellular localization, cell proliferation, and cell migration. *J. Cell Biol.* **125**, 447-460.

Paterson, H. F., Self, A. J., Garrett, M. D., Just, I., Aktories, K., and Hall, A. (1990). Microinjection of recombinant p21rho induces rapid changes in cell morphology. *J. Cell Biol.* **111**, 1001-1007.

Potter, D. A., Tirnauer, J. S., Janssen, R., Croall, D. E., Hughes, C. N., Fiacco, K. A., Mier, J. W., Maki, M., and Herman, I. M. (1998). Calpain regulates actin remodeling during cell spreading. *J. Cell Biol.* **141**, 647-662.

Racine-Samson, L., Rockey, D. C., and Bissell, D. M. (1997). The role of α1β1 integrin in wound contraction. *J. Biol. Chem.* **272**, 30911-30917.

35

Regen, C. M., and Horwitz, A. F. (1992). Dynamics of β1 integrin-mediated adhesive contacts in motile fibroblasts. *J. Cell. Biol.* **119**, 1347-1359.

Ridley, A. J., and Hall, A. (1992). The small GTP-binding protein rho regulates the assembly of focal adhesion and actin stress fibers in response to growth factors. *Cell.* **70**, 389-399.

Ridley, A. J., Comoglio, P. M., and Hall, A. (1995). Regulation of scatter factor/hepatocyte growth factor responses by ras, rac, and rho in MDCK cells. *Mol Cell Biol.* **15**, 1110-1122.

Romer, L. H., McLean, N., Turner, C. E., and Burridge, K. (1994). Tyrosine kinase activity, cytoskeletal organization, and motility in human vascular endothelial cells. *Mol. Biol. Cell.* **5**, 349-361.

Ruoslahti, E., and Pierschbacher, M. D. (1987). New perspectives in cell adhesion: RGD and integrins. *Science.* **238**, 491-497.

Santos, M. F., McCormack, S. A., Guo, Z., Okalicany, J., Zheng, Y., Johnson, L. R., and Tigyi, G. (1997). Rho proteins play a critical role in cell migration during the early phase of mucosal restitution. *J. Clin. Invest.* **100**, 216-225.

Saterbak, A., and Lauffenburger, D. A. (1996). Adhesion mediated by bonds in series. *Biotechnol. Prog.* **12**, 682-699.

Schaller, M. D., and Parsons, J. T. (1994). Focal adhesion kinase and associated proteins. *Curr. Opin. Cell Biol.* **6**, 705-710.

Schmidt, C., Horwitz, A.F., Lauffenburger, D. A., and Sheetz, M. P. (1993). Integrin/cytoskeleton interactions in migrating fibroblasts are dynamic, asymmetric, and regulated. *J. Cell. Biol.* **123**, 977-991.

Schmidt, C., Pommerenke, H., Durr, F., Nebe, B. and Rychly, J. (1998). Mechanical stressing of integrin receptors induces enhanced tyrosine phosphorylation of cytoskeletally anchored proteins. *J. Biol. Chem.* **273**, 5081-5085.

Schlaepfer, D. D. and Hunter, T. (1998). Integrin signalling and tyrosine phosphorylation: just the FAKs? *Trends Cell Biol.* **8**, 151-157.

Schwartz, M. A. (1997). Integrins, oncogenes, and anchorage independence. *J. Cell Biol.* **139**, 575-578.

Seftor, R. E., Seftor, E. A., Stetler-Stevenson, W. G., and Hendrix, M. J. (1993). The 72 kDa type IV collagenase is modulated via differential expression of αvβ3 and α5β1 integrins during human melanoma cell invasion. *Cancer Res.* **53**, 3411-3415.

Shaw, L. M. and Mercurio, A. M. (1994). Regulation of cellular interactions with laminin by integrin cytoplasmic domains: the A and B structural variants of the α6β1 integrin differently modulate the adhesive strength, morphology, and migration of macrophages. *Mol Biol. Cell.* **5**, 679-690.

Sheetz, M. P. (1994). Cell migration by graded attachment to substrates and contraction. *Sem. Cell Biol.* **5**, 149-155.

Shyy, J. Y.-J. and Chien, S. (1997). Role if integrins in cellular responses to mechanical stress and adhesion. *Curr. Opin. Cell Biol.* **9**, 707-713.

Smith, J. W. and Cheresh, D. A. (1988). The Arg-Gly-Asp binding domain of the vitronectin receptor. Photoaffinity cross-linking implicates amino acid residues 61-203 of the beta subunit. *J. Biol. Chem.* **263**, 18726-18731.

Sonnenberg, A. (1993). Integrins and their ligands. *Curr. Top. Microbiol. Immunol.* **184**, 7-35.

Springer, T. A. (1995). Traffic signals on endothelium for lymphocyte recirculation and leukocyte emigration. *Annu Rev. Physiol.* **57**, 827-872.

Stewart, M. P., McDowall, A., and Hogg, N. (1998). LFA-1 mediated adhesion is regulated by cytoskeletal restraint and by a Ca^{2+}-dependent protease, calpain. *J. Cell Biol.* **140**, 699-707.

Stossel, T. P. (1993). On the crawling of animal cells. *Science.* **260**, 1086-1094.

Svitkina, T. M., Verkhovsky, A. B., McQuade, K. M., and Borisy, G. G. (1997). Analysis of the actin-myosin II system in fish epidermal keratocytes: mechanism of cell body translocation. *J. Cell Biol.* **139**, 397-415.

Tapon, N., and Hall, A. (1997). Rho, rac and cdc42 GTPases regulate the organization of the actin cytoskeleton. *Curr. Opin. Cell Biol.* **9**, 86-92.

Toker, A., Meyer, M., Reddy, K. K., Falck, J. R., Aneja, R., Aneja, S., Parra, A., Burns, D. J., Ballas, L. M., and Cantley, L. C. (1994). Activation of protein kinase C family members by the novel polyphosphoinositides PtdIns-3,4-P2 and PtdIns-3,4,5-P3. *J. Biol. Chem.* **269**, 32358-32367.

Tolias, K. F., Cantley, L., and Carpenter, C. L. (1995). Rho family GTPases bind to phosphoinositide kinases. *J. Biol. Chem.* **270**, 17656-17659.

Van Roy, F., and Mareel, M. (1992). Tumour invasion: effects of cell adhesion and motility. *Trends Cell Biol.* **2**, 163-169.

Varnum-Finney, B., and Reichardt, L. F. (1994). Vinculin-deficient PC12 cell lines extend unstable lamellipodia and filopodia and have a reduced rate of neurite outgrowth. *J. Cell. Biol.* **127**, 1071-1084.

Verkhovsky, A. B., Svitkina, T. M., and Borisy, G. G. (1997). Polarity sorting of actin filaments in cytochalasin-treated fibroblasts. *J. Cell Sci.* **110**, 1693-1704.

Verkhovsky, A. B., Svitkina, T. M., and Borisy, G. G. (1995). Myosin II filament assemblies in the active lamella of fibroblasts: their morphogenesis and role in the formation of actin filament bundles. *J. Cell Biol.* **131**, 989-1002.

Waltz, D. A., Natkin, L. R., Fujita, R. M., Wei, Y., and Chapman, H. A. (1997). Plasmin and plasminogen activator inhibitor type 1 promote cellular motility by regulating the interaction between urokinase receptor and vitronectin. *J. Clin. Invest.* **100**, 58-67.

Wang, N., Butler, J. P., and Ingber, D. E. (1993). Mechanotransduction across the cell surface and through the cytoskeleton. *Science.* **260**, 1124-1127.

Wang, N., and Ingber, D. E. (1994). Control of cytoskeletal mechanics by extracellular matrix, cell shape, and mechanical tension. *Biophys. J.* **66**, 2181-2189.

Weber, C., Alon, R., Moser, B., and Springer, T. A. (1996). Sequential regulation of $\alpha 4 \beta 1$ and $\alpha 5 \beta 1$ integrin avidity by CC chemokines in monocytes: implication for tansendothelial chemotaxis. *J. Cell Biol.* **134**, 1063-1073.

Wei, Y., Lukashev, M., Simon, D. I., Bodary, S. C., Rosenberg, S., Doyle, M. V., and Chapman, H. A. (1996). Regulation of integrin function by the urokinase receptor. *Science.* **273**, 1551-1555.

Werb, Z., Tremble, P. M., Behrendtsen, O., Crowley, E., and Damsky, C. H. (1989). Signal transduction through the fibronectin receptor induces collagenase and stromelysin gene expression. *J. Cell Biol.* **109**, 877-889.

Wessels, D., Soll, D. R., Knecht, D., Loomis, W. F., DeLozanne, A., and Spudich, J. (1988). Cell motility and chemotaxis in Dictyostelium amoebae lacking myosin heavy chain. *Dev. Biol.* **128**, 164-177.

Wessels, D., Vawter-Hugart, H., Murray, J., and Soll, D. R. (1994). Three-dimensional dynamics of pseudopod formation and the regulation of turning during the motility cycle of Dictyostelium. *Cell Motil. Cytoskeleton.* **27**, 1-12.

Wilson, A. K., Gorgas, G., Claypool, W. D., and de Lanerolle, P. (1991). An increase or decrease in myosin II phosphorylation inhibits macrophage motility. *J. Cell Biol.* **114**, 277-283.

Woods, A., and Couchman, J. R. (1992). Protein kinase C involvement in focal adhesion formation. *J. Cell Sci.* **101**, 277-290.

Xie, H., Pallero, M. A., Gupta, K., Chang, P., Ware, M. F., Witke, W., Kwiatkowski, D. J., Lauffenburger, D. A., Murphy-Ulrich, J. A., and Wells, A. (1997). EGF receptor regulation of cell motility: EGF induces disassembly of focal adhesions independently of the motility-associated PLC-γ signaling pathway. *J. Cell Sci.* **111**, 615-624.

Zhang, J., King, W. C., Dillon, S., Hall, A., Feig, L., and Rittenhouse, S. E. (1993). Activation of platelet phosphatidylinositide 3-kinase requires the small GTP-binding protein rho. *J. Biol. Chem.* **268**, 22251-22254.

Zheng, Y., Bagrodia, S., and Cerione, R. A. (1994). Activation of phosphoinositide 3-kinase activity by cdc42Hs binding to p85. *J. Biol. Chem.* **269**, 18727-18730.

Zhong, C., Chrzanowska-Wodnicka, M., Brown, J., Shaub, A., Belkin, A. M., and Burridge, K. (1998). Rho-mediated contractility exposes a cryptic site in fibronectin and induces fibronectin matrix assembly. *J. Cell Biol.* **141**, 539-551.
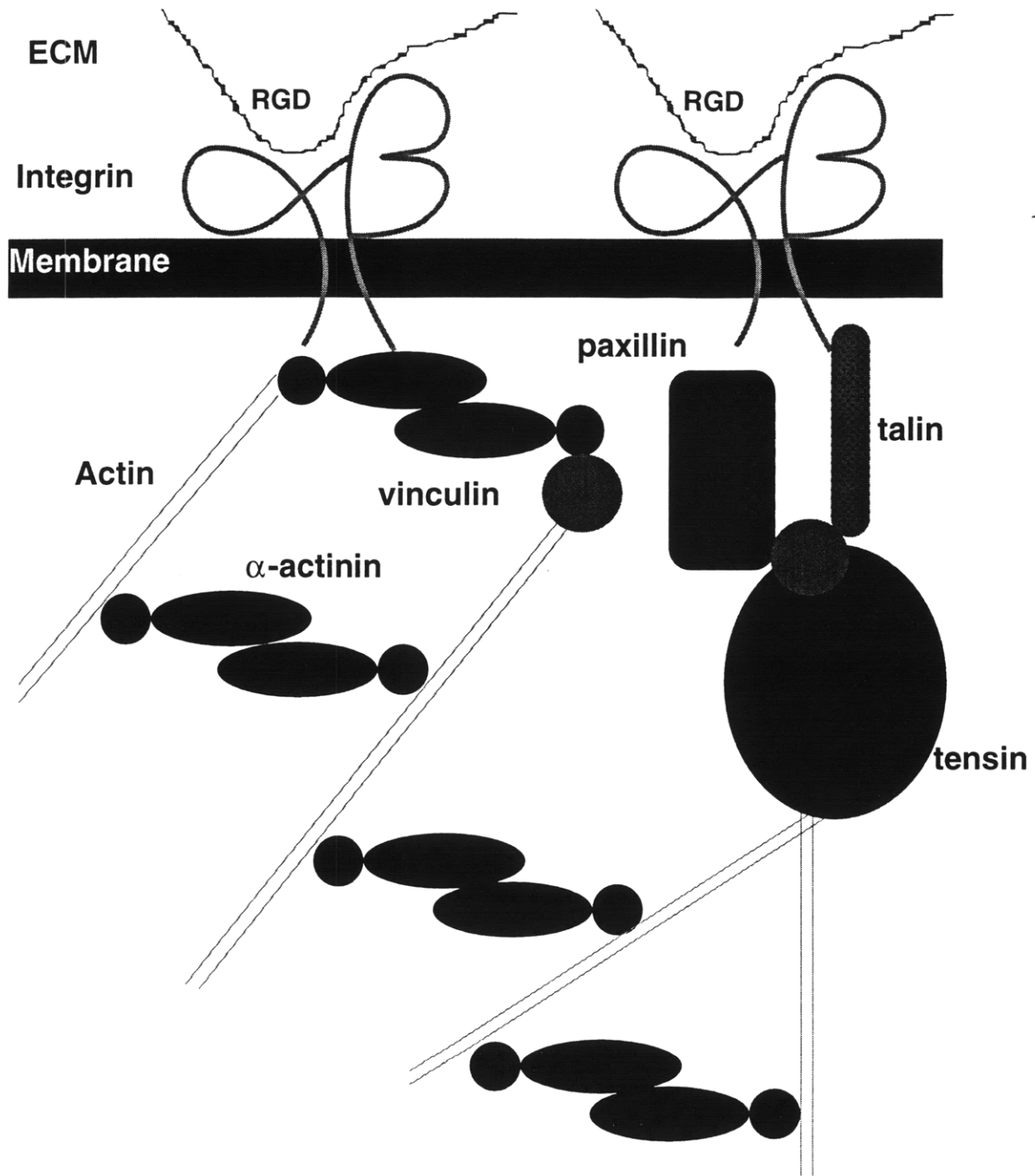
Figure 1.1 Schematic Representation of Physical Linkage between Extracellular Matrix, Integrins, and Cytoskeletal Proteins.
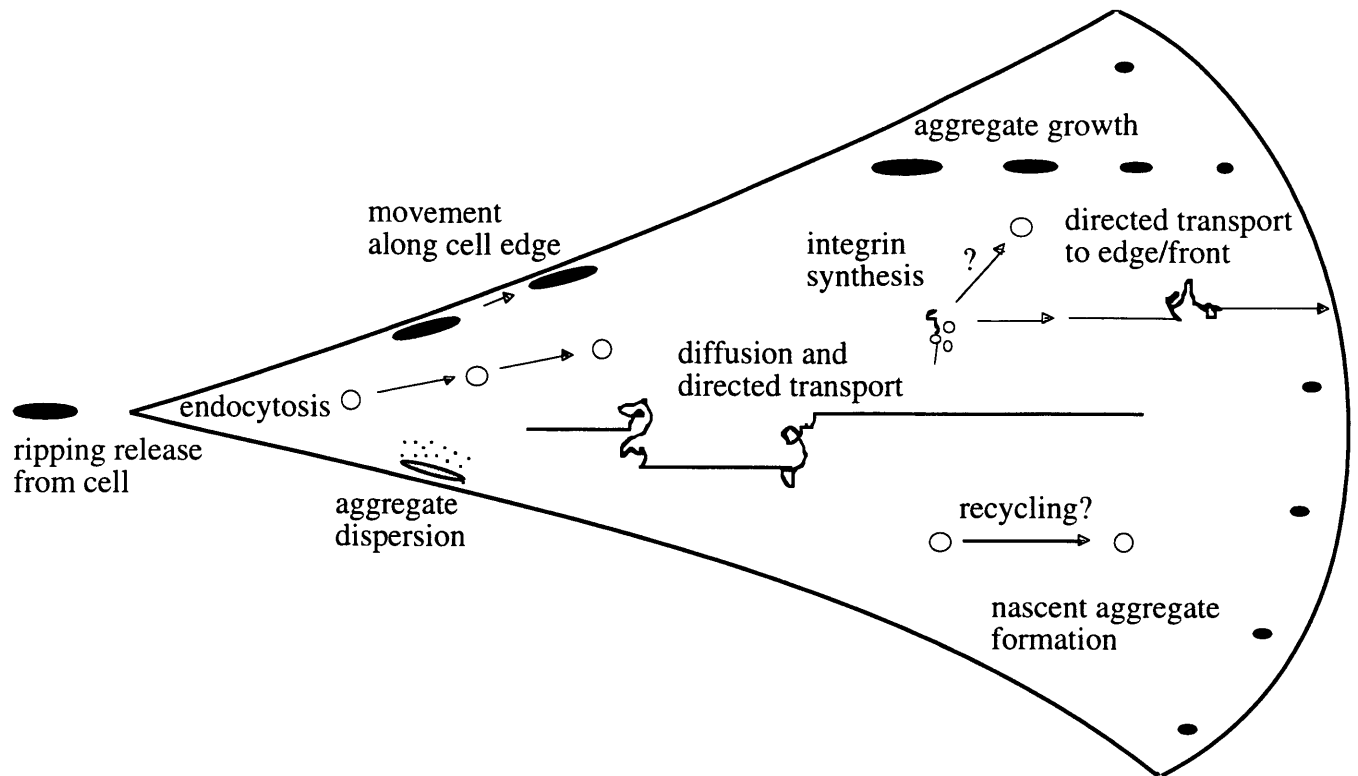
Figure 1.2 Integrin Dynamics during Cell Migration. Integrins are synthesized and inserted into the cell membrane where they move to the cell front by directed transport. There they participate in the formation of adhesion structures. The adhesions grow in size as the cells migrate over them. At the cell edge, adhesions can release from the cell and remain attached to the substratum behind the migrating cell. Alternatively, they can detach from the substratum and move along the cell edge until they reattach. Aggregated integrins can also disperse their integrins into the cell membrane. The dispersed integrins can return to the front of the cell by diffusion and/or directed transport or by endocytosis into vesicles.

A

B

graded polarity
actin bundle

bundle movement ⟶▷

ventral surface cell membrane
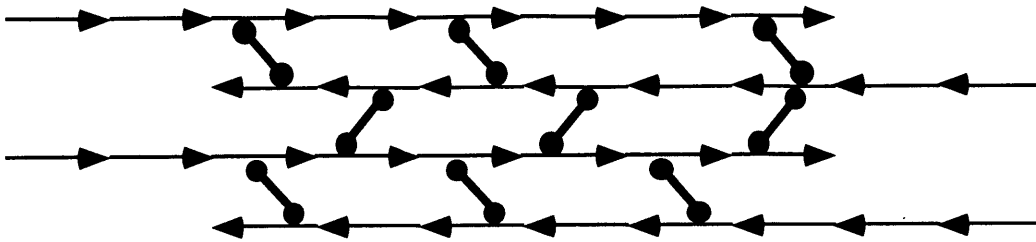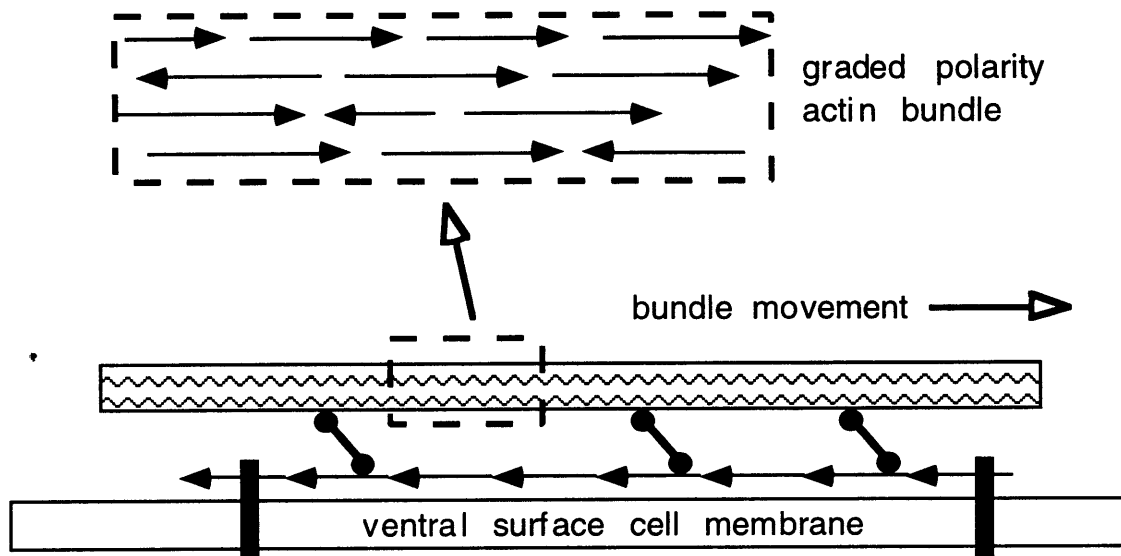
Figure 1.3 Models for Contractile Force Generation during Motility. (A) Individual filaments in actin bundles alternate in polarity (arrows point toward pointed end). Myosin II molecules (line with two balls) slide the actin filaments across each other to contract the bundle, as in a muscle sarcomere. This actin arrangement along the inner surface of the plasma membrane. (B) In the bundle/track mechanism, actin filaments (lines with arrows) are anchored (filled rectangles) to the substratum through cell membrane and remain stationary with respect to the cell surface. Bundles of actin filaments are attached to myosins which transport the bundles along the filament track. The actin bundles are composed of filaments with graded polarity. Near the front of the cell, actin barbed ends tend to face forward but near the rear of the cell actin pointed ends tend to face forward. This actin organization occurs along the entire length of the ventral surface of the cell.

41
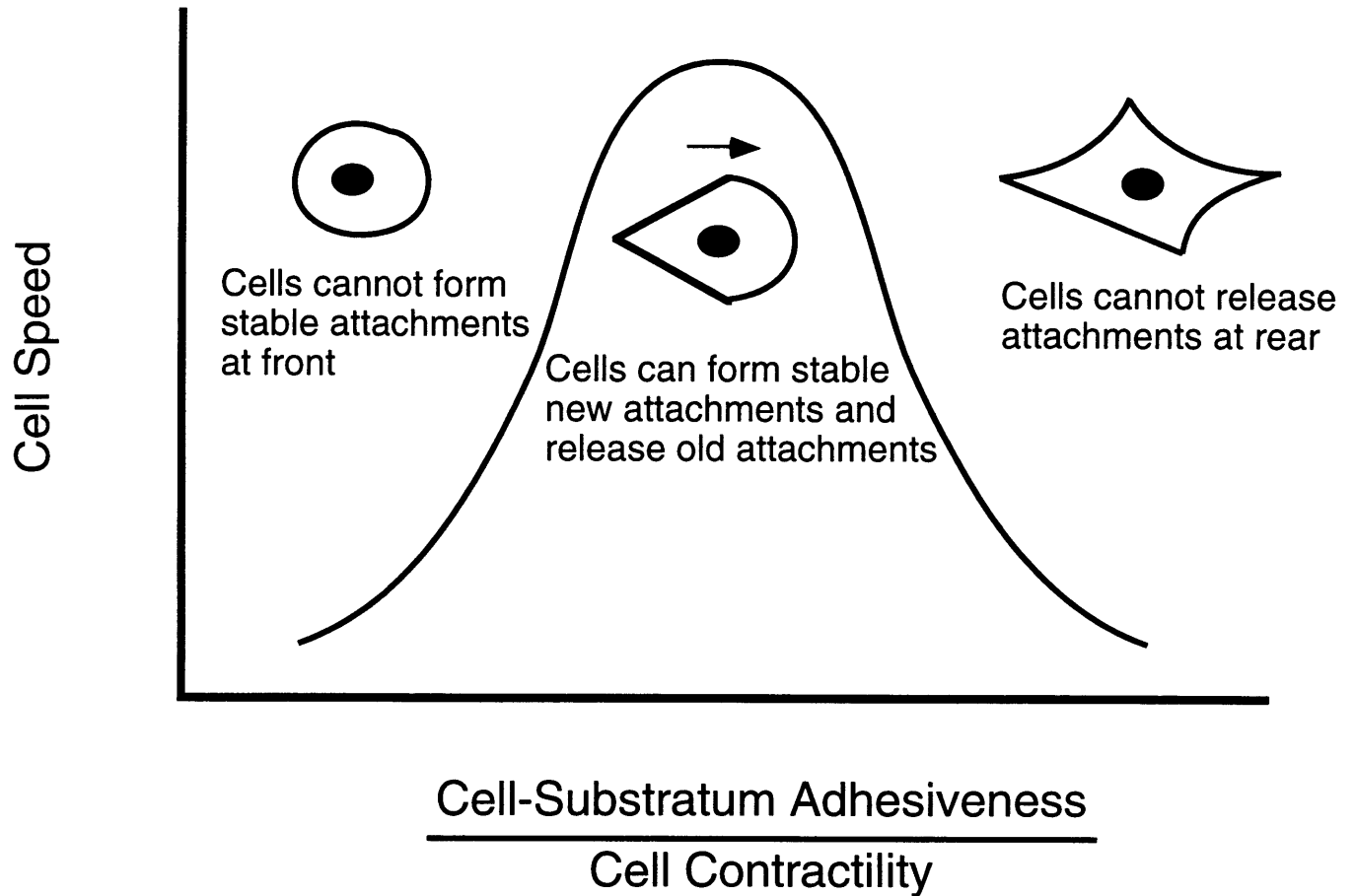
Figure 1.4 Cell-Substratum Adhesiveness Regulates Cell Migration Speed. At low adhesiveness, cells cannot form stable attachments to the substratum and generate traction forces required for migration. At high adhesiveness, adhesions at the cell rear are very strong and rear detachment limits cell speed. Cell speed is a maximum at intermediate adhesiveness where the cells can efficiently form adhesions at the cell front and detach adhesions at the cell rear.

Chapter 2: Experimental Systems for Studying Adhesive Regulation of Cell Speed

2.1 Measuring Speed as a Function of Adhesiveness

As described in Section 1.5, a quantitative cell migration model predicts principles governing the dependence of cell speed on integrin/ECM-ligand binding and cell mechanical properties (DiMilla et al., 1991). This model has been supported by several experimental studies which alter ligand concentration (DiMilla et al., 1993; Goodman et al., 1989), receptor number (Keely et al., 1995; Giancotti and Ruoslahti, 1990; Bauer et al., 1992), or receptor-ligand affinity (Huttenlocher et al., 1996). However, the use of different experimental systems and different adhesion and migration assays in each of these studies makes elucidating a clear, quantitative relationship between cell-substratum adhesiveness and migration speed difficult. We have devised experimental systems and quantitative assays to alter substrate ECM concentration, integrin expression, and integrin-ligand affinity to quantitatively test predictions concerning properties of the integrin-ECM linkage in mediating cell-substrate adhesiveness and cell migration speed.

2.2 Cell Systems

We chose a Chinese Hamster ovary (CHO) cells as a model system to study how integrin-ECM ligand binding affects cell speed. CHO cells are relatively easy to stably transfect, making genetic alterations in receptor expression or receptor-ligand affinity simple. Also, the function of $\alpha_{IIb}\beta_3$ integrins has been extensively studied in CHO cells (O'Toole et al., 1989; Bajt et al., 1992; Freilinger et al., 1991; O'Toole et al., 1994). CHO cells do not express endogenous $\alpha IIb\beta_3$ or other fibrinogen receptors. A CHO cell clone (B2), which expresses very low levels of α_5 integrin, was available for studying the effects of integrin expression on cell speed. Thus, we can use the CHO cell system to quantitatively vary 3 integrin-ECM binding parameters: ECM concentration, integrin expression, and integrin-ligand affinity.

The main disadvantage of using the CHO cell system is CHO cells are not as physiologically relevant as other cell types such as leukocytes or fibroblasts. However, the basic mechanisms governing migration speed through integrin-ligand binding are likely to be the same across many cell types. Changes in motile behavior are probably in a large part due to changes in the quantitative values of integrin-ligand binding parameters. We expect behaviors detected in CHO cells to be relevant for virtually all types of cell motility.

2.3 Materials and Reagents

Fibronectin and fibrinogen were obtained from Sigma Chemical Company (St. Louis, MO). The αIIbβ3 activating antibody mAb 62 which recognizes an epitope on β3 and the non-adhesion perturbing αIIbβ3 antibody D57 were used as previously described (O'Toole et al., 1990; Freilinger et al., 1991; O'Toole et al., 1994). The anti-human α5 antibody 6F4 was a gift of Dr. Ralph Isberg (Tufts University). The human α5 cDNA (Argraves et al., 1987) was a gift of Dr. Louis Reichardt and subcloned into the eukaryotic expression vector pRSVneo (Reszka et al., 1992; Sastry et al., 1996).

2.4 Cell Culture and Transfection

Wild-type CHO-LA cells were obtained from Dr. Andrew Belmont (University of Illinois at Urbana-Champaign) and low α5 expressing CHO-B2 cells were provided by Dr. Rudolph Juliano (University of North Carolina, Chapel Hill). Generation of αIIbβ3 and αIIbβ3(β1-2) expressing CHO cells is previously described (O'Toole et al., 1989; Bajt et al., 1992). The cells grow in DMEM containing 10% FBS, 2 mM glutamine (Sigma Chemical Co.), and 1% nonessential amino acids.

CHO B2 cells were transfected with human α5 cDNA using Lipofectamine (GIBCO-BRL) according to the manufacturer's protocols. The transfected cells were selected in DME containing 100 μg/ml G418 and maintained in DME containing 50 μg/ml G418. Cells expressing human α5 were selected from nonexpressors by flow cytometry.

Quantitative cell surface expression of integrins was determined by flow cytometry as described (Loftus et al., 1990) using 6F4 at 1:4 dilution of hybridoma supernatant to assay α5 expression and D57 at 1:200 dilution of mouse ascites to assay αIIbβ3 expression. The cells were washed with PBS and detached from plates with 0.02% EDTA in calcium-magnesium free HEPES-Hanks buffer (CMF-HH). Cells were incubated at 4°C for 30 minutes with primary antibody and then washed twice with blocking buffer (2% BSA in CMF-HH). Cells were then incubated at 4°C with the secondary antibody, fluorescein-conjugated goat anti-mouse IgG (Molecular Probes), for 30 minutes, washed twice with blocking buffer, and suspended in CMF-HH. A FACS-STAR (Becton-Dickson) was used to sort α5 expressing cells into populations with different relative expression levels and to sort αIIbβ3(β1-2) expressing cells into similar surface expression profiles as αIIbβ3 transfected cells. Surface expression of α5 transfected cells remained stable for more than 3 weeks while expression in αIIbβ3(β1-2) transfected cells is not stable for more than 5 days, so these cells were used within 5 days of sorting.

2.5 Cell Adhesion Assay

Cell substratum adhesiveness was quantitatively measured using shear flow detachment of cells. A surface coated with cells was exposed to a well-defined laminar flow. The flow chamber (Usami et al., 1993) induces Hele-Shaw flow patterns and produces a surface shear stress which varies linearly with position along the centerline according to the formula:

$$\tau_w = \frac{6\mu Q}{h^2 w_1}(1 - \frac{z}{L})$$

(2.1)

where τ_w is the surface shear stress, μ the fluid viscosity, Q the flowrate, h the channel height, w_1 the channel width at the origin of the flow field, z the distance from the origin along the centerline, and L the length of the flow field. The dimensions of the chamber are w_1=1.35 mm, L=5.65 cm, and h=365 mm. PBS with Ca^{2+} and Mg^{2+} is heated to 37°C in a constant head tank fitted with a stopcock to control flow. Construction and operation of the flow chamber is described in greater detail by Powers et al. (1996).

Glass slides (Fisher Scientific) were acid-washed in 20% HNO_3 for 1 hour, rinsed with deionized water overnight and silaned by exposure to hexamethyldisilazane vapor (Sigma Chemical Co.) for 30 minutes at 200°C (Regen and Horwitz, 1992) to block hydrophilic charged groups and reduce nonspecific cell adhesion to the glass surface. The surface was incubated at 4°C overnight with 2 ml ECM protein solution of the desired concentration diluted in PBS and blocked with 1% BSA in PBS for 1 hour at 37°C. Cells were harvested from plates using 0.02% EDTA in PBS and trituration. 10^5 cells in 1 ml serum-free OptiMEM-1 (GIBCO-BRL) were incubated on the slide at 37°C for 20 minutes, long enough for cells to attach to the surface but not long enough for significant organization of focal adhesions or cell spreading. The medium was gently aspirated from the slide and then the slide was mounted in the chamber which was prefilled with PBS. The chamber was placed on the stage of a Zeiss Axiovert 100 microscope with a 10X objective (Carl Zeiss), which gives a 0.5 mm^2 field of view. A Ludl 99S008 motorized microscope stage (Ludl Electronic Products, Hawthorne, NY), interfaced with a nuDrive amplifier (nuLogic Inc., Needham, MA), was used to provide precise motion control. Cells in 20 fields, spaced at 2.5 mm, along the centerline were counted. The stopcock was opened and flowrate was measured using a stopwatch and graduated cylinder. Cells were exposed to flow for 5 minutes and then cells in each of the fields were counted again. 99% of cells which detached due to shear stress did so within 5 minutes.

To calculate detachment force, both the shear stress and cell morphology must be known. Cell shape was estimated as a hemispherical cap. Mean cell diameter was measured using a Coulter Counter and mean hemispherical cap radius, r_p, was measured from images of fields in the linear flow chamber prior to initiation of flow. The height of the cap, h, was calculated assuming

45

constant cell volume. Shear force, F_s, on a hemispherical cap was calculated from (Truskey and Proulx, 1993):

$$F_s = 2.15\pi(r_p^2 + h^2)\tau_w. \tag{2.2}$$

A plot of fraction of cells detached as a function of shear force was fit with the integrals of logarithmic normal probability density function distributions (LNPDFD). The mean of the LNPDFD is reported as the mean cell detachment force. LNPDFDs also were used to analyze detachment of fibroblasts (Truskey and Pirone, 1990) and hepatocytes (Powers et al., 1996) under shear flow. 5 detachment assays were performed for each cell type at each ECM concentration and mean detachment forces were averaged. Error bars are 95% confidence intervals of the mean.

2.6 Cell Migration Assay

Cell migration speed was measured using real-time image analysis to track individual cell centroids. Microscopy plates were constructed by punching a hole out of the bottom of a 35-mm tissue culture dish. Acid-washed and silaned 18 mm No. 1 glass coverslips (Fisher Scientific) were attached to the bottoms of the dishes with clear silicone rubber sealant (Dow-Corning). Prior to use, the plates were sterilized with 70% ethanol and rinsed with sterile deionized water. Coverslips were coated with 60 µl ECM protein, to maintain the same volume to surface area ratio of solution as used in the adhesion assays, at the desired concentration overnight at 4°C and blocked with 1% BSA for 1 hour at 37°C. Cells were removed from tissue culture plates with 0.02% EDTA in CMF-PBS and trituration. The cells were centrifuged and resuspended in microscopy medium (OptiMEM I containing 20 mM HEPES buffer without sodium bicarbonate, supplemented with 50 units/ml penicillin and 50 µg/ml streptomycin). 1000 cells in 60 µl microscopy medium were seeded onto the coverslip and allowed to attach for 20 minutes before 3 ml microscopy medium was added to the plate. 4 ml light mineral oil (Sigma) was added to the plate to prevent evaporation of the medium. Cells were allowed to attach for 3 hours at 37°C prior to tracking. The plate was placed in a heated stage insert for a Ludl 99S008 motorized stage on a Zeiss Axiovert 35 microscope.

Real-time digital image processing was used to acquire images and calculate cell centroid position as a function of time. Images were acquired through a Sony CCD videocamera using a 10X objective. The experiments were videotaped on a time-lapse VCR. The image processing software was developed by Engineering Technology Center (Mystic, CT) to run under a LabVIEW (National Instruments, Austin, TX) and Concept Vi (Graftek Imaging, Mystic, CT) environment. The software identifies cell boundaries from phase contrast images by two-tailed thresholding, dilation, hole filling, erosion, and low pass filtering (Pratt, 1978). After image processing, the software measures cell centroid position and cell area and writes the data to a file. Cells from

multiple fields were tracked using a nuDrive amplifier to interface the software with the motorized stage.

5-10 cells per field in 10 different fields were scanned every 15 minutes for 12 hours. The cells did not noticeably change speeds during the course of the experiment. The "wind-rose displays" of individual cell tracks (Goodman et al., 1989) and videotape of the experiment were analyzed to discard cells which migrated out of the field of view, aggregates of more than one cell, or cells whose boundaries were not correctly identified by the image analysis software. The mean-squared displacement (MSD) as a function of time was calculated for each cell using nonoverlapping time intervals. Each cell track consists of n cell positions separated by a constant time increment, Dt. If x_{ik} is the squared displacement over the time interval $t_i=iDt$ at the kth time point, the measured MSD, x_i, is calculated as:

$$\overline{x_i} = \frac{1}{n_i} \sum_{k=0}^{n_i-1} x_{i,1+ki}$$ (2.3)

where

$$n_i = [\frac{n-i}{i}]$$ (2.4)

(Dickinson and Tranquillo, 1993).

x_i at each time point was averaged for 50-100 cells from at least 2 separate experiments. The data were fit to a persistent random walk model (Alt, 1990) to calculate cell speed, S, and persistence time, P:

$$< d^2(t) >= 2S^2P[t - P(1 - e^{-t/P})]$$ (2.5)

where $<d^2(t)>$ is the MSD as a function of time. S is the rate at which cells move while P can be interpreted as a measure of the average time between significant changes of direction. Since P is undefined when S=0, only cells which move at least 20 μm from their starting point during some part of the 12 hour experiment are used to calculate P. P is set and all of the cells, motile or immotile, are used to calculate S. 95% confidence intervals for speed are calculated by calculating 95% confidence intervals for the MSD, xi, at each time point based on the corresponding statistical t value. The upper and lower limits from the mean cell speed confidence interval were fit from the limits of the confidence intervals on the MSD vs. time plot. The reported error bars are 95% confidence intervals of the mean cell speed.

2.7 References

Argraves, W. S., Suzuki, S., Arai, H., Thompson, K., Pierschbacher, M. and Ruoslahti, E. (1987). Amino acid sequence of the human fibronectin receptor. *J. Cell Biol.* **105**, 1183-1190.

Bajt, M. L., Loftus, J. C., Gawaz, M. P., and Ginsberg, M. H. (1992). Characterization of a gain of function mutation of integrin αIIbβ3 (platelet glycoprotein IIb-IIIa). *J. Biol. Chem.* **267**, 22211-22216.

Bauer, J. S., Schreiner, C., Giancotti, F. G., Ruoslahti, E., and Juliano, R. L. (1992). Motility of fibronectin receptor-deficient cells on fibronectin and vitronectin: collaborative interactions among integrins. *J. Cell Biol.* **116**, 477-487.

Dickinson, R. B. and Tranquillo, R. T. (1993). Optimal estimation of cell movement indices from the statistical analysis of cell tracking data. *AIChE J.* **39**, 1995-2010.

DiMilla, P. A., Barbee, K., and Lauffenburger, D. A. (1991). Mathematical model for the effects of adhesion and mechanics on cell migration speed. *Biophys. J.* **60**, 15-37.

DiMilla, P. A., Stone, J. A., Quinn, J. A., Albeda, S. M., and Lauffenburger, D. A. (1993). Maximal migration of human smooth muscle cells on fibronectin and type IV collagen occurs at an intermediate attachment strength. *J. Cell Biol.* **122**, 729-737.

Frelinger, A.L., Du, X., Plow, E. F., and Ginsberg, M. H. (1991). Monoclonal antibodies to ligand-occupied conformer of integrin αIIbβ3 (glycoprotein IIb-IIa) alter receptor affinity, specificity and function. *J. Biol. Chem.* **266**, 17106-17111.

Giancotti, F. G., and Ruoslahti, E. (1990). Elevated levels of the α5β1 fibronectin receptor suppress the transformed phenotype of Chinese hamster ovary cells. *Cell.* **60**, 849-859.

Goodman, S. L., Risse, G., and von der Mark, K. (1989). The E8 subfragment of laminin promotes locomotion of myoblasts over extracellular matrix. *J. Cell Biol.* **109**, 799-809.

Huttenlocher, A, Ginsberg, M. H., and Horwitz, A. F. (1996). Modulation of cell migration by integrin-mediated cytoskeletal linkages and ligand-binding affinity. *J. Cell Biol.* **134**, 1551-1562.

Keely, P. J., Fong, A. M., Zutter, M. M., and Santoro, S. A. (1995). Alteration of collagen-dependent adhesion, motility, and morphogenesis by the expression of antisense α2 integrin mRNA in mammary cells. *J. Cell Sci.* **108**, 595-607.

Loftus, J. C., O'Toole, T. E., Plow, E. F., Glass, A., Frelinger, A. L., and Ginsberg, M. H. (1990). A β3 integrin mutation abolishes ligand binding and alters divalent cation-dependent conformation. *Science.* **249**, 915-918.

O'Toole, T. E., Loftus, J. C., Plow, E. F., Glass, A., Harper, J. R. and Ginsberg, M. H. (1989). Efficient surface expression of platelet GPIIb-IIIa requires both subunits. *Blood.* **74**, 14-18.

O'Toole, T. E., Loftus, J. C., Du, X., Glass, A. A., Ruggeri, Z. M., Shattil, S. J., Plow, E. F. and Ginsberg, M. H. (1990). Affinity modulation of the αIIbβ3 integrin (platelet GPIIbIIIa) is an intrinsic property of the receptor. *Cell Reg.* **1**, 883-893.

O'Toole, T. E., Katagiri, Y., Faull, R. J., Peter, K., Tamura, R., Quaranta, V., Loftus, J., Shattil, S. J. and Ginsberg, M. H. (1994). Integrin cytoplasmic domains mediate inside-out signal transduction. *J. Cell Biol.* **125**, 447-460.

Powers, M. J., Rodriguez, R. E., and Griffith, L. G. (1996). Cell-substratum adhesion strength as a determinant of hepatocyte aggregate morphology. *Biotech. Bioeng.* **53**, 415-423.

Regen, C. M., and Horwitz, A. F. (1992). Dynamics of $\beta 1$ integrin-mediated adhesive contacts in motile fibroblasts. *J. Cell. Biol.* **119**, 1347-1359.

Reszka, A., Hayashi, Y. and Horwitz, A. (1992). Identification of amino acid sequences in the integrin $\beta 1$ cytoplasmic domain implicated in cytoskeletal association. *J. Cell Biol.* **117**, 1321-1330.

Sastry, S., Lakonishok, M., Thomas, D. A., Muschler, J. and Horwitz, A. F. (1996). Integrin α subunit ratios, cytoplasmic domains, and growth factor synergy regulate muscle proliferation and differentiation. *J. Cell Biol.* **133**, 169-184.

Truskey, G. A. and Proulx, T. L. (1993). Relationship between 3T3 cell spreading and the strength of adhesion on glass and silane surfaces. *Biomaterials.* **14**, 243-254.

Truskey, G. A. and Pirone, J. S. (1990). The effect of fluid shear stress upon cell adhesion to fibronectin-treated surfaces. *J. Biomed. Mat. Res.* **24**, 1333-1353.

Usami, S., Chen, H. H., Zhao, Y., Chien, S., and Skalak, R. (1993). Design and construction of a linear shear stress flow chamber. *Ann. Biomed. Eng.* **21**, 77-83.

Chapter 3: Cell-Substratum Adhesiveness Regulates Cell Speed - Experimental Results

3.1 The Optimal Fibronectin Concentration for Promoting Cell Migration Decreases as α5 Expression Increases

Migration speeds, measured by individual cell tracking, of wild-type CHO LA and α5β1-deficient CHO B2 cells, which have about 1-2% intact surface α5β1 expression of wild-type cells (Schreiner et al., 1989), as fibronectin coating concentration varies are compared in Figure 3.1. After a 3 hour preincubation to allow the cells to attach to the substrate and begin migration, individual cell centroids were measured as a function of time for 12 hours. The cell paths were fit to a model of a persistent random walk to obtain cell speed and persistence time. Individual cell tracking offers several advantages over assays which measure the migration of cell populations. First, tracking individual cells allows calculation of both cell speed and persistence time. Although there is no evidence that persistence time (Equation 2.5), which is related to the length of time a cell migrates before it significantly changes direction, is related to cell adhesiveness, comparison of persistence times will tell if the cell locomotory behavior has changed in response to experimental conditions. Also, inspecting individual cell tracks gives a better measure of the range of cellular migration speeds. Fewer cells are required for individual cell tracking, reducing the amount of ECM proteins secreted into the medium by the cells. CHO LA cells exhibit a biphasic speed vs. fibronectin concentration relationship, with a maximum speed at 3.5 μg/ml fibronectin. CHO B2 cells only migrate at high fibronectin concentrations. Cell speed monotonically increases with fibronectin coating concentration up to 100 μg/ml.

To better define the role of integrin subunit expression in quantitatively determining cell adhesion and migration we generated cell populations with different α5 expression levels. CHO B2 cells were transfected with a human α5 cDNA and subpopulations with 3 different expression levels were selected from α5 expressors. Figure 3.2 shows that mean cell speed exhibits a biphasic dependence on fibronectin concentration at each α_5 expression level. Maximum attainable cell speed, however, does not appear to be a function of α_5 expression. At different fibronectin coating concentrations, the relationship between migration speed and α_5 expression changes. At low concentrations cell speed increases as a_5 expression increases, while at high concentrations cell speed increases as α_5 expression decreases. At intermediate fibronectin concentrations, intermediate α_5 expression levels result in highest cell speed.

Videotape observations of migrating cells indicate that at maximum migration speeds (10-20 μm/hour), CHO cells are moderately spread and move by extending multiple lamellae in different directions. One lamellipod dominates and moves the cell in the direction of its extension

while the others retract. This cycle repeats and causes the cell to change directions quite often, exploring a small area of the surface. At the maximum cell speed, about 80% of the cells are motile, as defined by moving at least 20 μm from its starting position, during some point in the experiment. Cell speed decreases from its maximum because fewer cells are motile and cells which are motile move more slowly. At fibronectin concentrations below the maximum speed the cells are more rounded but still extend lamellae which are smaller and shorter-lived than lamellae in migrating cells. The unstable lamellae cannot move the cell body, however. At fibronectin concentrations above the maximum speed the cells are very spread and extend lamellae similarly to migrating cells. The cell body does not move well, presumably because it cannot release adhesions to the substrate. Persistence time of motile cells ranges from 30-90 minutes for CHO LA, CHO B2, and each of the $\alpha5$-transfected CHO B2 cell populations, and does not appear to be a function of fibronectin coating concentration or $\alpha5$ expression level.

The fibronectin concentration allowing maximum migration speed is inversely proportional to the $\alpha5$ expression level so that the product of the fibronectin concentration at maximum cell speed and the $\alpha5$ expression level is constant over the range of $\alpha5$ expression levels in this study (Figure 3.3). This result is quantitatively consistent with a prediction of a mathematical model of cell migration (DiMilla et al., 1991), and indicates that cell receptor number and substratum ligand concentration are reciprocally related at maximum cell speed.

3.2 Short-Term Cell-Substrate Adhesiveness Increases Proportionally to the Potential Number of Cell-Substratum Bonds

Adhesion of CHO LA and CHO B2 cells under shear stress is compared in Figure 3.4. Cells were allowed to attach to a fibronectin-coated silaned glass slide for 20 minutes before the slide was placed on a linear shear stress flow chamber to measure cell-substrate adhesiveness by flow detachment. The 20 minute incubation allows cell-substratum bonds to form but the cells do not spread and organization of integrins and cytoskeletal elements into focal adhesions is not apparent. The measured force reflects the force required to detach loosely organized groups of bonds, as seen in migrating cells, rather than highly organized adhesion structures. The linear shear stress flow chamber provides an accurate measure of mean detachment force in the range of 10^{-8} to 10^{-6} N for unspread CHO cells. At lower detachment forces the cells detach upon placing the slide on the chamber while at higher detachment forces the chamber cannot accommodate flowrates required to detach most of the cells. The force required to detach 50% of the CHO LA cells increases as fibronectin coating concentration increases, but adhesion of CHO B2 cells does not increase with fibronectin concentration. CHO LA cells adhere more strongly to the substrate than CHO B2 cells at every fibronectin concentration.

51

Mean cell detachment force increases with fibronectin concentration at each α_5 expression level, shown in Figure 3.5. At any fibronectin concentration, mean detachment force increases as α_5 expression increases. Increases in fibronectin concentration or α_5 expression allow the cells to form more bonds with the substrate, resulting in increased adhesiveness.

Integrin-fibronectin bond formation is assumed to be a second-order equilibrium process, such that

$$R + L \Leftrightarrow C \tag{3.1}$$
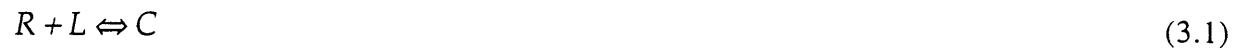
where L is the ligand, R the receptor, and C the receptor-ligand complex.

Neglecting receptor and ligand depletion due to binding,

$$[C] = K_a'[R_0][L_0] \tag{3.2}$$

so that the concentrations of cell-substratum bonds, [C], is related to the product of the integrin concentration, $[R_0]$, and the ECM-protein concentration $[L_0]$ by an association constant, K_a'. K_a' takes into account geometrical parameters of the immobilized ligand and the receptor diffusion in the plane of the cell membrane. Figure 3.6 shows the mean detachment force for each $\alpha 5$ expressing population plotted against the product of $\alpha 5$ expression and fibronectin concentration. For each $\alpha 5$ expression population, mean detachment force has the same linear relationship to the product of $\alpha 5$ expression and fibronectin concentration, suggesting that the short-term mean detachment force is proportional to the number of cell-substratum bonds.

3.3 Cell Migration Speed is a Biphasic Function of Cell-Substratum Adhesiveness at Different α_5 Expression Levels

Plotting the migration speed data from Figures 3.1 and 3.2 as a function of the detachment force data from Figures 3.4 and 3.5 shows that migration speed is a biphasic function of cell-substratum adhesiveness at each receptor expression level. The qualitatively different migration vs. fibronectin concentration behavior of CHO LA and B2 cells can be quantitatively explained by their differences in cell-substratum adhesiveness (Figure 3.7). CHO B2 cells express very little α_5 and cannot adhere to the fibronectin-coated surfaces and promote efficient migration. CHO LA cells achieve intermediate levels of adhesiveness which promote migration as well as high and low levels which do not permit migration.

Since the number of cell-substratum bonds appears to be constant at the maximum migration speed and the number of cell-substratum bonds appears to be proportional to mean detachment force, the mean detachment force should also be constant at maximum cell speed for the different $\alpha 5$-expressing populations. Figure 3.8 shows that the migration speed-cell-substratum adhesiveness relationships are in fact the same for each of the 3 $\alpha 5$ expression levels. This suggests that as $\alpha 5$ expression and fibronectin concentration changes, integrins quantitatively

mediate cell migration speed due to alterations in short-term adhesive interactions between the cell and substratum.

3.4 The Fibrinogen Concentration Promoting Optimal Migration Decreases as Integrin-Fibrinogen Affinity Increases

In addition to integrin expression level and ECM protein concentration, integrin-extracellular ligand affinity also influences cell-substratum adhesion. To assess quantitatively how integrin-ECM affinity affects cell migration and cell-substratum adhesiveness we used CHO cells transfected with wild-type $\alpha IIb\beta 3$ integrin or $\alpha IIb\beta 3(\beta 1-2)$, which has 6 amino acids from the putative fibrinogen binding domain of the $\beta 3$ subunit replaced with the corresponding sequence derived from the $\beta 1$ subunit. The mutation results in a higher affinity of the integrin for soluble fibrinogen (Bajt et al., 1992). $\alpha IIb\beta 3$ and $\alpha IIb\beta 3(\beta 1-2)$ can both be activated to a higher affinity state by incubation with mAb 62. mAb 62 activation results in a 3 order of magnitude increase in the affinity of $\alpha IIb\beta 3$ and a 10-fold increase in the affinity of $\alpha IIb\beta 3(\beta 1-2)$. $\alpha IIb\beta 3(\beta 1-2)$ has at least a 300-fold higher affinity for soluble fibrinogen than wild-type $\alpha IIb\beta 3$ in the resting state (200 nM vs. 7 μM) and a 3-fold higher affinity in the activated state (20 nM vs. 60 nM). Affinities between each integrin and soluble fibrinogen are given in Table 3.1.

Mean cell speed is a biphasic function of fibrinogen concentration for CHO cells transfected with $\alpha IIb\beta 3$ and $\alpha IIb\beta 3(\beta 1-2)$ in both the resting and mAb 62 activated states (Figure 3.9). Maximum cell speed mediated by $\alpha IIb\beta 3$ on fibrinogen is not a function of receptor-ligand affinity, and is the same as maximum cell speed mediated by $\alpha 5\beta 1$ on fibronectin (Figure 3.2). As affinity increases, however, lower substrate fibrinogen concentrations are required to permit optimal migration. At low fibrinogen concentrations (e.g. 0.1 μg/ml) cell speed increases as affinity increases while at high fibrinogen concentrations (e.g. 3 μg/ml) cell speed decreases as affinity increases. At intermediate fibrinogen concentrations, intermediate receptor-ligand affinity results in maximum migration speed. Cells migrating at maximum speed move by a series of rounding and spreading, similarly to $\alpha 5$-transfected CHO cells on fibronectin. Cells at fibrinogen concentrations below maximum speed are more rounded and cells at fibrinogen concentrations above maximum speed are more spread. Cell persistence time ranges from 90-180 minutes for cells expressing either $\alpha IIb\beta 3$ or $\alpha IIb\beta 3(\beta 1-2)$ in resting or activated states. Persistence time does not appear to be a function of integrin-fibrinogen affinity or fibrinogen concentration.

3.5 Short-Term Cell-Substrate Adhesiveness Increases with Increasing Integrin-ECM Ligand Affinity

Mean cell detachment force increases as receptor-ECM ligand affinity increases (Figure 3.10). $\alpha IIb\beta 3(\beta 1\text{-}2)$ expressing cells were selected for the same expression level as $\alpha IIb\beta 3$ expressing cells by FACS to eliminate effects due to receptor expression differences. In both resting and activated states, cells expressing $\alpha IIb\beta 3(\beta 1\text{-}2)$ adhere more strongly to the substratum than cells expressing $\alpha IIb\beta 3$ at all fibrinogen concentrations. Cells with antibody-activated receptors also adhere more strongly to the substratum than cells with receptors in the resting state, for both $\alpha IIb\beta 3$ and $\alpha IIb\beta 3(\beta 1\text{-}2)$.

3.6 Partial Integrin Activation Due to Ligand Binding Appears to Increase Short-Term Cell-Substratum Adhesiveness

Cell-substratum adhesion strength appears to correlate linearly with the number of cell-substratum bonds as receptor expression changes (Figure 3.6). However, this correlation does not exist as receptor-ECM ligand affinity changes. Assuming that integrin affinity for immobilized fibrinogen is proportional to integrin affinity for soluble fibrinogen, at constant receptor concentration the product of receptor-ligand affinity and fibrinogen surface concentration should be proportional to the number of bonds between the cell and substratum (Equation 3.2). A plot of mean detachment force as a function of the product of integrin-fibrinogen affinity and fibrinogen concentration (Figure 3.11) does not reveal a single linear relationship between short-term detachment force and apparent bond number. Activated $\alpha IIb\beta 3$ and $\alpha IIb\beta 3(\beta 1\text{-}2)$ show the same linear relationship but both resting integrins have a higher than expected detachment force at each apparent bond number. This is consistent with increased affinity of the resting state due to full or partial integrin activation. We can calculate an apparent affinity ($K_{a,app}$) of the non-Ab activated integrins by determining what value for K_a is required to cause the short-term detachment force vs. apparent bond number relationships (Figure 3.11) to be the same for both the nonactivated and activated integrins. We then calculate an activation index (I_A), defined as:

$$I_A = \frac{K_{a\,app} - K_{a,resting}}{K_{a\,activated} - K_{a\,resting}}.$$

(3.3)

In the adhesion assays $\alpha IIb\beta 3$ has an apparent affinity more than two orders of magnitude greater than the measured affinity for soluble fibrinogen and $\alpha IIb\beta 3(\beta 1\text{-}2)$ has an apparent affinity 3 times greater than the affinity for soluble fibrinogen (Table 3.2). Both fibrinogen receptors have a similar activation index, indicating that the $K_{a,app}$ values are consistent with full activation of about 25% of the receptors on the cell or partial activation of a larger fraction of receptors.

54

3.7 Cell Migration Speed is a Biphasic Function of Cell-Substratum Adhesiveness at Different Receptor-Ligand Affinity

Figure 3.12 shows a plot of the cell migration speed data from Fig 3.9 as a function of cell adhesion-substratum adhesiveness from Fig 3.10. Cell migration speed is a constant, biphasic function of cell-substratum adhesiveness as integrin-ECM affinity changes due to either an extracellular domain mutation or integrin activation by mAb 62. This relationship suggests that modulation of integrin affinity states can rationally alter cell migration speed through changes in the short-term adhesive interaction between the cell and substratum. ECM protein concentration, integrin expression, and integrin-ECM affinity all appear to contribute quantitatively to short-term cell adhesion by altering the number of cell-substratum bonds. These changes in short-term adhesiveness lead to predictable changes in cell migration speed.

3.8 Discussion of the Role of Adhesion in Regulating Cell Speed

In this chapter we have demonstrated how integrin-ECM bonds regulate cell adhesion and cell migration. This was done by varying 3 parameters which alter cell-substratum binding: (1) substrate ECM concentration, (2) receptor expression, and (3) receptor-ECM ligand affinity. Substrate ECM concentration was varied by adsorbing solutions of ECM at different concentrations to a silaned glass surface. Receptor number was varied by transfecting $\alpha 5$-deficient CHO B2 cells with the $\alpha 5$ integrin subunit and sorting expressors by FACS into different expression level populations. Integrin-ECM ligand affinity was varied using CHO cells transfected with wild-type human $\alpha IIb\beta 3$ integrin and $\alpha IIb\beta 3(\beta 1\text{-}2)$ high affinity mutant (Bajt et al., 1992) in both resting and mAb 62 activated states. We quantitatively measured cell migration speed by real-time videomicroscopic image analysis and cell-substratum adhesiveness by shear flow detachment. Our major findings are (a) the effect of changing receptor expression on cell migration correlates with changes in short-term cell/substratum adhesiveness and (b) the effect of changing integrin/ECM-ligand affinity correlates with changes in short-term cell/substratum adhesiveness. Both of these findings are consistent with the notion of the existence of an optimum adhesiveness for cell migration (DiMilla et al., 1991). Our results suggest that ECM protein density, integrin expression level, and integrin-ligand affinity can be useful targets to rationally alter cell migration speed in therapeutic applications, biomaterials design, and tissue engineering.

Another finding of our study is that cell substratum adhesion strength appears to linearly correlate with the number of cell-substratum bonds as receptor expression changes (Figure 3.6). As receptor-ligand affinity increases due to antibody activation, however, more apparent bonds are

required to achieve the same level of cell-substratum adhesiveness (Figure 3.11). These results are probably not due to more actual bonds between the cell and substratum, but rather to an increase in resting state integrin affinity for immobilized ligand due to full or partial integrin activation. The observations are consistent with full activation of 25% of the resting state integrins due to receptor binding or inside-out signaling, resulting in increased short-term adhesiveness. Partial activation of a larger fraction of integrins would also have the same effect. RGD peptide binding to $\alpha IIb\beta 3$ on platelets leads to receptor conformational changes and the acquisition of high affinity fibrinogen binding (Du et al., 1991). This change in affinity state may be attributable to a feedback loop where ligand binding and transmembrane signaling result in an altered association between the integrin and cytoskeleton which then stabilizes the interactions between the integrin and ligand (Fox et al., 1996). Purifications of $\alpha IIb\beta 3$ integrin from resting platelets suggest that about 10% of the receptors are in an activated conformation (Kouns et al., 1990; Kouns et al., 1991). In addition, fibrinogen adsorption to a surface changes the conformation of the protein (Zamarron et al., 1990), which may result in an increased affinity of the receptor for immobilized fibrinogen as compared to soluble fibrinogen by better exposing the integrin binding site.

Changes in short-term cell/substratum adhesiveness have the same effect on cell migration speed as ECM-substratum concentration, receptor expression, or receptor/ligand affinity change. The maximum migration speed occurs at a short-term adhesive force of about 2-4 X 10^{-8} N for both CHO cells using $\alpha 5\beta 1$ receptors to migrate on fibronectin or $\alpha IIb\beta 3$ receptors to migrate on fibrinogen (Figures 3.2 and 3.9). Migrating fibroblasts exert traction forces on the order of 20 X 10^{-8} N on deformable 2-dimensional substrata (Oliver et al., 1995). The DiMilla et al. migration model (1991) predicts that the cell migration speed is governed by the ratio of cell/substratum adhesiveness to intracellular motile force, suggesting that the $\alpha IIb\beta 3$ and $\alpha 5\beta 1$ form similar linkages to the intracellular force-generating machinery and transmit the forces of cell migration in a similar manner. Different receptors may mediate migration through different ligand recognition specificities, different receptor/ligand affinities, or different expression levels. Of course, additional variables such as lamellipodial extension, intracellular force generation, integrin clustering and avidity effects, and integrin signaling are clearly important to the processes of cell adhesion and cell migration (Lauffenburger and Horwitz, 1996; Huttenlocher et al., 1995). Overexpression of FAK in CHO cells results in increased cell migration but does not alter cell adhesion or spreading (Cary et al., 1996). Our results suggest that cell/substratum adhesiveness is rate-limiting in determining migration speed under the experimental conditions in this study.

High cell-substratum adhesiveness likely hinders cell migration by obstructing release of adhesions at the cell rear. Videotape observations of cells at high adhesiveness reveal lamellipod extension and retraction, but little movement of the cell body. In general, cell migration appears to be rate-limited by rear detachment rather than lamellipodial events on highly adhesive substrata.

The rate of lamellipodial extension in primary cultures of chick and mouse fibroblasts is approximately a factor of 5 greater than overall cell speed (Abercrombie et al., 1970; Felder and Elson, 1990). Inhibition of Ca^{2+} transients in neutrophils results in reduced migration rates on fibronectin and vitronectin; these cells often possess highly elongated tails (Marks et al., 1991). In *Dictyostelium*, loss of myosin-II-dependent contraction in the uropod correlates with diminished locomotion speed on highly adhesive substrata (Jay et al., 1995). At low cell-substratum adhesiveness, however, inhibition of rear release is an unlikely explanation for reduced migration rates. Except at the lowest levels of adhesiveness, the cells are still able to extend lamellae, but these lamellae are smaller and less frequently extended than in more adherent cells. Decreased rate of lamellipodial extension or decreased probability of formation of a stable attachment to the surface by the lamellae likely account for reduced migration at low adhesiveness. The rate of cell locomotion in *Dictyostelium* is proportional to the frequency of lamellipod extension (Wessels et al., 1994).

Besides ECM protein concentration, receptor expression, and receptor-extracellular ligand affinity, the integrin-cytoskeletal linkage is another potential control point for cell/substratum adhesiveness and cell migration speed (Williams et al., 1994). Previous studies suggest that intermediate levels of cytoskeletal molecules promote maximal migration (summarized in Huttenlocher et al., 1995). For example, a decrease in vinculin expression increases 3T3 cell motility (Fernandez et al., 1993) but inhibits neurite outgrowth (Varnum-Finney and Reichardt, 1994). One expects that optimal ligand density for migration would increase as integrin-cytoskeleton affinity decreases. $\alpha IIb\beta 3$ receptors with $\beta 3$ cytoplasmic domain deletions show that alterations in integrin-cytoskeletal interactions shift the migration vs. fibrinogen concentration relationship and that increased or decreased focal adhesion formation inhibits maximum cell migration speed (Huttenlocher et al., 1996). Quantitatively studying integrin-cytoskeletal associations is currently complex because measurement of intracellular affinities is difficult and any mutations which alter integrin-cytoskeleton affinity are also likely to affect integrin signaling properties, such as formation of adhesion structures. However, characterization of integrin/cytoskeletal interactions is necessary to further our understanding of the role of cell/substratum adhesiveness in mediating cell migration speed.

Our most significant finding is that cell migration speed can be rationally increased or decreased by altering cell/substratum adhesiveness in several different ways. Thus, at any substratum ECM concentration, an optimal receptor concentration exists to provide maximal migration. Relatively small changes in receptor expression or substrate ligand concentration can significantly change cell migration speed. In fact, at the maximum cell speed, receptor expression and ECM concentration are inversely related. The maximum attainable migration speed is not a function of receptor expression level.

Likewise, integrin/ECM ligand affinity also modulates cell migration speed through cell-substratum adhesiveness. Increased $\alpha IIb\beta 3$ affinity for fibrinogen, by mutations in the ligand-binding domain or antibody activation, correspondingly decreases the fibrinogen concentration which promotes optimum migration. Maximum migration speed is not a function of receptor-ligand affinity for cells migrating on a 2-dimensional surface, but maximum speed appears to decrease some with affinity in a random transwell assay (Huttenlocher et al., 1996). Reasons for this discrepancy are unclear but are likely related to differences in how the assays measure migration. CHO cells transfected with $\alpha IIb\beta 3$ mutants with reduced fibrinogen binding affinity compared to wild-type $\alpha IIb\beta 3$ (Bajt and Loftus, 1994) do not adhere to nor migrate upon a surface coated with any concentration of fibrinogen. Since integrins are very low affinity receptors it is difficult to generate a low affinity mutant which does not completely abrogate ligand binding.

This inter-relation between migration and adhesiveness has important implications in therapeutic applications, such as inhibition of neovascularization (Nicosia and Bonanno, 1991) or tumor metastasis (Rudolph and Cheresh, 1990; Ruoslahti, 1992). In these applications, where decreased cell migration is generally desirable, targeting receptor expression or receptor-ligand affinity are potentially effective strategies. In biomaterials and tissue engineering applications (Cima and Langer, 1993; Langer and Vacanti, 1993), increased migration is often desired. Altering substrate ECM-protein concentration promises to be the easiest method to alter cell-substratum adhesiveness, but soluble factor approaches to effectively change receptor number or receptor-ligand affinity may allow additional control of adhesiveness.

3.9 References

Abercrombie, M., Heaysman, J. E. M., and Pegrum, S. M. (1970). The locomotion of fibroblasts in culture. I. Movements of the leading edge. *Exp. Cell Res.* **59**, 393-398.

Bajt, M. L. and Loftus, J. C. (1994). Mutation of a ligand binding domain of β_3 integrin. *J. Biol. Chem.* **269**, 20913-20919.

Bajt, M. L., Loftus, J. C., Gawaz, M. P., and Ginsberg, M. H. (1992). Characterization of a gain of function mutation of integrin $\alpha IIb\beta 3$ (platelet glycoprotein IIb-IIIa). *J. Biol. Chem.* **267**, 22211-22216.

Cary, L. A., Chang, J. F., and Guan, J. L. (1996). Stimulation of cell migration by overexpression of focal adhesion kinase and its association with Src and Fyn. *J. Cell Sci.* **109**, 1787-1794.

Cima, L. G. and Langer, R. (1993). Engineering human tissue. *Chem. Eng. Progr.* June, 46-54.

DiMilla, P. A., Barbee, K., and Lauffenburger, D. A. (1991). Mathematical model for the effects of adhesion and mechanics on cell migration speed. *Biophys. J.* **60**, 15-37.

Du, X., Plow, E. F., Frelinger, A. L. III, O'Toole, T. E., Loftus, J. C. and Ginsberg, M. H. (1991). Ligands "activate" integrin αIIbβ3 (platelet GPIIb-IIa). *Cell.* **65**, 409-416.

Felder, S., and Elson, E. L. (1990). Mechanics of fibroblast locomotion: quantitative analysis of forces and motions at the leading lamellas of fibroblasts. *J. Cell Biol.* **111**, 2527-2536.

Fernandez, J. L. R., Geiger, B., Salomon, D., and Ben-Ze'ev, A. (1993). Suppression of vinculin expression by antisense transfection confers changes in cell morphology, motility, and anchorage-dependent growth of 3T3 cells. *J. Cell. Biol.* **122**, 1285-1294.

Fox, J. E. B., Shattil, S. J., Rathbone, R. L. K., Richardson, M., Packham, M. A., and Sanaan, D. A. (1996). The platelet cytoskeleton stabilizes the interaction between αIIbβ3 and its ligand and induces selective movements of ligand-occupied integrin. *J. Biol. Chem.* **271**, 7004-7011.

Huttenlocher, A, Ginsberg, M. H., and Horwitz, A. F. (1996). Modulation of cell migration by integrin-mediated cytoskeletal linkages and ligand-binding affinity. *J. Cell Biol.* **134**, 1551-1562.

Huttenlocher, A., Sandborg, R. R., and Horwitz, A. F. (1995). Adhesion in cell migration. *Curr Opin. Cell Biol.* **7**, 697-706.

Jay, P. Y., Pham, P. A., Wong, S. A., and Elson, E. L. (1995). A mechanical function of myosin II in cell motility. *J. Cell Sci.* **108**, 387-393.

Kouns, W. C., Wall, C. D., White, M. M., Fox, C. F. and Jennings, L. K. (1990). A conformation-dependent epitope of human platelet glycoprotein IIIa. *J. Biol. Chem.* **265**, 20594-20601.

Kouns, W. C., Hadvary, P., Haering, P. and Steiner, B. (1992). Conformational modulation of purified glycoprotein (GP) IIb-IIIa allows proteolytic generation of active fragments from either active or inactive GPIIb-IIIa. *J. Biol. Chem.* **267**, 18844-18851.

Langer, R. and Vacanti, J. (1993). Tissue Engineering. *Science.* **260**, 920-926.

Lauffenburger, D. A. and Horwitz, A. F. (1996). Cell migration: a physically integrated molecular process. *Cell.* **84**, 359-369.

Marks, P. W., Hendey B. and Maxfield, F. R. (1991). Attachment to fibronectin or vitronectin makes human neutrophil migration sensitive to alterations in cytosolic free calcium concentration. *J. Cell. Biol.* **112**, 149-158.

Nicosia, R. and Bonnano, E. (1991). Inhibition of angiogenesis in vitro by Arg-Gly-Asp-containing synthetic peptide. *Am. J. Pathol.* **138**, 829-833.

Oliver, T., Dembo, M., and Jacobson, K. (1995). Traction forces in locomoting cells. *Cell Motility Cyto.* **31**, 225-240.

Rudolph, R. and Cheresh, D. (1990). Cell adhesion mechanisms and their potential impact on wound healing and tumor metastasis. *Clin. Plast. Surg.* **17**, 457-462.

59

Ruoslahti, E. (1992). Control of cell motility and tumor invasion by extracellular matrix interactions. *Brit. J. Canc.* **66**, 239-242.

Schreiner, C. L., Bauer, J. S., Danilov, Y. N., Hussein, S., Sczekan, M. M. and Juliano, R. L. (1989). Isolation and characterization of Chinese hamster ovary cell variants deficient in the expression of fibronectin receptor. *J. Cell Biol.* **109**, 3157-3167.

Varnum-Finney, B., and Reichardt, L. F. (1994). Vinculin-deficient PC12 cell lines extend unstable lamellipodia and filopodia and have a reduced rate of neurite outgrowth. *J. Cell. Biol.* **127**, 1071-1084.

Wessels, D., Vawter-Hugart, H., Murray, J., and Soll, D. R. (1994). Three-dimensional dynamics of pseudopod formation and the regulation of turning during the motility cycle of Dictyostelium. *Cell Motil. Cytoskeleton.* **27**, 1-12.

Williams, M. J., Hughes, P. E., O'Toole, T. E. and Ginsberg, M. H. (1994). The inner world of cell adhesion: integrin cytoplasmic domains. *Trends Cell Biol.* **4**, 109-112.

Zamarron, C, Ginsberg, M. H. and Plow, E. F. (1990). Monoclonal antibodies specific for a conformationally altered state of fibrinogen. *Thromb. Haemo.* **64**, 41-46.

TABLE 3.1. Soluble ^{125}I-Fibrinogen Binding Affinities (K_a) to Recombinant Integrins (from Bajt et al., 1992)

	αIIbβ3	αIIbβ3(β1-2)
Resting	$<1.4 \times 10^4$ M^{-1} ($K_d > 7$ mM)	$4.85 \pm 0.84 \times 10^6$ M^{-1} ($K_d = 206$ nM)
mAb 62 Activated	$1.66 \pm 0.33 \times 10^7$ M^{-1} ($K_d = 60$ nM)	$4.55 \pm 0.77 \times 10^7$ M^{-1} ($K_d = 22$ nM)

TABLE 3.2. Apparent Integrin-Fibrinogen Binding Affinities ($K_{a,app}$) and Activation Indices (I_A) for Resting State $\alpha IIb\beta3$ and $\alpha IIb\beta3(\beta1-2)$ Integrins.

	$\alpha IIb\beta3$	$\alpha IIb\beta3(\beta1-2)$
$K_{a,app}$	4.0×10^6 M^{-1} ($K_{d,app} = 250$ nM)	1.4×10^7 M^{-1} ($K_{d,app} = 71$ nM)
I_A	0.24	0.23
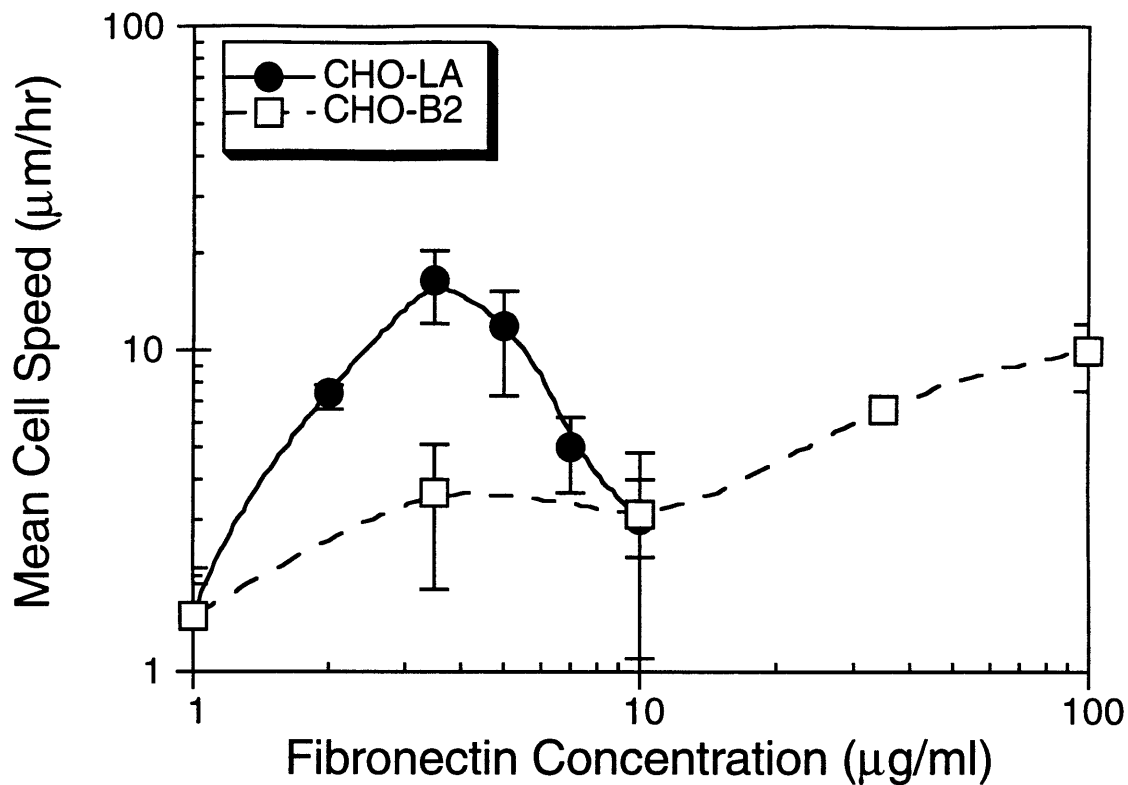
Figure 3.1. α5β1-Mediated Migration Depends on Substrate Fibronectin Concentration and α5 Expression Level. Mean cell migration speed is determined using videomicroscopy and image analysis to track cell centroids of CHO cells migrating on a fibronectin-coated glass coverslip as a function of time, as described in Chapter 2. Error bars indicate 95% confidence intervals for the mean cell speed. Wild-type CHO LA cells exhibit a biphasic dependence of cell speed on fibronectin concentration while α5-deficient CHO B2 cells exhibit a monotonic dependence
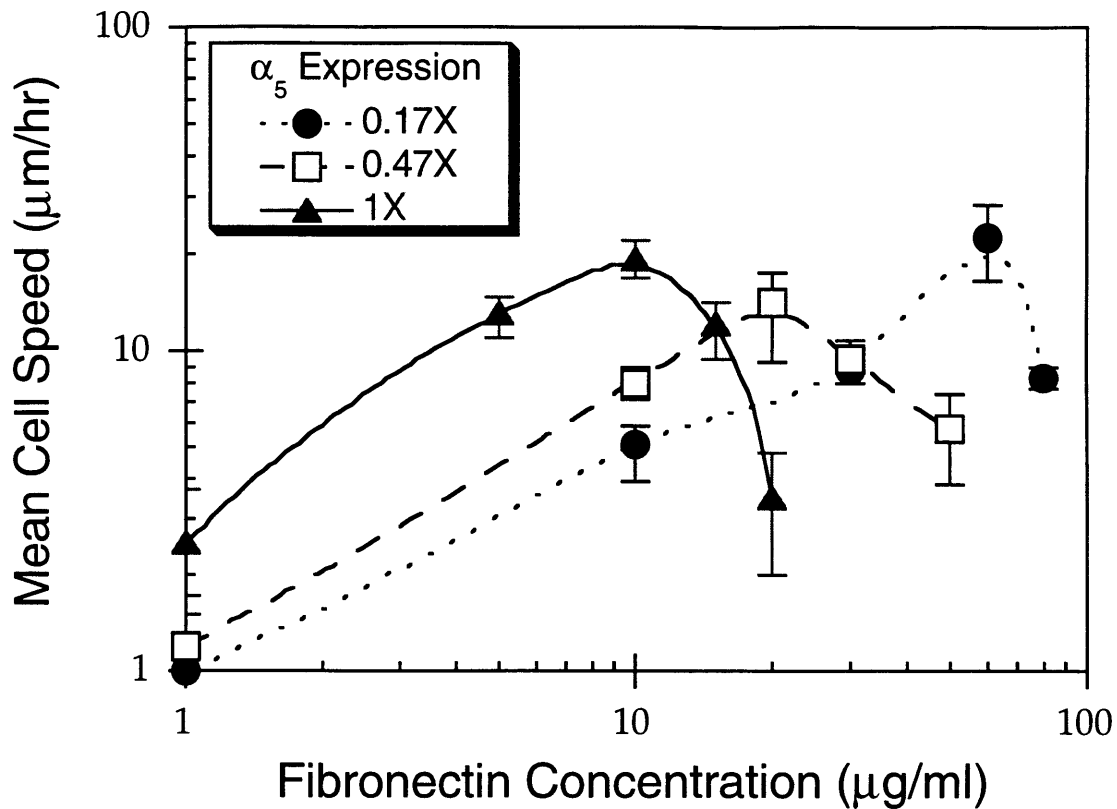
Figure 3.2. The Rate of α5β1-Mediated Migration Depends on Substrate Fibronectin Concentration and α5 Expression Level. Mean cell migration speed is determined using videomicroscopy and image analysis to track cell centroids of CHO cells migrating on a fibronectin-coated glass coverslip as a function of time, as described in Chapter 2. Error bars indicate 95% confidence intervals for the mean cell speed. CHO cell populations expressing different relative amounts of α5 integrin all have a biphasic migration speed dependence on fibronectin concentration (B). As α5 expression increases, the fibronectin concentration promoting maximal migration decreases. At low fibronectin concentrations, migration speed increases as α5 expression increases while at high fibronectin concentrations migration speed decreases as α5 expression increases. At intermediate fibronectin concentrations, intermediate α5 expression supports optimal migration speed. Maximum attainable migration speed is not a function of α5 expression.
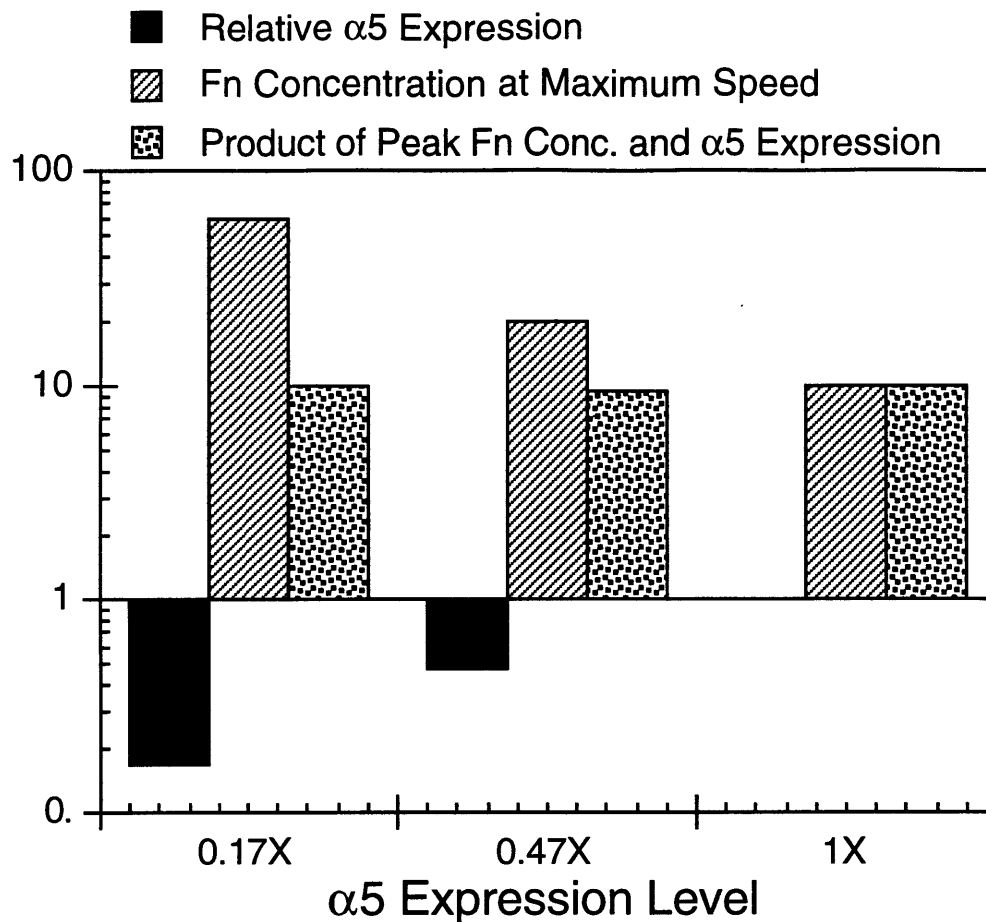
Figure 3.3. Fibronectin Concentration Promoting Maximal Cell Speed is Inversely Proportional to the α5 Expression Level. Migration speed of CHO cell populations expressing different relative amounts of α5 is measured using videomicroscopy and image analysis to track cell centroids of CHO cells migrating on glass coverslips coated with different fibronectin concentrations. As the α5 expression increases, the fibronectin concentration promoting optimal migration decreases. The product of α5 expression and fibronectin concentration, which is proportional to the number of bonds between the cell and substratum, remains a constant at the maximal migration speed.
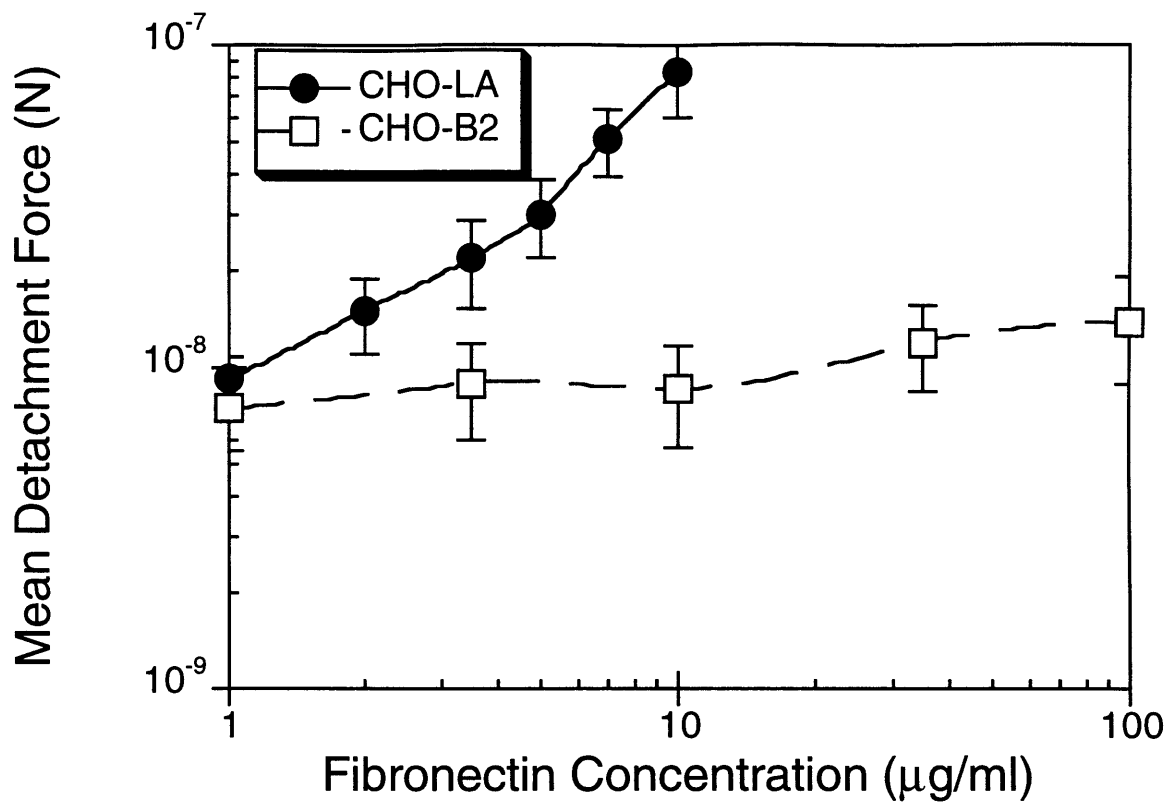
Figure 3.4. α5β1-Mediated Cell Adhesion to Fibronectin of CHO Cells Expressing Different Levels of α5 Integrin. Short-term mean cell detachment force, the force which detaches 50% of the cells, is measured by shear flow detachment of cells, as described in Chapter 2. Error bars represent 95% confidence intervals for the mean detachment force. Mean detachment force increases with fibronectin concentration for wild-type CHO LA cells but is independent of fibronectin concentration for α5-deficient CHO B2 cells.
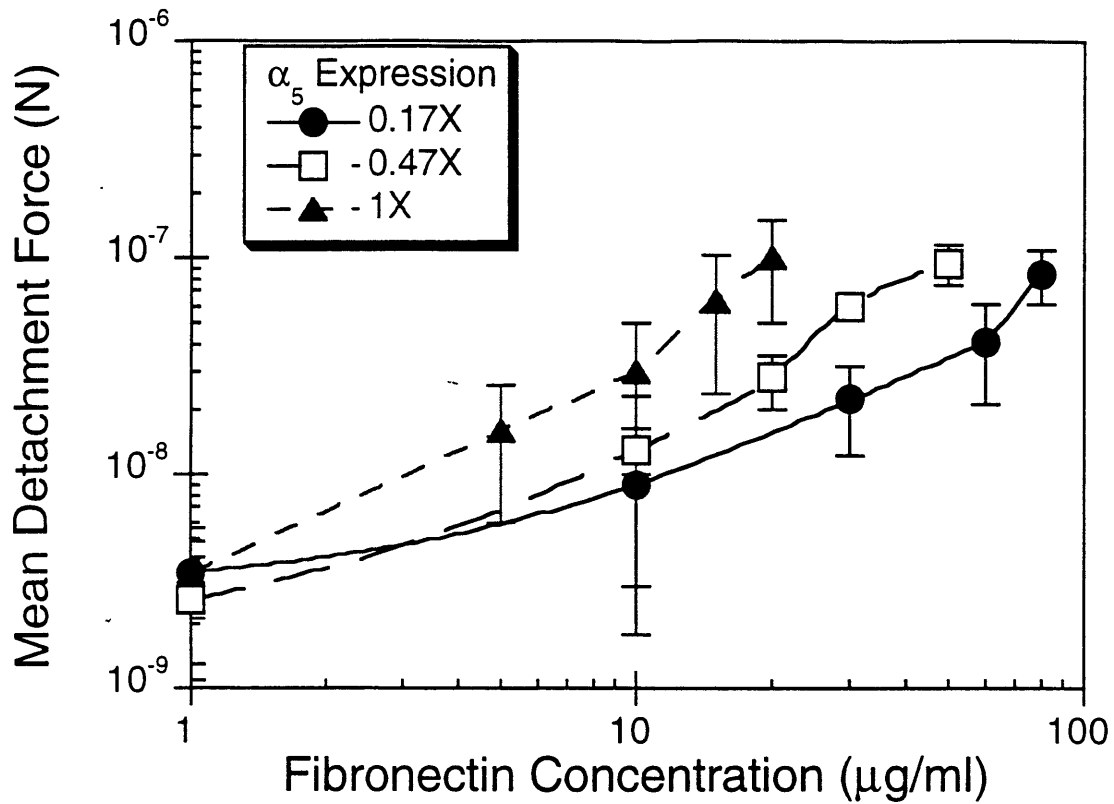
Figure 3.5. α5β1-Mediated Cell Adhesion to Fibronectin of CHO Cells Expressing Different Levels of α5 Integrin. Short-term mean cell detachment force, the force which detaches 50% of the cells, is measured by shear flow detachment of cells, as described in Chapter 2. Error bars represent 95% confidence intervals for the mean detachment force. CHO B2 cells were transfected with a human α5 cDNA and sorted by FACS into populations with different expression levels. Relative expression is denoted as a fraction of maximum expression. In each population the mean detachment force increases with the fibronectin concentration. For every fibronectin concentration, the mean detachment force increases as α5 expression increases.
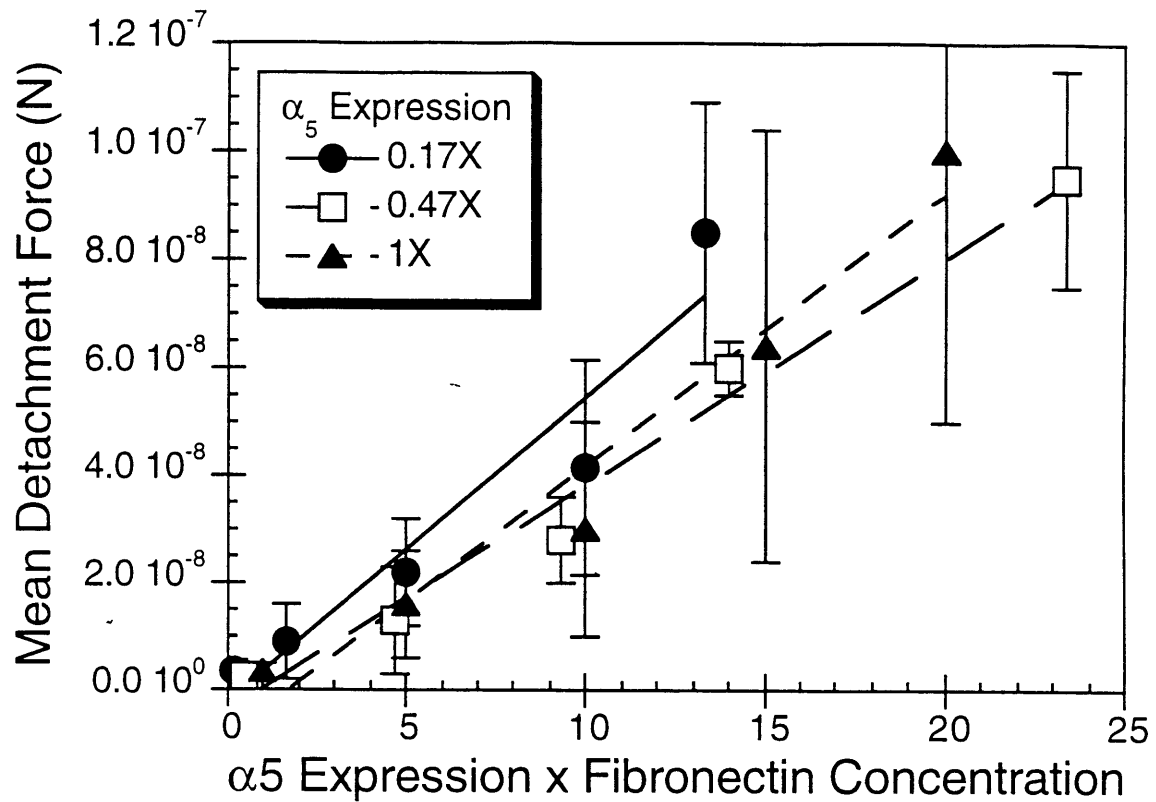
Figure 3.6. Short-Term Mean Cell Detachment Force is Linearly Related to the Apparent Number of Bonds Formed between the Cell and Substrate. The mean cell detachment force for CHO cells with different relative $\alpha 5$ expression levels is plotted against the product of the relative $\alpha 5$ expression and the substratum fibronectin concentration. This product is linearly proportional to the number of bonds between the cell and substratum (Equation 3.2). Error bars represent 95% confidence intervals for the mean detachment force. Each $\alpha 5$ expressing population has the same linear relationship between cell-substratum adhesiveness and cell-substratum bond number.
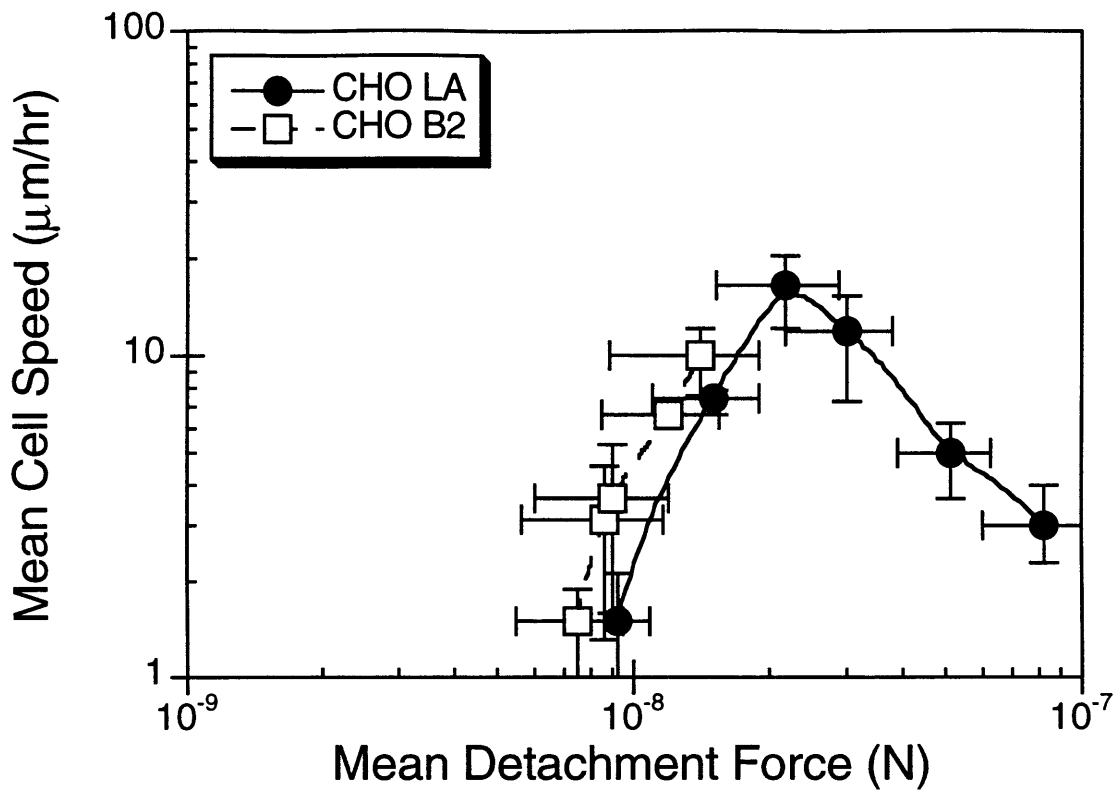
Figure 3.7. Changes in α5 Expression and Surface Fibronectin Concentration Modulate Cell Migration Speed by Altering Cell-Substratum Adhesiveness. Short-term mean cell detachment force is measured by shear flow detachment and mean cell migration speed is determined using videomicroscopy and image analysis to track cell centroids of CHO cells migrating on a fibronectin-coated glass coverslip as a function of time, as described in Chapter 2. Error bars represent 95% confidence intervals of the mean detachment force or mean cell speed. Wild-type CHO LA cells display a biphasic dependence of mean cell speed on short-term detachment force. CHO B2 cells cannot attain high enough adhesiveness to the substratum to promote optimal migration.
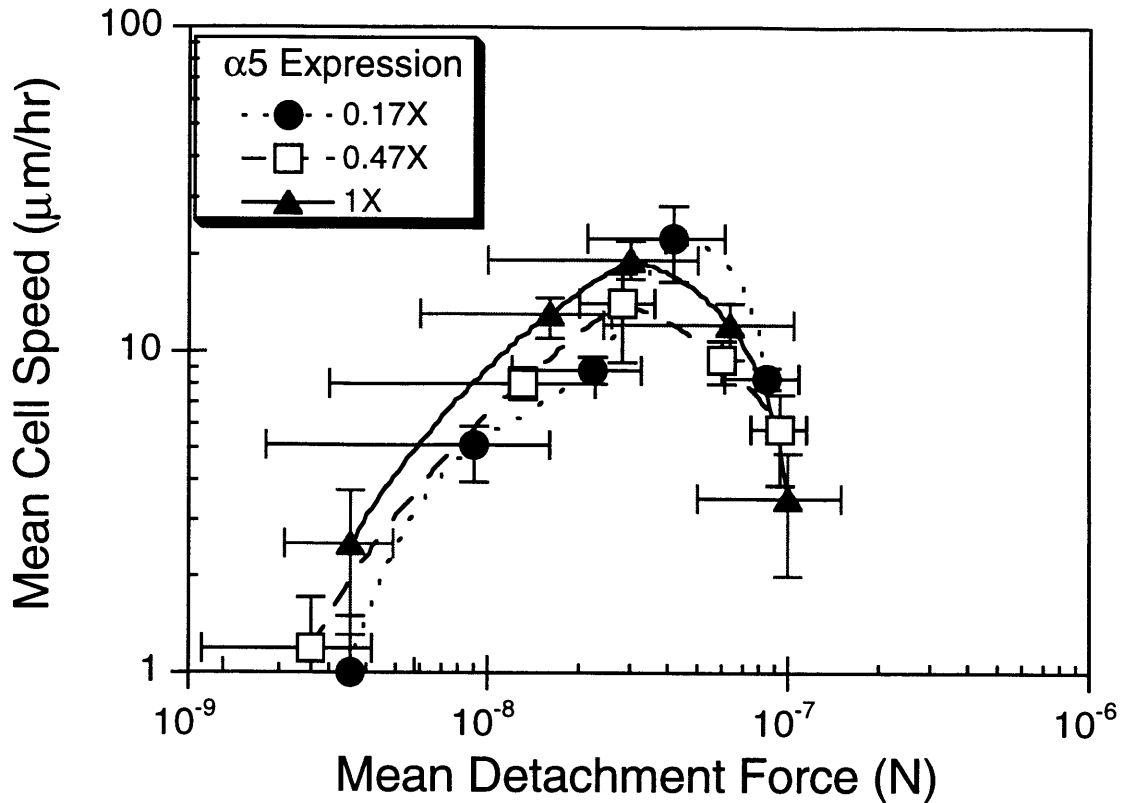
Figure 3.8. Changes in α5 Expression and Surface Fibronectin Concentration Modulate Cell Migration Speed by Altering Cell-substratum Adhesiveness. Short-term mean cell detachment force is measured by shear flow detachment and mean cell migration speed is determined using videomicroscopy and image analysis to track cell centroids of CHO cells migrating on a fibronectin-coated glass coverslip as a function of time, as described in Chapter 2. Error bars represent 95% confidence intervals of the mean detachment force or mean cell speed. CHO B2 cells transfected with human α5 and sorted into populations with different relative α5 expression demonstrate that as fibronectin substratum concentration or α5 expression change, the relationship between migration speed and mean detachment force is a constant, biphasic function.
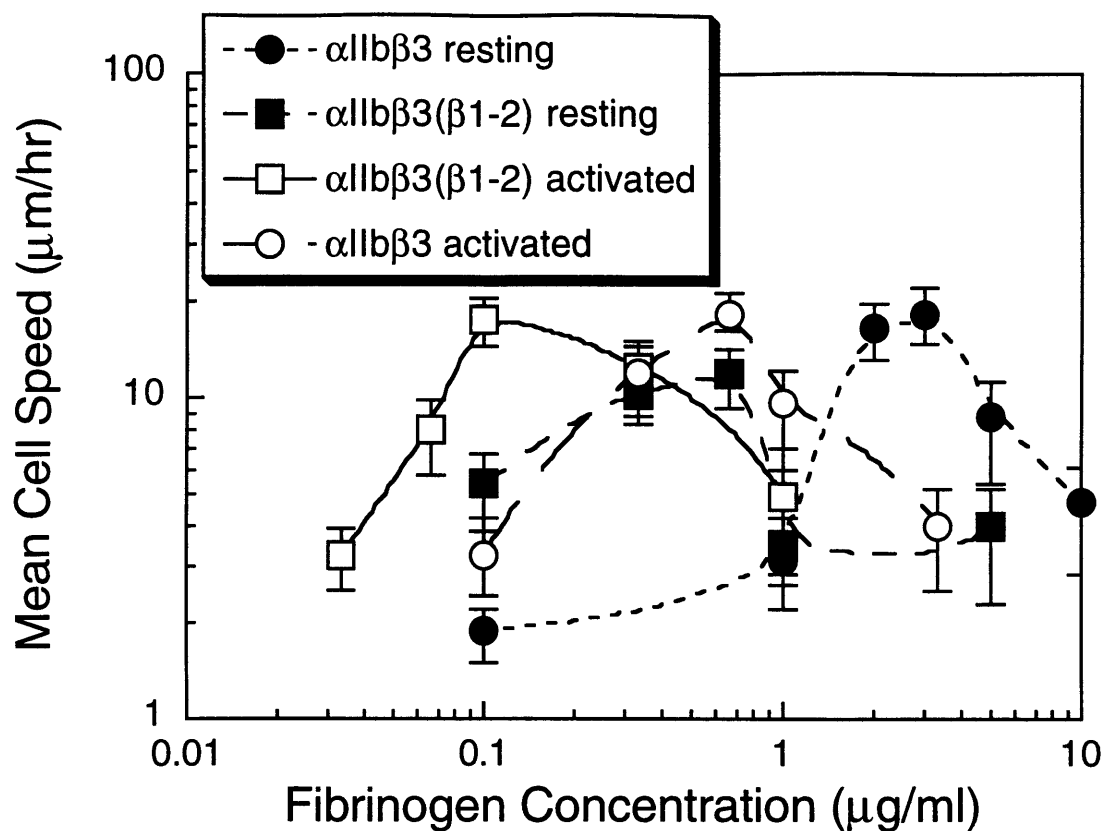
Figure 3.9. αIIbβ3-Mediated Migration Depends on Substrate Fibrinogen Concentration and αIIbβ3-Fibrinogen Binding Affinity. Mean cell migration speed is determined using videomicroscopy and image analysis to track cell centroids of CHO cells migrating on a fibronectin-coated glass coverslip as a function of time, as described in Chapter 2. Error bars indicate 95% confidence intervals for the mean cell speed. CHO cells are transfected with wild-type αIIbβ3 integrin or αIIbβ3(β1-2), a high affinity mutant. Both integrins are activated to a higher-affinity conformation by incubation with mAb 62. Receptors in each affinity state promote migration which has a biphasic dependence on fibrinogen concentration. Increasing receptor-ligand affinity reduces the fibrinogen concentration which promotes maximum cell migration. Maximum attainable migration speed is not a function of receptor-ligand affinity.
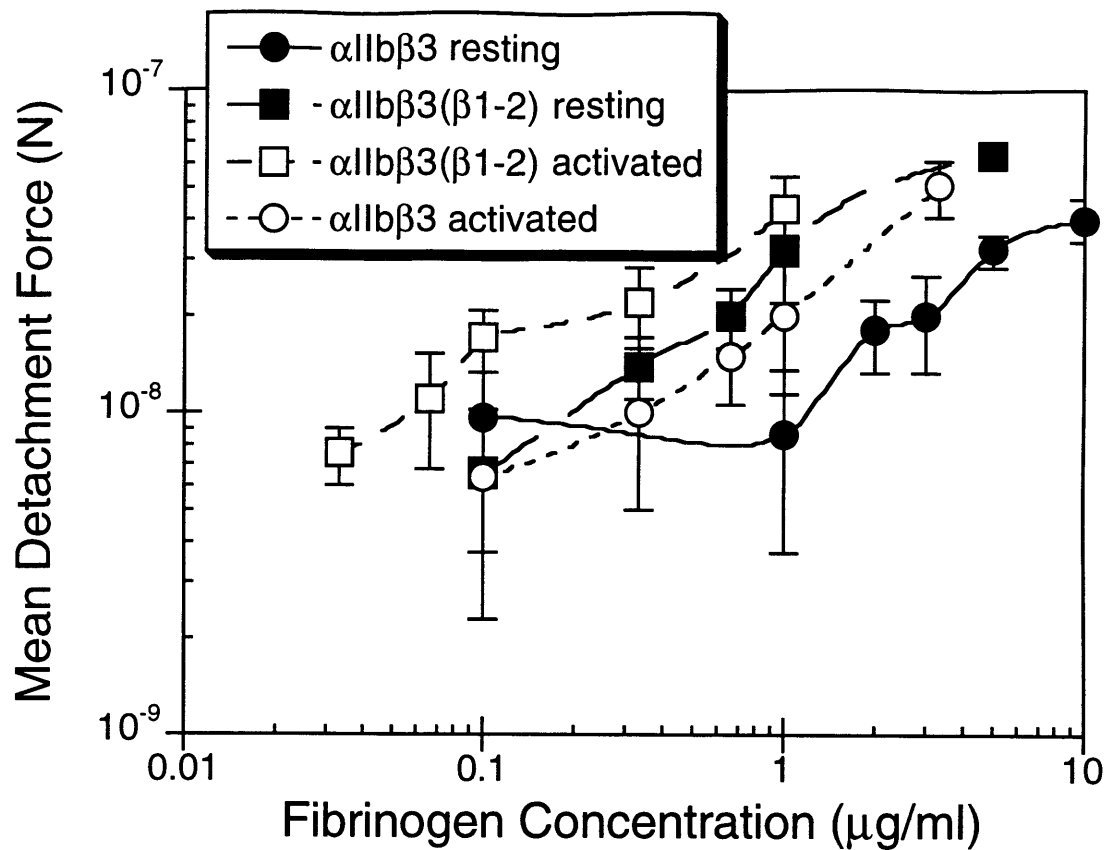
Figure 3.10. Adhesion of CHO Cells Transfected with αIIbβ3 Integrin Increases as Receptor-Ligand Affinity Increases. CHO cells are transfected with wild-type αIIbβ3 integrin or αIIbβ3(β1-2), a high affinity mutant. Both integrins are activated to a higher-affinity conformation by incubation by mAb 62. Short-term mean cell detachment force is measured by shear flow detachment, as described in Chapter 2. Error bars represent 95% confidence intervals of the mean detachment force. Short-term mean detachment force increases with fibrinogen concentration for each receptor-ligand affinity state. At any fibrinogen concentration, detachment force increases as affinity increases due to the β3 to β3(β1-2) mutation or antibody activation.
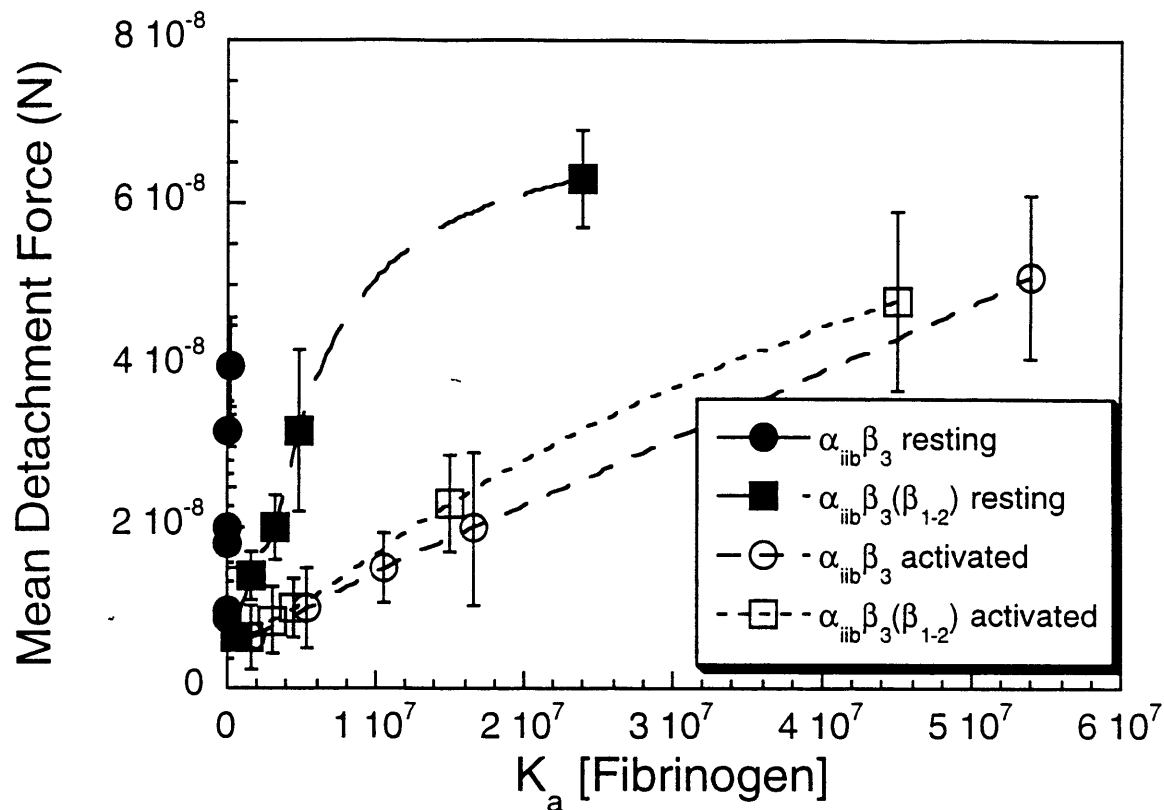
Figure 3.11. Activated αIIbβ3 Has a Higher Detachment Force at Each Apparent Bond Number than Resting State αIIbβ3. CHO cells are transfected with wild-type αIIbβ3 integrin or αIIbβ3(β1-2), a high affinity mutant. Both integrins are activated to a higher-affinity conformation by incubation with mAb 62. Short-term mean cell detachment force is measured by shear flow detachment, as described in the Materials and Methods. Error bars represent 95% confidence intervals of the mean detachment force. The product of receptor-ligand affinity and fibrinogen concentration is proportional to the apparent number of bonds between the cell and substratum. mAb 62 activated αIIbβ3 and αIIbβ3(β1-2) have the same linear relationship between detachment force and apparent bond number. Non Ab-activated αIIbβ3 and αIIbβ3(β1-2) have a higher detachment force at each apparent bond number than activated integrins. These data are consistent with integrin activation due to binding of immobilized ligand.
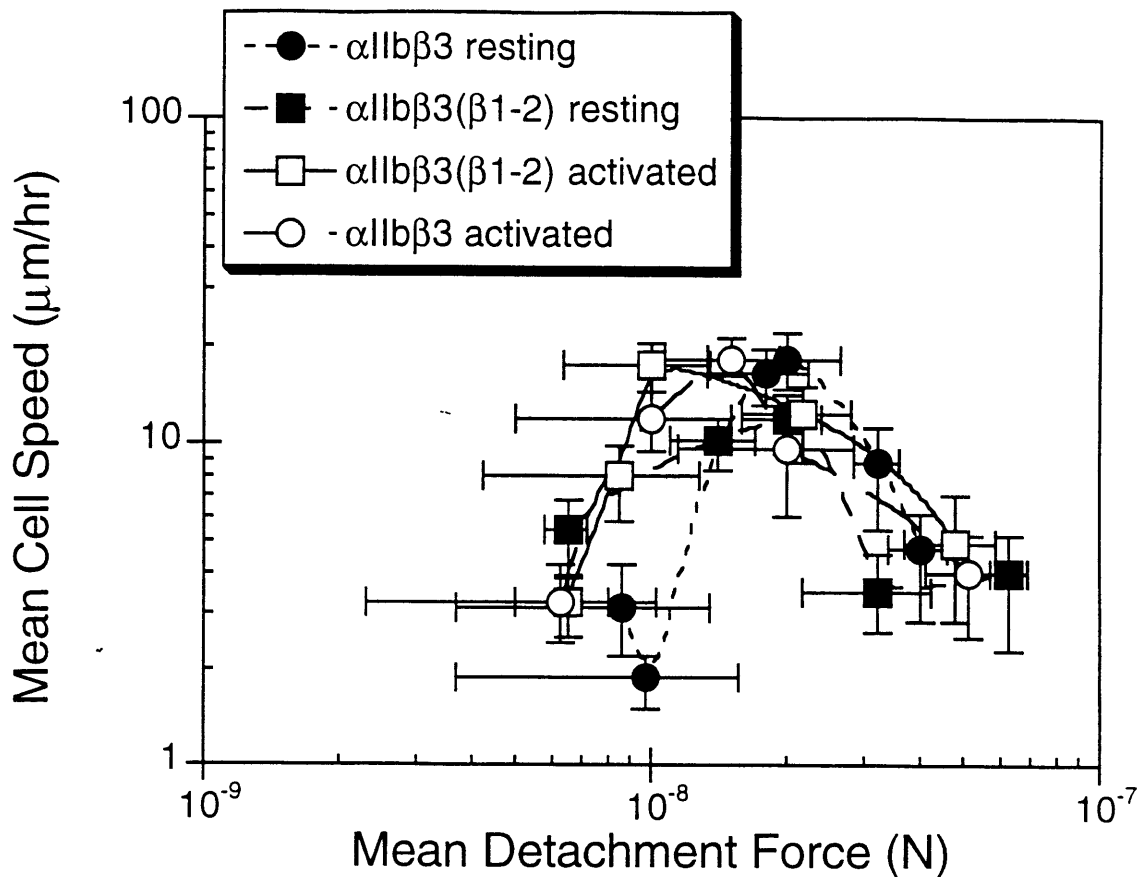
Figure 3.12. Cell Migration Speed Correlates with Cell-Substratum Adhesiveness as $\alpha IIb\beta3$-Fibrinogen Affinity and Surface Fibrinogen Concentration Change. Short-term mean cell detachment force is measured by shear flow detachment and mean cell migration speed is determined using videomicroscopy and image analysis to track cell centroids of CHO cells migrating on a fibronectin-coated glass coverslip as a function of time, as described in Chapter 2. Error bars represent 95% confidence intervals of the mean detachment force or mean cell speed. CHO cells are transfected with wild-type $\alpha IIb\beta3$ integrin or $\alpha IIb\beta3(\beta1-2)$, a high affinity mutant. Both integrins are activated to a higher-affinity conformation by incubation with mAb 62. As $\alpha IIb\beta3$-fibrinogen affinity increases due to the $\beta3$ to $\beta3(\beta1-2)$ mutation or mAb 62 activation, the cell migration speed dependence on short-term adhesiveness remains a constant, biphasic relationship.

Chapter 4: Regulation of Cell-Substratum Detachment through Integrin-Mediated Linkages

4.1 Introduction to Rear Detachment

As discussed in Chapter 1.1, the complex process of migration can be usefully conceived of as a dynamic arrangement of a number of distinct events, including membrane protrusion, formation of stable contacts between the cell and extracellular matrix (ECM), cytoskeletal contraction, cell body translocation, and release of cell-substratum adhesions at the rear of the cell (Stossel, 1993; Sheetz, 1994; Lauffenburger and Horwitz, 1996; Mitchison and Cramer, 1996). In some circumstances, proteolytic degradation of extracellular matrix is also required to allow a cell to release connections to its environment (Werb, 1997). Cell migration is not likely to be universally limited over a comprehensive range of movement environments by any single one of these individual motility processes (Lauffenburger and Horwitz, 1996). For instance, in some circumstances migration speed seems to be governed by lamellipod extension and attachment (Wessels et al., 1994), whereas in others rear detachment appears to be limiting (Marks et al., 1991; Jay et al., 1995). In general, quantitative studies elucidating conditions under which various motility processes are rate-limiting for cell migration speed have not yet been pursued.

Cell migration is regulated, at least in part, through cell-substratum adhesive interactions with maximum speed occurring at an intermediate adhesiveness (Chapter 3; Goodman et al., 1989; Duband et al., 1991; DiMilla et al., 1993; Keely et al., 1995; Huttenlocher et al., 1996). At low adhesiveness, cytoskeletal forces disrupt cell-substratum attachments so that cells are unable to generate the traction needed for locomotion. At high adhesiveness, cytoskeletal forces are insufficient to break cell-substratum attachments, leaving cells spread but incapable of locomotion. At intermediate adhesiveness cytoskeletal forces are roughly in balance with adhesion so that traction can be maintained at the cell front while it can be disrupted at the cell rear, permitting net cell body movement (DiMilla et al., 1991; Sheetz, 1994; Huttenlocher et al., 1995).

In environments where rear detachment limits cell migration speed, it can be hypothesized that breakage of cell-substratum attachments is an important local regulatory event. Breakage of cell-substratum attachments needed to allow locomotion can, in principle, occur by either intracellular or extracellular fracture of the cytoskeletal-integrin-ECM linkage. For fibroblasts migrating in vitro, a large fraction of integrins in adhesion structures has been found to be released from the cell and left on the substratum (Regen and Horwitz, 1992; Palecek et al., 1996). The remaining integrins release from the substratum and either move forward along the cell edge as an aggregate to form a new adhesion or disperse into the cell membrane. Interestingly, integrin release from the cell membrane also appears to occur during the migration through extracellular

75

matrices by corneal fibroblasts in vivo (Hay, 1985) and by tumor cell lines in vitro (Niggemann et al., 1997). Mechanisms of rear release include contributions from cytoskeletal contractility. Dictyostelium expressing myosin II mutants show inhibited migration on adhesive substrata (Jay et al., 1995) and antibodies against myosin light chain kinase inhibit migration when injected into macrophages (Wilson et al., 1991).

In this chapter we address the issue of how the release of adhesions at the cell rear can regulate the rear detachment rate and cell speed. We track integrins at the rear of migrating CHO cells as we vary cell-substratum adhesiveness through ECM concentration, receptor expression, and receptor-ligand affinity. Using a fluorophor conjugated to anti-integrin monoclonal antibodies we can visualize and quantitate the relative fraction of integrin which detaches from the cell upon rear retraction.

4.2 Experimental System

4.2.1 Cell Systems

The CHO cell systems used in Chapters 2 and 3 to study regulation of speed through cell adhesiveness were also used to study the fate of integrin-cytoskeleton and integrin-matrix bonds at the rear of migrating cells. The CHO B2 system, transfected with the $\alpha 5$ subunit and selected into subpopulations with different $\alpha 5\beta 1$ integrin expression, was used to determine the effects of ECM concentration and integrin expression on cell detachment. CHO cells with $\alpha IIb\beta 3$ integrins in different affinity states were used to determine the effects of ECM concentration and receptor-ligand affinity on cell detachment.

Previously, chick skeletal muscle fibroblasts have been used to study molecular events during rear detachment (Palecek et al., 1996; Regen and Horwitz, 1992). Fibroblasts are more polarized than CHO cells, allowing easier identification of the cell rear, and form larger integrin aggregates than CHO cells. CHO cells are much more amenable to genetic manipulations and allow us to study rear detachment over a wider range of integrin-ligand binding conditions.

4.2.2 Antibodies and Reagents

Fibronectin was prepared from human plasma as described previously (Ruoslahti et al., 1982). Fibrinogen was obtained from Sigma Chemical Company. The $\alpha IIb\beta 3$ activating monoclonal antibody mAb62, which recognizes an epitope on $\beta 3$, and the non-adhesion perturbing $\alpha IIb\beta 3$ monoclonal antibody D57 were used as described previously (O'Toole et al., 1990;

Frelinger et al., 1991; O'Toole et al., 1994). The anti-human $\alpha5$ monoclonal antibody 6F4 was a gift of Dr. Ralph Isberg (Tufts University).

D57 MAb was conjugated to Oregon Green 488 carboxylic acid, succinimidyl ester (Molecular Probes) and 6F4 MAb was conjugated to carboxy-X-rhodamine, succinimidyl ester (Molecular Probes). 180 µl of MAb diluted to 1.25 mg/ml in 0.1 M sodium bicarbonate at pH 8.3 were stirred for 1 hour at room temperature with 10 µl of the fluorophor dissolved in DMSO at 10 mg/ml. 10 ml of 1.5 M hydroxylamine pH 8.5 were stirred with the reaction mixture for 1 hour at room temperature to stop the reaction and remove dye from unstable conjugates. Conjugated MAb was separated from free dye by gel filtration on Sephadex G-25 minicolumns, prepared as follows. The ends of glass Pasteur pipettes were broken off and the remaining center cylinder was acid-washed and silaned to reduce protein adsorption to the glass surface. A small piece of cotton was placed in the bottom of the pipette and 1 ml Sephadex G-25 (Pharmacia Inc.), swelled in PBS, was added to the pipette and allowed to settle while the column was rinsed with several volumes of pH 8.3 NaHCO3. The MAb-dye solution was added to the top of the column and allowed to drain into the column. pH 8.3 NaHCO3 was added to the column and the first fluorescent peak was collected, aliquoted, wrapped in foil, and stored under argon at -80 °C.

4.2.3   Immunofluorescence and Phase-Contrast Microscopy

Cells were allowed to attach to the microscopy plate for 2 hours prior to staining. The cells were then incubated for 30 minutes at 37 °C with Oregon Green-conjugated MAb D57 or rhodamine-conjugated MAb 6F4, diluted to 40 µg/ml in warm CCM1. The cells were rinsed 5X with warm CCM1 and 3 ml of warm CCM1 was added to the plate. Stained cells were placed in a temperature-regulated, humidified chamber, described previously (Regen and Horwitz, 1992), mounted on the inverted microscope stage. Warmed, humidified 10% CO_2 was passed over the cells to maintain correct pH. A field with 3-5 cells which were stained brightly with respect to the background was selected. Fluorescent images of the cells were acquired every 30 minutes for 2 hours using a 3 second exposure. Cell position as a function of time was determined by acquiring phase contrast images immediately after the fluorescence images.

A Nikon Diaphot inverted microscope with a x60/1.4 NA phase planapochromat objective was used for immunofluorescent studies. An electronic shutter (Uniblitz, Vincent Associates, Rochester, NY) controlled the fluorescence illumination by a 100 W mercury lamp. Phase contrast images were illuminated using a 50 W halogen lamp. A cooled CCD camera (CE200A, Photometrics, Tucson, AZ) acquired and digitized images were sent to a Quadra 950 (Apple Computer) for analysis. Oncor Image software (Oncor Imaging, Rockville, MD) was used to control the camera shutter and process the images.

77

4.2.4 Image Analysis

Cell perimeter at each time point was determined by manually tracing cell edges on the phase contrast images. The cell area which retracted between t1 and t2 was determined by subtracting a mask of the cell area at t2 from the mask at t1. The fraction of integrin which ripped from the cell upon rear retraction between t1 and t2 was calculated as the ratio of mean fluorescent intensity in the retraction area after detachment to the mean fluorescent intensity in the retraction area before detachment. Average intensity outside the cell was subtracted from the mean intensities to correct for background fluorescence. Retractions of lamellipodia were neglected and retraction areas less than 2 μm wide were also not used. If a cell retracted from the same area more than once, only the first retraction was used. 75-150 different detachments in at least 8 different cells were measured at each condition. Fluorescence diminishment due to photobleaching was negligible for the exposure times used. Intensity of integrin patches which ripped from the cell remained constant for several hours after detachment.

4.3 Rear Detachment is Rate-Limiting for Cells Migrating at High Adhesiveness

Intuitively, one expects cell speed to be limited by the formation of adhesions and the generation of traction forces at low cell-substratum adhesiveness and by release of adhesions at high adhesiveness. We addressed the issue of release at high adhesiveness by comparing the rate of cell-substratum detachment to cell speed. Cell-substratum detachment rate was measured by outlining areas of a cell which detached from the substrate during a 30 minute time interval and cell speed was assayed by measuring cell centroid displacement at 15 minute time intervals and fitting the path to a persistent random walk model.

If rear detachment were the rate-limiting step for migration speed, the rate of detachment should roughly equal the cell speed. Cell speed, normalized to cell diameter, is plotted as a function of detachment rate in Figure 4.1. Mean cell diameter and area were calculated from phase contrast images of more than 50 cells at each ECM concentration. At very low adhesiveness, detachment rates are significantly higher than cell speed. This means that the cell is detaching from the substratum in multiple directions simultaneously, resulting in little movement of the cell centroid. Very low detachment rates correspond to high adhesiveness. In this regime, cell speed is about equal to detachment rate. At intermediate adhesiveness, the detachment rate and migration speed are both high.

The ratio of migration speed to detachment rate provides a quantitative measure of how efficiently the cell detaches. A high ratio of speed to detachment rate indicates that most of the

detachments lead to a change in cell centroid position and suggests that cell speed is limited by the rate of detachment (Figure 4.2). A low ratio indicates that the detachments do not effectively produce movement of the cell centroid and that speed is limited by another aspect of motility. At low adhesiveness ($< 10^{-8}$ N) the ratio of speed to detachment rate ranges from 0.2 - 0.4, suggesting that cell speed is not limited by rear detachment under these conditions. However, at adhesiveness of 2 X 10^{-8} N -- where the cells migrate at maximum speed -- and above, the ratio of speed to detachment rate is 0.6 - 0.8. Under these conditions cell speed is limited by rear detachment rate.

When locomotion occurs at essentially a steady state, the rate of detachment must equal the rate of formation of new attachments to maintain an approximately constant cell area. Time-lapse videomicroscopy indicates that at high ECM concentrations these cells extend membrane at rates significantly greater than they locomote or retract stable adhesions, indicating that membrane protrusion does not limit cell speed at high adhesiveness. The probability of these protrusions forming stable attachments to the substratum may also limit cell speed. However, the probability of forming-stable adhesions is likely to increase as cell adhesiveness increases, so adhesion formation is not consistent with limiting cell speed at high adhesiveness.

4.4 Integrin Release from the Rear of Migrating Cells Increases with ECM Concentration, Integrin Expression, and Integrin-ECM Affinity

Since the detachment rate limits cell speed at high adhesiveness, molecular parameters which affect cell detachment will also limit cell speed at high adhesiveness. One expects that the rate of rear detachment is primarily a function of the contractile force generated at the cell rear and the strength of integrin-mediated linkages between the cell and substrate. At high adhesiveness, for example, more cell-substratum bonds exist, inhibiting rear retraction. We explored the locus of cell-substratum linkage fracture in regulating cell detachment, and the consequential effects on cell speed, as a function of adhesiveness. If the integrin-ECM linkage were to fracture, the integrins would detach from the substratum and remain in the cell but if integrin-cytoskeleton or other cytoskeletal bonds were to fracture, the integrins would rip from the cell membrane and remain attached to the substratum. Thus the amount of integrin which rips from the cell is a measure of the relative strength of integrin-ligand bond compared to other bonds in the linkage, with the weaker bonds preferentially fracturing. A mechanism of active linkage release would likely act intracellularly and lead to an increase in the amount of integrin which rips from the cell during rear retraction.

We determined the locus of fracture of the cytoskeleton-ECM-integrin linkage by tracking integrins at the rear of migrating cells. We used nonadhesion-perturbing anti-integrin MAbs

79

conjugated with fluorescent dyes to determine the fate of integrin adhesion receptors at the rear of migrating CHO cells. We used phase contrast imaging to determine the cell retraction area and quantitative fluorescence microscopy to measure the fraction of integrin which ripped from the cell in this area upon rear retraction. Cell-substratum adhesiveness was varied by altering the number of cell-substratum bonds through three variables: ECM protein concentration, receptor expression level, and receptor ligand affinity. $\alpha 5$-deficient CHO B2 cells were transfected with a human $\alpha 5$ cDNA and sorted by flow cytometry into populations with three different relative $\alpha 5$ expression levels (0.17X, 0.47X, and 1X) to vary $\alpha 5\beta 1$ fibronectin receptor expression. To vary integrin-ECM affinity we used CHO cells transfected with the $\alpha IIb\beta 3$ fibrinogen receptor, an extracellular domain mutation of the $\beta 3$ subunit in which 6 amino acids of the ligand (Bajt et al., 1992) binding domain are replaced with sequences derived from the $\beta 1$ integrin subunit. This mutation increases the affinity of the integrin for fibrinogen. An even higher affinity state occurs when $\alpha IIb\beta 3(\beta 1-2)$ is activated with anti-LIBS2 antibody (Frelinger et al, 1991). Soluble fibrinogen binding affinities for $\alpha IIb\beta 3$ and $\alpha IIb\beta 3(\beta 1-2)$ in resting and MAb 62 activated state are shown in Table 3.1.

Migrating CHO cells organize integrins into smaller, less concentrated clusters than migrating fibroblasts. Integrins form larger clusters as ECM concentration, integrin expression level, and integrin-ECM affinity increase. The resolution of individual adhesion structures was too low to determine accurately their sizes and intensities, however, so we focused on comparing the amount of integrin in the entire membrane retraction area pre- and post-retraction. Endocytic vesicles containing integrins tend to accumulate in the perinuclear region of CHO cells, as in fibroblasts (Regen and Horwitz, 1992; Palecek et al., 1996). Figure 4.3 shows wild-type $\alpha IIb\beta 3$ integrin movement in CHO cells migrating on different concentrations of fibrinogen. At low fibrinogen concentrations (Figure 4.3A,B) the majority of the integrin in the rear retraction area detaches from the substratum and moves with the cell. At high fibrinogen concentrations the majority of the integrin in the retraction area rips from the cell and remains attached to the surface as an integrin trail (Figure 4.3C,D). At intermediate fibrinogen concentrations, an intermediate amount of integrin tends to detach from the cell (Figure 4.3E,F). Average pixel intensities before (I_1) and after (I_2) detachment and average background intensities (I_B) are shown in Table 4.1. The fraction of fluorescent intensity (F) remaining in the detachment area after rear retraction is calculated as: $F=(I_1-I_B)/(I_2-I_B)$.

Figure 4.4 shows histograms of the fraction of $\alpha IIb\beta 3$ integrin that is left in the retraction area from each detachment event after the cell rear detaches from substrates coated with different amounts of fibrinogen. At each fibrinogen concentration a wide range of fractions exists, ranging from virtually no integrin to virtually all of the integrin in the retraction area ripping from the cell. At low fibrinogen concentrations less integrin tends to rip from the cells than at higher concentrations, consistent with visual observations (Figure 4.3). A small fraction of integrin

(<20%) is commonly left on the surface at 0.6 µg/ml fibrinogen, when the cells are not adherent enough to migrate well. At least some integrin is almost always left when the cells are on fibrinogen concentrations where they migrate optimally (2 µg/ml) or too adherent to migrate optimally (5 µg/ml). The mean fraction of integrin deposited on the surface increases from 0.27 ± 0.18 at 0.6 µg/ml fibrinogen to 0.46 ± 0.15 at 5 µg/ml fibrinogen.

Integrins become more likely to release from the cell as ECM concentration increases (Figure 4.4). To determine whether this is generally due to an increase in cell-substratum adhesiveness and a corresponding increase in the number of cell-substratum bonds, we measured integrin release in CHO cells expressing different levels of α5 integrin or αIIbβ3 integrins with different affinities for fibrinogen. In CHO cells expressing different levels of α5, integrin release increases with fibronectin concentration at each of the expression levels (Figure 4.5). At each fibronectin concentration, integrin release increases as receptor expression increases. Receptor clustering may also increase as ECM concentration increases, so that integrin clustering could correlate with increased integrin release onto the substratum. The linkage fracture point is a function of integrin-ECM and intracellular avidities, so as integrin-ECM affinity increases we expect an increase in integrin release. Our observations verify this idea; at each fibrinogen concentration, integrin release increases as receptor-ligand affinity increases (Figure 4.6). Integrin release also increases as fibrinogen concentration increases for each αIIbβ3-fibrinogen affinity state.

4.5 Integrin Release from the Rear of Migrating Cells Correlates with Cell-Substratum Adhesiveness

Integrin release onto the substratum increases as cell-substratum adhesiveness increases due to changes in ECM concentration, receptor number, and receptor-ligand affinity. Cell speed is also a constant function of adhesiveness as these three variables change (Chapter 3). Therefore, if integrin release were to limit cell speed, one would expect that integrin release would also be a constant function of cell-substratum adhesiveness. Short-term cell-substratum adhesiveness is reported for each of these cell populations at the same experimental conditions we used to measure integrin release (Chapter 3). Cell-substratum adhesiveness was determined by shear flow detachment of cells after a 20 minute incubation. During this incubation period cells attach to the surface but do not organize integrins into focal adhesions or begin spreading. The reported mean detachment force is the shear force required to remove 50% of the cells from the substratum. Cell-substratum adhesiveness increases as ECM concentration, receptor expression, and receptor-ligand affinity increase and is linearly proportional to the number of cell-substratum bonds. To relate integrin release to adhesiveness, we plotted the mean fraction of integrin released from the cell

during rear detachment as a function of short term cell-substratum adhesiveness which we measured previously (Chapter 3). A constant, monotonically increasing relationship exists between the amount of integrin which releases from the cell and the adhesiveness as either receptor expression (Figure 4.7) or receptor ligand affinity (Figure 4.8) changes. This suggests that the mechanism of release of adhesions at the rear of migrating cells depends upon the adhesiveness, and thus the number of bonds, which exists between the cell and substratum. If release of adhesions at the rear of the cell was purely a biochemical mechanism we would expect the amount of integrin which releases from a cell to be independent of adhesiveness. Since there is a correlation between adhesiveness and integrin release, it appears that physical forces also play a role in release of adhesions.

4.6 Cell Speed has an Inverse Relationship to Integrin Release when Rear Detachment Limits Cell Locomotion Rate

Since speed and integrin release both correlate with cell-substratum adhesiveness, we plotted integrin release as a function of cell speed to determine whether integrin release limits cell speed. At high adhesiveness, where rear detachment limits cell speed, one expects stronger adhesions and the integrin-ECM bond is less likely to fracture because intracellular release becomes limiting for rear detachment.

Mean cell speed is also reported for each of the CHO cell populations we used to study integrin release (Chapter 3). Speed was measured by videomicroscopic tracking of centroids of individual cells. Cell speed exhibits a biphasic dependence on ECM protein concentration at each receptor expression level and receptor-ligand affinity state. Speed is also a constant, biphasic function of cell-substratum adhesiveness. Plotting fraction of integrin released as a function of mean cell speed, we find that a monotonic relationship does not exist between integrin release and mean cell speed (Figures 4.9 and 4.10) over the entire range of speeds. At maximum cell speed an intermediate amount of integrin releases from the cell. As cell speed decreases from the maximum due to increased adhesiveness, more integrin releases from the cell while as cell speed decreases due to decreased adhesiveness, less integrin releases from the cell. However, at intermediate to high adhesiveness where rear detachment limits cell speed, speed decreases as integrin release increases. These results indicate that cytoskeletal release of the integrins at the cell rear is likely to limit rear detachment rate, and thus cell migration speed, at intermediate and high cell-substratum adhesiveness.

4.7 Discussion of the Release of Integrin Linkages during Cell Migration

A mathematical model for cell migration (DiMilla et al., 1991), along with compilation of experimental findings (Sheetz, 1994; Huttenlocher et al., 1995; Lauffenburger and Horwitz, 1996), suggests that cell migration speed should be governed by motility processes at the cell front or the cell rear under different conditions. Conceptually, detachment of cell-substratum interactions at the cell rear can be predicted to limit cell migration speed in situations of high cell-substratum adhesiveness, with lamellipod extension and attachment at the cell front limiting migration speed in situations of low adhesiveness; in situations of intermediate adhesiveness, both cell front and cell rear processes likely act in coordination.

To our knowledge, no studies to date have explored the conditions under which motility processes occurring at either the cell front or cell rear govern locomotion, although a number of investigations have reported aspects of rate-limitation in specific situations. The rate of locomotion of *Dictyostelium* cells can be governed by lamellipod extension (Wessels et al., 1994), but on highly-adhesive substrata their locomotion is limited by their ability to detach at the rear (Jay et al., 1995). The rate of lamellipodial extension in primary cultures of chick and mouse fibroblasts has been found to be approximately 5-fold greater than the overall cell speed (Abercrombie et al, 1970; Felder and Elson, 1990). Protrusion rate is relatively constant in spread fibroblasts while retraction rate governs changes in cell area (Dunn and Zicha, 1995), and speed does not strongly correlate with rate of membrane flow (Condeelis, 1993). Often, lamellipodia are not able to form stable attachments to the substratum and retract (Bard and Hay, 1975). In some cases, rear detachment and lamellipodal extension have been observed to be correlated: protrusion of the leading edge appears to sometimes be required for rear retraction in *Dictyostelium* cell locomotion (Weber et al., 1995), and in chick heart fibroblasts lamellipodal spreading could be found to increase rapidly following retraction at the trailing edge of the cell (Chen, 1979).

Therefore, a first aim of our work described in this chapter was to examine the relationship between the rates of cell body translocation and cell rear detachment across a range of cell-substratum adhesiveness conditions, for CHO cells transfected with $\alpha IIb\beta 3$ integrins migrating on fibrinogen-coated surfaces. As shown in Figure 4.1, we have found that the rate of cell body translocation is approximately equal to the rate of cell rear detachment under conditions of intermediate and high adhesiveness, whereas translocation is substantially slower than rear detachment under conditions of low adhesiveness. These data are consistent with our predictions, and are not in contradiction with the literature reports of specific situations cited above.

Understanding the regulatory mechanism of adhesion release is crucial to rational manipulation of cell speed at conditions where release is rate-limiting. To investigate these mechanisms, we probed the fate of integrin adhesion receptors at the rear of CHO cells during

α5β1 integrin-mediated migration on fibronectin or αIIbβ3 integrin-mediated migration on fibrinogen. We labeled integrins on live cells with a nonadhesion-perturbing MAb conjugated to a fluorescent probe and measured the fraction of integrins which release from the cell and the fraction of integrins which remain with the cell upon rear retraction. This allows us to determine whether the cytoskeletal linkage or extracellular linkage is more stable, and to locate the locus of regulation of adhesion release. We measured integrin release as a function of cell-substratum adhesiveness by varying ECM protein concentration, integrin expression, and integrin-ligand affinity. We then correlated integrin release to cell migration speed at adhesive regimes where rear retraction rates limit cell speed. Our results indicate that a significant, though variable, amount of integrin detaches from the rear of migrating CHO cells upon rear retraction. The detachment of integrins at the rear of migrating CHO cells is similar to the detachment of β1 integrins reported in chick skeletal muscle fibroblasts migrating on laminin (Regen et al., 1992; Palecek et al., 1996). The amount of integrin which releases from the cell increases as receptor clustering and integrin-ECM avidity increase due to changes in ECM protein concentration, receptor expression, or receptor-ligand affinity. In fact, integrin release from the cell rear is a constant function of cell-substratum adhesiveness and the number of cell-substratum bonds. We demonstrated that at intermediate and high adhesiveness, where rear detachment rate limits cell speed, cell speed correlates inversely with integrin release.

The constant, increasing relationship between the amount of integrin released from the cell during rear retraction and the cell-substratum adhesiveness indicates that the avidity of cell-substratum interactions influences cell rear detachment. Short-term cell-substratum adhesiveness measurements are linearly proportional to the number of cell-substratum bonds (Chapter 3). If relatively few bonds exist, the integrins are more likely to release from the substratum. If many bonds exist the adhesion receptors are more likely to release from the cell and remain attached to the substratum. Increased receptor organization may also play a role in the increased integrin release at high adhesiveness since integrin clustering increases as integrin or ECM concentration and integrin-ECM affinity increases. Concentration of cytoskeletal proteins may alter the avidity of individual bonds within the linkage. Alternatively, signaling or regulatory molecules for rear release which weaken the intracellular linkage may be concentrated at focal adhesions. The relationship between integrin release and bond number suggests that the mechanism for rear release involves a physical component due to tension at the rear of the cell. If linkage release were purely biochemical, we would expect integrin release to be independent of cell-substratum adhesiveness.

Cell adhesiveness not only determines the amount of integrin which releases from the rear of migrating cells and adhesiveness but also regulates cell speed, so integrin release from cells likely influences cell speed (Chapter 3). Cell migration speed exhibits a biphasic dependence upon cell-substratum adhesiveness. Maximum cell speed is a function of adhesiveness as ECM

concentration, integrin expression, or integrin-ECM ligand affinity change (Chapter 3) One might expect integrin release to be inversely proportional to cell speed since fast cells (e.g. neutrophils) tend to release very few integrins during rear retraction (Huttenlocher and Palecek, unpublished observations) while slow cells (e.g. fibroblasts or CHO cells) release a significant proportion of their integrins. In this scenario, the release of cytoskeletal linkages at the cell rear would be rate-limiting for migration speed. However, integrin release is not a monotonic function of cell speed over the entire range of cell-substratum adhesiveness. At intermediate and high adhesiveness, where rear detachment rate limits migration speed, an inverse relationship exists between integrin release and cell speed. The molecular-level event which governs release of the cell from the substratum, and thus regulates cell speed, appears to be release of linkages between integrins and the cytoskeleton. At low adhesiveness and low migration speed, less integrin releases from the cells than at intermediate adhesiveness and high speed, indicating that release of adhesions is not rate-limiting for cell speed at low adhesiveness. Detachment rate data in Figure 4.1 show that the cell can detach from the substratum faster than it migrates. At low adhesiveness the cells retract from many directions evenly, causing very little movement in the cell centroid. Lamellipod extension or formation of new adhesions may be rate-limiting under these conditions.

Dissociation of cytoskeletal linkages appears to be regulated by biochemical mechanisms as well as tension forces from cytoskeletal contraction. Dissociation of integrin-ECM linkages is likely to depend only on physical forces and integrin-ECM bond affinity. An analysis of bonds in series under force (Saterbak and Lauffenburger, 1996) predicts that the probability of linkage fracture at each point is related logarithmically to the affinities of each of the individual bonds. The large amount of variation in the linkage fracture location during rear release suggests that the affinities of the individual bonds in the adhesion complex are quite close, allowing a high probability of both intracellular and extracellular bonds breaking. Biochemical regulation of integrin linkages is relatively unknown and will be addressed in Chapter 5.

4.8   References

Bajt, M. L., Loftus, J. C., Gawaz, M. P., and Ginsberg, M. H. (1992). Characterization of a gain of function mutation of integrin αIIbβ3 (platelet glycoprotein IIb-IIIa). *J. Biol. Chem.* **267**, 22211-22216.

Bard, J. B. L., and Hay, E. D. (1975). The behavior of fibroblasts from the developing avian cornea. *J. Cell Biol.* **67**, 400-418.

Chen, W. -T. (1981). Mechanism of retraction of the trailing edge during fibroblast movement. *J. Cell Biol.* **90**, 187-200.

Condeelis, J. (1993). Life at the leading edge. *Annu. Rev. Cell Biol.* **9**, 411-444.

DiMilla, P. A., Stone, J. A., Quinn, J. A., Albeda, S. M., and Lauffenburger, D. A. (1993). Maximal migration of human smooth muscle cells on fibronectin and type IV collagen occurs at an intermediate attachment strength. *J. Cell Biol.* **122**, 729-737.

DiMilla, P. A., Barbee, K., and Lauffenburger, D. A. (1991). Mathematical model for the effects of adhesion and mechanics on cell migration speed. *Biophys. J.* **60**, 15-37.

Duband, J. L., Dufour, S., Yamada, S. S., Yamada, K. M., and Thiery, J. P. (1991). Neural crest cell locomotion induced by antibodies to β1 integrins. A tool for studying the roles of substratum molecular avidity and density in migration. *J. Cell Sci.* **98**, 517-532.

Dunn, A. D. and Zicha, D. (1995). Dynamics of fibroblast spreading. *J. Cell Sci.* **108**, 1239-1249.

Frelinger, A.L., Du, X., Plow, E. F., and Ginsberg, M. H. (1991). Monoclonal antibodies to ligand-occupied conformer of integrin αIIbβ3 (glycoprotein IIb-IIa) alter receptor affinity, specificity and function. *J. Biol. Chem.* **266**, 17106-17111.

Goodman, S. L., Risse, G., and von der Mark, K. (1989). The E8 subfragment of laminin promotes locomotion of myoblasts over extracellular matrix. *J. Cell Biol.* **109**, 799-809.

Hay, E. D. (1985). Interaction of migrating embryonic cells with extracellular matrix. *Exp. Biol. Med.* **10**, 174-193.

Huttenlocher, A., Palecek, S. P., Lu, Q., Zhang, W., Mellgren, R. L., Lauffenburger, D. A., Ginsberg, M. H., and Horwitz, A. F. (1997). Regulation of cell migration by the calcium-dependent protease calpain. *J. Biol. Chem.* **272**, 32719-32722.

Huttenlocher, A, Ginsberg, M. H., and Horwitz, A. F. (1996). Modulation of cell migration by integrin-mediated cytoskeletal linkages and ligand-binding affinity. *J. Cell Biol.* **134**, 1551-1562.

Huttenlocher, A., Sandborg, R. R., and Horwitz, A. F. (1995). Adhesion in cell migration. *Curr Opin. Cell Biol.* **7**, 697-706.

Jay, P. Y., Pham, P. A., Wong, S. A., and Elson, E. L. (1995). A mechanical function of myosin II in cell motility. *J. Cell Sci.* **108**, 387-393.

Keely, P. J., Fong, A. M., Zutter, M. M., and Santoro, S. A. (1995). Alteration of collagen-dependent adhesion, motility, and morphogenesis by the expression of antisense α2 integrin mRNA in mammary cells. *J. Cell Sci.* **108**, 595-607.

Lauffenburger, D. A. and Horwitz, A. F. (1996). Cell migration: a physically integrated molecular process. *Cell.* **84**, 359-369.

Mitchison, T. J., and Cramer, L. P. (1996). Actin-based cell motility and cell locomotion. *Cell.* **84**, 371-379.

Niggimann, B., Maaser, K., Lu, H., Kroczek, R., Zanker, K. S., and Friedl, P. (1997). Locomotory phenotypes of human tumor cell lines and T lymphocytes in a three-dimensional collagen lattice. *Cancer Lett.* **118**, 173-180.

O'Toole, T. E., Loftus, J. C., Du, X., Glass, A. A., Ruggeri, Z. M., Shattil, S. J., Plow, E. F. and Ginsberg, M. H. (1990). Affinity modulation of the αIIbβ3 integrin (platelet GPIIbIIIa) is an intrinsic property of the receptor. *Cell Reg.* **1**, 883-893.

O'Toole, T. E., Katagiri, Y., Faull, R. J., Peter, K., Tamura, R., Quaranta, V., Loftus, J., Shattil, S. J. and Ginsberg, M. H. (1994). Integrin cytoplasmic domains mediate inside-out signal transduction. *J. Cell Biol.* **125**, 447-460.

Palecek, S. P., Schmidt, C. E., Lauffenburger, D. A., and Horwitz, A. F. (1996). Integrin dynamics on the tail region of migrating fibroblasts. *J. Cell Sci.* **109**, 941-952.

Regen, C. M., and Horwitz, A. F. (1992). Dynamics of β1 integrin-mediated adhesive contacts in motile fibroblasts. *J. Cell. Biol.* **119**, 1347-1359.

Ruoslahti, E., Hayman, E.G., Pierschbacher, M. and Engvall, E. (1982). Fibronectin: purification, immunochemical properties, and biological activities. *Methods Enzymol.* **82**, 803-831.

Saterbak, A., and Lauffenburger, D. A. (1996). Adhesion mediated by bonds in series. *Biotechnol. Prog.* **12**, 682-699.

Sheetz, M. P. (1994). Cell migration by graded attachment to substrates and contraction. *Sem. Cell Biol.* **5**, 149-155.

Stossel, T. P. (1993). On the crawling of animal cells. *Science.* **260**, 1086-1094.

Weber, I., Wallraff, E., Albrecht, R., and Gerisch, G. (1995). Motility and substratum adhesion of *Dictyostelium* wild-type and cytoskeletal mutant cells: a study by RICM/bright-field double-view image analysis. *J. Cell Sci.* **108**, 1519-1530.

Werb, Z., Tremble, P. M., Behrendtsen, O., Crowley, E., and Damsky, C. H. (1989). Signal transduction through the fibronectin receptor induces collagenase and stromelysin gene expression. *J. Cell Biol.* **109**, 877-889.

Wessels, D., Vawter-Hugart, H., Murray, J., and Soll, D. R. (1994). Three-dimensional dynamics of pseudopod formation and the regulation of turning during the motility cycle of Dictyostelium. *Cell Motil. Cytoskeleton.* **27**, 1-12.

Wilson, A. K., Gorgas, G., Claypool, W. D., and de Lanerolle, P. (1991). An increase or decrease in myosin II phosphorylation inhibits macrophage motility. *J. Cell Biol.* **114**, 277-283.

Table 4.1. Quantitative Analysis of Integrin Release during Rear Retraction.

Retraction Number (See Fig. 4.3)	Average Intensity Before Detachment I_1	Average Intensity After Detachment I_2	Average Background I_B	Fraction Intensity Detached F
1 (0.6 µg/ml)	2371	1327	1058	0.205
2 (0.6 µg/ml)	1623	1131	1003	0.207
3 (0.6 µg/ml)	2577	1067	1040	0.011
4 (0.6 µg/ml)	1804	1262	1044	0.352
5 (2 µg/ml)	1612	1414	945	0.703
6 (2 µg/ml)	1472	1363	930	0.799
7 (2 µg/ml)	1530	1485	927	0.926
8 (5 µg/ml)	1189	934	658	0.528
9 (5 µg/ml)	1423	1026	669	0.474
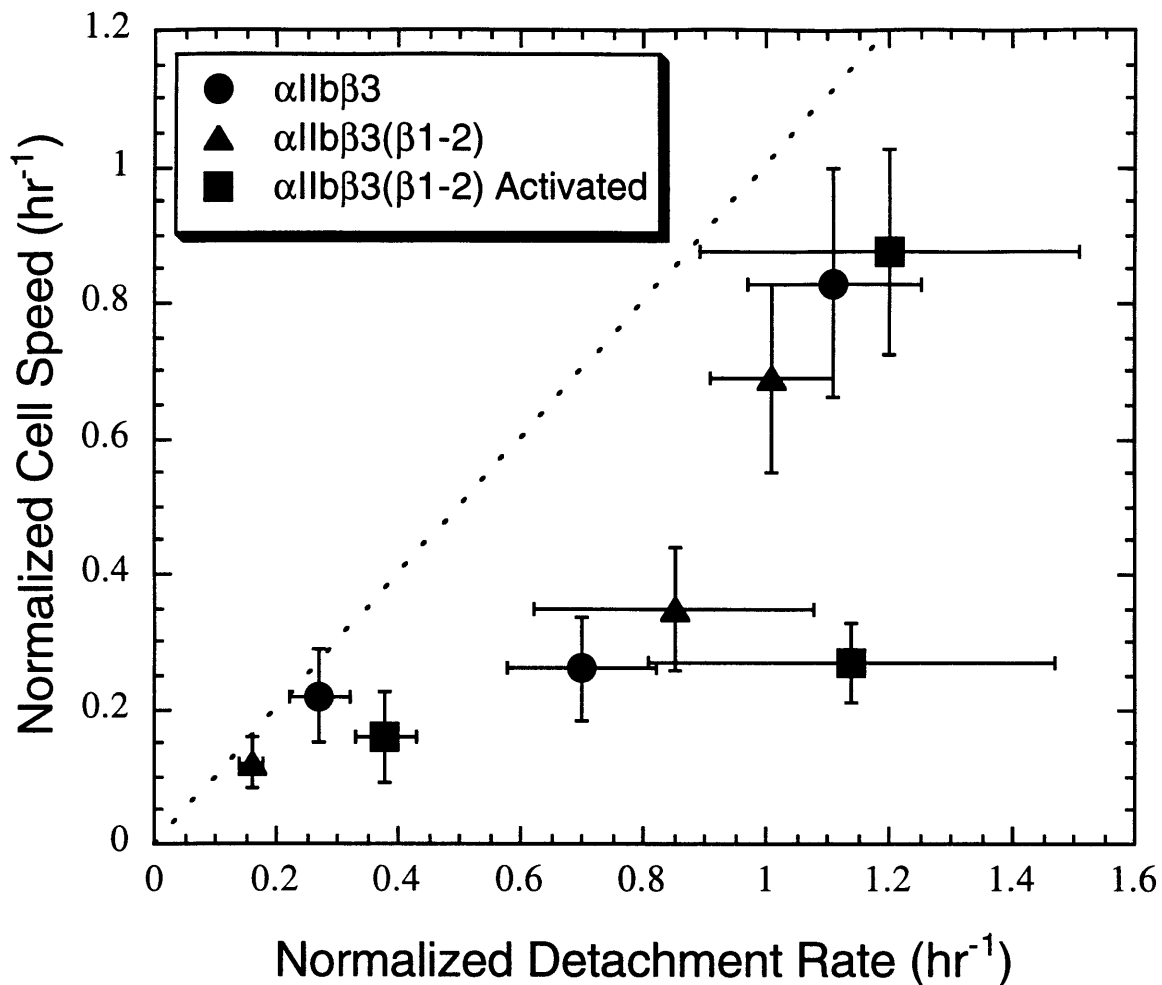
Figure 4.1. The Rate of Rear Release Limits Cell Migration Speed at Intermediate and High, but not Low, Adhesiveness. Cell speed, normalized to cell diameter, is plotted as a function of rear detachment rate, normalized to cell area, for CHO cells expressing $\alpha IIb\beta3$ and $\alpha IIb\beta3(\beta1-2)$ integrins on different concentrations of fibrinogen. Mean cell diameter and mean cell area were calculated from phase contrast images of more than 50 cells at each fibrinogen concentration. The dotted line indicates where speed equals detachment rate. Error bars represent s.e.m.
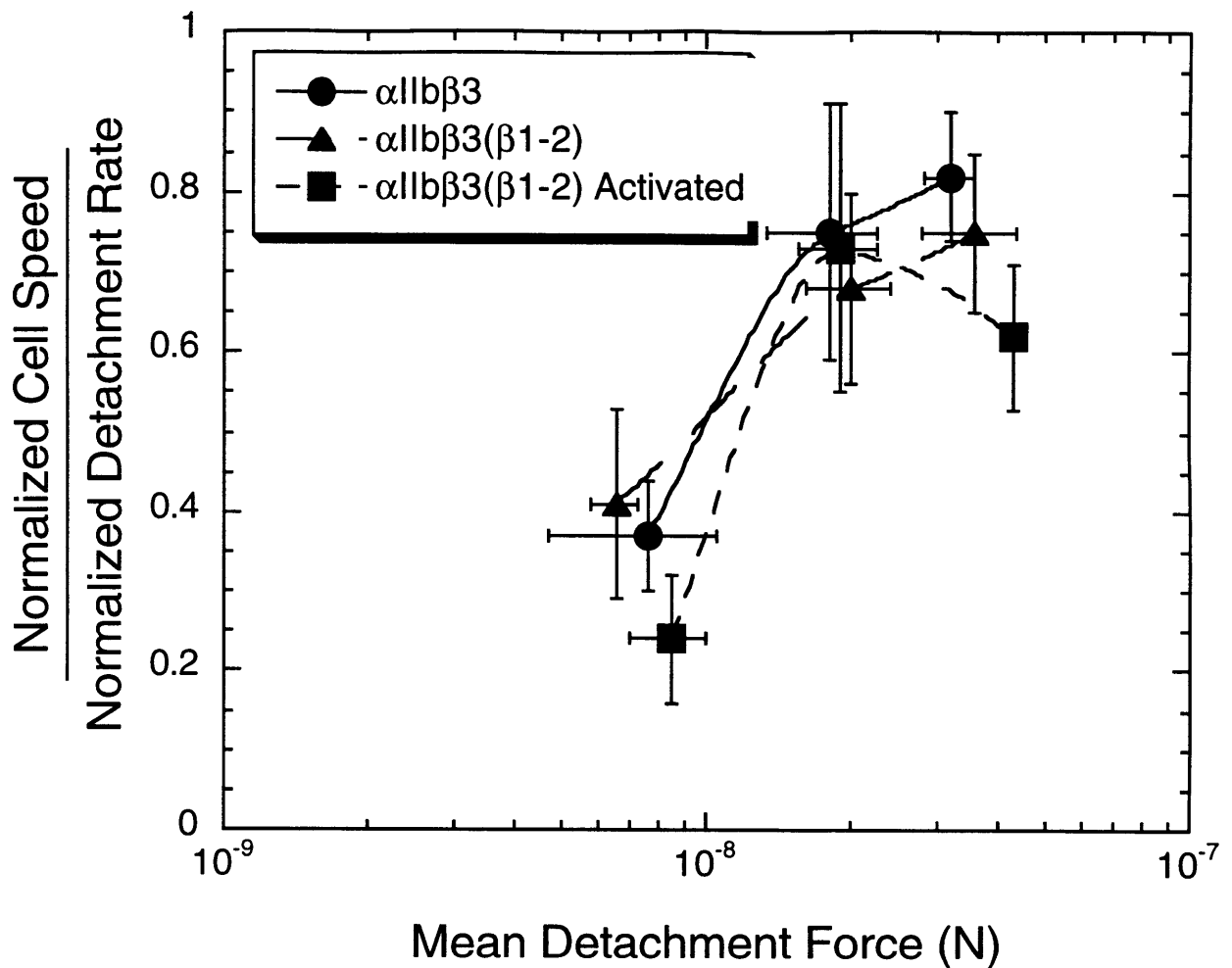
Figure 4.2. The Rate of Rear Release Limits Cell Migration Speed at Intermediate and High, but not Low, Adhesiveness. The ratio of speed to detachment rate indicates how efficiently the detachments move the cell centroid. Speed to detachment ratio is plotted as a function of cell-substratum adhesiveness (B). Short-term mean detachment force was measured by shear flow detachment of cells after a 20 minute incubation on the surface (Chapter 2). At adhesiveness values below 10^{-8} N, where the cells are not adherent enough to migrate well, the ratio of speed to detachment rate is below 0.4. At adhesiveness above 2 x 10^{-8} N, where the cells migrate at maximum speed, the ratio of speed to detachment rate is above 0.6. These results suggest that at intermediate and high adhesiveness cell detachment rate is limits overall migration speed. Error bars on detachment force represent 95% confidence intervals on the mean and error bars on speed and detachment rates represent s.e.m.

90
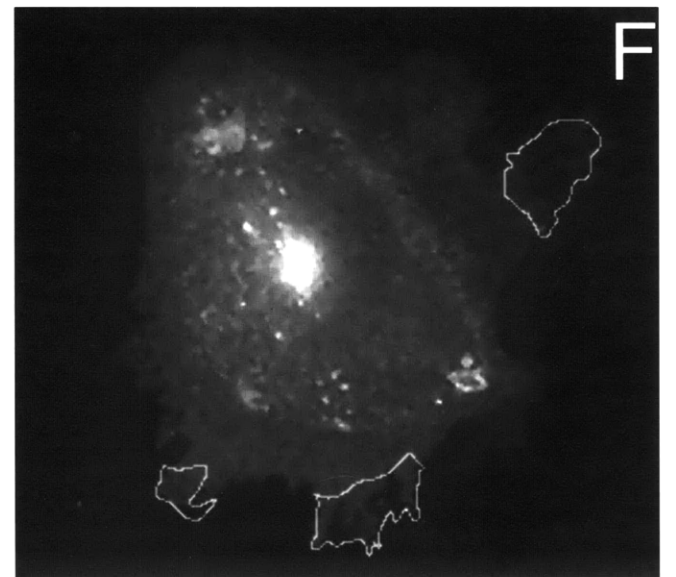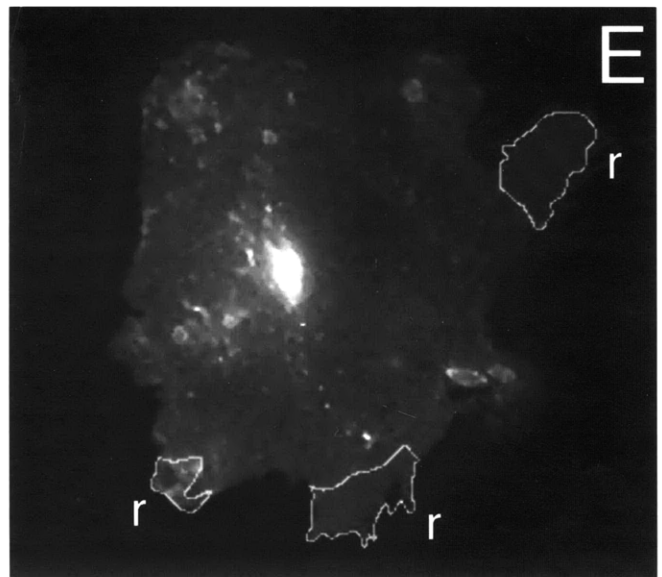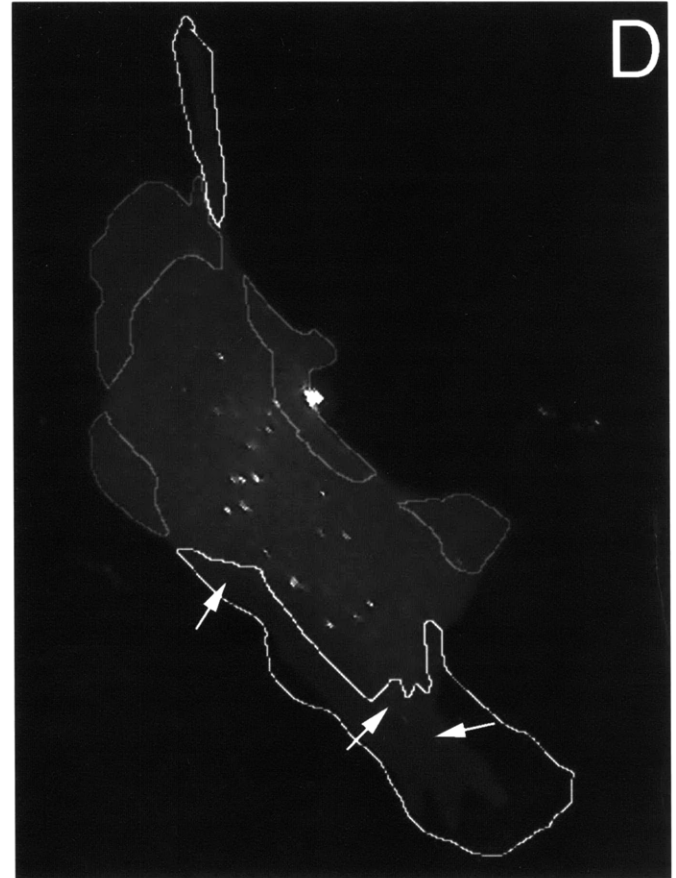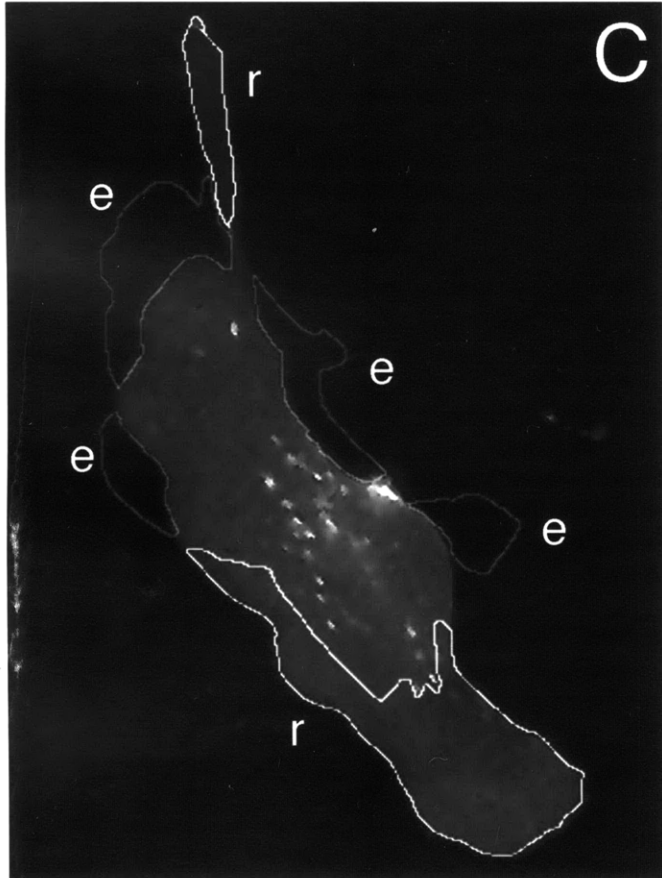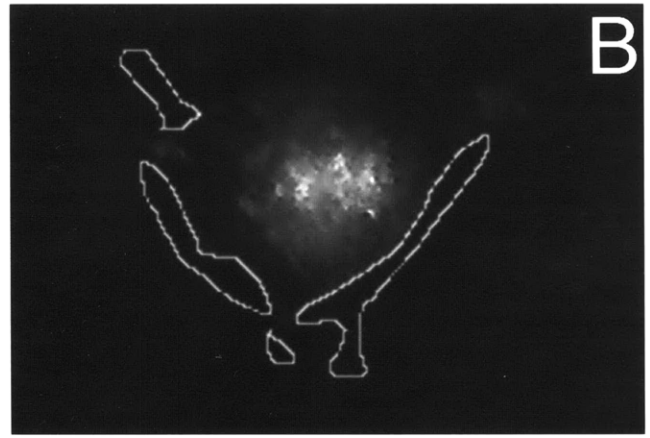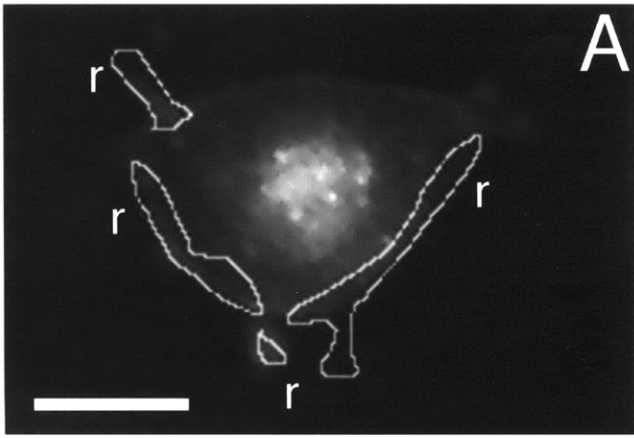
Figure 4.3. Integrins Release from the Rear of CHO Cells during Migration. Anti-αIIbβ3 integrin immunofluorescence images of single living cells labeled with the non-adhesion perturbing MAb D57 conjugated to Oregon Green fluorophor show the movement of integrins during rear retraction on 0.6 μg/ml (A, B), 5 μg/ml (C, D), and 2 μg/ml (E, F) fibrinogen. The area of the cell which retracts between 0 minutes (A, C, E) and 30 minutes (B, D, F) was determined from phase contrast images and is traced on the fluorescent images in light gray and labeled with an r. Areas of the cell which extend are traced in dark gray and labeled with an e. Retraction areas are numbered and average pixel intensities before and after detachment are shown in Table 4.1. At 0.6 μg/ml fibrinogen (A, B), cells are quite round and when they retract, most of the integrins dissociate from the substratum and remain with the cell. At 5 μg/ml fibrinogen (C, D), cells are spread and release most of their integrin onto the substratum upon rear retraction. At 2 μg/ml fibrinogen (E, F) an intermediate the cells release an intermediate amount of integrin on the substratum. Examples of patches of integrin which have detached from the cell are indicated with arrowheads in D and F. Bar, 10 μm.

A
0.6 μg/ml fibrinogen

B
2 μg/ml fibrinogen

C
5 μg/ml fibrinogen
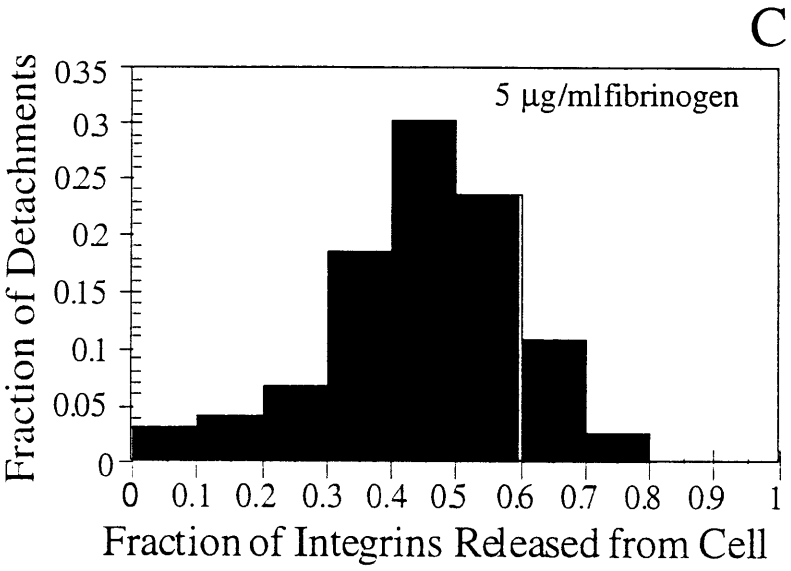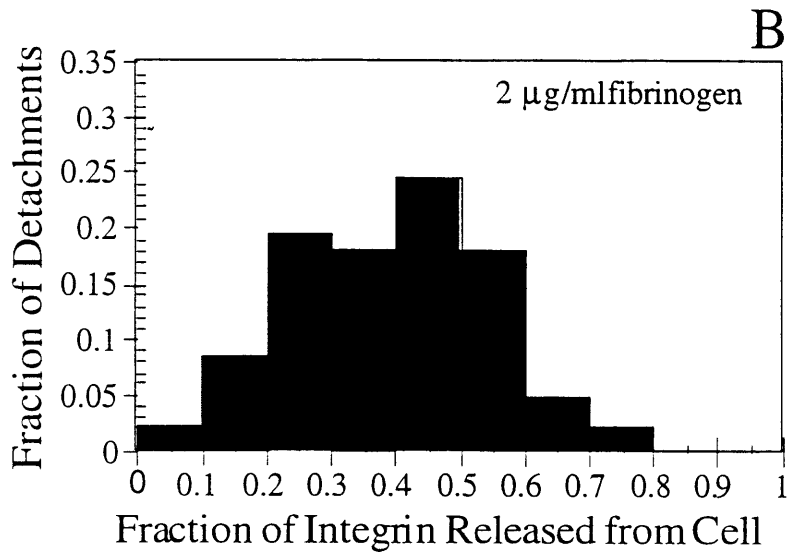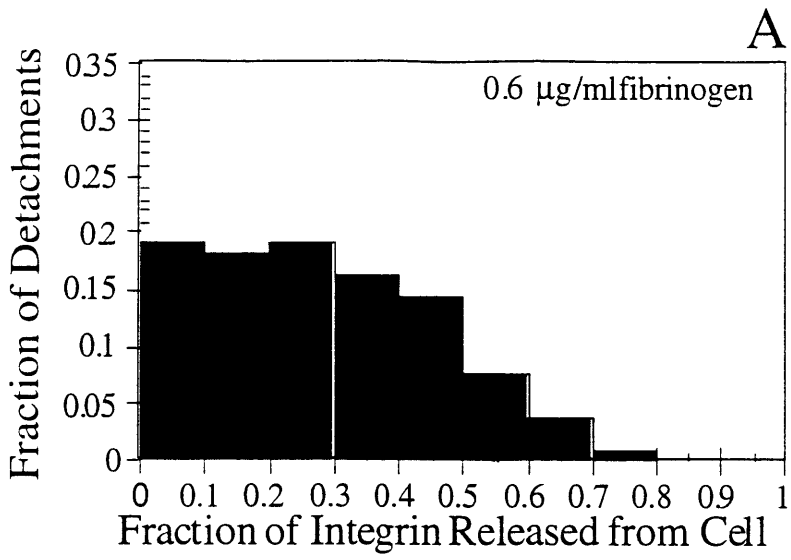
Figure 4.4. Histograms Showing the Amount of Integrin Released from CHO cells Migrating on 0.6 µg/ml (A), 2 µg/ml (B), and 5 µg/ml (C) Fibrinogen for Different Rear Retraction Events. The amount of integrin which releases from the cell in the detachment area at the rear of a migrating cell was measured by quantitative immunofluorescence of anti-integrin MAbs. At each fibrinogen concentration a variable range of integrin, ranging from 0 to 80 percent, can be released from the cell. The distribution is different at each fibrinogen concentration, however. At 0.6 µg/ml fibrinogen (A) 0 to 30 percent of the integrin in the detachment area is usually released from the cell. At 2 (B) and 5 (C) µg/ml fibrinogen, 30 to 60 percent of the integrin in the detachment area is typically released from the cell. N = 104 (A), 81 (B), 119 (C).
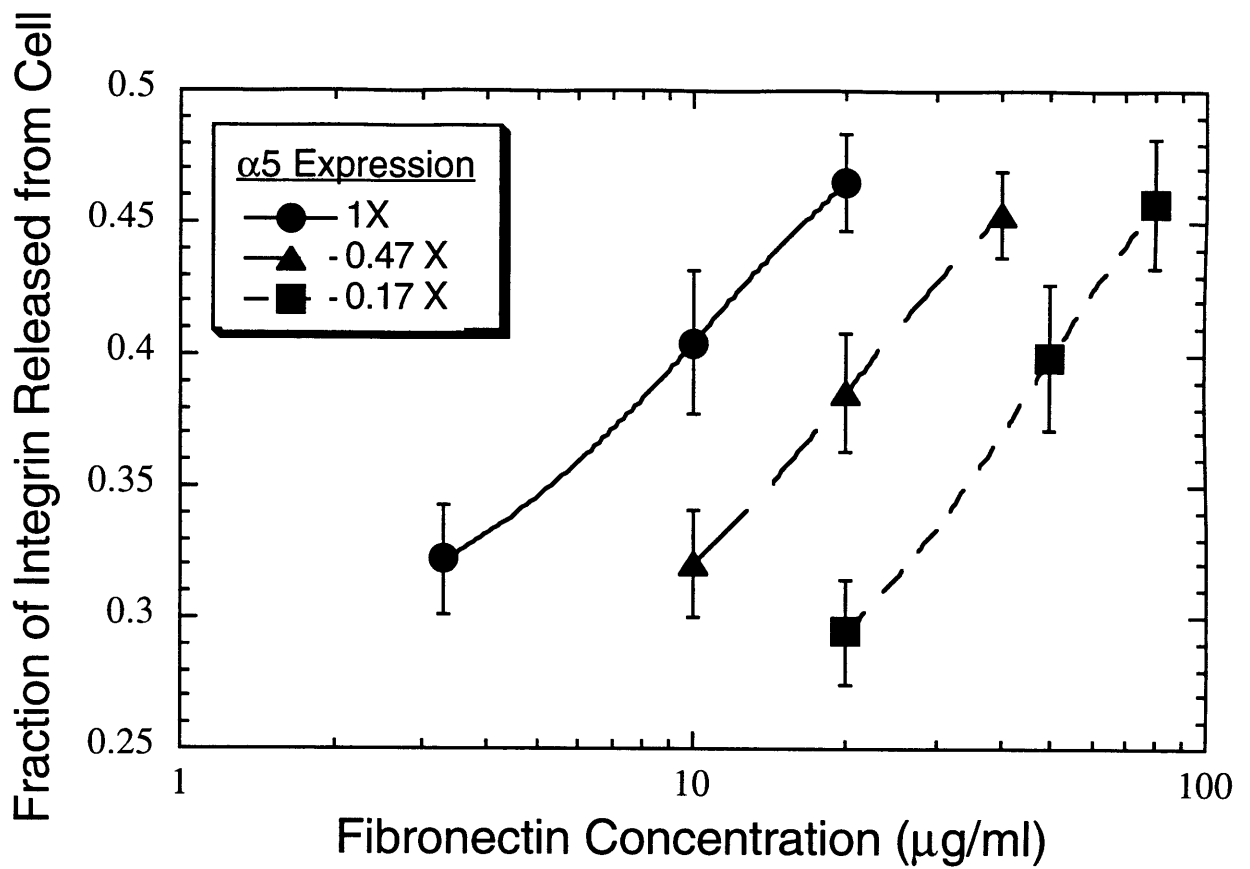
Figure 4.5. Integrin Release Increases as Receptor Number and Substrate Concentration Increases. The amount of integrin which releases from the detachment area of migrating cells was measured in CHO cells expressing different levels of α5 integrin. As ECM concentration or integrin expression increases, the amount of integrin released from the rear of migrating CHO cells increases. Error bars represent s.e.m.
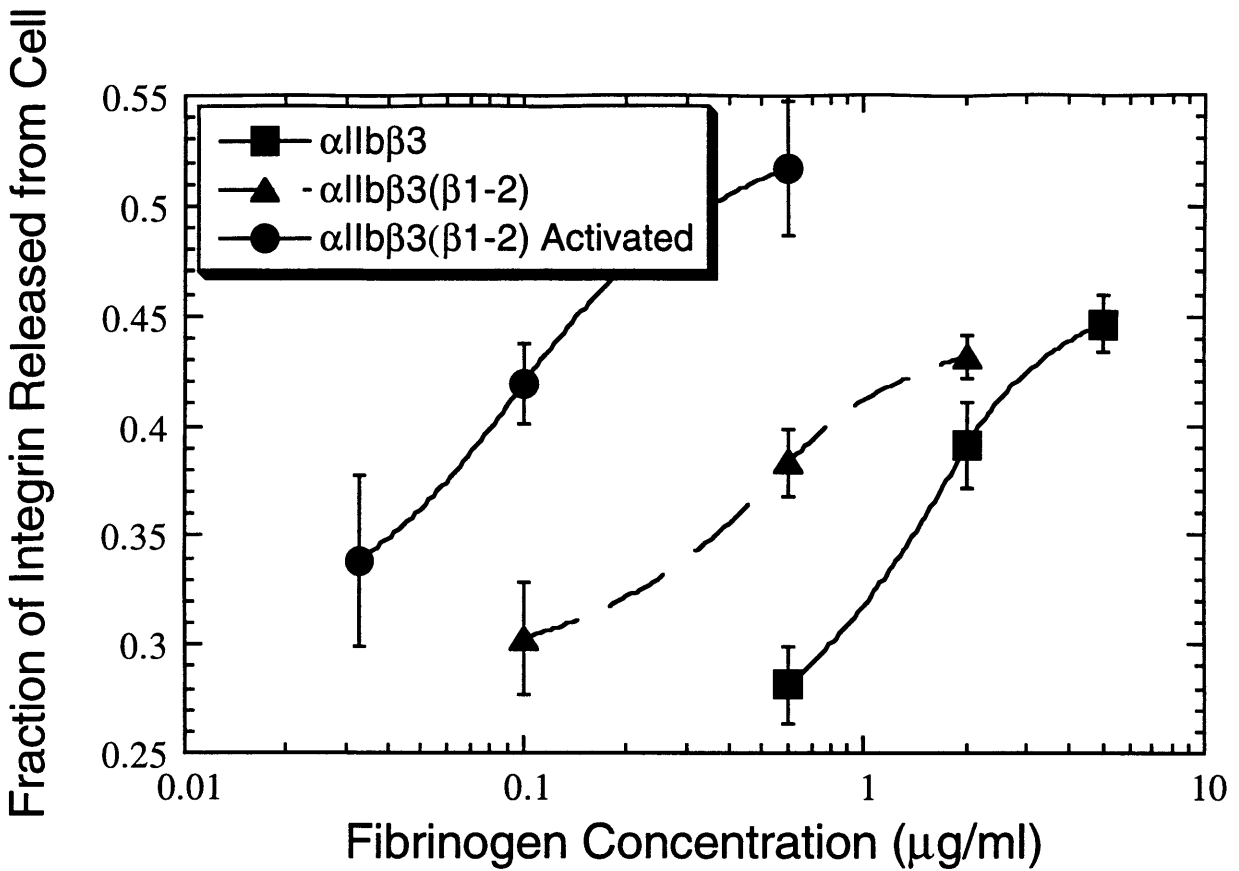
Figure 4.6. Integrin Release Increases as Ligand Affinity and Substrate Concentration Increases. The amount of integrin which releases from the detachment area of migrating cells was measured in CHO cells expressing αIIbβ3 integrins with different affinities for fibrinogen. As ECM concentration or integrin-ligand affinity increases, the amount of integrin released from the rear of migrating CHO cells increases. Error bars represent s.e.m.
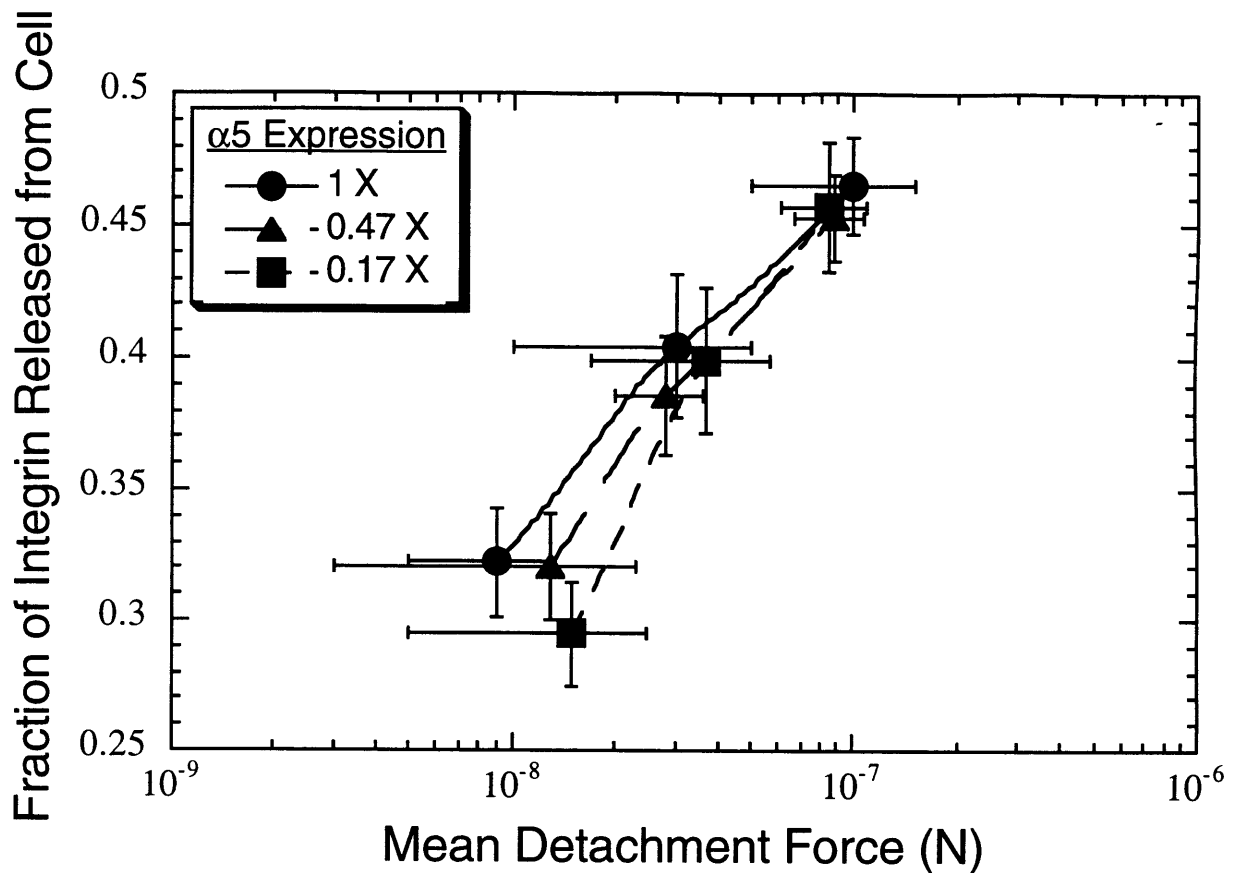
Figure 4.7. Integrin Release Correlates with Cell-Substratum Adhesiveness at Different Integrin Expression Levels. The amount of integrin which releases from migrating CHO cells during rear retraction was measured for cells expressing different levels of $\alpha 5$ integrin. Adhesiveness was also altered by varying substrate fibronectin or fibrinogen concentrations. Short-term mean detachment force was measured by shear flow detachment of cells after a 20 minute incubation on the surface (Chapters 2 and 3). As cell-substratum adhesiveness increases in cells expressing different levels of $\alpha 5$ integrins more integrin is released from the cell. Error bars on mean detachment force represent 95% confidence intervals on the mean and error bars on fraction of integrin released represent s.e.m.
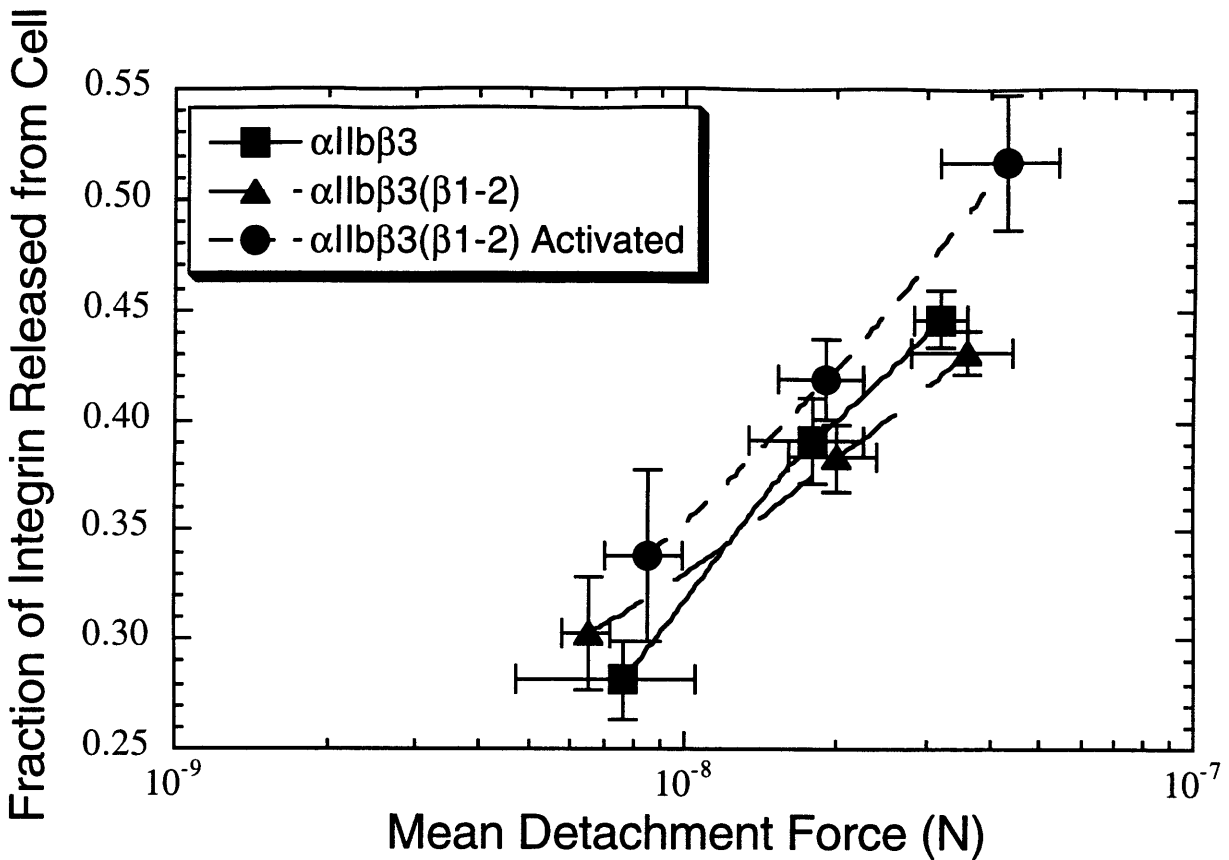
Figure 4.8. Integrin Release Correlates with Cell-Substratum Adhesiveness at Different Integrin-Ligand Affinities. The amount of integrin which releases from migrating CHO cells during rear retraction was measured for cells expressing $\alpha IIb\beta 3$ integrins with different affinities for fibrinogen. Adhesiveness was also altered by varying substrate fibronectin or fibrinogen concentrations. Short-term mean detachment force was measured by shear flow detachment of cells after a 20 minute incubation on the surface (Chapters 2 and 3). As cell-substratum adhesiveness increases in cells expressing $\alpha IIb\beta 3$ integrins in different affinity states, more integrin is released from the cell. Error bars on mean detachment force represent 95% confidence intervals on the mean and error bars on fraction of integrin released represent s.e.m.
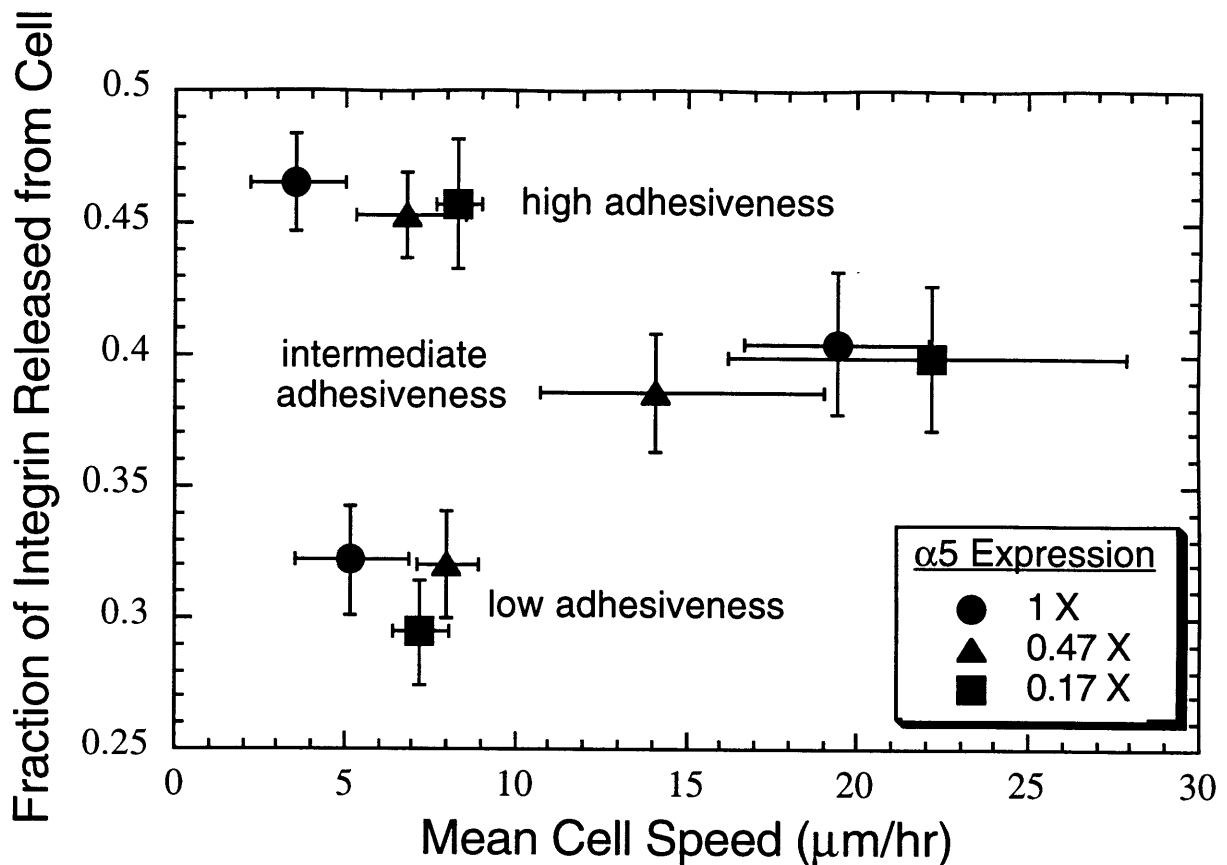
Figure 4.9. Integrin Release Correlates Inversely with Cell Speed when Rear Detachment Limits Migration Speed. The amount of integrin which releases from migrating CHO cells during rear retraction was measured for cells expressing different levels of $\alpha 5$ integrin. Mean cell migration speed was determined using image analysis to track the centroids of individual cells (Chapters 2 and 3). The amount of integrin which releases from the rear of migrating cells is not a monotonic function of cell speed. As cell speed increases from low adhesiveness to the intermediate adhesiveness which promotes maximum cell speed, integrin release increases. Over the range of adhesiveness where cell speed is limited by rear detachment (intermediate to high adhesiveness), integrin release has an inverse relationship with cell speed. Error bars on mean cell speed represent 95% confidence intervals on the mean and error bars on fraction of integrin released represent s.e.m.

Figure 4.10. Integrin Release Correlates Inversely with Cell Speed when Rear Detachment Limits Migration Speed. The amount of integrin which releases from migrating CHO cells during rear retraction was measured for CHO cells expressing αIIbβ3 integrins with different affinities for fibrinogen. Mean cell migration speed was determined using image analysis to track the centroids of individual cells (Chapters 2 and 3). The amount of integrin which releases from the rear of migrating cells is not a monotonic function of cell speed. As cell speed increases from low adhesiveness to the intermediate adhesiveness which promotes maximum cell speed, integrin release increases. Over the range of adhesiveness where cell speed is limited by rear detachment (intermediate to high adhesiveness), integrin release has an inverse relationship with cell speed. Error bars on mean cell speed represent 95% confidence intervals on the mean and error bars on fraction of integrin released represent s.e.m.
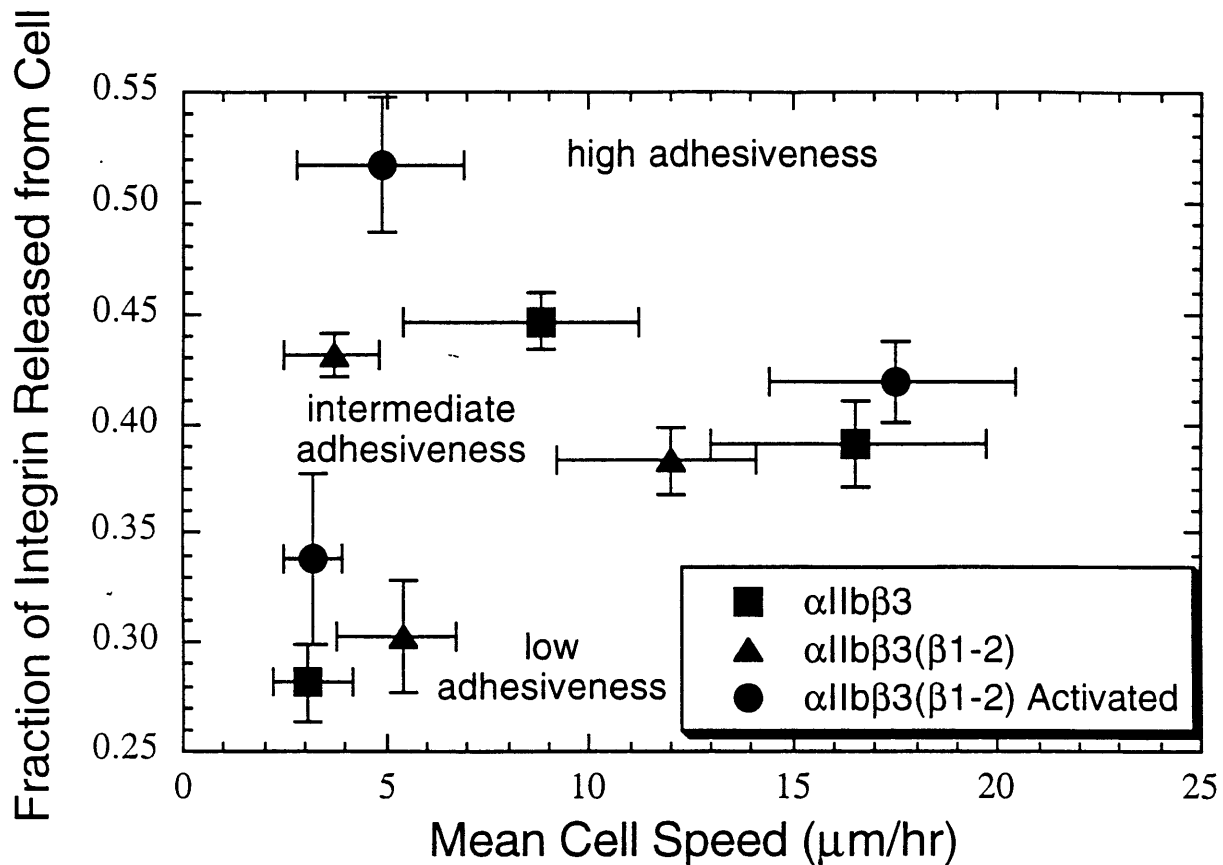
101

Chapter 5   Regulation of the Integrin-Cytoskeleton Linkage by Calpain during Cell Migration

5.1   Evidence for Biochemical Regulation of Integrin-Cytoskeletal Linkages

The fracture location of cell substratum linkages changes from predominantly integrin-ECM to predominantly integrin-cytoskeletal as cell-substratum adhesiveness increases (Chapter 4). These results suggest that as rear detachment events become the rate-limiting steps for cell migration, integrin-cytoskeleton bonds must fracture to allow the cell to migrate. Forces from cytoskeletal contraction are transmitted through these linkages and play a role in linkage fracture. The role of biochemical events in linkage release is unclear, however. In this chapter we explore the role of calpain, a calcium-dependent protease, in regulating integrin-cytoskeletal linkages during cell migration.

Previous experimental reports indicate that the mechanism which allows intracellular release of cytoskeletal connections at the rear of a migrating cell is likely to involve a regulated, biochemical process. The addition of ATP to permeabilized fibroblasts (Crowley and Horwitz, 1995) results in the rapid breakdown of focal adhesions, detachment from the substratum, and integrin tracks where cells resided prior to detachment. This is attributed to tyrosine phosphorylation of cytoskeletal components and tension generated by cell contraction. Surges in intracellular Ca^{2+} levels have been detected during rear release in neutrophils (Marks et al., 1991). These calcium transients have been implicated in adhesive release of neutrophils migrating on vitronectin through the Ca^{2+}-calmodulin dependent phophatase calcineurin (Maxfield, 1993; Hendey et al., 1992). Calpain localizes to focal adhesions in vivo (Beckerle et al., 1987) In vitro, calpain cleaves the cytoplasmic domain of the β subunit of integrins as well as other cytoskeletal molecules including focal adhesion kinase (FAK) and talin (Du et al., 1996; Cooray et al., 1996; Inomata et al., 1996).

Calpain is a cysteine protease with two characterized isoforms, calpain I (μ-calpain) and II (m-calpain). Both contain an 80 kDa catalytic subunit and a 30 kDa regulatory domain. Activation requires calcium concentrations in the μM range and mM range for calpain I and II, respectively (Saido et al., 1994; Sorimachi et al., 1994). The increases in calcium seen in migrating cells appear to be within the range to support activation of calpain (Maxfield, 1993). In this chapter we use pharmacological inhibition of calpain to show that calpain regulates rear detachment by weakening integrin-cytoskeletal linkages. Thus, calpain can be an important target for controlling cell speed under conditions where rear detachment limits cell speed. The experiments in this chapter were performed in collaboration with Dr. Anna Huttenlocher at the University of Illinois.

5.2 Experimental System

5.2.1 Cell Systems and Reagents

We used the CHO cell system described in Chapter 2.2 to investigate the effects of calpain inhibition on rear detachment and cell speed. We have characterized speed and adhesiveness of these cells (Chapter 3), as well as detachment behavior (Chapter 4), at different ECM concentration, integrin expression level, and integrin-ligand affinity states. CHO cells contain calpain I and II at a 1:9 ratio (Huttenlocher et al., 1997).

CHO K1 cells were obtained from American Type Culture Collection (Rockville, MD). A CHO SH1 clone, which expresses very low levels of calpain I (Mellgren et al., 1996), and a CHO A4 clone, which expresses 4 times the amount of calpain I as CHO SH1, were provided by Dr. Ronald Mellgren. The A4 clone was prepared by cotransfecting SHI cells with pSBC-muL plasmid containing human calpain I large subunit and a neo selection vector, pMC1Neo using lipofectamine. The SH1 and A4 clones allow us to compare the effects of genetically reducing calpain expression to pharmacologically reducing calpain activity.

Stock solutions of calpain inhibitor I (Boehringer Mannheim, Indianapolis, IN) were prepared at a concentration of 10 mg/ml in ethanol. Calpain inhibitor I was used at a concentration of 50 μg/ml. Cells were preincubated with calpain inhibitor for 30 minutes prior to the experiments and maintained in media containing calpain inhibitor throughout the experiments. These inhibitors have no toxicity effects up to concentrations of 100 μg/ml. Benzyloxycarbonyl-Leu-Leu-Tyr diazomethyl ketone, ZLLY-CHN2, (Enzyme System Products, Dublin, CA), was prepared in DMSO at a concentration of 35 mM and used at a final concentration of 50 mM.

5.2.2 Experimental Assays

Time lapse videomicroscopy and modified Boyden chamber transwell assays were performed to measure cell speed. Cells were washed and resuspended in serum free hybridoma media CCM1 (Hyclone Laboratories Inc., Logan, UT) and pretreated with calpain inhibitors for 20 minutes prior to plating for time lapse videomicroscopy and transwell assays. Plates were coated with ECM substrate, fibronectin or fibrinogen, and blocked with 2% BSA for 30 minutes prior to use. Cells were tracked by time lapse videomicroscopy for 3-6 hours. Random transwell assays were performed using membranes coated with substrate on both sides (CoStar Corp., Cambridge, MA). Assays were run for 3 hours and cells were then fixed with methanol and stained with methylene blue (Fisher leukostat staining kit, Sigma Chemical Co.). Each experiment was performed a minimum of three times.

The rear detachment rate and integrin tracking assays are described in Chapter 4.2.3 and 4.2.4.

5.3 Calpain Inhibition Affects Cell Speed in an Inhibitor- and ECM Concentration-Dependent Manner

Treatment of cells with calpain inhibitor I reduces cell speed on both fibronectin and fibrinogen (Figure 5.1). The reduction of cell speed increases as calpain inhibitor I concentration increases. Inhibition of cell speed begins at 2.6 mM calpain inhibitor I and increases to almost full inhibition (60-75%) at 130 mM. At 260 mM, calpain inhibitor I causes cell rounding and toxicity in about 20% of the cells.

The CHO SH1 cell clone, which has low endogenous levels of calpain I but expresses normal levels of calpain II and cathepsins (Mellgren et al., 1996), also shows 60% inhibition of cell speed on fibronectin-coated surfaces. The CHO A4 clone transfected with human calpain I cDNA has a speed similar to wild-type cells. These results suggest that decreased levels of calpain activity are responsible for reducing cell speed.

Calpain inhibitor I reduces cell speed to a greater extent at high ECM concentrations than low ECM concentrations. The ratio of CHO SH1 cell speed to wild-type CHO K1 cell speed also decreases as ECM concentration increases. These results are consistent with calpain reducing cell speed by inhibition of rear retraction. At low substrate concentrations cell speed is likely to be inhibited by the ability to form stable attachments at the cell front, while at high substrate concentrations cell speed is more likely to be limited by rear detachment (Chapter 4.3). At low ECM concentrations, cells migrate at the same speed in the presence or absence of calpain inhibitor I, suggesting that calpain inhibitor I is not cytotoxic at these concentrations.

5.4 Calpain Inhibition Reduces Cell-Substratum Detachment Rate

To demonstrate more directly that calpain inhibition affects release at the cell rear, we quantitated the rates of rear retraction for cells migrating in the presence of calpain inhibitors (Figure 5.2). At a low fibrinogen concentration (0.6 μg/ml), calpain inhibitors have no detectable effect on the rate of rear retraction. At an intermediate fibrinogen concentration (2 μg/ml), which supports maximum migration, calpain inhibitor I shows a five fold inhibition in the rate of rear retraction. Significant inhibition of the retraction rate is also seen with calpain inhibitor I, II and diazomethyl ketone as compared to control cells at high substrate concentrations. Our results suggest that treatment with calpain inhibitors blocks migration by specifically inhibiting cell-substrate detachment at the rear of the cell.

5.5 Calpain Inhibition Hinders Rear Release by Strengthening Cytoskeletal Linkages

Release of adhesions at the cell rear clearly involves a physical mechanism reliant upon cytoskeletal contraction. The tension forces presumably fracture the linkage at the weakest point. It is likely that a biochemical mechanism exists to facilitate rear release by weakening this linkage intracellularly. To search for such a mechanism, we investigated the role of the Ca^{2+}-dependent protease, calpain, in regulating this linkage. Calpain inhibition by pharmacological or genetic means inhibits rear retraction by stabilizing cytoskeletal structures (Huttenlocher et al., 1997). Presumably, calpain acts by severing cytoskeletal linkages, allowing the integrins to release from the cell. We measured the fraction of integrin which releases from the rear of migrating CHO cells in which calpain has been inhibited by calpain inhibitor I.

The effect of calpain inhibition on integrin release at the cell rear depends upon substrate concentration. The amount of integrin released from the cell increases as fibrinogen concentration increases in control cells but is independent of fibrinogen concentration in cells treated with calpain inhibitor I (Figure 5.3). At 2 and 5 μg/ml fibrinogen, where rear retraction limits cell speed, calpain inhibitor I significantly reduces the amount of integrin which releases at the rear of migrating cells. At 0.6 μg/ml fibrinogen, where rear release is not likely to limit migration speed, calpain inhibition has no effect on the cytoskeletal release of integrins during migration. Calpain appears to be an important regulatory molecule for controlling release of adhesions at the rear of cells migrating on substrates with high adhesiveness by fracturing cytoskeletal linkages. Thus, calpain activity will allow integrins to preferentially release from within cell rather than from the substratum.

5.6 Discussion of Biochemical Mechanisms Facilitating Cell-Substratum Detachment

Dissociation of cytoskeletal linkages appears to be regulated by biochemical mechanisms as well as tension forces from cytoskeletal contraction. Dissociation of integrin-ECM linkages is likely to depend only on physical forces and integrin-ECM bond affinity. An analysis of bonds in series under force (Saterbak and Lauffenburger, 1996) predicts that the probability of linkage fracture at each point is related logarithmically to the affinities of each of the individual bonds. The large amount of variation in the linkage fracture location during rear release suggests that the affinities of the individual bonds in the adhesion complex are quite close, allowing a high probability of both intracellular and extracellular bonds breaking.

Calpain is one mechanism which appears to regulate rear retraction of some cells at intermediate and high adhesiveness. Maximum cell speed decreases when rear release is impeded by inhibition of calpain (Huttenlocher et al., 1997). This raises the question of what governs the maximum speed a cell can attain, and what range of environmental conditions can sustain that maximum speed. A mathematical model of cell migration predicts that a front-vs.-rear asymmetry in adhesiveness or contractility is a major parameter that governs maximum cell speed and the range of conditions sustaining it (DiMilla et al., 1991). The greater this asymmetry, the greater the maximum speed and the greater the sustaining range. This asymmetry requirement can be satisfied in a number of ways. The spatial distribution of adhesion receptors due to preferential trafficking or localization into adhesion complexes may lead to higher adhesiveness at the cell front than the cell rear. Asymmetries in adhesion receptor-ECM ligand affinity could also result in an adhesive gradient in the cell. Locking integrins in a high affinity state, thereby eliminating receptor-ligand affinity gradients, inhibits eosinophil, lymphocyte, and fibroblast migration (Kuijpers et al., 1993; Dustin et al., 1997; Huttenlocher, et al., 1996). Adhesion receptor-cytoskeleton linkage avidity appears to exhibit a spatial asymmetry in the cell; integrin linkages to cytoskeleton in migrating NIH 3T3 fibroblasts have been found to be more prevalent in the cell front than at the cell rear (Schmidt et al., 1993). Spatial concentrations of signaling molecules may also contribute to the asymmetry. For example, intracellular Ca^{2+} or phophoinositide levels may regulate adhesion or contractile forces. In migrating leukocytes, calcium concentration, and myosin-II based contractility, increases from the front to rear of the cell (Hahn et al., 1992). Also, intracellular calcium transients are required for detachment of the cell rear during neutrophil migration via the phosphatase calcineurin (Maxfield, 1993). Proteases including calpain may also be activated by intracellular calcium transients at the rear of migrating cells.

Calpain is likely to aid cell migration by increasing adhesive asymmetry within the cell by weakening cytoskeletal linkages at the cell rear. Inhibition of calpain stabilizes cytoskeletal linkages with respect to integrin-ECM linkages, resulting in preferential fracture of integrin-ECM linkages. Calpain activity appears to regulate rear release by cleavage of cytoskeletal linkages, destabilizing adhesions at the cell rear with respect to adhesions at the cell front, thereby increasing the front vs. rear asymmetry in adhesiveness. If inhibition of calpain decreases adhesive asymmetry, cells with low calpain activity should migrate over a smaller range of substrate ECM concentrations and not be able to attain as high of a maximum cell speed as cells with a higher calpain activity. Experimental measurements quantitatively agree with this prediction (Huttenlocher et al., 1997). Increasing calpain activity above normal levels may allow us to increase maximum cell speed. However, at a certain point, calpain activity will likely impede formation of cytoskeletal linkages and reduce maximum speed. Thus, an intermediate calpain activity theoretically will provide maximum cell speed.

Our results suggest a model for rear detachment regulated by both applied tension from cytoskeletal contraction and biochemical modifications of cytoskeletal linkages (Figure 5.4). High cell-substratum adhesiveness (Figure 5.4A) may represent integrin aggregation into complexes which are under tension due to cytoskeletal contraction. This tension may not be high enough to sever adhesion complex bonds, however. Calpain activity and/or other biochemical mechanisms may weaken bonds within the cytoskeletal linkage enough for the applied tension to fracture the linkage, allowing the integrins in the adhesion complex to rip from the cell. Tyrosine phosphorylation and cytoskeletal tension are involved in ATP-dependent release of adhesions at the rear of migrating fibroblasts (Crowley and Horwitz, 1995). Conversely, low adhesiveness (Figure 5.4B) may represent integrins in a less-aggregated state. In this case, the biochemical signal for rear release may not localize to individual adhesions and rear release will be regulated primarily by applied force, allowing the integrin-ECM bonds to preferentially sever. Alternatively decreased avidity due to lack of integrin clustering at low adhesiveness may not necessitate a biochemical release mechanism -- the applied tension at the rear of the cell may be great enough to peel diffuse integrins from the ECM without biochemical cleavage of cytoskeletal linkages. In addition to accounting for migration of cells at different adhesiveness, this model for rear detachment also explains different detachment modes for different cell types. Fibroblasts, which form strong focal adhesions and adhere strongly to the substratum, apparently require integrin release for migration under many conditions. More highly motile cells, in contrast could exhibit dissociation of the integrin-ECM bonds as the primary detachment mode.

5.7 References

Beckerle, M. C., Burridge, K., DeMartino, G. N., and Croall, D. E. (1987). Colocalization of calcium-dependent protease II and one of its substrates at sites of cell adhesion. *Cell.* **51**, 569-577.

Cooray, P., Yuan, Y., Schoenwaelder, S. M., Mitchell, C. A., Salem, H. H., and Jackson, S. P. (1996). Focal adhesion kinase (pp125Fak) cleavage and regulation by calpain. *Biochem. J.* **318**, 41-47.

Crowley, E., and Horwitz, A. F. (1995). Tyrosine phosphorylation and cytoskeletal tension regulate the release of fibroblast adhesions. *J. Cell Biol.* **131**, 525-537.

DiMilla, P. A., Barbee, K., and Lauffenburger, D. A. (1991). Mathematical model for the effects of adhesion and mechanics on cell migration speed. *Biophys. J.* **60**, 15-37.

Du, X., Saido, T. C., Tsubuki, S., Indig, F. E., Williams, M. J., and Ginsberg, M. H. (1996). Calpain cleavage of the cytoplasmic domain of the integrin β3 subunit. *J. Biol. Chem.* **270**, 26146-26151.

Dustin, M. L., Bromley, S. K., Kan, Z., Peterson, D. A., and Unanue, E. R. (1997). Antigen receptor engagement delivers a stop signal to migrating T lymphocytes. *Proc. Natl. Acad. Sci. USA.* **94**, 3909-3913.

Hahn, K., DeBiasio, R., and Taylor, D. L. (1992). Patterns of elevated free calcium and calcineurin activation in living cells. *Nature.* **359**, 736-738.

Hendey, B., Klee, C. B., and Maxfield, F. R. (1992). Inhibition of neutrophil chemotaxis on vitronectin by inhibitors of calcineurin. *Science.* **258**, 296-299.

Huttenlocher, A., Palecek, S. P., Lu, Q., Zhang, W., Mellgren, R. L., Lauffenburger, D. A., Ginsberg, M. H., and Horwitz, A. F. (1997). Regulation of cell migration by the calcium-dependent protease calpain. *J. Biol. Chem.* **272**, 32719-32722.

Huttenlocher, A, Ginsberg, M. H., and Horwitz, A. F. (1996). Modulation of cell migration by integrin-mediated cytoskeletal linkages and ligand-binding affinity. *J. Cell Biol.* **134**, 1551-1562.

Inomata, M., Hayashi, M., Ohno-Iwashita, Y., Tsubuki, S., Saido, T.C. and Kawahima, S. (1996). Involvement of calpain in integrin-mediated signal transduction. *Arch. Biochem. Biophys.* **328**, 129-134.

Kuijpers, T. W., Mul, E. P. J., Blom, M., Kovach, N. L., Gaeta, F. C. A., Tollefson, V., Elices, M. J., and Harlan, J. M. (1993). Freezing adhesion molecules in a state of high-avidity binding blocks eosinophil migration. *J. Exp. Med.* **178**, 279-284.

Marks, P. W., Hendey B. and Maxfield, F. R. (1991). Attachment to fibronectin or vitronectin makes human neutrophil migration sensitive to alterations in cytosolic free calcium concentration. *J. Cell. Biol.* **112**, 149-158.

Maxfield, F. R. (1993). Regulation of leukocyte locomotion by Ca^{2+}. *Trends Cell Biol.* **3**, 386-391.

Mellgren. R. L., Lu, Q., Zhang, W., Lakkis, M., Shaw, E., and Mericle, M. T. (1996). Isolation of a Chinese hamster ovary cell clone possessing decreased μ-calpain content and a reduced proliferative growth rate. *J. Biol. Chem.* **271**, 15568-15574.

Saido, T. C., Sorimachi, H., and Suzuki, K. (1994). Calpain: new perspectives in molecular diversity and physiological-pathological involvement. *FASEB J.* **8**, 814-822.

Saterbak, A., and Lauffenburger, D. A. (1996). Adhesion mediated by bonds in series. *Biotechnol. Prog.* **12**, 682-699.

Schmidt, C., Horwitz, A.F., Lauffenburger, D. A., and Sheetz, M. P. (1993). Integrin/cytoskeleton interactions in migrating fibroblasts are dynamic, asymmetric, and regulated. *J. Cell. Biol.* **123**, 977-991.

Sorimachi, H., Saido, T. C., and Suzuki, K. (1994) New era of calpain research. Discovery of tissue-specific calpains. *FEBS Lett.* **343**, 1-5.

% Migration Speed

100 —

0 —

| CON | CPI | CON | CPI | CON | CPI | CON | CPI | CON | SHI | A4 | CON | SHI |

High **Low** **High** **Low** **High** **Low**

$\alpha IIb\beta 3$ $\alpha 5\beta 1$ $\alpha 5\beta 1$
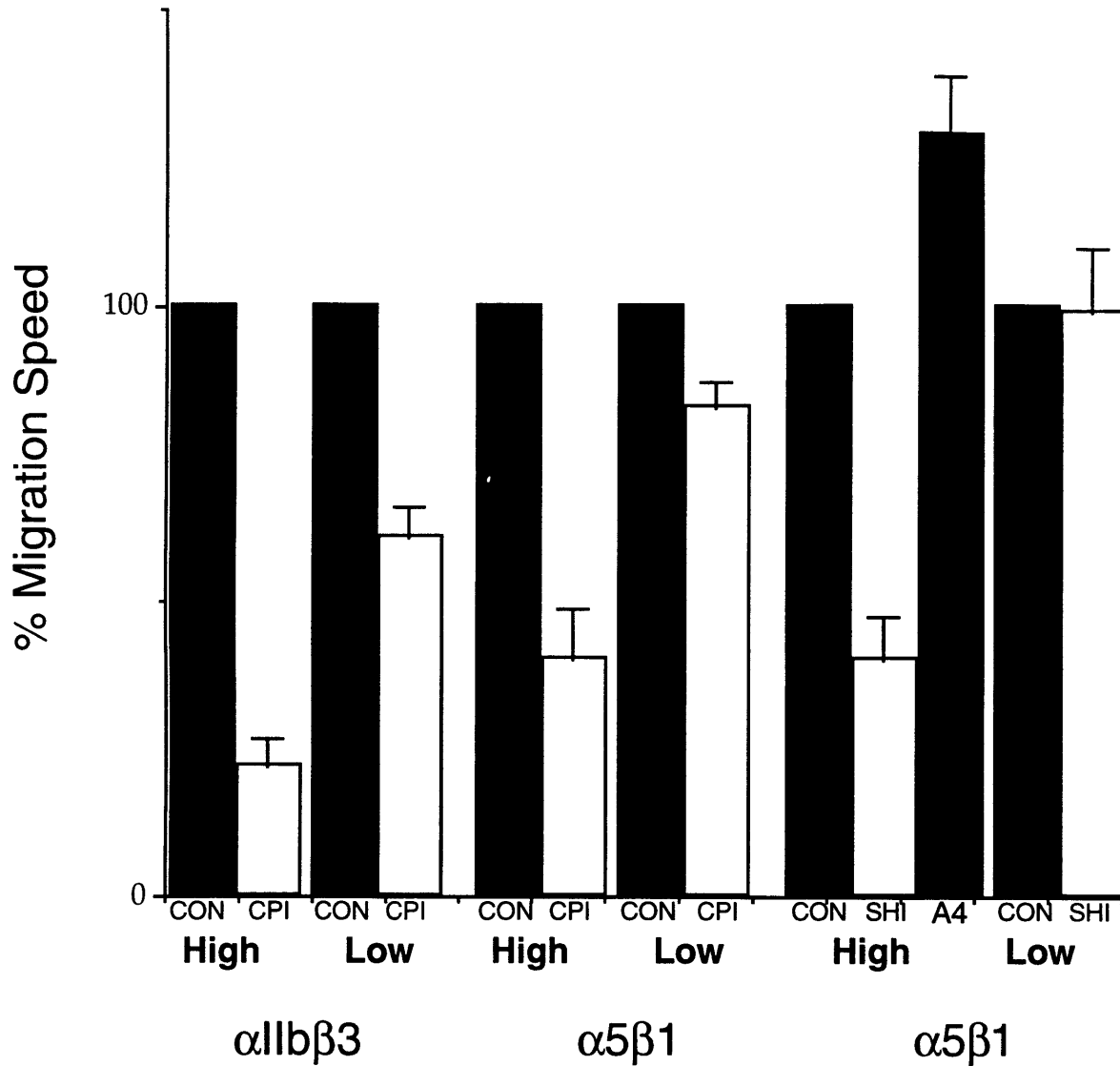
Figure 5.1. Calpain Inhibitor I Inhibits both $\beta 1$ and $\beta 3$ Integrin-Mediated Cell Migration. CHO cell clone, SHI, which expresses low levels of calpain I, also shows reduced migration rates. Rescue of this phenotype is demonstrated by transfecting SHI cells with human calpain I cDNA (A4). Reduced migration with calpain inhibition is substrate concentration dependent. Migration of CHO cells ectopically expressing $\alpha IIb\beta 3$ and untransfected CHO cells was studied on 10 µg/ml of fibrinogen and 10 µg/ml of fibronectin respectively (high). Migration was also measured at lower substrate concentrations, 1 µg/µl of fibrinogen and 0.1 µg/ml of fibronectin (low) respectively. Migration is expressed as the percentage of untreated control cells (CON) that migrate on both fibrinogen ($\alpha IIb\beta 3$) and fibronectin ($\alpha 5\beta 1$) over three hours. Each data point represents the average of a minimum of three separate experiments with error bars indicating s.d. Treatment with calpain inhibitor I (CPI) inhibits both $\alpha IIb\beta 3$ and $\alpha 5\beta 1$-mediated cell migration.
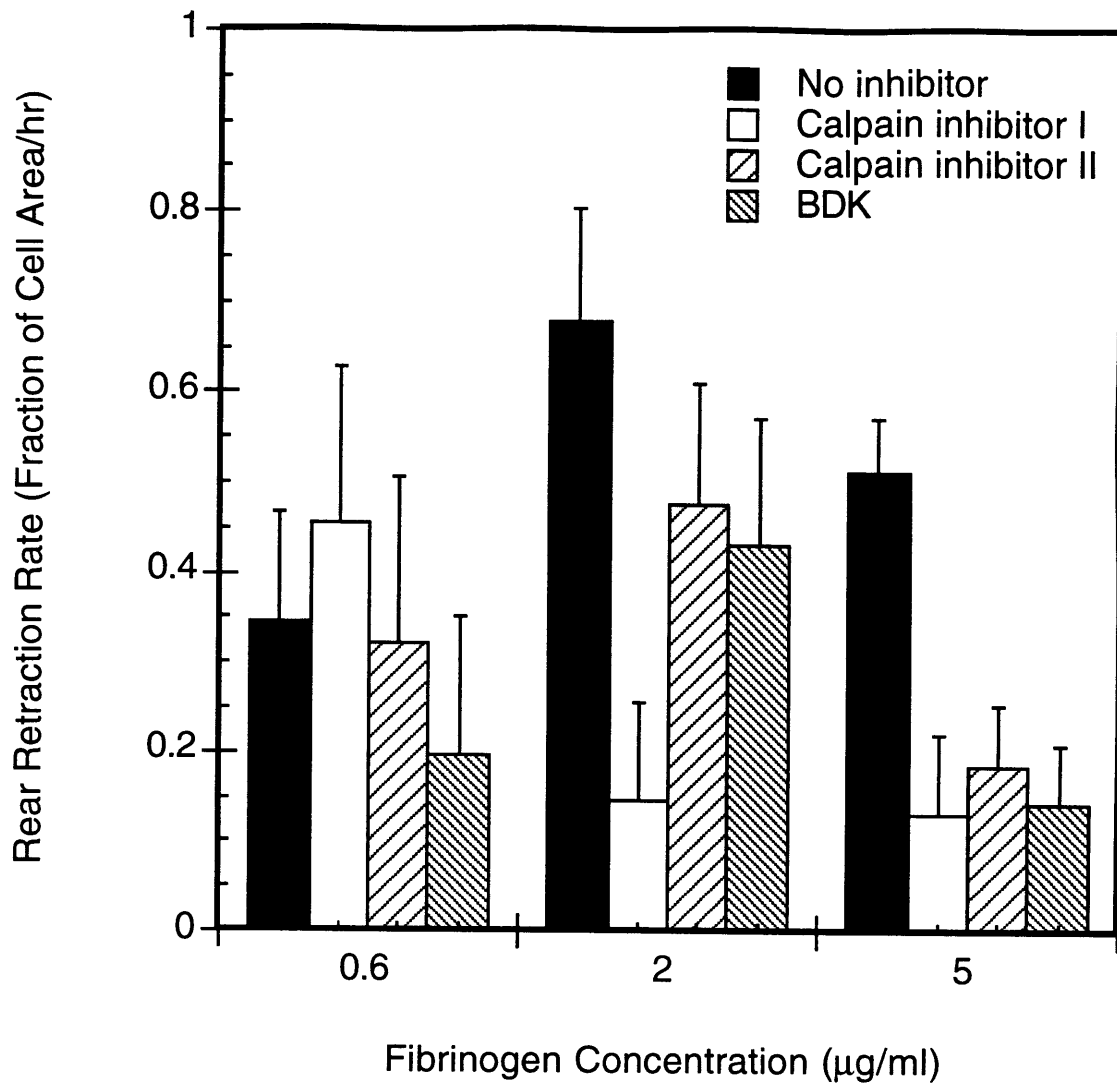
Figure 5.2. Calpain Inhibitors Reduce the Rate of Retraction of the Cell Rear during Migration at High Fibrinogen Concentrations. Detachment rate is measured by tracing cell outlines on phase contrast images and normalizing the area of the cell rear which detaches to the total cell area. Error bars represent standard deviations of detachment rate measurements. Calpain inhibitors I and II were used at 50 μg/ml and the diazomethyl ketone (BDK) was used at 50 μM. At high fibrinogen concentrations (5 μg/ml), calpain inhibitor I inhibits retraction rate by a factor of 5 while calpain inhibitor II and BDK partially inhibit rear retraction rate. At low fibrinogen concentrations (0.6 μg/ml) rear retraction is not inhibited by calpain inhibitors.
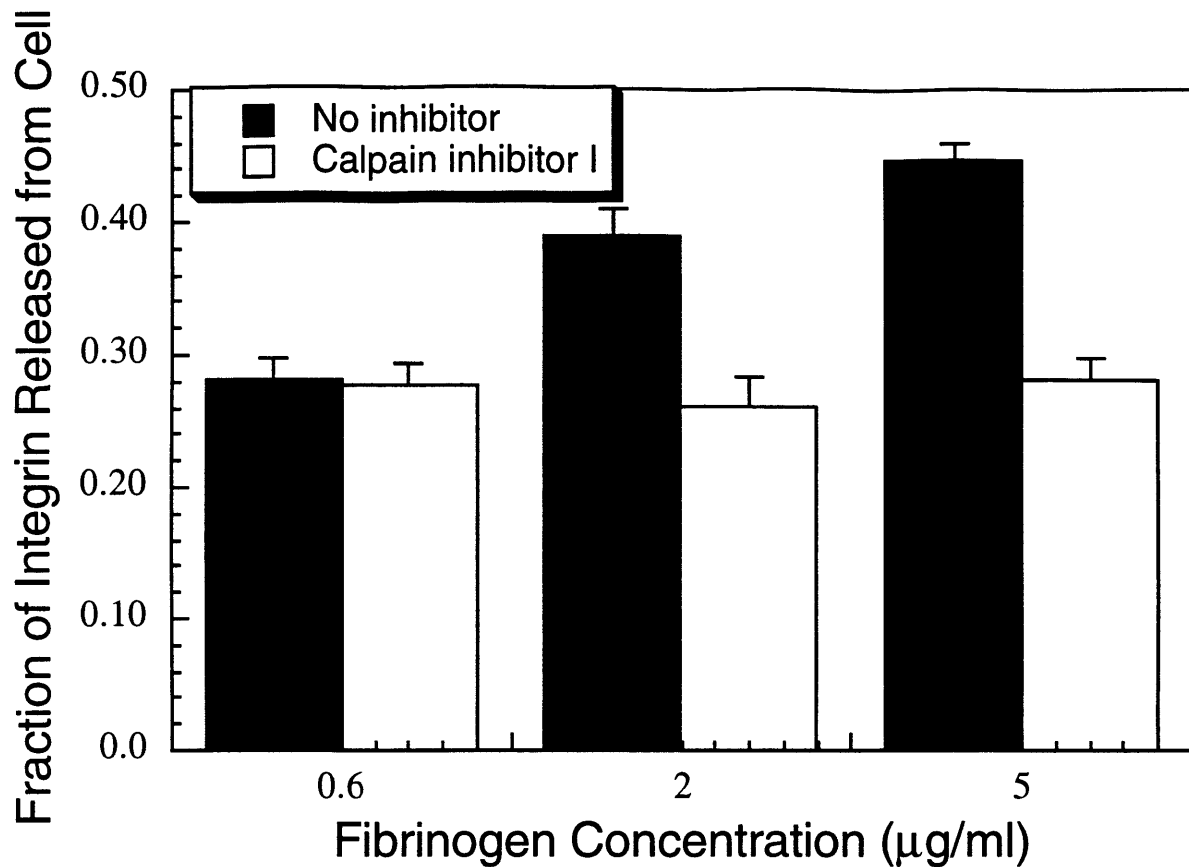
Figure 5.3. Calpain Facilitates Cytoskeletal Linkage Release at High Cell-Substratum Adhesiveness. The amount of integrin which releases from the rear of CHO cells migrating on fibrinogen was measured for cells which express αIIbβ3 integrin. At high fibrinogen concentrations (2 or 5 μg/ml) calpain inhibitor I causes less integrin to release from the cell upon rear retraction. This reduction in the amount of integrin on the substratum suggests a relative strengthening of the integrin-cytoskeleton bond compared to the integrin-ECM bond. At low fibrinogen concentrations (0.6 μg/ml), calpain inhibition has no effect on integrin release during cell migration. Error bars represent s.e.m.
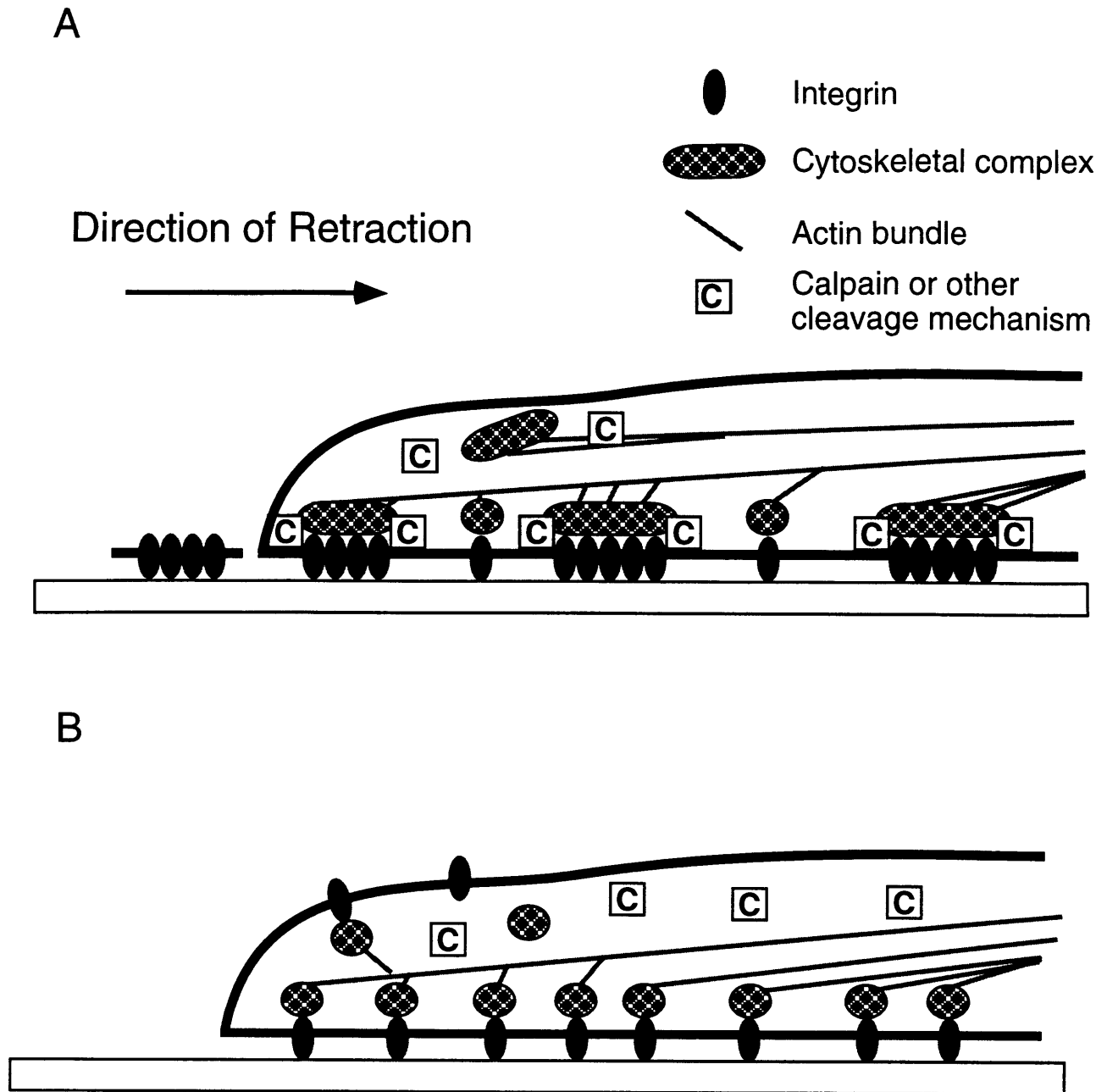
Figure 5.4. A Model for Release of Cytoskeleton-Integrin-ECM Linkages at the Rear of Cells which Migrate Using (A) Adhesion Complexes of Organized Integrins, or (B), Diffuse Integrins (B). Aggregated integrins are bound to cytoskeletal molecules which link them to the actin cytoskeleton. Calpain or other regulatory molecules localize to the adhesion structures in an inactive state. Contraction of the actin cytoskeleton applies tension which is generally insufficient to fracture the linkages, until the calpain is activated and cleaves cytoskeletal linkages. This results in the release of integrins from the rear of the migrating cell. Less organized integrins are similarly linked to the actin cytoskeleton but applied tension from cytoskeletal contraction is strong enough to peel the integrin-ECM bonds without calpain-mediated cytoskeletal bond cleavage. Integrins then dissociate from the substratum and remain within the cell membrane.

Chapter 6: Modeling Rear Detachment during Cell Migration

6.1 Model Overview

We developed a kinetic model for rear detachment in migrating cells to predict the detachment rate and mechanism as a function of integrin-ECM binding parameters, intracellularly generated force, and calpain activity. We can then compare the model predictions of detachment rate and the amount of integrin which rips from the cell with the experimental data to determine if our experimental results can be quantitatively explained by the effects of force and proteolysis on integrin-mediated linkages.

The model consists of two time phases -- (1) an attachment phase during which cell-substratum linkages form in the absence of force and calpain activity and (2) a detachment phase during which force and calpain activity are applied to the linkages until the cell detaches from the substratum. The attachment phase corresponds to the time an area of the cell is in contact with the substratum before it reaches the "rear region." For the purposes of the model, the rear of the cell is defined as the area which bears a high force and which possesses activated calpain. For the attachment phase, kinetic equations for formation of integrin-ECM and integrin-cytoskeletal bonds and mass balances on integrins, ECM ligands, and cytoskeletal elements are solved.

During the detachment phase the rear of the cell is divided into compartments. A compartment corresponds to the area of the cell which acts as a fracture unit. Therefore, all links between the cell and matrix in a compartment must fracture in order for the cell to detach that compartment from the substratum. Compartment size may roughly be equal to focal adhesion density. A cell with very few focal adhesions will have a few large compartments while a cell with many focal adhesions will have many smaller compartments. To induce cell-substratum detachment, a force is applied across the cell and calpain activity is initiated. The application of force and calpain activity is assumed to occur simultaneously. Such a scenario can be envisioned by local calcium release which induces actin-myosin contractility (Warrick and Spudich, 1987; Spudich, 1990) and calpain activity (Saido et al., 1994; Sorimachi et al., 1994). Force increases bond dissociation rate constants, as described by Bell (1978). We assume that forces are applied evenly through the cell membrane so that any integrin-ECM bond is subjected to force whether or not it is bound to cytoskeletal elements. Calpain irreversibly cleaves integrin cytoplasmic domains as well as cytoskeletal elements. This assumption can be relaxed to only cleave integrins or cytoskeletal elements, however. The bond formation differential equations are integrated through time until less than one bond per compartment exists and the force at the rear of the cell is great enough to extract from the cell membrane any integrins remaining bound to the ECM. This time required to detach the membrane allows us to calculate a detachment rate. We can also calculate the

amount of integrin ripped from the cell as the fraction of integrin-ECM bonds which remain intact and rip from the cell membrane at the detachment time.

6.2 Model Equations - Attachment Phase

In the model, integrins can exist in 4 different states: (1) bound to both cytoskeleton and matrix, (2) bound to cytoskeleton only, (3) bound to matrix only, or (4) bound to neither cytoskeleton nor matrix. Figure 6.1 is a schematic representation of the different occupancy states integrins, ECM ligands, and cytoskeletal elements may have in the model.

This model assumes only one bond between the integrin and cytoskeleton. In actuality, integrins link to the actin cytoskeleton through a series of bonds which may be crosslinked (see Figure 1.1). Since little is known about the interaction of the cytoskeletal molecules in an adhesion structure, we lump these interactions together into one bond. The integrin-cytoskeletal connection in our model corresponds to all of the bonds between the integrin and actin cytoskeleton.

We ean calculate the number of bonds a cell forms with the surface from the time an area on the membrane makes contact with the substratum to the time the area reaches the cell rear by solving a set of differential equations on bond formation and equations for conservation of receptors, ligands, and cytoskeleton Variables representing receptor states are definied in Figure 6.1

$$\frac{dq}{du} = k_{f1}rc - k_{r1}q - k_{f3}ql + k_{r3}t \tag{6.1}$$

$$\frac{ds}{du} = k_{f2}rl - k_{r2}s - k_{f4}sc + k_{r4}t \tag{6.2}$$

$$\frac{dt}{du} = k_{f3}ql - k_{r3}t + k_{f4}sc - k_{f4}t \tag{6.3}$$

$$R_T = r + q + s + t \tag{6.4}$$

$$L_T = l + s + t \tag{6.5}$$

$$C_T = c + q + t \tag{6.6}$$

To calculate the number of each species at the cell rear these equations are integrated through time until $u=u_A$ with the following initial condition:

@u=0; r=R$_T$ (6.7)

6.3 Model Equations - Detachment Phase

At u=uA, force is applied across bond linkages and protease activity is initiated at the cell rear, simultaneously. Both have several effects on the model equations.

Upon induction of protease activity, cytoskeletal elements and receptor cytoplasmic domains become inactivated. This agrees with data that shows calpain can cleave both integrin β subunit cytoplasmic domains as well as cytoskeletal molecules such as talin (Du et al., 1996; Inomata et al., 1996). Once inactivated, these elements can no longer participate in receptor-cytoskeletal bonding. In addition, we assume that cleavage of an intact receptor-cytoskeleton bond dissolves the bond and inactivates both the cytoskeletal element and the receptor cytoplasmic domain. The rate of receptor-ligand binding are assumed to be unchanged due to cleavage of the receptor cytoplasmic domain. Experiments have shown that cytoskeletal deletions can either increase or decrease integrin affinity for ligand, depending on the deletion site and the receptor type (Hughes et al., 1996; Lub et al., 1997; Lu and Springer, 1997). Inactivated cytoskeletal elements are denoted as c*, cleaved receptors are r*, and cleaved receptors bound to ligand are s*.

We assume a force distribution such that all bonds at the cell rear are equally stressed. This stress does not affect rate constants of bond formation (k$_f$) but increases dissociation rate constants (k$_r$), as described by Bell (1978):

$$k_r = k_r^0 \exp\left(\frac{\gamma F_b}{k_b \theta}\right)$$ (6.8)

Here, γ is the characteristic length of the unstressed bond, k_b is the Boltzmann constant, and θ is the absolute temperature. The force per bond, F_b, is:

$$F_b = \frac{F_T}{A_r(t+s+s*)}$$ (6.9)

This expression assumes that integrin-ligand bonds can transmit the same stresses as complete cytoskeleton-integrin-ECM bonds over the area of interest. Since the receptors cluster into regions of high density upon ligand binding, this is probably a reasonable assumption. We also assume that receptors not linked to the matrix are not allowed to transmit forces. Any force applied to these receptors will move the receptors in the plane of the cell membrane. In the presence of force and protease activity, the set of model equations becomes:

$$\frac{dq}{du} = k_{f1}rc - k_{r1}q - k_{f3}ql + k_{r3}t\left[\exp\left(\frac{\gamma F_b}{k_b \theta}\right)\right] - k_c pq$$ (6.10)

115

$$\frac{ds}{du} = k_{f2}rl - k_{r2}s\left[\exp\left(\frac{\gamma F_b}{k_b\theta}\right)\right] - k_{f4}sc + k_{r4}t\left[\exp\left(\frac{\gamma F_b}{k_b\theta}\right)\right] - k_c ps \qquad (6.11)$$

$$\frac{dt}{du} = k_{f3}ql - k_{r3}t\left[\exp\left(\frac{\gamma F_b}{k_b\theta}\right)\right] + k_{f4}sc - k_{r4}t\left[\exp\left(\frac{\gamma F_b}{k_b\theta}\right)\right] - k_c pt \qquad (6.12)$$

$$\frac{ds^*}{du} = k_c pt + k_c ps - k_{r2}s^*\left[\exp\left(\frac{\gamma F_b}{k_b\theta}\right)\right] + k_{f2}r^*l \qquad (6.13)$$

$$\frac{dr^*}{du} = k_c pr + k_c pq + k_{r2}s^*\left[\exp\left(\frac{\gamma F_b}{k_b\theta}\right)\right] - k_{f2}r^*l \qquad (6.14)$$

$$\frac{dc^*}{du} = k_c pc + k_c pq + k_c pt \qquad (6.15)$$

$$R_T = r + q + s + t + r^* + s^* \qquad (6.16)$$

$$L_T = l + s + t + s^* \qquad (6.17)$$

$$C_T = c + q + t + c^* \qquad (6.18)$$

Initial conditions for q, s, and t in the detachment model are the values for q, s, and t at $u=u_A$ in the attachment model. r^*, s^*, and c^* are 0 initially in the detachment model.

This model neglects the effects of integrin and cytoskeletal element endocytosis or synthesis, secretion and organization of ECM ligands, and integrin and cytoskeleton transport during the course of detachment. Experimentally, the time scales of detachment for different cell types range from seconds to minutes (Chapters 4 and 5; Chen, 1981) while the time scales for synthesis and transport are minutes to hours (Lawson and Maxfield, 1995; Jacobson et al., 1987; Duband et al., 1988).

6.4 Model Analysis

We nondimensionalize the model using the following dimensionless parameters:

116

$$\tau = k_{r1}u \qquad R = \frac{r}{R_T} \qquad Q = \frac{q}{R_T} \qquad S = \frac{s}{R_T} \qquad S^* = \frac{s^*}{R_T} \qquad T = \frac{t}{R_T}$$

$$R^* = \frac{r^*}{R_T} \qquad L = \frac{l}{R_T} \qquad C = \frac{c}{C_T} \qquad C^* = \frac{c^*}{C_T} \qquad \theta_1 = \frac{k_{f1}C_T}{k_{r1}} \qquad \theta_2 = \frac{k_{f2}L_T}{k_{r2}}$$

$$\theta_3 = \frac{k_{f3}L_T}{k_{r3}} \quad \theta_4 = \frac{k_{f4}C_T}{k_{r4}} \quad \kappa_2 = \frac{k_{r2}}{k_{r1}} \quad \kappa_3 = \frac{k_{r3}}{k_{r1}} \quad \kappa_4 = \frac{k_{r4}}{k_{r1}} \quad \kappa_c = \frac{k_c p}{k_{r1}}$$

$$\eta_{RL} = \frac{R_T}{L_T} \qquad \eta_{RC} = \frac{R_T}{C_T} \qquad \psi = \frac{\gamma F_T A_R}{k_B \theta R_T} \tag{6.19}$$

The attachment model equations become:

$$\frac{dQ}{d\tau} = \theta_1 RC - Q - \theta_3 \kappa_3 QL + \kappa_3 T \tag{6.20}$$

$$\frac{dS}{d\tau} = \theta_1 \kappa_2 RL - \kappa_2 S - \theta_4 \kappa_4 SC + \kappa_4 T \tag{6.21}$$

$$\frac{dT}{d\tau} = \theta_3 \kappa_3 QL - \kappa_3 T + \theta_4 \kappa_4 SC - \kappa_4 T \tag{6.22}$$

$$1 = R + Q + S + T \tag{6.23}$$

$$1 = L + \eta_{RL}[S + T] \tag{6.24}$$

$$1 = C + \eta_{RC}[Q + T] \tag{6.25}$$

with initial condition
$$\tau = 0 \quad R = 1 \tag{6.26}$$

The detachment model equations become:

$$\frac{dQ}{d\tau} = \theta_1 RC - Q - \theta_3 \kappa_3 QL + \kappa_3 T\left[\exp\left(\frac{\psi}{T + S + S^*}\right)\right] - \kappa_c Q \tag{6.27}$$

117

$$\frac{dS}{d\tau} = \theta_2 \kappa_2 RL - \kappa_2 S\left[\exp\left(\frac{\psi}{T + S + S^*}\right)\right] - \theta_4 \kappa_4 SC + \kappa_4 T - \kappa_c S \tag{6.28}$$

$$\frac{dT}{d\tau} = \theta_3 \kappa_3 QL - \kappa_3 T\left[\exp\left(\frac{\psi}{T + S + S^*}\right)\right] + \theta_4 \kappa_4 SC - \kappa_4 T - \kappa_c T \tag{6.29}$$

$$\frac{dS^*}{d\tau} = \kappa_c T + \kappa_c S - \kappa_2 S^*\left[\exp\left(\frac{\psi}{T + S + S^*}\right)\right] + \theta_2 \kappa_2 R^* L \tag{6.30}$$

$$\frac{dR^*}{d\tau} = \kappa_c R + \kappa_c Q + \kappa_2 S^*\left[\exp\left(\frac{\psi}{T + S + S^*}\right)\right] - \theta_2 \kappa_2 R^* L \tag{6.31}$$

$$\frac{dC^*}{dt} = \kappa_c[C + \eta_{RL}[Q + T]] \tag{6.32}$$

$$1 = R + Q + S + T + R^* + S^* \tag{6.33}$$

$$1 = L + \eta_{RL}[S + T + S^*] \tag{6.34}$$

$$1 = C + C^* + \eta_{RC}[Q + T] \tag{6.35}$$

The attachment model is integrated through time during the attachment phase. The values of R, Q, S, and T at the end of the attachment phase are used as the initial conditions during the detachment portion of the model.

6.4.1 Compartmentalization

During the detachment phase of the model, the rear of the cell is divided up into a number of compartments. The physical relevance of compartment size is the smallest area of the rear which will completely detach from the substratum if all linkages between the cell and the substratum are broken in that area. Detachment of one compartment is therefore independent of integrin-ECM or integrin-cytoskeleton binding in adjacent compartments. One can think of compartment size as being related to the size and density of focal adhesion structures. Cells with many, small adhesion structures will have very small compartments while cells with fewer, large adhesion structures will have large compartments.

6.4.2 Model Solution Procedure

The detachment equations are integrated in each compartment until two conditions are met. First, less than one cytoskeleton-integrin-ECM bond must remain intact in the compartment. Mathematically, this is:

$$T < \frac{R_T A_r}{N_C} \tag{6.36}$$

Second, the force at the rear of the cell must be sufficient to extract the integrins bound to ECM ligands from the membrane. We assume that the force required to extract multiple receptors is linearly proportional to the force required to extract a single receptor. Since receptors are extracted by pulling lipids from the cell membrane, clustered receptors may require less force to extract as a group than they would to extract individually. Our approximation is valid for diffuse receptors and probably overestimates force required to extract clustered receptors. This condition for detachment is mathematically expressed as:

$$S + S^* < R_T F_R A_r \tag{6.37}$$

The time for detachment, τ_d, is τ at the time which these two conditions are first met. The fraction of integrin which rips from the cell upon detachment is S+S* at $\tau=\tau_d$.

6.4.3 Parameter Values

Computations were performed with a range of parameter values to cover the range of behavior among many different cell types. The values for dimensional parameters we used are shown in Table 6.1 with corresponding references. A model sensitivity analysis to the various dimensionless parameters was performed by varying one dimensionless parameter over a physiologically relevant range while holding the other dimensionless parameters constant. This analysis allows us to determine how effectively we can regulate rear retraction rate and mechanism by quantitatively altering molecular interactions in the cell.

6.5 References

Akiyama, S. K. and Yamada, K. M. (1985). Interaction of plasma fibronectin with fibroblastic cells in suspension. *J. Biol. Chem.* **260**, 4492-4500.

Bajt, M. L., Loftus, J. C., Gawaz, M. P., and Ginsberg, M. H. (1992). Characterization of a gain of function mutation of integrin αIIbβ3 (platelet glycoprotein IIb-IIIa). *J. Biol. Chem.* **267**, 22211-22216.

Bell, G. I., Dembo, M., and Bongrand, P. (1984). Cell adhesion. Competition between nonspecific repulsion and specific bonding. *Biophys. J.* **45**, 1051-1064.

Bell, G. I. (1978). Models for the specific adhesion of cells to cells. *Science.* **200**, 618-627.

Burridge, K. and Connell, L. (1983). Talin: a cytoskeletal component concentrated in adhesion plaques and other sites of actin-membrane interaction. *Cell Motil.* **3**, 405-417.

Chen, W. -T. (1981). Mechanism of retraction of the trailing edge during fibroblast movement. *J. Cell Biol.* **90**, 187-200.

Du, X., Saido, T. C., Tsubuki, S., Indig, F. E., Williams, M. J., and Ginsberg, M. H. (1996). Calpain cleavage of the cytoplasmic domain of the integrin β3 subunit. *J. Biol. Chem.* **270**, 26146-26151.

Duband, J.-L., Nuckolls, G. H., Ishihara, A., Hasegawa, T., Yamada, K. M., Thiery, J. P., and Jacobson, K. (1988). Fibronectin receptor exhibits high lateral mobility in embryonic locomoting cells but is immobile in focal contacts and fibrillar streaks in stationary cells. *J. Cell Biol.* **107**, 1385-1396.

Evans, E. A., Berk, D., and Leung, A. (1991a). Detachment of agglutinin-bonded red blood cells. I. Forces to rupture molecular-point attachments. *Biophys. J.* **59**, 838-848.

Evans, E. A., Berk, D., Leung, A., and Mohandas, N. (1991b). Detachment of agglutinin-bonded red blood cells. II. Mechanical energies to separate large contact areas. Biophys. J. **59**, 849-860.

Fath, K. R., Edgell, C. J., and Burridge, K. (1989). The distribution of integrins in focal contacts is determined by the substratum composition. *J. Cell Sci.* **92**, 67-75.

Feltkamp, C. A., Pijnenburg, M. A., and Roos, E. (1991). Organization of talin and vinculin in adhesion plaques of wet-cleaved chicken embryo fibroblasts. *J. Cell Sci.* **100**, 579-587.

Galbraith, C. G., and Sheetz, M. P. (1997). A micromachined device provides a new bend on fibroblast traction forces. *Proc. Natl. Acad. Sci, USA.* **94**, 9114-9118.

Goodman, S. L., Risse, G., and von der Mark, K. (1989). The E8 subfragment of laminin promotes locomotion of myoblasts over extracellular matrix. *J. Cell Biol.* **109**, 799-809.

Harris, A. K., Wild, P., and Stopak, D. (1980). Silicone rubber substrata: a new wrinkle in the study of cell locomotion. *Science.* **208**, 177-179.

Horwitz, A. F., Duggan, K., Buck, C., Beckerle, M. C., and Burridge, K. (1986). Interaction of plasma membrane fibronectin receptor with talin. A transmembrane linkage. *Nature.* **320**, 531-532.

Hughes, P. E., Diaz-Gonzales, F., Leong, L., Wu, C., McDonald, J. A., Shattil, S. J., and Ginsberg, M. H. (1996). Breaking the integrin hinge. A defined structural constraint regulates integrin signaling. *J. Biol. Chem.* **271**, 6571-6574.

Inomata, M., Hayashi, M., Ohno-Iwashita, Y., Tsubuki, S., Saido, T.C. and Kawahima, S. (1996). Involvement of calpain in integrin-mediated signal transduction. *Arch. Biochem. Biophys.* **328**, 129-134.

Jacobson, K., Ishihara, A., and Inman, R. (1987). Lateral diffusion of proteins in membranes. *Annu. Rev. Physiol.* **49**, 163-175.

Kuntz, R. M., and Saltzman, W. M. (1997). Neutrophil motility in extracellular matrix gels: mesh size and adhesion affect speed of migration. *Biophys. J.* **72**, 1472-1480.

Lane, R. D., Allan, D. M., and Mellgren, R. L. (1992). A comparison of the intracellular distribution of μ-calpain, m-calpain, and calpistatin in proliferating human A431 cells. *Exp. Cell. Res.* **203**, 5-16.

Lawson, M. A., and Maxfield, F. R. (1995). Ca^{2+}-and calcineurin-dependent recycling of an integrin to the front of migrating neutrophils. *Nature.* **377**, 75-79.

Leckband, D., Muller, W., Schmitt, F. J., and Ringsdorf, H. (1995). Molecular mechanisms determining the strength of receptor-mediated intermembrane adhesion. *Biophys. J.* **69**, 1162-1169.

Lee, J., Leonard, M., Oliver, T., Ishihara, A., and Jacobson, K. (1994). Traction forces generated by locomoting keratocytes. *J. Cell Biol.* **127**, 1957-1964.

Lu, C. F. and Springer, T. A. (1997). The α subunit cytoplasmic domain regulates the assembly and adhesiveness of integrin lymphocyte function-associated antigen-1. *J. Immunol.* **159**, 268-278.

Lub, M., van Vliet, S. J., Oomen, S. P., Pieters, R. A., Robinson, M., Figdor, C. G., and van Kooyk, Y. (1997). Cytoplasmic tails of β1, β2, and β7 integrins differently regulate LFA-1 function in K562 cells. *Mol. Biol. Cell.* **8**, 719-728.

Murachi, T. and Yoshimura, N. (1985). Intracellular localization of low and high calcium-requiring forms of calpain. *Prog. Clin. Biol. Res.* **180**, 165-174.

Regen, C. M., and Horwitz, A. F. (1992). Dynamics of β1 integrin-mediated adhesive contacts in motile fibroblasts. *J. Cell. Biol.* **119**, 1347-1359.

Saido, T. C., Sorimachi, H., and Suzuki, K. (1994). Calpain: new perspectives in molecular diversity and physiological-pathological involvement. *FASEB J.* **8**, 814-822.

Sczekan, M. M. and Juliano, R. L. (1990). Internalization of the fibronectin receptor is a constitutive process. *J. Cell. Phys.* **142**, 575-580.

Sorimachi, H., Saido, T. C., and Suzuki, K. (1994) New era of calpain research. Discovery of tissue-specific calpains. *FEBS Lett.* **343**, 1-5.

Spudich, J. A. S. (1990). Motor molecules in motion. *Nature.* **348**, 284-285.

Suzuki, K., Saido, T. C., and Hirai, S. (1992). Modulation of cellular signals by calpain. *Ann. NY Acad. Sci.* **674**, 218-227.

Warrick, H. M. and Spudich, J. A. (1987). Myosin structure and function in cell motility. *Annu. Rev. Cell Biol.* **3**, 379-421.

Table 6.1. Estimates for Dimensional Parameters.

Parameter	Definition	Range	Reference
A_r	Cell rear area	10^1-10^3 mm^2	Chen, 1981
$k_b\Theta$	Thermal Energy	4.1×10^{-14} ergs	
γ	Unstressed Receptor-Ligand Bond Length	10^{-8}-10^{-7} m	Bell et al., 1984
k_r	Reverse reaction rates	10^{-5}-10^1 s^{-1}	Bell, 1978
$K_{d2,3}$	Receptor-ligand equilibrium constants	10^{-8}-10^{-6} M^{-1}	Horwitz et al., 1986; Akiyama and Yamada, 1985
$K_{d1,4}$	Receptor-cytoskeleton equilibrium constants	10^{-8}-10^{-6} M^{-1}	Horwitz et al., 1986
R_T	Receptor number	10^4-10^7	Sczekan and Juliano, 1990; Bajt et al., 1992
F_T	Force at cell rear	10^{-1}-10^1 nN/μm2	Galbraith and Sheetz, 1997; Harris et al., 1980; Lee et al., 1994
F_R	Force to extract an integrin from cell membrane	0.1-100 μdyne	Leckband et al., 1995; Evans et al., 1991
C_T	Cytoskeletal element density	10^9-10^{12} cm^{-2}	Feltkamp et al., 1991
L_T	Ligand density	10^6-10^{13} cm^{-2}	Goodman et al., 1989
N_C	Compartment number	10^1-10^4	Burridge and Connell, 1983; Fath et al., 1989; Regen and Horwitz, 1992
p	Calpain concentration	10^{-9}-10^{-6} M	Murachi and Yoshimura, 1985; Lane et al., 1992
k_c	Calpain rate constant	10^2-10^6 M^{-1}s^{-1}	Mellgren, personal communication; Suzuki et al., 1992
u_A	Cell attachment time	10^2-10^5 s	Chen, 1981; Kuntz and Saltzman, 1997
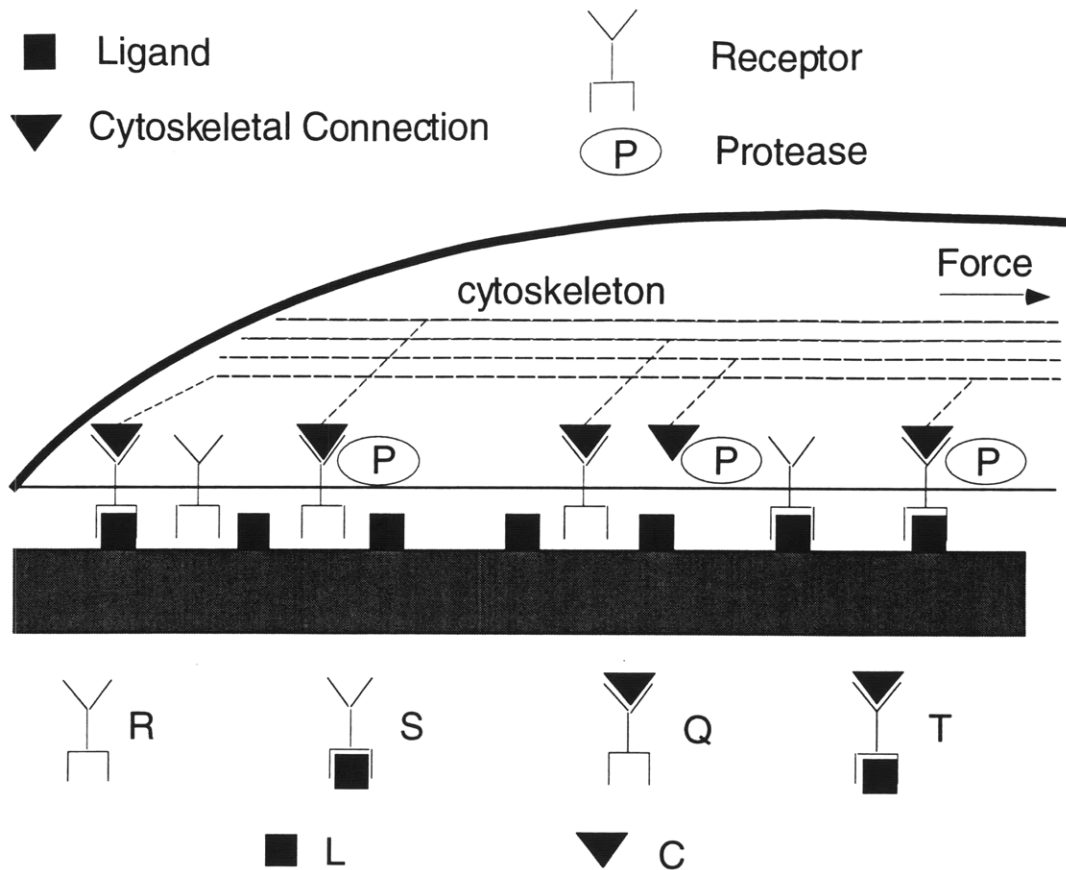
Figure 6.1. A Schematic Representation of Linkages between the Cell and Substratum during Rear Retraction. Integrins can exist in 4 states: unbound (R), bound to ECM ligand only (S), bound to the cytoskeleton only (Q), or bound to both ECM and cytoskeleton (T). Ligands can either be free (L) or bound to integrins (S). Cytoskeletal elements can also be free (C) or bound to integrins (Q). Upon activation, proteases (P), can cleave integrin-cytoskeletal linkages.

Chapter 7: Model Results and Analysis

7.1 Modeling Strategy

We developed a mathematical model to simulate the detachment of adhesion structures at the rear of a migrating cell from its substratum due to both forces applied across cytoskeleton-integrin-ECM linkages and protease activity which cleaves and deactivates integrins and cytoskeletal elements. This model can predict both the detachment rate and detachment mechanism, referring to the relative contribution of integrin-matrix vs. integrin-cytoskeleton bond dissociation.

We focused on how cytoskeleton-integrin-ligand binding affinities, cytoskeleton-integrin-ligand concentrations, calpain activity, and applied force affect detachment rate and mechanism. We were particularly interested in determining how each of these parameters can alter detachment mechanism and the corresponding influence on detachment rate. Then we can compare model predictions to phenotypic differences in rear detachment among different cell types. We conclude that cells can detach through a rapid, force-dominated mechanism which tends to dissociate integrin ECM linkages or a slower, protease-dominated mechanism which cleaves integrin-cytoskeletal linkages. The amount of integrin which is extracted at the rear of the migrating cell is an excellent indicator of which phenotype the cell exhibits.

7.2 Temporal Profiles of Bond States Indicate Two Detachment Phenotypes

First, we analyzed how the number of free, bound, cleaved, and uncleaved receptors, ligands, and cytoskeletal elements changed through times at different values of ψ, dimensionless force. Figure 7.1 shows how T, the number of complete cytoskeleton-integrin-ECM linkages, changes through time at different ψ. One condition for detachment is that less than one complete linkage exists per compartment. During this simulation, that condition corresponds to T<0.001. T decreases through time as force and calpain activity are activated. At low forces ($\psi<2.07$), T and detachment time are relatively insensitive to ψ. At higher forces ($\psi>2.08$), T and detachment time become a strong function of ψ.

Two different phenotypes of detachment exist. These phenotypes can be better illustrated by looking at all of the different receptor states through time at different forces. At $\psi=2$ (Figure 7.2) detachment takes over 4 τ. An initial rapid decrease in T is accompanied by an increase in Q and S. T, Q, and S all decrease as S* and R* increase. Applied force appears to break about half of the complete linkages then calpain activity is required to release the rest of the linkages. This

125

bond profile is typical for ψ<2.07. Therefore, slow detachment is limited by integrin-cytoskeleton cleavage due to calpain activity.

Rapid detachment is limited by force-dependent dissociation of integrin-ligand bonds, however. At ψ=3 (Figure 7.3), an initial decrease in T is accompanied by an increase in Q and S. After τ=0.01, T and S rapidly decrease while Q and R increase as integrin-ligand bonds dissociate. Receptor cleavage is negligible during rapid detachment. This bond profile is typical for ψ>2.08. The transition between rapid and slow detachment is very abrupt at ψ=2.07.

7.3 Phase Plots of Bond States at Different Detachment Phenotypes

In order to characterize the detachment mechanisms for both rapid and slow detachment, we constructed a phase plot of cytoskeleton-integrin-ECM linkages, T, vs. cytoskeleton-integrin linkages, Q, (Figure 7.4) at the same dimensionless parameters as figures 7.1-7.3. During rapid detachment (ψ>2.08), a significant number of cytoskeleton-integrin linkages remain intact at detachment. The number of cytoskeleton-integrin linkages increases as ψ increases. During slow detachment (ψ<2.07), cytoskeleton-integrin linkages form as complete linkages dissociate. Essentially all cytoskeleton-integrin linkages must fracture to allow slow detachment, however. The condition for detachment requires T to approach 0. At slow detachment Q approaches 0, consistent with cytoskeleton-integrin bond cleavage as the dominant detachment mechanism. During rapid detachment Q does not approach 0 so cytoskeleton-integrin cleavage is not a condition for rapid detachment.

The presence of intact integrin-cytoskeleton bonds at detachment appears to be one sign which would allow us to differentiate between slow and rapid detachment. This is a very difficult parameter to measure experimentally. We can measure the fraction of integrin-ligand bonds which remain intact at detachment, however. Chapter 5 describes an immunofluorescent assay to determine the amount of integrin which is extracted from the membrane upon detachment. In terms of this model, that fraction corresponds to S+S* at detachment. We constructed a phase plot of T vs. S+S* to determine if the presence of intact integrin-ligand bonds also indicates rapid or slow detachment (Figure 7.5). Slow detachment conditions (ψ<2.07) results in a significant number of integrin-ligand bonds (>50%) remaining intact. During rapid detachment (ψ>2.08) less than 10% of integrins remain bound to ligand. The amount of integrin which is extracted at the rear of a migrating cell is a good sign for whether rear retraction is in the rapid, integrin-ligand dissociation regime or the slow, cytoskeleton-integrin cleavage regime. It is fairly easy to measure the amount of integrin which extracts from the cell membrane and there is a large difference between the amounts which release from the cell in each regime.

126

7.4 Calpain Activity Regulates Slow Detachment but not Rapid Detachment

We varied intracellular calpain activity during the detachment phase of the model to predict the effects a proteolytic mechanism can have on rear retraction rate and bond detachment mechanism. Figure 7.6A illustrates how η_{RL}, the ratio of receptor concentration to ligand concentration, affects detachment rate at different levels of calpain activity. At $\eta_{RL} < 3$, the time required for detachment is virtually independent of η_{RL} but does depend on calpain activity. An order of magnitude increase in calpain activity corresponds to an order of magnitude decrease in τ_D. At low η_{RL}, detachment rate directly correlates with calpain activity. For η_{RL} above 3, detachment rate decreases with increasing η_{RL} and is independent of calpain activity. Cleavage of cytoskeleton-integrin bonds has no effect on detachment rate at high η_{RL}. By decreasing integrin expression or increasing ligand concentration we can move from protease-limited to integrin-ligand dissociation-limited detachment. By only changing calpain activity we cannot switch between detachment phenotypes but we can alter the rate of detachment if we are operating in the protease-limited regime. If calpain concentration or activity is zero, then the protease-limited detachment regime does not exist and cells cannot detach from the substratum at low η_{RL}.

We also find that the amount of integrin which rips from the cell membrane upon rear retraction correlates with detachment phenotype as η_{RL} changes (Figure 7.6B). At low η_{RL} and slow detachment, we see significant amounts of integrin-ligand bonds which remain intact as the rear retracts. At high η_{RL} and rapid detachment, very few integrin-ligand bonds remain intact. Interestingly, calpain activity does not affect the bond detachment mechanism, even at low η_{RL} where it affects detachment rate. Changing calpain activity does not change the number of cytoskeleton-integrin bonds which must fracture, only the rate at which they fracture.

7.5 Integrin-Ligand Binding Parameters can Affect the Transition between Detachment Phenotypes

Integrin-ligand binding affinity (θ_2, θ_3) can alter the value of η_{RL} which results in the transition from slow to rapid detachment as shown in Figure 7.7A. An increase in integrin-ligand affinity causes an increase in the integrin:ligand concentration ratio which allows rapid detachment. An increase in affinity can compensate for a decrease in ligand concentration to keep the cell attachment strength great enough that the applied force cannot sever the bonds without protease activity. If the cells are in the slow detachment regime, detachment rate is not a function of either η_{RL} or $\theta_{2,3}$. Therefore, integrin-ligand binding parameters can regulate the transition from slow to rapid detachment but not the detachment rate in the slow detachment regime. As changes in η_{RL} and $\theta_{2,3}$ result in the transition from slow to rapid detachment, a corresponding decrease in the

fraction of integrin extracted at the rear of the cell occurs (Figure 7.7B). Conditions promoting rapid detachment cause about 5% of the integrin to extract from the cell membrane while conditions resulting in slow detachment cause 20-100% of the integrin to remain attached to the substratum behind the cell.

At any η_{RL}, changes in $\theta_{2,3}$ can affect how changes in ψ cause the transition from slow to rapid detachment (Figure 7.8A). As affinity increases, a higher force is required to sever all of the cell-substratum attachments and cause rapid detachment. Detachment rate in the slow release regime is relatively independent of $\theta_{2,3}$ or ψ. During the slow detachment regime at low ψ, significant amounts of integrin is extracted from the cell membrane but at rapid detachment rates very little integrin is extracted (Figure 7.8B). In the rapid detachment regime, increases in ψ do result in increased integrin extraction because cytoskeleton-integrin-ligand linkages fracture into cytoskeleton-integrin or integrin-ligand linkages so rapidly that integrin-ligand linkages are extracted before they fracture. This behavior is probably a modeling artifact and would not occur experimentally because membrane stiffness would probably not allow the lipid bilayer to support the forces required to extract the receptors in the μs time scale of bond fracture at high forces.

Three different parameters can affect the transition of detachment rate from the slow, protease-limited to the faster, bond-dissociation limited regime. These are η_{RL}, $\theta_{2,3}$, and ψ. By changing the integrin-ligand binding parameters or the intracellularly generated force we can change the detachment phenotype. Figure 7.9 illustrates how these three parameters interact at the transition between phenotypes. The transition point is most sensitive to changes in ψ due to the exponential effect of ψ on dissociation rate constants. At high η_{RL} the transition point is relatively insensitive to $\theta_{2,3}$ but at low η_{RL} the transition point is very sensitive to $\theta_{2,3}$. Likewise, the sensitivity of the transition point to η_{RL} increases as $\theta_{2,3}$ increases. If these parameters are not altered enough to switch to the rapid phenotype, however, they will have little effect on detachment rate. These parameters will affect detachment rate within the rapid release phenotype because they affect the kinetics of integrin-ligand release. This will probably not result in changes in cell migration speed, however, because at detachment rates this fast other cellular process will limit overall cell speed.

7.6 Cytoskeleton-Integrin Binding Parameters Affect the Rate of Protease-Limited Detachment

Since linkage fracture between either the cytoskeleton-integrin or integrin-ligand bond can allow detachment, we varied the affinities of these two bonds simultaneously to see how each affects detachment rate (Figure 7.10A) and detachment mechanism (Figure 7.10B). Changes in integrin-ligand affinity (θ_2 and θ_3), but not changes in cytoskeleton-integrin affinity (θ_1 and θ_4)

can affect the transition from rapid detachment to slow detachment. During rapid detachment at low integrin-ligand affinity, detachment rate is a function of integrin-ligand binding affinity but not integrin-cytoskeleton binding affinity. Under these conditions, very little integrin rips from the cell membrane, so one expects integrin-ligand dissociation to limit detachment rate. As more integrin-ligand bonds form due to increased affinity, detachment slows. During slow detachment at high integrin-ligand affinity, detachment rate is relatively independent of integrin-ligand affinity but is a function of cytoskeleton-integrin affinity. In this slow detachment regime, a large fraction of integrins are extracted upon detachment indicating that cytoskeleton-integrin fracture is limiting detachment. As cytoskeleton-integrin affinity increases, more linkages must be cleaved and detachment time increases. Interestingly, integrin extraction is a function of integrin-ligand affinity but not of integrin-cytoskeleton affinity, except at very low θ_1, θ_2, θ_3 and θ_4.

We also simultaneously varied the receptor:ligand concentration ratio (η_{RL}) and the receptor:cytoskeleton concentration ratio (η_{RC}) to determine the effects of each of these parameters on detachment rate (Figure 7.11A) and detachment mechanism (Figure 7.11B). Similar to changing integrin-ligand or cytoskeleton-integrin affinity, changes in η_{RL} but not η_{RC} can affect the transition from slow detachment to rapid detachment. At low η_{RL}, the intracellularly generated force is not sufficient to fracture all of the cytoskeleton-integrin-ligand linkages and calpain cleavage of cytoskeleton-integrin bonds limits detachment rate. Under these conditions, τ_D is a function of η_{RC} but not η_{RL} and a significant fraction of integrins is extracted from the cell membrane. At high η_{RL} the applied force can fracture all of the cytoskeleton-integrin-ligand linkages to allow rear retraction. Here, detachment of integrin-ligand bonds limits detachment rate and an increase in η_{RL} decreases τ_D.

The detachment mechanism in this model depends on the number and nature of integrin-ligand bonds but is independent of the number and nature of cytoskeleton-integrin bonds. Only by changing the integrin-ligand concentration or affinity can we cause the transition between slow and rapid detachment. In the slow detachment regime cytoskeleton-integrin cleavage limits the rate of detachment so changes in integrin-cytoskeleton affinity and concentrations affect detachment rate but integrin-ligand binding parameters do not. Conversely, in the rapid detachment regime, integrin-ligand dissociation limits retraction rate. Altering integrin-ligand affinity and concentrations will affect detachment rate in the rapid regime but cytoskeleton-integrin binding parameters do not.

7.7 Receptor Clustering Increases Detachment Time in the Slow Detachment Regime

Cell types such as fibroblasts cluster integrins into areas of close contact (Regen and Horwitz, 1992; Palecek et al., 1996) while cell types such as leukocytes do not (Maxfield, 1993). Our model allows us to account for integrin clustering by varying the compartment size, or the area of the cell in which all cytoskeleton-integrin-ligand linkages must fracture to permit that area to retract. A large compartment size, or low compartment number, corresponds to a high degree of integrin clustering. As integrins become more diffuse, compartment number approaches the number of complete linkages. Figure 7.12 shows that changing compartment number does not affect the transition from slow to rapid detachment or detachment rate during rapid detachment. During slow detachment, however, increasing the number of compartments decreases τ_D. As the receptors become more diffuse, fewer cytoskeleton-integrin-ECM linkages exist per compartment at any value of η_{RL}, so fewer linkages must fracture for the compartment to detach from the substratum. The number of compartments has no effect on the detachment mechanism.

7.8 Cooperative Binding of Integrins Does not Affect Transition between Slow and Rapid Detachment

Most of the model calculations were performed assuming integrin-ligand and cytoskeleton-integrin binding are independent events. However, integrin-ligand and cytoskeleton-integrin binding have been shown to induce conformational changes in the integrin which can presumably enhance integrin binding to both the ligand and cytoskeleton (O'Toole et al., 1994; Fox et al., 1996; Hughes et al., 1996; Tsuchida et al., 1998). For example, integrins bound to ligand have a higher affinity for cytoskeletal elements than integrins not bound to ligand. The magnitude of the affinity change is unknown however. To test the effects of enhanced binding due to cooperativity we varied θ_3 and θ_4 while holding θ_1 and θ_2 constant. The degree of cooperativity does not affect the value of η_{RL} which causes the transition from slow to rapid detachment. Increasing cooperativity does decrease detachment rate during both slow and rapid detachment by increasing the number of cytoskeleton-integrin-ECM linkages and decreasing the number of cytoskeleton-integrin and integrin-ligand linkages (Figure 7.13). The change in detachment times is very small though. An order of magnitude increase in θ_3 and θ_4 only increases τ_D by about 20%. Cooperativity also has no effect on the bond fracture mechanism during rear retraction. Therefore, the rapid integrin-ligand dissociation dependent mechanism of release and the slower integrin-cytoskeleton cleavage dependent mechanism occur in the presence or absence of integrin binding

cooperativity but the rates of detachment in either regime may vary depending on the enhancement of binding.

7.9 Comparison to Experiments

Several of the model predictions have been tested in different experimental systems. Perhaps the most interesting prediction of the model is two different phenotypes for detachment. One phenotype is very rapid and limited by the rate of receptor-ECM ligand dissociation. The other phenotype is slower and limited by receptor-cytoskeleton bond cleavage. The model also predicts that the extent of integrin extraction is an indicator of detachment phenotype. Rapid detachment is primarily between the integrin and ECM ligand so very little integrin extracts from the membrane at the rear of the cell. Conversely, slow detachment occurs primarily due to integrin-cytoskeleton bond proteolysis and many integrin-ligand bonds remain intact. These integrins are extracted from the cell membrane and leave a trail of adhesion receptors behind the migrating cell.

These two different detachment phenotypes exist among different cell types. Cells such as fibroblasts or Chinese hamster ovary (CHO) cells are rate-limited by rear retraction, especially at high adhesiveness (Chapter 4). These cells often possess elongated tails and rear retraction events occur on the timescale of minutes (Chen, 1981, Huttenlocher et al., 1997). These cells also release a substantial fraction of their integrin onto the substratum upon rear retraction in vitro (Regen and Horwitz, 1992; Palecek et al., 1996; Chapter 4) and apparently in vivo (Bard and Hay, 1975). Cells such as keratocytes move by gliding over the substratum. They do not have elongated tails at the cell rear and detach much more quickly than fibroblasts (Lee et al., 1994). Neutrophils and T lymphocytes also move much more rapidly than fibroblasts and their migration speed does not seem to be limited by rear retraction under most conditions (Maxfield, 1993; Niggimann et al., 1997). Membrane extraction has not been as extensively studies in these rapidly-detaching cells as in slowly-detaching cells. However, T-lymphocytes do not leave patches of membrane attached to the substratum (Niggimann et al., 1997). β_2 integrin subunits do not appear to extract from the rear of migrating neutrophils either (Huttenlocher and Palecek, unpublished observations).

The model predicts that a cell can switch between rapid, integrin-ECM dominated dissociation and slower, integrin-cytoskeleton dominated fracture by quantitatively altering the integrin:ECM concentration, the integrin-ligand affinity, or the intracellularly generated force. We previously demonstrated that at high ligand concentration or integrin-ligand affinity CHO cells detach from the substratum very slowly and leave a large fraction of their integrin attached to the substratum (Chapter 4). As we decrease ligand concentration or integrin-ligand affinity, migration speed increases due to increased detachment rate and the amount of integrin which extracts from

131

the cell decreases. Although rear detachment no longer limits cell speed, the CHO cells still cannot move as quickly as neutrophils or keratocytes, possibly because other factors are limiting cell speed. Cells which typically migrate by rapid detachment can also switch phenotype to slow detachment. The formation of focal adhesions in fish epidermal keratocytes results in an elongated cell shape and decreased cell speed (Lee and Jacobson, 1997). As these highly motile cells become more adherent, they appear to migrate with a morphology more typical of fibroblasts. The semicircular morphology characteristic of keratocyte locomotion, and the higher speed, can be restored by competitive inhibition of the formation of the focal adhesions by RGD peptides or monoclonal antibodies (de Beus et al., 1997). Increasing ligand concentrations causes neutrophil tails to elongate and greatly reduces cell speed (Mandeville and Maxfield, 1997). The detachment mechanism of these cells is unknown, however.

According to the model, inhibiting calpain activity should decrease the rate of detachment for cells in the predominately integrin-cytoskeletal cleavage regime but should not affect detachment in the integrin-ECM release regime. Both of these situations have been observed experimentally. Pharmacological or genetic inhibition of calpain activity inhibits rear retraction rate at high ligand concentrations but not at low ligand concentrations (Huttenlocher et al., 1997; Chapter 5). Calpain inhibitors also have no effect on rear retraction in neutrophils (Huttenlocher, unpublished results). Changes in calpain activity should not affect a transition between slow and rapid detachment, according to the model. Marks et al. (1991) observed uropod elongation and a corresponding reduction in neutrophil speed when intracellular calcium transients are buffered. Preventing intracellular calcium transients at the rear of the cell should prevent calpain activity (Saido et al., 1994; Sorimachi et al., 1994), but may also affect other cellular process, such as the production of force by altering actin-myosin interactions (Warrick and Spudich, 1987). The model predicts that calpain activity will not affect integrin extraction as it alters detachment rate. In contrast, we found that inhibition of calpain decreases the amount of integrin which rips from the rear of a migrating cell (Chapter 5). This difference is probably due to stoichastic variations in parameter values at different locations in the cell. Areas of the cell with fewer bonds may show the rapid detachment phenotype while areas of the cell which are more adherent may be limited by integrin-cytoskeletal cleavage. The experiments in Chapter 5 may have measured proportionally more rapid detachment events which can still occur in the absence of calpain activity than in the presence of calpain activity. This would account for an observed decrease in the amount of integrin which extracts from the rear of the cell.

The model predictions of the effects of force and integrin-cytoskeleton binding parameters on rear retraction rate and mechanism are largely unknown. Cytoskeleton element concentration could be varied by transfecting or microinjecting the cells with talin. Integrin-cytoskeleton affinity can be altered using integrins with cytoplasmic domain mutations or deletions. Typically, these

mutations affect integrin-ligand binding or integrin clustering as well as integrin-cytoskeleton binding, complicating experimental interpretation.

7.10   Discussion of Model Results

We have described a simple mathematical model for biophysical and biochemical detachment of adhesions at the rear of a migrating cell. Integrin-ligand and integrin-cytoskeleton bonds from in the absence of force. As these linkages reach the rear of the cell a force is applied to the linkages and intracellular proteases are activated simultaneously. For example, intracellular calcium transients, which occur at the rear of migrating cells, can stimulate both contractility and protease activity and may be stimulated by bound adhesion receptors (Marks et al., 1991; Alteraifi and Zhelev, 1997). This localization of high cell forces to the cell rear is supported by experimental observations in keratocytes (Lee et al., 1994) and fibroblasts (Galbraith and Sheetz, 1997). Calpain has also been shown to promote rear retraction by weakening connections between integrins and the cytoskeleton at the rear of migrating CHO cells (Huttenlocher et al., 1997; Chapter 5). The rear of the cell is divided into compartments to account for integrin clustering. The occupancy state of the integrins in each compartment is followed as a function of time until less than one cytoskeleton-integrin-ECM bond exists per compartment. If the force at the cell rear is sufficient to extract from the cell membrane the integrins which are still bound to the ECM, the rear retracts. This model allows us to calculate the rate and mechanism of cell detachment at many different conditions.

The main goal of our approach is to generate clear predictions for how altering different parameters can aid us in our goal of regulating cell speed through rear detachment. The model is consistent with many previous experimental studies on how integrin-ligand binding (Chapter 4; Mandeville and Maxfield, 1997) and calpain activity (Huttenlocher et al., 1997; Chapter 5) affect cell migration. In addition the model generates predictions which have not yet been experimentally tested. These predictions primarily deal with how integrin-cytoskeleton binding, intracellular force, and integrin organization affect rear retraction rate and mechanism.

In our model, the force required to extract integrins from the cell membrane did not impede rear retraction at physiologically relevant parameter values. We assumed that the lipid bilayer surrounding the integrin fractures while the lipid-integrin interactions remain intact. This assumption is supported in cellular systems (Bard and Hay, 1975) as well as in isolated membranes (Leckband et al., 1995; Evans et al., 1991). We also assumed that the force required to extract multiple aggregated receptors is the sum of the forces to extract the individual receptors. Depending on the packing of integrins in the cluster, ripping the entire cluster as a whole may

133

require less force than ripping the individual integrins so we may have overestimated the forces required to extract the integrins.

We predict two different rear retraction phenotypes in which detachment occurs by distinct mechanisms. In the force-dominated phenotype, rear retraction rate is dependent upon the rate at which the applied force can dissociate the integrin-ligand bonds. If the force is not sufficient to dissociate all of the complete cytoskeleton-integrin-ECM linkages, detachment enters the cleavage-dominated phenotype. Here, retraction rate is limited by cleavage of cytoskeleton-integrin linkages. Force-dominated retraction is much more rapid than cleavage-dominated because the bond dissociation rates are much greater than the proteolytic cleavage rates. This has implications for overall cell migration speed. If rear retraction occurs on the order of seconds or less, as is typical for force-dominated detachment, rear release is unlikely to be the rate-limiting step in cell migration. Altering the rate of force-dominated detachment is unlikely to have much effect on overall cell speed. However, if rear retraction occurs on the order of minutes or more, as is typical for cleavage-dominated detachment, rear detachment may limit cell speed. Therefore, parameters which affect the rate of cleavage-dominated detachment, such as integrin-cytoskeleton binding parameters or calpain activity, or parameters which affect the transition between phenotypes, such as integrin-ligand binding parameters or applied force, may or may not affect overall cell speed, depending on the experimental conditions.

The fact that the cytoskeleton-integrin-ECM linkage fractures at different locations in the two different regimes allows us to experimentally measure which phenotype exists. If a large fraction of the integrin rips from the rear of a migrating cell, retraction is cleavage-dominated. If very little integrin is extracted, retraction is force-dominated. This prediction can be experimentally tested since the fate of integrins at the rear of migrating cells can be quantitatively measured by immunofluorescent tracking of labeled integrins (Regen and Horwitz, 1992; Palecek et al., 1996, Chapter 4).

We assume intracellular control of the integrin-cytoskeleton linkage occurs through a protease which cleaves both the integrins and cytoskeletal elements. There is experimental evidence for the cleavage of both the cytoplasmic domain of the integrin and talin (Du et al., 1996; Tranqui and Block, 1995). However, the substrate for calpain in vivo is unknown. We predict that the majority of integrins have their cytoplasmic domain cleaved at the rear of migrating cells. This prediction has not yet been verified.

Experimental probes of cytoskeleton-integrin binding show that these linkages are weaker at the rear of a cell than the front (Schmidt et al., 1993). Cells probably use mechanisms other than protease activity to regulate integrin-cytoskeletal linkages. Recently, evidence of control mechanisms which may allow the cell to strengthen integrin-cytoskeleton linkages have been found. For example, phosphorylation of the β3 integrin cytoplasmic domain can result in

increased cytoskeleton-integrin binding (Jenkins et al., 1998). Integrin-cytoskeleton bond strengthening occurs when integrins are mechanically stressed (Wang and Ingber, 1994). This strengthening may be the result of tyrosine phosphorylation of cytoskeletal proteins (Schmidt et al., 1998). This model predicts that any mechanism a cell uses to alter the cytoskeleton-integrin linkage will only affect the detachment rate in the "protease-dominated" phenotype. The transition between protease and force-dominated regimes will be unaffected.

The prediction that changing cytoskeleton-integrin affinity does not affect bond fracture location appears to contradict a model of cell detachment for adhesion mediated by several bonds in series (Saterbak et al., 1996). The models are only comparable in the force-dominated regime of detachment. The Saterbak et al. model predicts that linkage rupture location is a function of the relative bond affinities while our model predicts that integrin-ECM dissociation dominates in virtually all circumstances. The reason for this discrepancy is our model allows lateral transmission of forces through adhesion complexes or the cell membrane to intact integrin-ECM bonds as long as the cell has not detached, while the Saterbak et al. model has no mechanism to laterally transmit forces. In our model integrin-ECM bonds will continue to feel the effects of force, even after cytoskeletal linkages have ruptured, and this will allow for almost complete rupture of integrin-ECM bonds upon rear detachment.

The role of these two different detachment phenotypes may give insight into why some cells are able to glide over substrates without retraction at the cell front while others move in discrete steps of directed extension and retraction. Some degree of asymmetry is required in adhesiveness between the front and rear of a cell for it to migrate (Lauffenburger and Horwitz, 1996; Sheetz, 1994). If the cell is migrating so that the front is in the "slow-detachment" regime while the rear is in the "rapid detachment" regime it should be able to glide over the substratum by rapidly detaching the rear without affecting adhesions at the front. Experimental measurements of local traction forces exerted by migrating cells indicate that adhesions at the front of migrating cells experience much less force than adhesions at the rear of the cell (Lee et al., 1994; Galbraith and Sheetz, 1997). These differences in forces may be enough to switch from one phenotype to the other, since the transition is very sensitive to changes in force (Figure 7.1). Intracellular gradients in integrin concentration or integrin-ligand affinity may also result in different detachment phenotypes in the front and rear of the cell but the phenotype transition point is much less sensitive to these variables than to force.

In conclusion, we hope that results of this model will stimulate further experimental studies towards understanding how both physical and chemical molecular interactions affect the complex process of cell migration.

7.11 References

Alteraifi, A. M. and Zhelev, D. V. (1997). Transient increases of free cytosolic calcium during neutrophil motility responses. *J. Cell Sci.* **110**, 1967-1977.

Bard, J. B. L., and Hay, E. D. (1975). The behavior of fibroblasts from the developing avian cornea. *J. Cell Biol.* **67**, 400-418.

Chen, W. -T. (1981). Mechanism of retraction of the trailing edge during fibroblast movement. *J. Cell Biol.* **90**, 187-200.

de Beus, E., de Beus, A., and Jacobson, K. (1997). The role of β1-integrin mediated adhesions in Xenopus laevis keratocyte locomotion. *Mol. Biol. Cell Suppl.* **8**, 264a.

DiMilla, P. A., Barbee, K., and Lauffenburger, D. A. (1991). Mathematical model for the effects of adhesion and mechanics on cell migration speed. *Biophys. J.* **60**, 15-37.

Du, X., Saido, T. C., Tsubuki, S., Indig, F. E., Williams, M. J., and Ginsberg, M. H. (1996). Calpain cleavage of the cytoplasmic domain of the integrin β3 subunit. *J. Biol. Chem.* **270**, 26146-26151.

Evans, E. A., Berk, D., and Leung, A. (1991a). Detachment of agglutinin-bonded red blood cells. I. Forces to rupture molecular-point attachments. *Biophys. J.* **59**, 838-848.

Evans, E. A., Berk, D., Leung, A., and Mohandas, N. (1991b). Detachment of agglutinin-bonded red blood cells. II. Mechanical energies to separate large contact areas. Biophys. J. **59**, 849-860.

Fox, J. E. B., Shattil, S. J., Rathbone, R. L. K., Richardson, M., Packham, M. A., and Sanaan, D. A. (1996). The platelet cytoskeleton stabilizes the interaction between αIIbβ3 and its ligand and induces selective movements of ligand-occupied integrin. *J. Biol. Chem.* **271**, 7004-7011.

Galbraith, C. G., and Sheetz, M. P. (1997). A micromachined device provides a new bend on fibroblast traction forces. *Proc. Natl. Acad. Sci, USA.* **94**, 9114-9118.

Hughes, P. E., Diaz-Gonzalez, F., Leong, L., Wu, C., McDonald, J. A., Shattil, S., and Ginsberg, M. H. (1996). Breaking the integrin hinge: a defined structural constraint regulates integrin signaling. *J. Biol. Chem.* **271**, 6571-6574.

Huttenlocher, A., Palecek, S. P., Lu, Q., Zhang, W., Mellgren, R. L., Lauffenburger, D. A., Ginsberg, M. H., and Horwitz, A. F. (1997). Regulation of cell migration by the calcium-dependent protease calpain. *J. Biol. Chem.* **272**, 32719-32722.

Jenkins, A. L., Nannizzi-Alaimo, L., Silver, D., Sellers, J. R., Ginsberg, M. H., Law, D. A., and Phillips, D. R. (1998). Tyrosine phosphorylation of the β3 cytoplasmic domain mediates integrin-cytoskeletal interactions. *J. Biol. Chem.* **273**, 13878-13885.

Lauffenburger, D. A. and Horwitz, A. F. (1996). Cell migration: a physically integrated molecular process. *Cell.* **84**, 359-369.

Leckband, D., Muller, W., Schmitt, F. J., and Ringsdorf, H. (1995). Molecular mechanisms determining the strength of receptor-mediated intermembrane adhesion. *Biophys. J.* **69**, 1162-1169.

Lee, J. and Jacobson, K. (1997). The composition and dynamics of cell-substratum adhesions in locomoting fish keratocytes. *J. Cell Sci.* **110**, 2833-2844.

Lee, J., Leonard, M., Oliver, T., Ishihara, A., and Jacobson, K. (1994). Traction forces generated by locomoting keratocytes. *J. Cell Biol.* **127**, 1957-1964.

Mandeville, J. T. and Maxfield, F. R. (1997) Effects of buffering intracellular free calcium on neutrophil migration through three-dimensional matrices. *J. Cell. Physiol.* **171**, 168-178.

Marks, P. W., Hendey B. and Maxfield, F. R. (1991). Attachment to fibronectin or vitronectin makes human neutrophil migration sensitive to alterations in cytosolic free calcium concentration. *J. Cell. Biol.* **112**, 149-158.

Maxfield, F. R. (1993). Regulation of leukocyte locomotion by Ca^{2+}. *Trends Cell Biol.* **3**, 386-391.

Niggimann, B., Maaser, K., Lu, H., Kroczek, R., Zanker, K. S., and Friedl, P. (1997). Locomotory phenotypes of human tumor cell lines and T lymphocytes in a three-dimensional collagen lattice. *Cancer Lett.* **118**, 173-180.

O'Toole, T. E., Katagiri, Y., Faull, R. J., Peter, K., Tamura, R., Quaranta, V., Loftus, J., Shattil, S. J. and Ginsberg, M. H. (1994). Integrin cytoplasmic domains mediate inside-out signal transduction. *J. Cell Biol.* **125**, 447-460.

Palecek, S. P., Schmidt, C. E., Lauffenburger, D. A., and Horwitz, A. F. (1996). Integrin dynamics on the tail region of migrating fibroblasts. *J. Cell Sci.* **109**, 941-952.

Regen, C. M., and Horwitz, A. F. (1992). Dynamics of $\beta 1$ integrin-mediated adhesive contacts in motile fibroblasts. *J. Cell. Biol.* **119**, 1347-1359.

Saido, T. C., Sorimachi, H., and Suzuki, K. (1994). Calpain: new perspectives in molecular diversity and physiological-pathological involvement. *FASEB J.* **8**, 814-822.

Saterbak, A., and Lauffenburger, D. A. (1996). Adhesion mediated by bonds in series. *Biotechnol. Prog.* **12**, 682-699.

Schmidt, C., Horwitz, A.F., Lauffenburger, D. A., and Sheetz, M. P. (1993). Integrin/cytoskeleton interactions in migrating fibroblasts are dynamic, asymmetric, and regulated. *J. Cell. Biol.* **123**, 977-991.

Schmidt, C., Pommerenke, H., Durr, F., Nebe, B., and Rychly, J. (1998). Mechanical stressing of integrin receptors induces enhanced tyrosine phosphorylation of cytoskeletally anchored proteins. *J. Biol. Chem.* **273**, 5081-5085.

Sheetz, M. P. (1994). Cell migration by graded attachment to substrates and contraction. *Sem. Cell Biol.* **5**, 149-155.

Sorimachi, H., Saido, T. C., and Suzuki, K. (1994) New era of calpain research. Discovery of tissue-specific calpains. *FEBS Lett.* **343**, 1-5.

Tranqui, L. and Block, M. R. (1995). Intracellular processing of talin occurs within focal adhesions. *Exp. Cell Res.* **217**, 149-156.

Tsuchida, J., Uoki, S., Takada, Y., Saito, Y., and Takagi, J. (1998). The 'ligand-induced conformational change' of α5β1 integrin. *J. Cell Sci.* **111**, 1759-1766.

Wang, N., and Ingber, D. E. (1994). Control of cytoskeletal mechanics by extracellular matrix, cell shape, and mechanical tension. *Biophys. J.* **66**, 2181-2189.

Warrick, H. M. and Spudich, J. A. (1987). Myosin structure and function in cell motility. *Annu. Rev. Cell Biol.* **3**, 379-421.
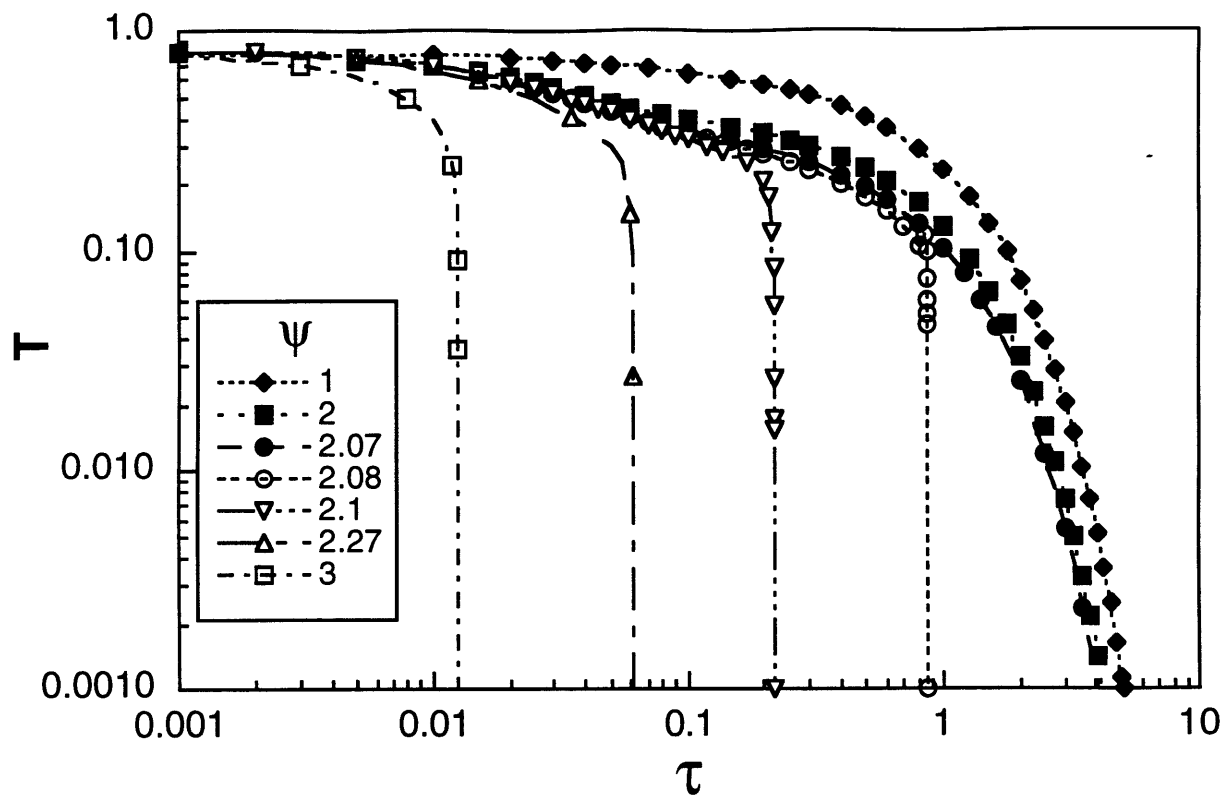
Figure 7.1. At High ψ (>2.08), Cytoskeleton-Integrin-ECM Linkages Dissociate Rapidly at a ψ-Dependent Rate. At low ψ (<2.07), cytoskeleton-integrin-ECM linkages dissociate slowly at a rate which is not a strong function of ψ. Detachment occurs at T<0.001. $\theta_1=\theta_2=\theta_3=\theta_4=100$, $\kappa_2=\kappa_3=\kappa_4=1$, $\kappa_c=1$, $\eta_{RL}=\eta_{RC}=1$, $N_c=100$, $R_T=10^5$.
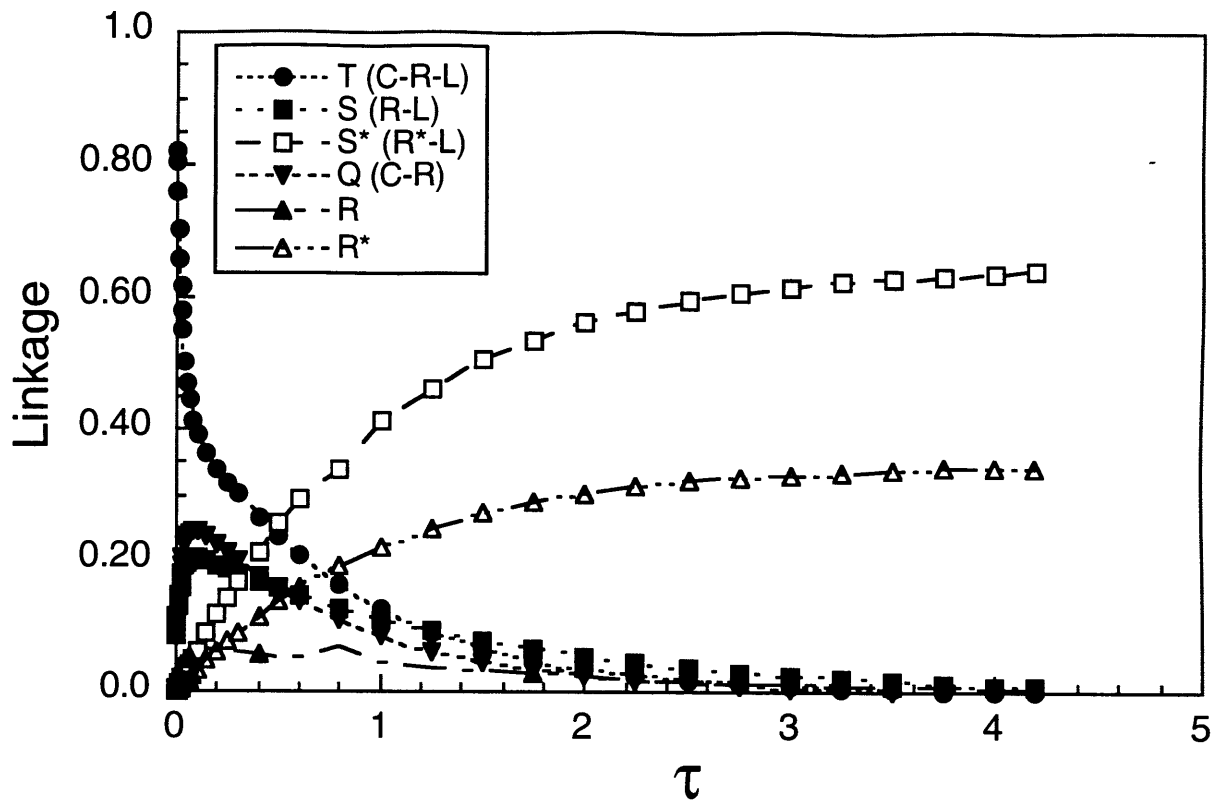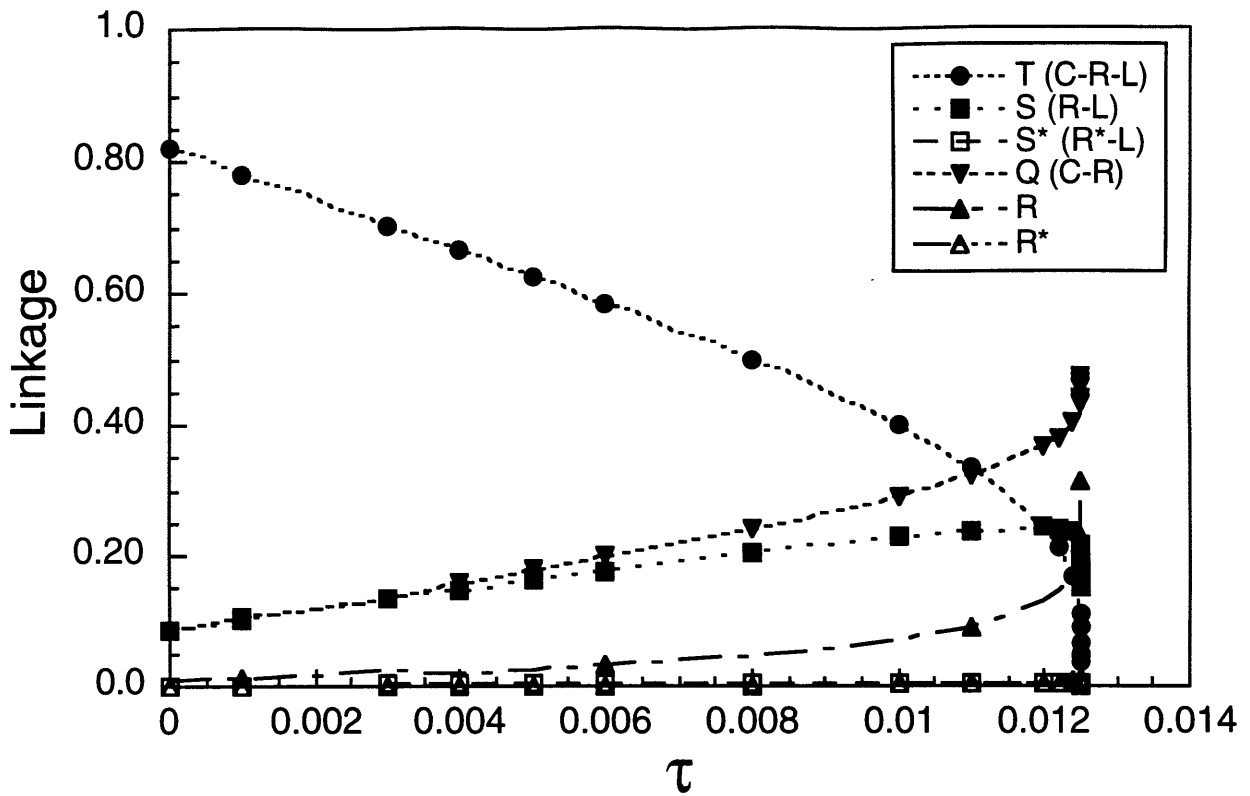
Figure 7.2. Integrin Occupancy State as a Function of Time during Slow Detachment. Initially, force dissociates integrins bound to the cytoskeleton and ECM (T) into ligand-bound (S) or cytoskeleton-bound (Q) states. This force is not sufficient to sever all linkages. Protease activity cleaves the remaining linkages at detachment most integrins are in cleaved (S^* or R^*) states. $\psi=2$, $\theta_1=\theta_2=\theta_3=\theta_4=100$, $\kappa_2=\kappa_3=\kappa_4=1$, $\kappa_c=1$, $\eta_{RL}=\eta_{RC}=1$, $N_c=100$, $R_T=10^5$.

Figure 7.3. Integrin Occupancy State as a Function of Time during Rapid Detachment. Force dissociates integrins bound to the cytoskeleton and ECM (T) into ligand-bound (S) or cytoskeleton-bound (Q) states. Ligand-bound integrins are fractured into free receptors (R). At detachment, most integrins are either unbound or cytoskeletally-bound. Virtually no integrins are cleaved by protease activity. $\psi=3$, $\theta_1=\theta_2=\theta_3=\theta_4=100$, $\kappa_2=\kappa_3=\kappa_4=1$, $\kappa_c=1$, $\eta_{RL}=\eta_{RC}=1$, $N_c=100$, $R_T=10^5$.
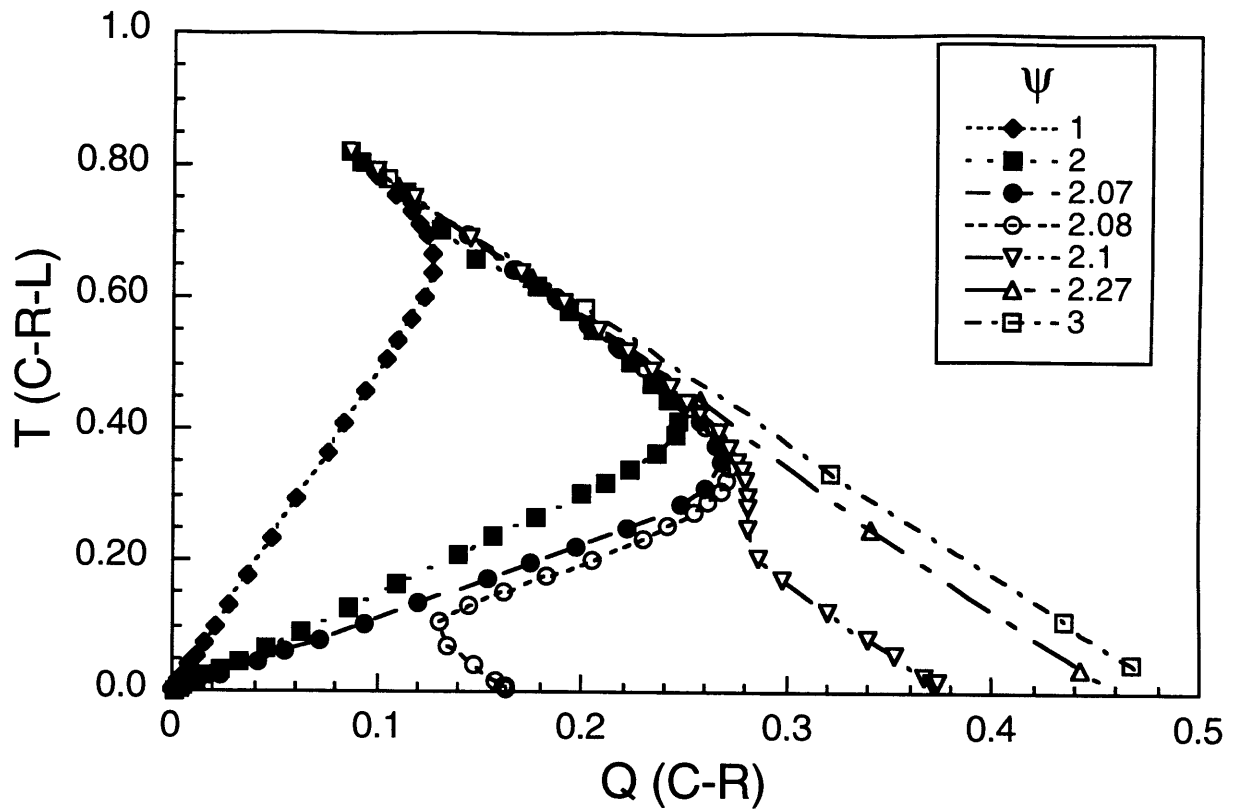
Figure 7.4. Phase Plot of Cytoskeleton-Integrin-ECM Linkages (T) as a Function of Cytoskeleton-Receptor Linkages (Q). At high forces (ψ>2.1), decreases in T are accompanied by increases in Q until detachment. At lower forces (ψ<2.07), initial decreases in T are accompanied by increases in Q, but then Q also decreases as proteases cleave integrin-cytoskeleton linkages. The absence of cytoskeleton-integrin linkages at detachment indicates a slow detachment mechanism while the presence of cytoskeleton linkages corresponds to rapid detachment. $\theta_1=\theta_2=\theta_3=\theta_4=100$, $\kappa_2=\kappa_3=\kappa_4=1$, $\kappa_c=1$, $\eta_{RL}=\eta_{RC}=1$, $N_c=100$, $R_T=10^5$.
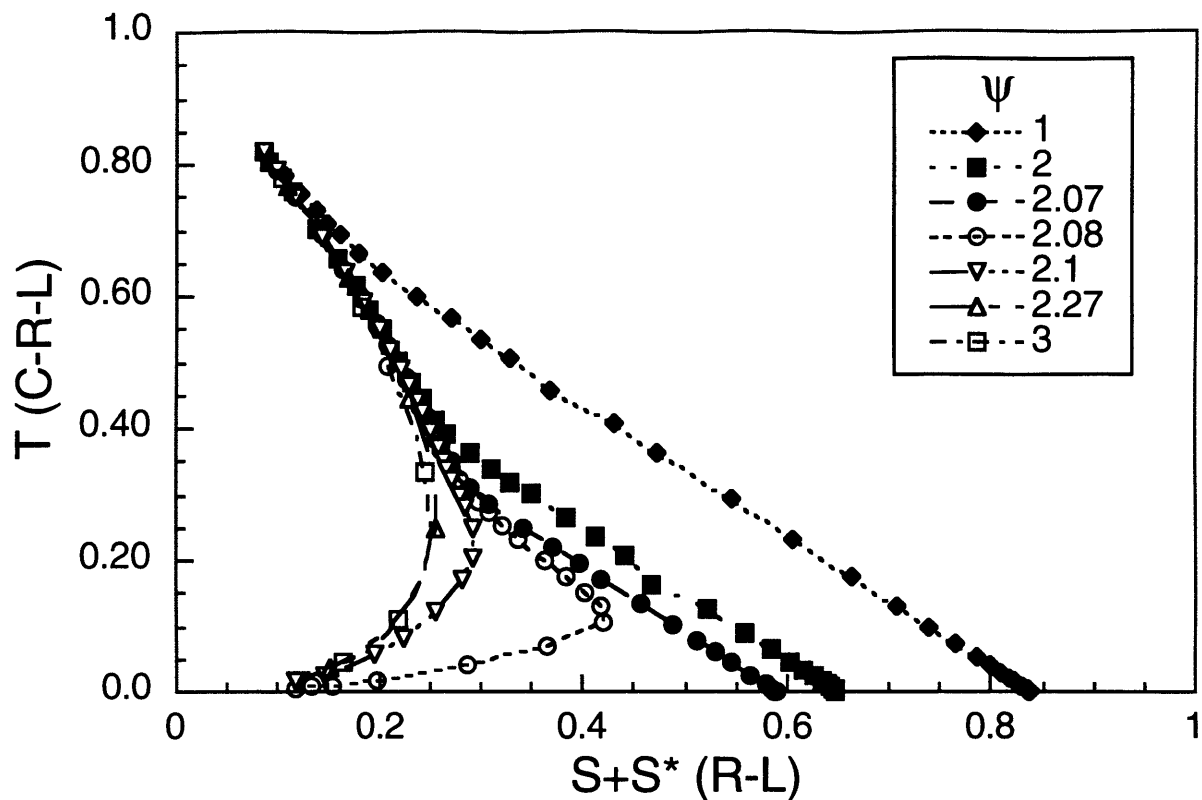
Figure 7.5. Phase Plot of Cytoskeleton-Integrin-ECM Linkages (T) as a Function of Integrin-ECM Ligand Linkages, with the Cytoplasmic Domain Intact (S) or Cleaved (S*). At low forces (ψ<2.07), decreases in T are accompanied by increases in S+S* until detachment. At higher forces (ψ>2.08), initial decreases in T are accompanied by increases in S+S*, but then S+S* also decreases as the applied force dissociates ligand-bound receptors into free receptors. The relative absence of integrin-ligand linkages at detachment indicates a rapid detachment mechanism while the presence of significant quantities of integrin which extracts upon rear retraction corresponds to rapid detachment. $\theta_1=\theta_2=\theta_3=\theta_4=100$, $\kappa_2=\kappa_3=\kappa_4=1$, $\kappa_c=1$, $\eta_{RL}=\eta_{RC}=1$, $N_c=100$, $R_T=10^5$.
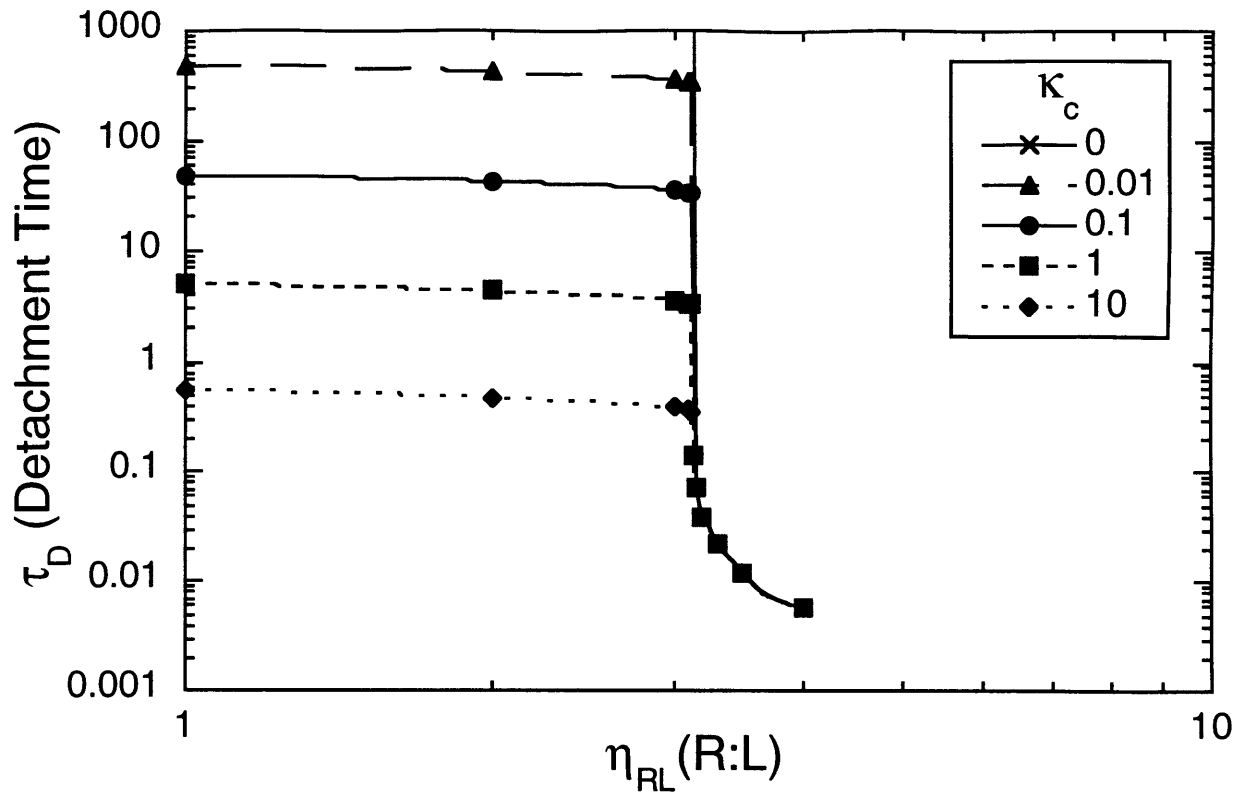
Figure 7.6A. Calpain Activity Affects Detachment Rate at Low Receptor:Ligand Concentration (η_{RL}) but not at High η_{RL}. During slow detachment ($\eta_{RL}<3$), detachment time is a function of κ_C but not η_{RL}. For $\eta_{RL}>3$, detachment time decreases as η_{RL} decreases and is not a function of calpain activity. Calpain appears to only be relevant during slow detachment and does not affect the transition between slow and rapid detachment mechanisms. $\theta_1=\theta_2=\theta_3=\theta_4=100$, $\kappa_2=\kappa_3=\kappa_4=1$, $\eta_{RC}=1$, $\psi=1.32$, $N_c=100$, $R_T=10^5$.
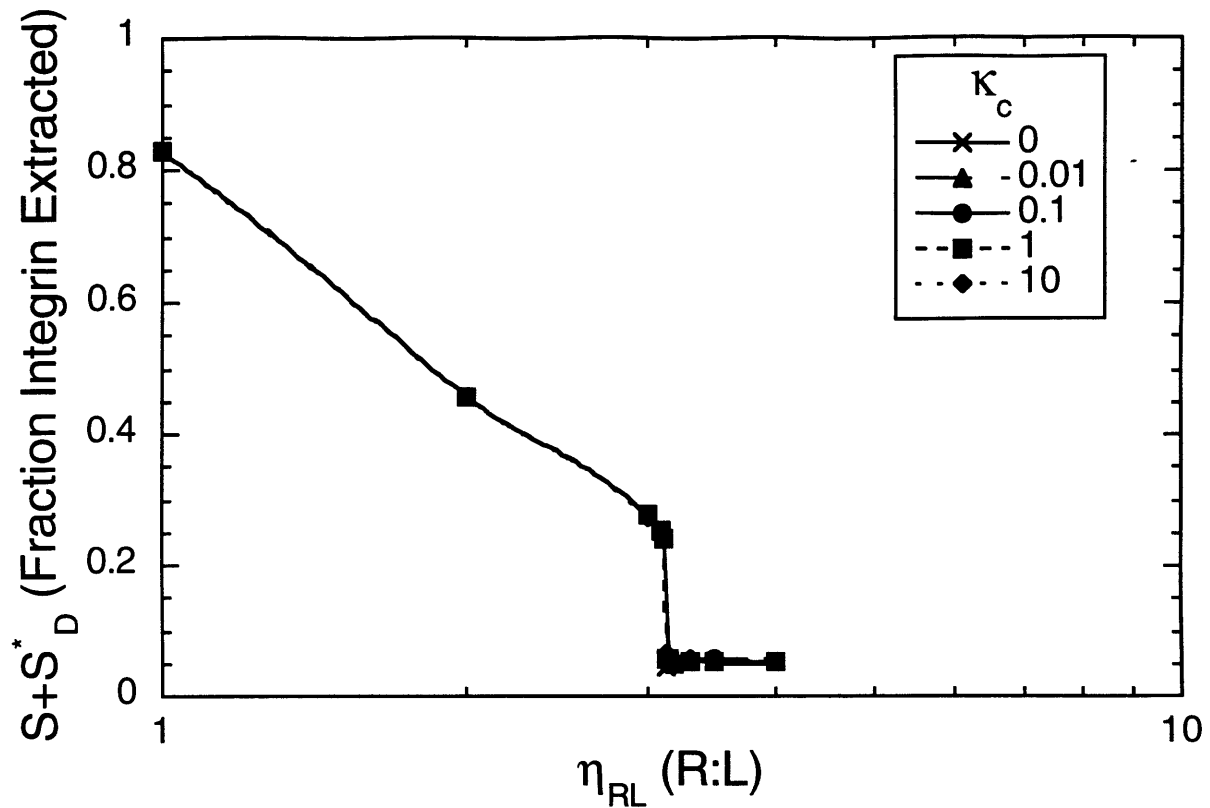
Figure 7.6B. Calpain Activity Does not Affect Integrin Extraction during Rear Retraction. At low receptor:ligand concentration (η_{RL} <3) where detachment rate is relatively slow, significant amounts of integrin extracts from the cell membrane as the cell detaches from the substratum. At η_{RL} above 3 where detachment rate is rapid, virtually no integrin extracts from the cell membrane. Calpain activity affects detachment rate in the slow detachment regime by altering the rate but not the number of cytoskeleton-integrin bonds which must be cleaved. $\theta_1=\theta_2=\theta_3=\theta_4=100$, $\kappa_2=\kappa_3=\kappa_4=1$, $\eta_{RC}=1$, $\psi=1.32$, $N_c=100$, $R_T=10^5$.

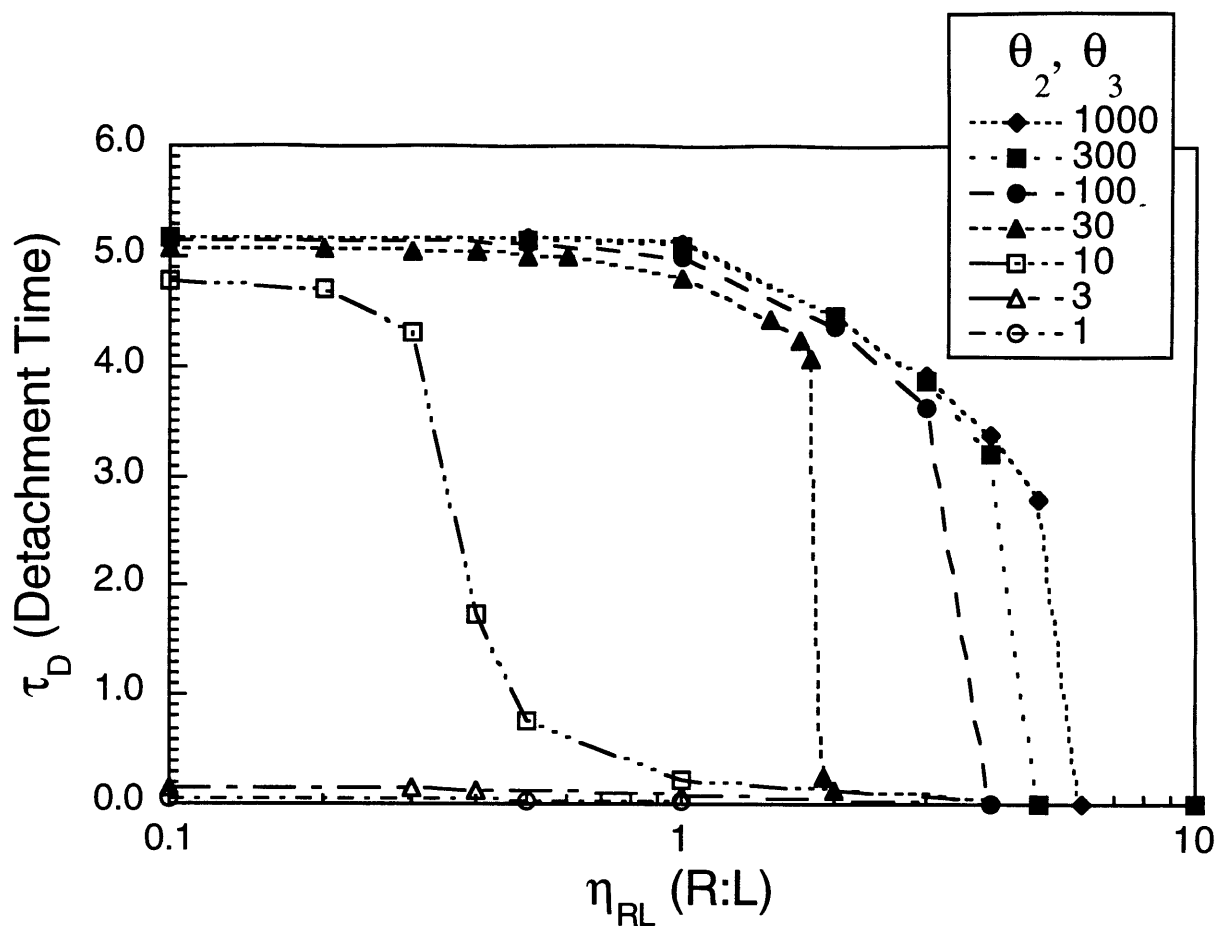**Figure 7.7A.** Integrin-Ligand Affinity (θ_2, θ_3) and Concentration Ratio (η_{RL}) Affect the Transition from Slow to Rapid Rear Detachment. As η_{RL} increases, higher θ_2 and θ_3 is required for rapid detachment. $\theta_1 = \theta_4 = 100$, $\kappa_2 = \kappa_3 = \kappa_4 = 1$, $\kappa_c = 1$, $\eta_{RC} = 1$, $\psi = 1.32$, $N_c = 100$, $R_T = 10^5$.
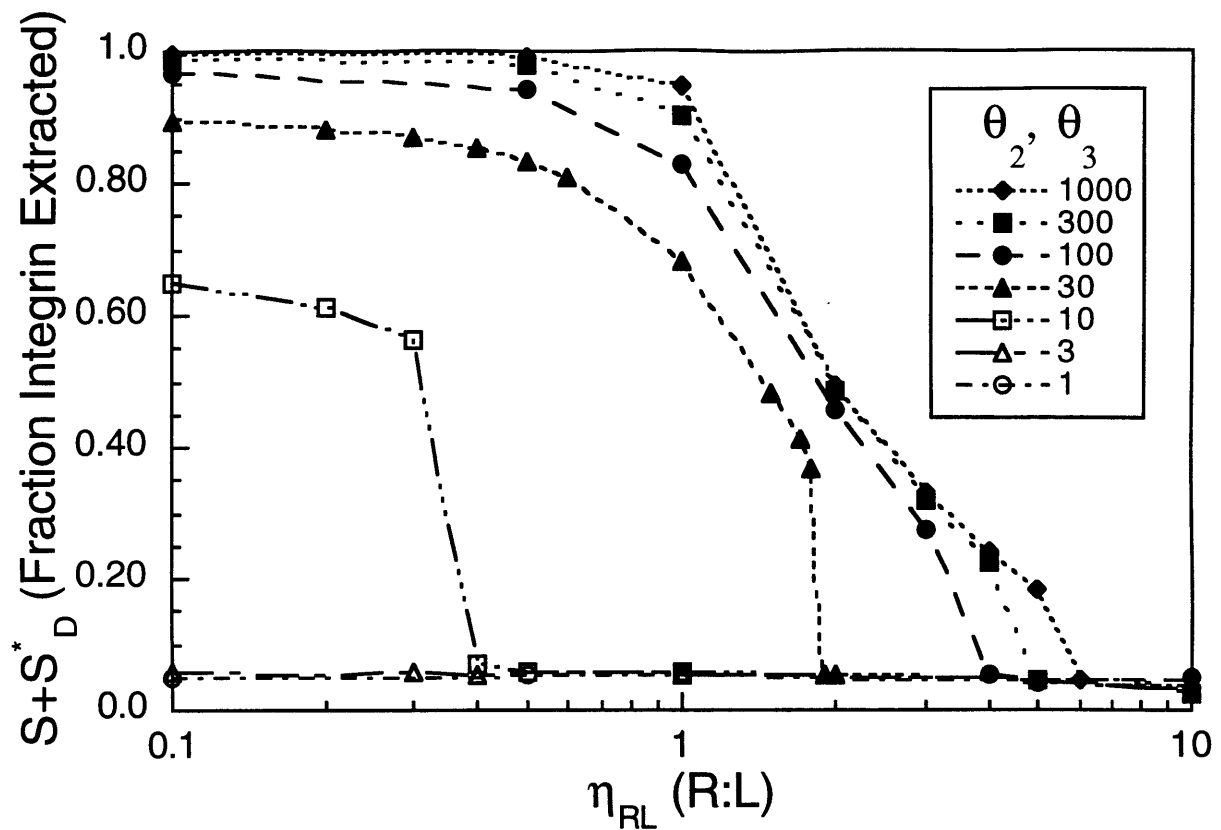
Figure 7.7B. Integrin-Ligand Affinity (θ_2, θ_3) and Concentration Ratio (η_{RL}) Affect Integrin Extraction during Rear Release. As η_{RL} increases or θ_2 and θ_3 decrease rear retraction changes from a mechanism which extracts large amounts of integrins from the rear of the cell to a mechanism in which integrin-ligand bonds primarily dissociate. The transition point of this bond release mechanism corresponds to a transition between rapid and slow detachment (Figure 7.7A). $\theta_1=\theta_4=100$, $\kappa_2=\kappa_3=\kappa_4=1$, $\kappa_c=1$, $\eta_{RC}=1$, $\psi=1.32$, $N_c=100$, $R_T=10^5$.
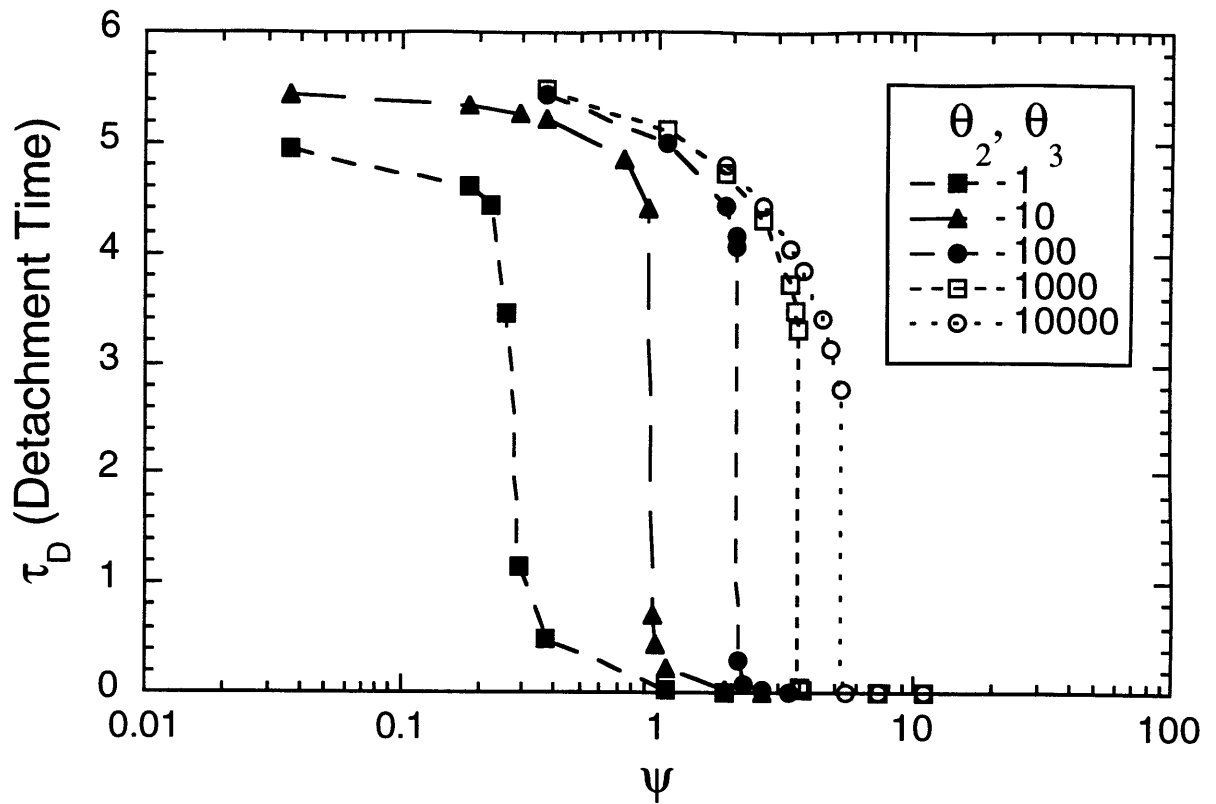
Figure 7.8A. Integrin-Ligand Affinity (θ_2, θ_3) and Force (ψ) Affect the Transition from Slow to Rapid Detachment. As θ_2 and θ_3 increase, higher ψ is required to allow rapid detachment. $\theta_1=\theta_4=100$, $\kappa_2=\kappa_3=\kappa_4=1$, $\kappa_c=1$, $\eta_{RL}=\eta_{RC}=1$, $N_c=100$, $R_T=10^5$.
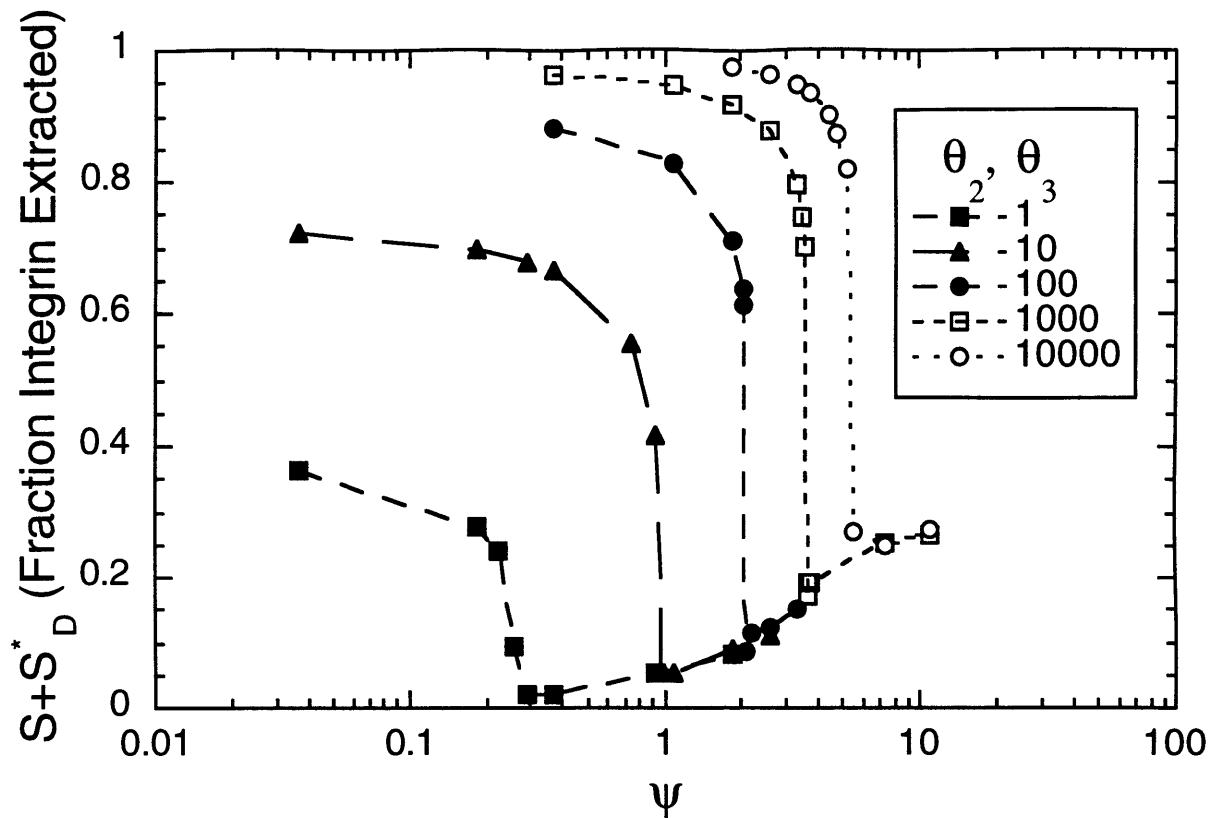
Figure 7.8B. Integrin-Ligand Affinity (θ_2, θ_3) and Force (ψ) Affect Integrin Extraction during Rear Release. As ψ increases or θ_2 and θ_3 decrease rear retraction changes from a mechanism which extracts large amounts of integrins from the rear of the cell to a mechanism in which integrin-ligand bonds primarily dissociate. The transition point of this bond release mechanism corresponds to a transition between rapid and slow detachment (Figure 7.8A). $\theta_1=\theta_4=100$, $\kappa_2=\kappa_3=\kappa_4=1$, $\kappa_c=1$, $\eta_{RL}=\eta_{RC}=1$, $N_c=100$, $R_T=10^5$.
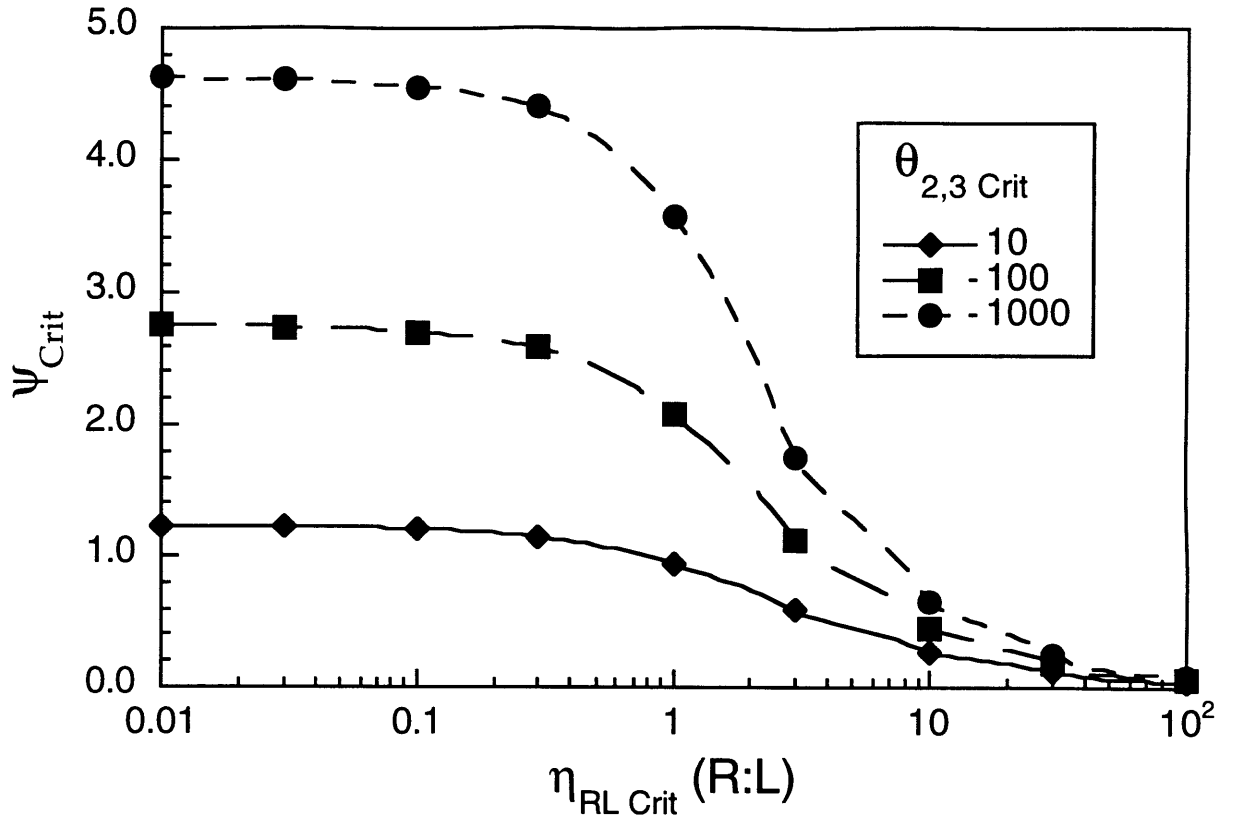
Figure 7.9. Phase Space of Rapid and Slow Detachment. Three parameters (ψ, η_{RL}, and $\theta_{2,3}$) affect the transition from slow, primarily cytoskeleton-integrin dissociation to fast, primarily integrin-ECM dissociation. This plot shows the values of these parameters at the transition point. The space above the curves corresponds to rapid detachment while the space below corresponds to slow detachment. As η_{RL} decreases, high ψ or $\theta_{2,3}$ is required for rapid detachment. As ψ decreases, low $\theta_{2,3}$ or high η_{RL} is required for rapid detachment. $\theta_1=\theta_4=100$, $\kappa_2=\kappa_3=\kappa_4=1$, $\kappa_c=1$, $\eta_{RC}=1$, $N_c=100$, $R_T=10^5$.
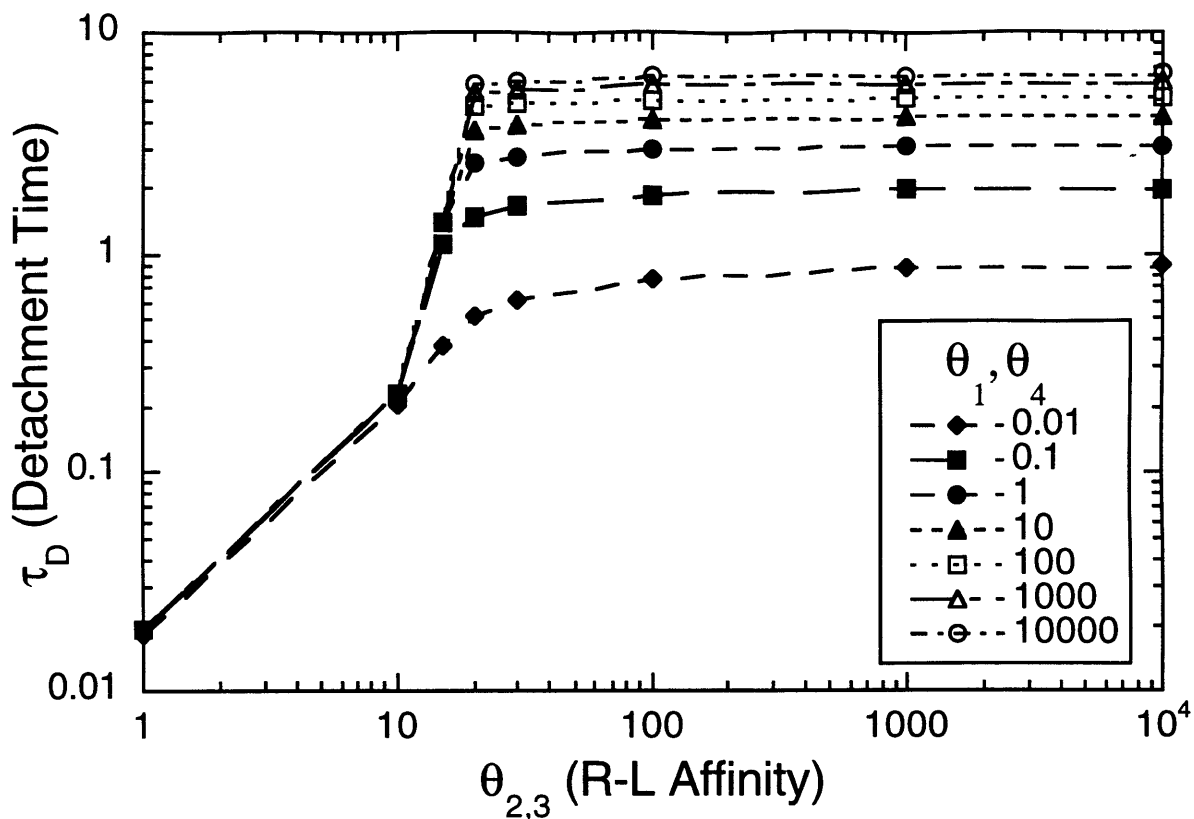
150

Figure 7.10A. Receptor-Ligand Affinity ($\theta_{2,3}$) Affects Rapid Detachment while Cytoskeleton-Receptor Affinity ($\theta_{1,4}$) Affects Slow Detachment. Changing $\theta_{2,3}$, but not $\theta_{1,4}$, can induce the transition between slow and rapid detachment. In the slow detachment regime, increasing $\theta_{1,4}$ will increase detachment time but altering $\theta_{2,3}$ has no effect on detachment rate. During rapid detachment, decreasing $\theta_{2,3}$ will decrease detachment time but changing $\theta_{1,4}$ has no effect on detachment rate. $\kappa_2 = \kappa_3 = \kappa_4 = 1$, $\kappa_c = 1$, $\eta_{RL} = \eta_{RC} = 1$, $\psi = 1.32$, $N_c = 100$, $R_T = 10^5$.
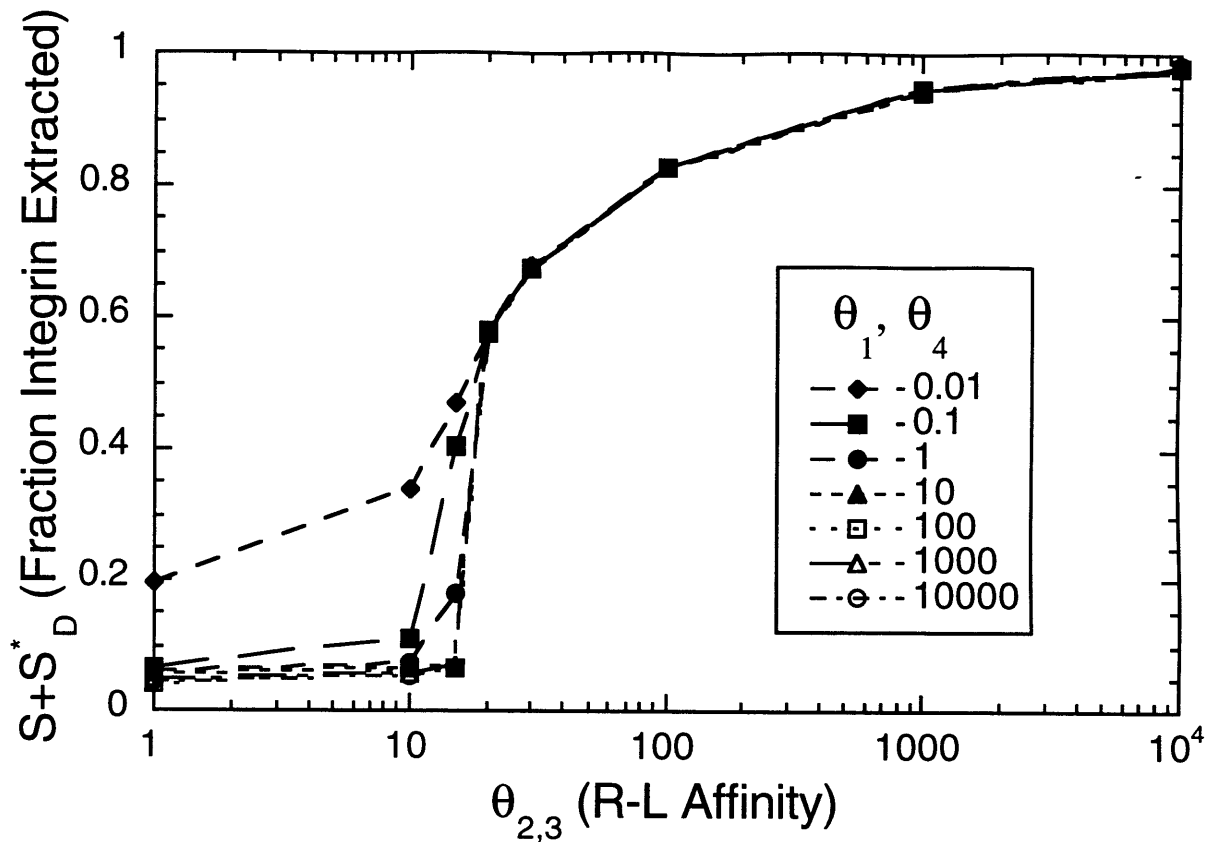
Figure 7.10B. Integrin Extraction is a Function of Integrin-ECM Affinity ($\theta_{2,3}$) but not Cytoskeleton-Integrin Affinity ($\theta_{1,4}$). At $\theta_{2,3} > 10$ cytoskeleton-integrin bond fracture is the primary mode of rear detachment and at $\theta_{2,3} < 10$ integrin-ECM dissociation dominates. Detachment mode is independent of $\theta_{1,4}$ except at very low cytoskeleton-receptor affinity. The switch in detachment mode also corresponds to a switch in detachment rate between slow and very rapid (Figure 7.10A). $\kappa_2 = \kappa_3 = \kappa_4 = 1$, $\kappa_c = 1$, $\eta_{RL} = \eta_{RC} = 1$, $\psi = 1.32$, $N_c = 100$, $R_T = 10^5$.
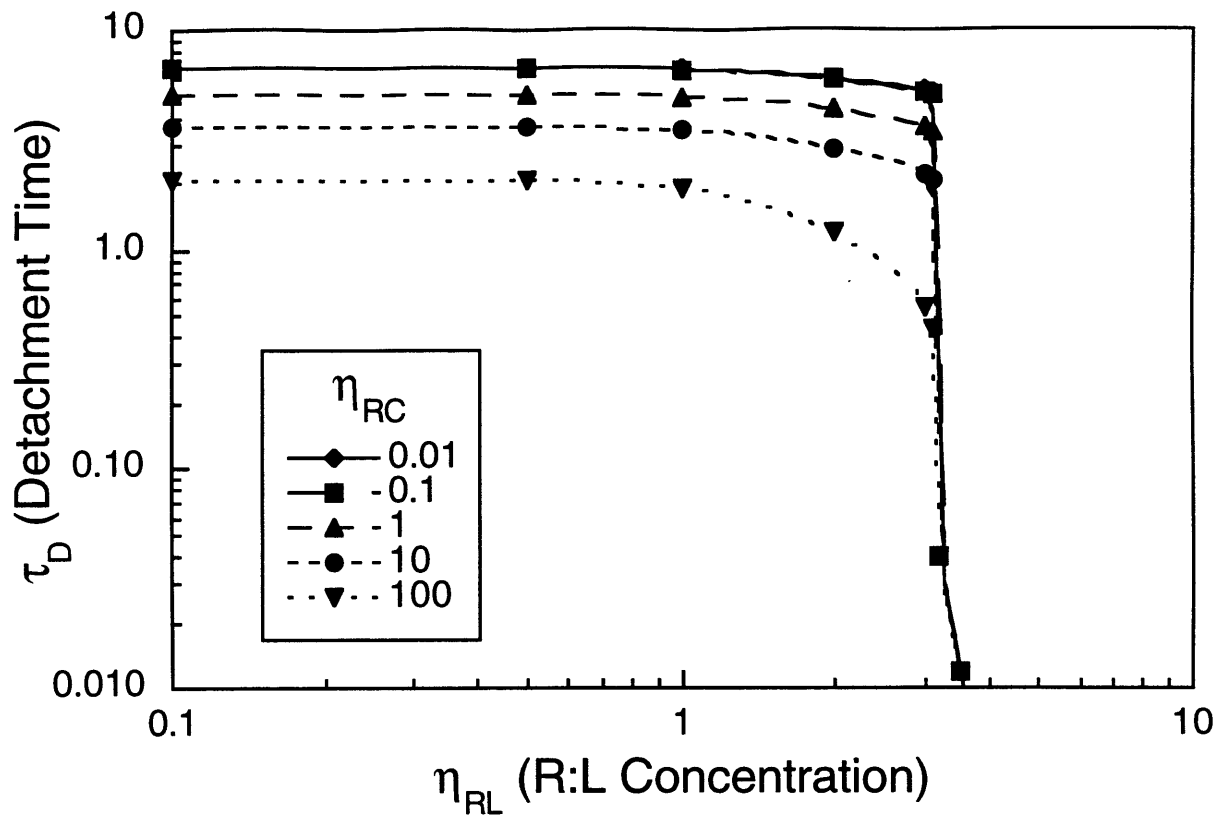
Figure 7.11A. Receptor:Ligand Concentration (η_{RL}) Affects Rapid Detachment while Cytoskeleton:Receptor Concentration (η_{RC}) Affects Slow Detachment. Changing η_{RL} but not η_{RC}, can induce the transition between slow and rapid detachment. In the slow detachment regime, decreasing η_{RC} will increase detachment time but altering η_{RL} has no effect on detachment rate. During rapid detachment, increasing η_{RL} will decrease detachment time but changing η_{RC} has no effect on detachment rate. $\theta_1=\theta_2=\theta_3=\theta_4=100$, $\kappa_2=\kappa_3=\kappa_4=1$, $\kappa_c=1$, $\psi=1.32$, $N_c=100$, $R_T=10^5$.
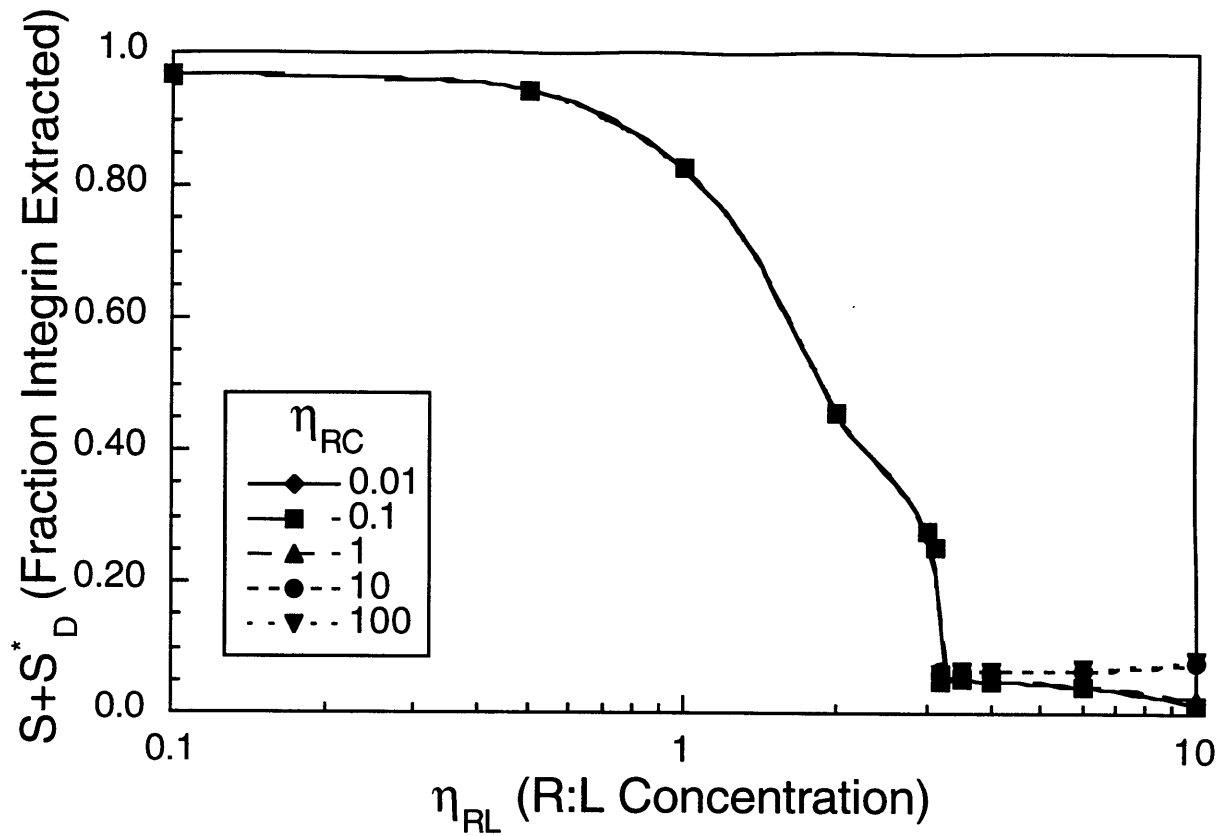
Figure 7.11B. Integrin Extraction is a Function of Integrin:ECM Concentration (η_{RL}) but not Cytoskeleton:Integrin Concentration (η_{RC}). At $\eta_{RL}<3$ cytoskeleton-integrin bond fracture is the primary mode of rear detachment and at $\eta_{RL}>3$ integrin-ECM dissociation dominates. Detachment mode is independent of η_{RC}. The switch in detachment mode also corresponds to a switch in detachment rate between slow and very rapid (Figure 7.11A). $\theta_1=\theta_2=\theta_3=\theta_4=100$, $\kappa_2=\kappa_3=\kappa_4=1$, $\kappa_c=1$, $\psi=1.32$, N_c, $R_T=10^5$.
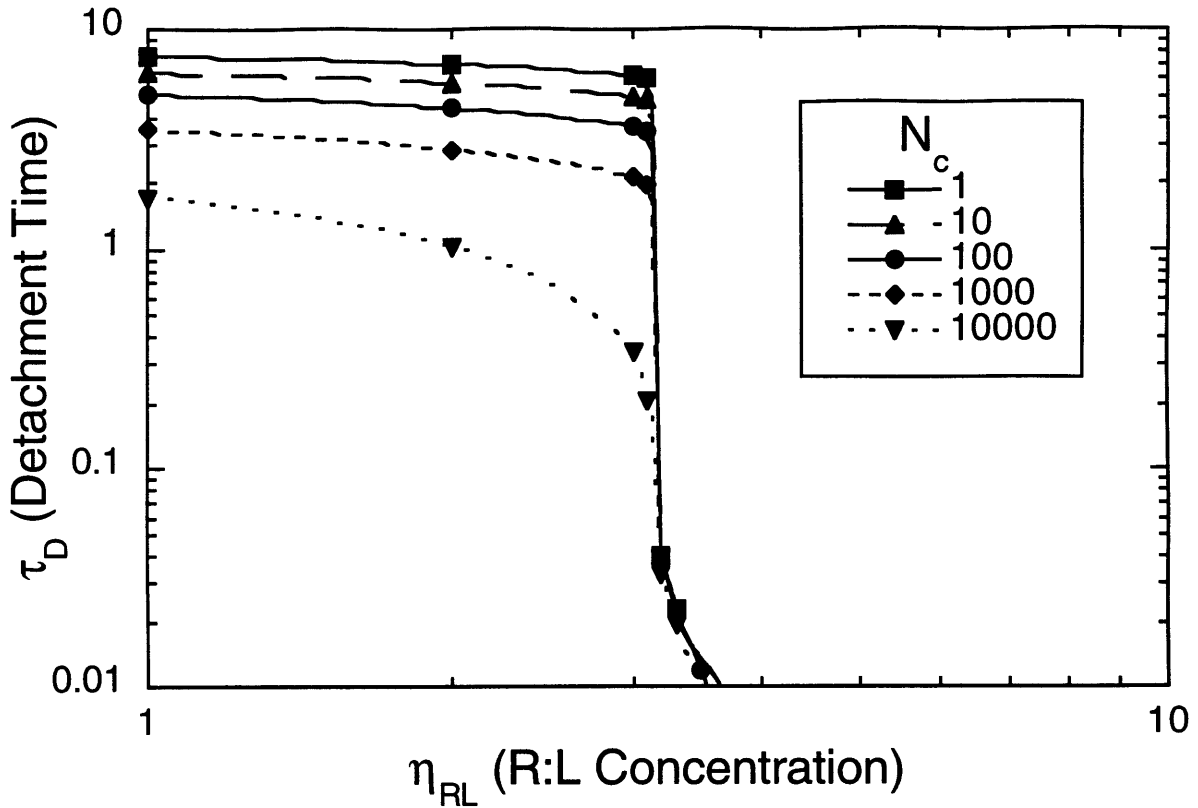
Figure 7.12. Integrin Clustering Affects Detachment Rate in the Slow Detachment Regime. Detachment time decreases as the number of compartments increases at low η_{RL} (<3). When detachment becomes rapid at high η_{RL} (>3), the number of compartments has not effect on detachment rate. Compartment number has no effect on the transition from slow to rapid detachment. $\theta_1=\theta_2=\theta_3=\theta_4=100$, $\kappa_2=\kappa_3=\kappa_4=1$, $\kappa_c=1$, $\eta_{RC}=1$, $\psi=1.32$, $R_T=10^5$.
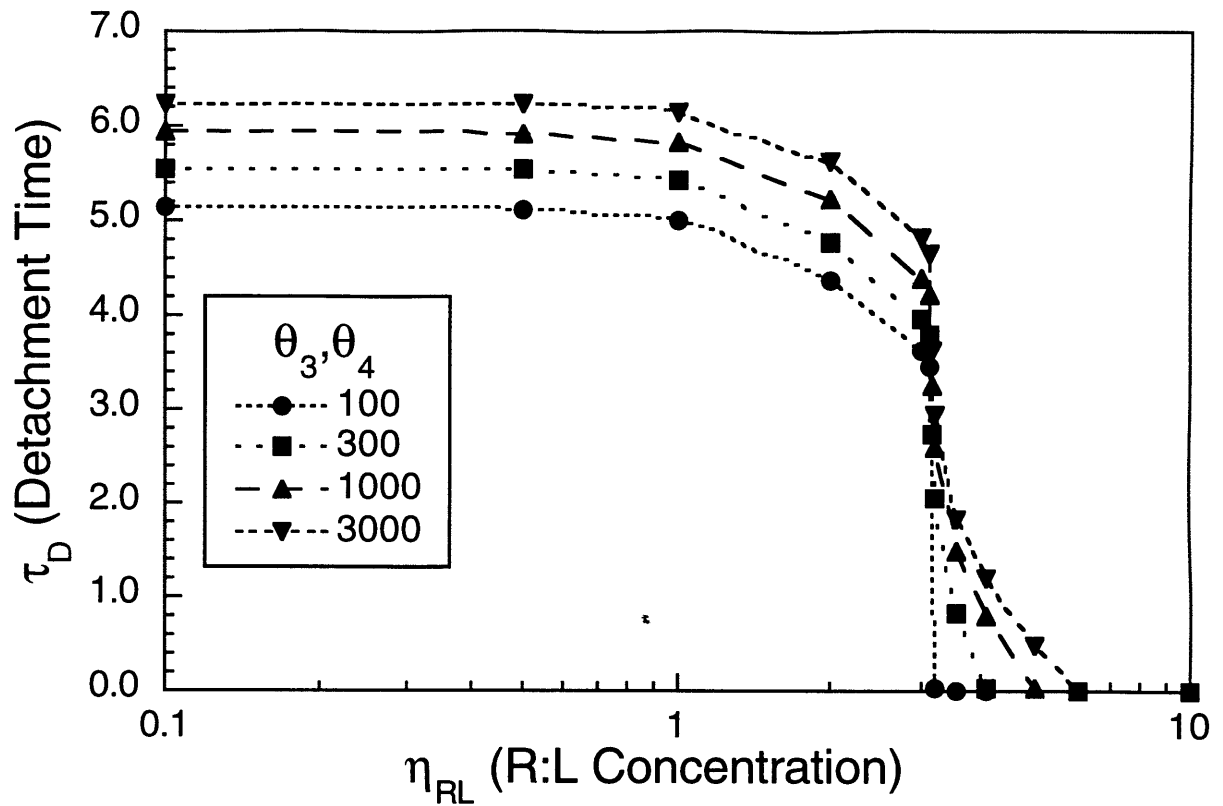
Figure 7.13. Integrin Cooperativity can Affect Detachment Rate but not the Transition between Detachment Mechanisms. At low η_{RL} (<3) increasing the affinity of ligand-bound integrin for the cytoskeleton or cytoskeleton-bound integrin for the ligand increases detachment time slightly. However, detachment rate still becomes very rapid at $\eta_{RL}=3$. $\theta_1=\theta_2=100$, $\kappa_2=\kappa_3=\kappa_4=1$, $\kappa_c=1$, $\eta_{RC}=1$, $\psi=1.32$, $N_c=100$, $R_T=10^5$.

Chapter 8: Conclusions

8.1 Summary of Results

We have developed an experimental system and a mathematical model to test the hypothesis that we can rationally enhance or inhibit cell migration speed by altering molecular interactions in the cytoskeleton-integrin-ECM ligand linkage. Using both experiments and computations we have quantitatively characterized how integrin-mediated linkages regulate cell adhesiveness, cell-substratum detachment, and cell speed. The ability to alter the number and nature of bonds between a cell and its environment is an important tool in designing therapies to modify cell speed. Many of the parameters contributing to motility must be optimized for maximum cell speed, so comprehension of how these parameters interact as a system is crucial to understanding how altering a single parameter will affect cell speed. This knowledge will aid efforts to control cell speed in a therapeutic setting, such as inhibiting tumor metastasis or stimulating wound healing, and in the design of engineered tissues.

A CHO cell system was constructed to allow us to simultaneously vary ECM concentration, integrin expression, and integrin ligand affinity. We developed assays to quantitatively measure migration speed and adhesion strength of these cells. As expected, cell adhesiveness increases as ECM concentration, integrin expression, or integrin-ECM affinity increase. Cell speed is a biphasic function of each of these parameters. Increasing integrin expression or affinity state decreases the amount of ligand required to promote maximum cell speed. Maximum attainable cell speed is not a function of integrin-ligand binding parameters, however. Plotting speed as a function of adhesiveness demonstrates that speed is a constant biphasic function of adhesiveness, with maximum speed always occurring at the same intermediate level of adhesiveness. These results are in agreement with previous experimental and theoretical studies (DiMilla et al., 1991; DiMilla et al., 1993; Lauffenburger and Horwtiz, 1996). Therefore, we can regulate cell speed by quantitatively altering the adhesive interactions between the cells and the substratum.

At high adhesiveness, cell speed is limited by the ability of the cell to detach from the substratum. This phenomenon involves the ability of the cytoskeleton to generate a force to fracture either integrin-cytoskeleton or integrin-ligand bonds. To determine which of this bonds in the linkage breaks, we developed an assay to track integrins at the rear of migrating cells. Quantitative fluorescent time-lapse microscopy is used to determine the fraction of integrins which rip from the rear of the cell upon rear detachment. We found that integrin linkage fracture location correlates with cell adhesiveness as we vary ECM concentration, integrin expression, or integrin-

157

ECM affinity. At low adhesiveness integrin-ECM bonds tend to dissociate while at high adhesiveness integrin-cytoskeletal bonds preferentially release.

The release of integrin-cytoskeletal bonds suggests an active cell detachment mechanism which may play a role in speed regulation at high adhesiveness. To search for such a mechanism, we investigated the role of calpain, a calcium-dependent protease, in allowing rear retraction during cell migration. We used pharmacological agents to inhibit calpain activity in migrating cells at different levels of cell substratum adhesiveness. At low adhesiveness, calpain activity has no effect on cell speed or retraction rate. At high adhesiveness, calpain inhibition greatly slows both speed and retraction rate. Additionally, integrin-cytoskeleton bond dissociation is greatly reduced when calpain is inhibited. These results suggest that calpain allows cell migration at high adhesiveness by weakening integrin-cytoskeletal connections.

Next, we constructed a mathematical model to integrate how the biophysical interactions between integrins, the cytoskeleton, and matrix and biochemical alterations of these interactions by calpain affect rear retraction and linkage dissociation mechanism. Our model also examines how applied forces and integrin clustering affect retraction kinetics. The model predicts that two different detachment mechanisms can occur. In the first mechanism, detachment is very fast, dominated by integrin-ECM dissociation, and occurs at high forces or low adhesiveness. In the second, detachment is much slower, is dominated by integrin-cytoskeleton dissociation, and occurs at low forces or high adhesiveness. The amount of integrin which is extracted from the rear of the cell is an assay for detachment phenotype. During rapid detachment cells leave very little integrin on the substratum while during slow detachment a large fraction of integrin rips from the membrane. This model may help explain why some cell types, such as leukocytes or keratocytes, are typically able to detach easily and move very quickly while other cell types, such as fibroblasts, tend to migrate more slowly and release many more integrins during detachment.

8.2 Implications and Future Directions

Our experimental studies and mathematical model indicate that control of cell speed through integrin-ligand and cytoskeleton-integrin linkages is a complex process. Interactions among different parameters can have varied effects on cell speed, depending on the values of the parameters. This study has raised further questions which must be addressed to achieve our goal of understanding how molecular interactions between a cell and its substratum regulate cell speed. In this section we will suggest directions for future work in this area.

First, our model for cell detachment has made a number of predictions which have not been experimentally verified. Experimental evidence supports the prediction that cell detachment phenotype can vary as integrin-ligand binding parameters vary but the prediction that integrin-

cytoskeleton binding cannot affect this transition has not been tested. The best way to initially address this issue may be to alter the expression of a cytoskeletal linker, such as talin, in the CHO cells. Alternatively, one could vary cytoskeleton integrin affinity using different $\beta 1$ splice variants. For example, the $\beta 1D$ splice variant binds talin with a higher affinity than the $\beta 1A$ (Pfaff et al., 1998). $\beta 1B$ and $\beta 1C$ disrupt cytoskeletal associations. Our model predicts that intracellular force generation may be a powerful way to control rear detachment and cell speed. Very small changes in force can have large effects on the transition between detachment phenotypes. Experimental techniques exist to measure local traction forces in migrating cells (Lee et al., 1994; Galbraith and Sheetz, 1997). Unfortunately, experimentally altering cellular force generation may prove to be difficult. Altering myosin levels may be one way to control force generation (Wessels et al., 1998; Jay et al., 1995). Alternatively, pharmacological agents which stimulate or inhibit actin-myosin contractility could be added to the cells.

In our study we were not able to probe specific cytoskeletal interactions during rear detachment. The actual bonds which break in the cytoskeletal linkage when integrins are extracted from the cell membrane are unknown. We may be able to answer this question by fusing green fluorescent proteins (GFPs) to cytoskeletal proteins, then tracking the cytoskeletal proteins during rear retraction. Fluorescence resonance energy transfer (FRET) microscopy may also be useful in determining the specific interactions between cytoskeletal proteins as cytoskeleton-integrin linkages fracture. The intracellular substrates for calpain are not known either. One way to examine which proteins calpain can cleave are to modify integrin cytoplasmic domains or cytoskeletal proteins to eliminate the calpain cleavage site. If calpain inhibitors have no effect on the rear detachment and migration speed of these mutants at high adhesiveness, we can conclude that the mutation is in the physiologic calpain cleavage site. One potential problem with this approach is there may be calpain cleavage sites on many proteins, so cells may be able to compensate for mutations in the cleavage site in one protein by cleaving other proteins. Also, these mutations may affect cytoskeleton binding affinities or rates, further complicating the analysis.

While we focused on the role of integrin binding on regulating cell motility through cell speed, we also measured other parameters which affect motility. We did not find that integrin-ligand binding affects cell persistence, although CHO cells may not be a very good system for analyzing persistence effects. CHO cells do not polarize well and tend to have a very low persistence. Perhaps persistence effects could be determined in cells such as fibroblasts. We have reported population cell speed, which is comprised of both individual cell speeds as well as the fraction of cells which migrate. It has been suggested that population speed is solely a function of fraction of cells which migrate. This assumes a bimodal distribution of cell speed centered around a speed of zero and a fixed speed which is dependent upon cell type. In our experiments this was not the case. We have analyzed individual cell speeds as well as the fraction of cells which

migrate. As population speed increases, the fraction of cells which migrates increases, but the speed of individual cells which are migrating increases too. Understanding the contributions of individual cell speed and a "switch" which can turn migration on or off may prove to be useful in designing therapies to regulate cell speed.

We chose to perform our experiments using cells migrating on a 2-dimensional substratum because the ease of cell tracking, adhesion assays, and quantitative fluorescence microscopy outweighs the nonphysiological nature of the system. The physical interactions which govern migration on 2D substrates will also be important for migration through 3D matrices and in vivo. Recent studies in 3D matrices support this claim (Niggimann et al., 1997; Kuntz and Saltzman, 1997). However, it is still important to test our conclusions and evaluate the quantitative interaction between the system parameters for migration in more physiological systems. As advances are made in imaging technologies and data management, the feasibility of 3D and in vivo studies will improve. We chose the CHO cell line because a significant amount of integrin biochemistry has been studied in these cells and the cells are easy to manipulate genetically. Testing our conclusions in more physiologically motile cell types, such as leukocytes or neutrophils, is also important to bring our results closer to practical applications.

This study has focused on the mechanical role of integrins in mediating cell adhesion and migration. Integrins also play an important role in transmitting signals from the ECM to the cell (Lo and Chen, 1994; Sastry and Horwitz, 1993), as well as from the cell to the ECM (Ginsberg et al., 1992). For example, focal adhesion kinase (FAK) associates with the cytoplasmic domain of integrins (Schaller and Parsons, 1994) and overexpression of FAK enhances CHO cell motility on fibronectin (Cary et al., 1996). Understanding how integrin binding generates biochemical signals and how these signals are further transmitted to mechanical events is important to understand how we can regulate cell migration through integrin activity.

Our approach has been to study the complex process of cell migration by dividing it into physical process and concentrating on cell-substratum detachment. We further divided detachment into molecular interactions between cytoskeletal proteins, adhesion receptors, and ECM ligands. We have demonstrated the ability to control cell migration speed through cell-substratum adhesiveness. At high adhesiveness molecular interactions which rear retraction can regulate cell speed. It is also very important to understand the molecular interactions which govern other cellular processes, such as lamellipod extension, adhesion formation, and force generation. The ability to synthesize these process into a model for migration and to understand the conditions where each of these processes is important.

8.3 References

Cary, L. A., Chang, J. F., Guan, J. L. (1996). Stimulation of cell migration by overexpression of focal adhesion kinase and its association with Src and Fyn. *J. Cell Sci.* **109**, 1787-1794.

DiMilla, P. A., Barbee, K., and Lauffenburger, D. A. (1991). Mathematical model for the effects of adhesion and mechanics on cell migration speed. *Biophys. J.* **60**, 15-37.

DiMilla, P. A., Stone, J. A., Quinn, J. A., Albeda, S. M., and Lauffenburger, D. A. (1993). Maximal migration of human smooth muscle cells on fibronectin and type IV collagen occurs at an intermediate attachment strength. *J. Cell Biol.* **122**, 729-737.

Galbraith, C. G., and Sheetz, M. P. (1997). A micromachined device provides a new bend on fibroblast traction forces. *Proc. Natl. Acad. Sci. USA.* **94**, 9114-9118.

Ginsberg, M. H., X. Du, and Plow, E. F. (1992). Inside-out integrin signaling. *Curr. Opin. Cell Biol.* **4**, 766-771.

Jay, P. Y., Pham, P. A., Wong, S. A., and Elson, E. L. (1995). A mechanical function of myosin II in cell motility. *J. Cell Sci.* **108**, 387-393.

Kuntz, R. M., and Saltzman, W. M. (1997). Neutrophil motility in extracellular matrix gels: mesh size and adhesion affect speed of migration. *Biophys. J.* **72**, 1472-1480.

Lauffenburger, D. A. and Horwitz, A. F. (1996). Cell migration: a physically integrated molecular process. *Cell.* **84**, 359-369.

Lee, J., Leonard, M., Oliver, T., Ishihara, A., and Jacobson, K. (1994). Traction forces generated by locomoting keratocytes. *J. Cell Biol.* **127**, 1957-1964.

Lo, S. H. and Chen, L. B. (1994). Focal adhesion as a signal transduction organelle. *Canc. Metast. Rev.* **13**, 9-24.

Niggimann, B., Maaser, K., Lu, H., Kroczek, R., Zanker, K. S., and Friedl, P. (1997). Locomotory phenotypes of human tumor cell lines and T lymphocytes in a three-dimensional collagen lattice. *Cancer Lett.* **118**, 173-180.

Pfaff, M., Liu, S., Erle, D. J., and Ginsberg, M. H. (1998). Integrin β cytoplasmic domains differently bind to cytoskeletal proteins. *J. Biol. Chem.* **273**, 6104-6109.

Sastry, S. and Horwitz, A. F. (1993). Integrin cytoplasmic domains: mediators of cytoskeletal linkages and extra- and intracellular initiated transmembrane signaling. *Curr. Opin. Cell Biol.* **5**, 819-831.

Schaller, M. D. and Parsons, J. T. (1994). Focal adhesion kinase and associated proteins. *Curr. Opin. Cell. Biol.* **6**, 705-710.

Wessels, D., Soll, D. R., Knecht, D., Loomis, W. F., DeLozanne, A., and Spudich, J. (1988). Cell motility and chemotaxis in Dictyostelium amoebae lacking myosin heavy chain. *Dev. Biol.* **128**, 164-177.